P2X$_7$ receptor and Sepsis- Induced Acute Kidney Injury

Nishkantha Arulkumaran

A thesis submitted to University College London in candidature for the degree of

Doctor of Philosophy

Bloomsbury Institute of Intensive Care Medicine

Division of Medicine

University College London

Gower Street, London WC1E 6BT

Affiliations:

Centre for Nephrology (& London Epithelial Group)

Rowland Hill Street, Royal Free Campus, University College London, NW3 2PF

Imperial College Kidney and Transplant Institute

5th Floor Commonwealth Building, Hammersmith Hospital, Du Cane Road, London W12 0HS

Declaration of originality

I, Nishkantha Arulkumaran confirm that the work presented in this thesis is my own. Where information has been derived from other sources, I confirm that this has been indicated in the thesis.

Signed:

Date:

Abstract

Acute kidney injury (AKI) is a common clinical problem within the intensive care unit. Sepsis is implicated in half the cases of AKI; in those patients requiring acute renal replacement therapy there is an associated mortality of 50%. However, other than maintenance of an adequate circulation, no specific therapy exists for septic AKI. This is in large part related to a poor understanding of the underlying pathophysiology..

I used a 72 hr clinically relevant, fluid-resuscitated rat model of sepsis and recovery to undertake a detailed temporal characterization of the pathophysiology of septic AKI and relevant biomarkers of kidney injury and dysfunction, and to assess the impact of targeted treatments. As with human studies, renal histology demonstrated minimal tissue injury or early inflammatory cell infiltration, however renal recovery was associated with a marked increase in renal macrophage infiltration. A panel of 8 renal biomarkers revealed that urine NGAL was the most sensitive marker, having risen by 3 hours' post-insult and elevated for 24hrs.

Renal blood flow was maintained over the first 24 hrs, however a fall in renal cortical oxygenation occurred despite similar renal oxygen delivery and utilization at 24 hrs. Though electron microscopy showed normal mitochondrial structure, I found an increased expression of mitochondrial uncoupling protein-2 (UCP-2); this may further uncouple mitochondrial respiration. Multiphoton imaging of live healthy kidney slices incubated in either sham or septic serum showed a rise in tubular reactive oxygen species (ROS) and falls in NADH and mitochondrial membrane potential in the septic serum group, findings that are consistent with uncoupling. Pre-incubation with the ROS scavenger, 4-OH-TEMPO, prevented these effects.

The NLRP3 inflammasome plays an important role in pro-inflammatory cytokine production. A NLRP3 inflammasome inhibitor, $P2X_7$ antagonist, prevented LPS-induced IL-1β production by peripheral blood monocytes *in vitro*, however this was related in part to its diluent vehicle, dimethyl sulfoxide (DMSO). In the kidney, proximal tubular $P2X_7$ and caspase-1 expression was seen both *in vivo* and *ex vivo* during sepsis. DMSO/$P2X_7$ antagonist treatment after the onset of sepsis was associated with reduced renal IL-1β expression and improvements in tachycardia, stroke volume, albumin and lactate however effects on renal function were inconclusive. Further studies targeting the NLRP3 inflammasome in sepsis are warranted.

Acknowledgements

Funding and Awards

2014:   Intensive Care Society (UK)- Research Gold Medal Award

2013**:**   Intensive Care Society (UK)- New Investigator Award (£13,800)

2011:   Wellcome Trust Fellowship (£242,000)

Presented Work

ORAL PRESENTATIONS

1. **Novel insights into sepsis induced acute kidney injury**

   Gold Medal Award, Intensive Care Society

   Intensive Care Society State of the Art Meeting, London, Dec 2014

2. **Mitochondrial dysfunction contributes to sepsis-induced acute kidney injury**

   E Greco, **N Arulkumaran**, M Sixma, H Courtneidge, M Duchen, F Tam, R J Unwin, M Singer

   27th Annual Congress of the European Society of Intensive Care Medicine, Barcelona, Spain, October 2014

3. **Mitochondrial uncoupling contributes to fever in sepsis**

   E Greco, **N Arulkumaran**, A Dyson, M Singer

   27th Annual Congress of the European Society of Intensive Care Medicine, Barcelona, Spain, October 2014

4. **Temporal changes in renal haemodynamics and oxygenation in a rat model of sepsis**

   N Arulkumaran, M Sixma, P Bass, F Tam, RJ Unwin, M Singer

   26th Annual Congress of the European Society of Intensive Care Medicine, Paris, France, October 2013

5. **Renal macrophage infiltration in a rat model of sepsis and recovery**

   N. Arulkumaran, M. Sixma, S Saeed, G Bhangal, P Bass, F Tam, M. Singer

   26th Annual Congress of the European Society of Intensive Care Medicine, Paris, France, October 2013

POSTER PRESENTATIONS

1. **Temporal changes in systemic and renal inflammation and histology in a 72-hour rat model of faecal peritonitis**

   N Arulkumaran, M Sixma, E Ceravola, E Jentho, P Bass, RJ Unwin, F Tam, M Singer.

   27th Annual Congress of the European Society of Intensive Care Medicine, Barcelona, Spain, October 2014

2. **P2X$_7$ Receptor and Haemorrhage-reperfusion- Induced Acute Tubular Injury**

   M Sixma, A Dyson, **N Arulkumaran**, P Bass, RJ Unwin, F Tam, M Singer

   26th Annual Congress of the European Society of Intensive Care Medicine, Paris, France, October 2013

3. **P2X$_7$ receptor and sepsis- induced acute tubular injury**

   N Arulkumaran, A Dyson, C Turner, R Unwin, FW Tam, M Singer

   25th Annual Congress of the European Society of Intensive Care Medicine, Lisbon, Portugal, 13-17 October 2012

Published Work

1. C Turner, **N Arulkumaran**, M Singer, RJ Unwin, FWK Tam. Is the inflammasome a potential therapeutic target in renal disease? BMC Nephrology. Jan 2014.

2. *N Arulkumaran*, C Turner, M Sixma, M Singer, RJ Unwin and FWK Tam. Purinergic signaling in inflammatory renal disease. Frontiers in physiology. Aug 2013

3. *Arulkumaran N*, Unwin RJ, Tam FW. A potential therapeutic role for $P2X_7$ receptor ($P2X_7R$) antagonists in the treatment of inflammatory diseases. *Expert Opin Investig Drugs* 2011; 20, 897-915

Content from these manuscripts (text, tables, and figures), written by myself but edited by colleagues and supervisors, has been included in the thesis.

Table of contents

Abbreviations

Abbreviation	Full
APC	activated protein C
ADP	adenosine diphosphate
ADQI	Acute Dialysis Quality Initiative
AIM-2	absent in melanoma-2
AKI	Acute kidney injury
AKIN	Acute Kidney Injury Network
ALP	alkaline phosphatase
ALT	alanine amino transferase
AMP	adenosine monophosphate
AP-1	activator protein-1
APC	antigen presenting cells
ASC	apoptosis-associated Speck-like protein containing a C-terminal CARD
AST	aspartate aminotransferase
ATN	acute tubular necrosis
ATP	adenosine triphosphate
AuROC	area under the receiver operated characteristic curve
BBG	Brilliant Blue G
BCA	bicinchoninic acid assay
Bz-ATP	2′(3′)-O-(4-Benzoylbenzoyl)adenosine 5′-triphosphate triethylammonium
cAMP	cyclic AMP
CARD	caspase recruitment domain
CCL2	C-C motif ligand 2
CKD	chronic kidney disease
CLP	caecal ligation and puncture
CLRs	C-type lectin receptors

CO	cardiac output
COX	cytochrome oxidase
CPPD	calcium pyrophosphate dehydrate
CrCl	creatinine clearance
CV	coefficient of variation
CVC	central venous catheter
CVP	central venous pressure
DAMP	danger associated molecular pattern
DMEM	Dulbecco's Modified Eagle's medium
DMSO	dimethyl sulfoxide
DNA	deoxyribonucleic acid
DO2	oxygen delivery
DTEC	distal tubular epithelial cell
EDV	end-diastolic volume
eGFR	estimated glomerular filtration rate
ELISA	enzyme linked immunosorbent assay
EM	electron microscopy
ENaC	epithelial sodium channel
ESV	end-systolic volume
ETC	electron transport chain
$FADH_2$	flavin adenine dinucleotide
GFR	glomerular filtration rate
GN	glomerulonephritis
HBSS	Hank's buffered saline solution
hCAP18	human cationic antimicrobial protein-18
Het	dihydroethidium
HO-1	heme oxygenase-1
HR	heart rate
hr	hour

HR	heart rate
ICE	interleukin 1b Converting enzyme
ICU	intensive care unit
IL-18	interleukin-18
IL-1β	interleukin-1ß
INF-γ	interferon-γ
iNOS	inducible nitric oxide synthase
IRAK-1	type I interleukin-1 receptor-associated protein kinase
IRI	ischaemia reperfusion injury
IV	intravenous
JGA	juxtaglomerular apparatus
KDIGO	Kidney Disease: Improving Global Outcomes
KIM-1	kidney injury molecule-1
KO	knockout
LD50	50% lethal dose
LPS	lipopolysaccharide
LV	left ventricle
LVEF	left ventricular ejection fraction
MAP	mean arterial pressure
MCP-1	monocyte chemotactic protein
MDP	muramyl dipeptide
MDRD	modification of diet in renal disease
MFI	microcirculatory flow index
MHC	major histocompatibility
MinDC	minimum detectable concentration
MMP	matrix metalloproteinase
MnSOD	manganese superoxide dismutase
MODS	multiorgan dysfunction syndrome
MRS	magnetic resonance spectroscopy

MSU	monosodium urate crystals
MSU	monosodium urate
NAC	n-acetyl cysteine
NADH	nicotinamide adenine dinucleotide
NF-κB	nuclear factor kappa-B
NGAL	neutrophil gelatinase-associated lipocalin
NLRP	NLR family, pyrin domain containing 1
NLRP3	NACHT, LRR and PYD domains-containing protein 3
NLRs	nod-like receptors
NO	nitric oxide
NRIS	near-infrared spectroscopy
OPN	osteopontin
$P2X_7$	$P2X_7$ receptor
PAMPs	pathogen-associated molecular patterns
PAS	periodic acid-Schiff
PBMCs	peripheral blood mononuclear cell
PRR	pattern recognition receptor
PSS	physiological saline solution
PTEC	proximal tubular epithelial cell
PYD	N-terminal pyrin domain
RBF	renal blood flow
RIFLE	Risk- Injury- Failure- Loss- Endstage
RIG-1	retinoic acid inducible gene-I
RIPA	radioimmunoprecipitation assay homogenizing buffer
RNA	ribonucleic acid
RNS	reactive nitrogen species'
ROS	reactive oxygen species
RRT	renal replacement therapy
SBP	systolic blood pressure

SD	standard deviation
SDF	sidestream dark field imaging
SDS	sodium dodecyl sulfate
SIRS	Systemic Inflammatory Response Syndrome
SIRT1	sirtuin-1
SV	stroke volume
SVR	systemic vascular resistance
TEMPO	4-Hydroxy -2,2,6,6-tetramethylpiperidin-1 -oxyl
TGF	tubular glomerular feedback
TGF-ß	transforming growth factor-beta
TLR	toll-like receptor
TMRM	tetramethylrhodamine methylester
TNF-alpha	tumor necrosis factor alpha
tPO_2	tissue oxygen tension
TRAF6	TNF receptor (TNFR)-associated factor
TTE	transthoracic echocardiography
TUNEL	terminal deoxyribonucleotidyl transferse (TdT)-mediated biotin-16-dUTP nick-end labelling
UCP-2	uncoupling protein-2
UO	urine output
UUO	unilateral ureteric obstruction
VO2	oxygen consumption
Vti	velocity-time integral
WBC	white blood cell

1 Sepsis

1.1 *Epidemiology and definitions*

Sepsis is a common and serious global health issue, accounting for 20% of all admissions to intensive care units (ICU), and is the leading cause of death in non-cardiac ICUs (Angus et al. 2001). Although there has been a modest decrease in the mortality of sepsis over time, a third of patients still do not survive (Levy et al. 2010). While the systemic inflammatory response syndrome ('SIRS') criteria are sensitive but non-specific criteria of generalized inflammation, they are an over-simplification of the physiological changes associated with sepsis. As such, criteria for the systemic manifestations of infection have been elaborated further (Table 1). An underlying localized or generalized infection triggering a systemic inflammatory response syndrome, is associated with tissue dysoxia, organ failure and death (Levy et al. 2003).

Sepsis, as defined by the international Surviving Sepsis Campaign, is the presence of infection (either suspected or proven) along with features of systemic inflammation (Table 1) (Dellinger et al. 2013). *Sepsis-induced hypotension* is defined as a systolic blood pressure (SBP) <90 mmHg or mean arterial pressure (MAP) <70 mmHg or a SBP decrease >40 mmHg, or more than two standard deviations below normal for age in the absence of other causes of hypotension. *Septic shock* is defined as sepsis-induced hypotension persisting despite adequate fluid resuscitation. When accompanied by signs of infection-induced hypotension, organ dysfunction or tissue hypoperfusion (e.g. hyperlactataemia or oliguria) *severe sepsis* is said to have occurred.

In order to improve outcomes, a rapid diagnosis is pivotal to prompt instigation of cardiovascular resuscitation. Because of the multiphasic nature of sepsis, an understanding of the sequence of temporal changes is essential to initiate context- and time-specific interventions.

24

Organ failure is a hallmark of severe sepsis and septic shock. Yet little is understood about the evolutionary drive behind organ failure in critical illness. Clinical trials in sepsis have been highly disappointing with multiple drug and interventional strategies all failing to show outcome benefit in large randomized controlled trials. These repeated failures highlight the major complexities presented by sepsis where multiple pathways are simultaneously affected, and where marked fluctuations occur over time.

It is becoming increasingly apparent that many of the biological and physiological alterations previously viewed as pathological may actually be adaptive and protective, and that our well-meaning but misguided attempts to normalize or over-correct perceived abnormality may actually be injurious. Likewise, the host response to Infection is highly variable both between individuals as well as over time. An appropriately dosed intervention at one time point may thus cause harm when given earlier or later in the disease process. Similarly, the assumption that sepsis simply represents a pro-inflammatory state has also been laid bare. Many patients, even on admission to intensive care, are in a state of immunosuppression. Thus, the addition of an immunosuppressive therapy may further compromise the host response, increasing the risk of secondary infection and a poor outcome (Boomer et al. 2011, Conway Morris et al. 2013). Some small studies have shown that immunostimulatory therapies may be beneficial in the right patient subset (Boomer et al. 2014). A personalized medicine approach where patients can be individually targeted by relevant biomarkers to receive appropriate therapies given at optimal dose and duration will lead to better patient selection and, hopefully, improved outcomes.

Table 1 Diagnostic criteria for sepsis (Dellinger et al. 2013)

Variable	Infection (documented or suspected) and 'some' of the following:
General	Fever (>38.3°C) or hypothermia (core temperature <36°C)
	Heart rate >90 beats/min
	Tachypnea
	Altered mental status
	Significant oedema or positive fluid balance (>20 ml/kg over 24 hrs)
	Hyperglycaemia (plasma glucose >7.7 mmol/L) in absence of diabetes
Inflammatory	Leukocytosis (WBC count >12,000/μl)
	Leukopenia (WBC <4000/μl)
	Normal WBC count with greater than 10% immature forms
	Plasma C-reactive protein >2 SD above the normal value
	Plasma procalcitonin >2 SD above the normal value
Haemodynamic	Arterial hypotension (SBP <90 mmHg, MAP <70 mmHg, or SBP decrease >40 mmHg in adults, or >2 SD below normal for age
Organ dysfunction	Arterial hypoxaemia (PaO$_2$/FIO$_2$ ratio < 300)
	Acute oliguria (urine output < 0.5 ml/kg/hr for at least 2 hrs despite adequate fluid resuscitation)
	Creatinine rise >0.5 mg/dl or 44.2 μmol/L
	Coagulation abnormalities (INR >1.5 or aPTT >60s)
	Ileus (absent bowel sounds)
	Thrombocytopenia (platelet count <100,000/ μ L)
	Hyperbilirubinaemia (plasma total bilirubin >4 mg/dl or 70 μmol/L)
Tissue hypoperfusion	Hyperlactataemia >1 mmol/L
	Decreased capillary refill or mottling

1.2 Global haemodynamic indices

The traditional cornerstone of resuscitation in severe sepsis is the optimization of haemodynamic variables to achieve an oxygen delivery adequate to meet metabolic needs. It is essential to recognize tissue hypoperfusion early in the disease process, as this allows timely intervention to limit organ dysfunction (Jones and Puskarich 2009). However, it is unclear what the 'ideal' cardiac output or oxygen delivery indices should be for a particular patient with sepsis, indeed, attempts to augment cardiac output and global oxygen delivery in sepsis to set endpoints have failed to show benefit (Gattinoni et al. 1995, Hayes et al. 1994).

Tissue hypoxia may develop due to impaired blood flow secondary to a low perfusion pressure. However, it is unclear to which level MAP should be increased during septic shock to improve outcomes. Targeting MAP values of 80-85 mm Hg, as compared with 65-70 mm Hg was not associated with improved survival (Asfar et al. 2014). In a *post hoc* analysis of control group data from a multicentre trial including 290 septic shock patients, MAP levels ≥70 mmHg was associated with worse outcomes, especially with augmentation of the vasopressor dose (Dunser et al. 2009). It is therefore prudent to assess blood pressure targets in the context of both flow and tissue perfusion, as patients with high lactate levels and no hypotension ('cryptic shock') may have mortality levels as high, if not higher, as patients who present with hypotension yet a normal lactate (Howell et al. 2007).

Central venous pressure (CVP) reflects the right arterial pressure and has been used for many years as an index of preload. However, the predictive value of CVP as a surrogate of preload is extensively debated, with no conclusive evidence demonstrating its reliability. A recent meta-analysis evaluating the absolute value of CVP and change (delta CVP) in predicting fluid responsiveness reported a poor predictive value for both parameters (Marik et al. 2008). Subsequent studies targeting CVP as a fluid resuscitation

target confirmed the poor correlation between CVP values and other resuscitation endpoints (Michard et al. 2000).

It therefore remains unsurprising that recent clinical trials of protocolized care guided by the above parameters have failed to demonstrate benefit (Peake et al. 2014, Yealy et al. 2014).

1.3 Microcirculation

Although the main therapies for treating sepsis are traditionally targeted at correcting macrovascular disturbances and tissue perfusion, the role of the microcirculation is becoming increasingly investigated. Patients may proceed to organ dysfunction despite correcting cardiovascular instability, possibly because microcirculatory dysfunction may lead to tissue hypoxia despite a normal or even elevated global oxygen delivery.

Patients with sepsis demonstrate a reduction in microvascular blood flow as demonstrated by sublingual microvascular visualization techniques (sidestream dark field imaging, SDF) (Spanos et al. 2010). These microcirculatory changes are more pronounced in septic non-survivors (De Backer et al. 2002). An increase in microcirculatory flow index (MFI) on initial resuscitation was associated with reduced organ failure without substantial differences in global haemodynamics, implying that the microcirculation may be a potential therapeutic target (Trzeciak et al. 2008). Following the acute early phase of sepsis when fluid resuscitation is needed, further supplementary intravenous fluid therapy has little impact on haemodynamics. (Ospina-Tascon et al. 2010).

Tissue oxygenation or, more accurately, microvascular oxygenation, may be measured non-invasively using near-infrared spectroscopy (NIRS) whereby near-infrared light can measure oxy- and deoxy-hemoglobin within the microvasculature. Measurements are usually taken on the thenar muscle or may be transcranial (Lichtenstern et al. 2012). Patients with severe sepsis have longer tissue oxygen saturation recovery times and

lower NIRS-derived local oxygen consumption values compared to healthy volunteers (Creteur et al. 2007, Doerschug et al. 2007, Skarda et al. 2007). Vasopressor administration aimed at achieving a MAP >65 mmHg in patients with septic shock was associated with an improvement of NIRS variables measured at the level of the thenar eminence (Georger et al. 2010). Further studies are required to evaluate the utility of microvascular flow indices as targets in the management of severe sepsis and septic shock.

1.4 Mitochondria

Severe sepsis is characterized by profound disturbances in global haemodynamics and organ perfusion. The traditional dogma that MODS was primarily due to tissue hypoperfusion has been undermined by the finding in resuscitated septic patients that skeletal muscle oxygen tension is elevated, suggesting oxygen availability yet a decrease in oxygen consumption (Boekstegers et al. 1991, Sair et al. 2001). Histology also remains relatively normal despite significant organ dysfunction (Hotchkiss et al. 1999, Lerolle et al. 2010).

Decreased oxygen consumption (VO_2) may represent, at least in part, an adaptive mechanism (Mongardon et al. 2009). Mitochondria, the primary consumer of O_2 within the body, can regulate metabolism though determining availability of energy substrate (i.e. ATP). A prolonged inflammatory result can result in decreased mitochondrial activity through inhibition of mitochondrial respiration by increased production of nitric oxide and other mediators (Brealey 2002). Respiratory protein subunits and transcripts are also down-regulated (Brealey et al. 2002, Carre et al. 2010). This reduction in energy availability may divert the body from its normal activities and direct its efforts towards dealing with the acute stressor of infection. However, with overwhelming inflammation, this response may become exaggerated, resulting in decompensation with organ dysfunction and, ultimately, death in many cases. A clear association was reported

between the degree of mitochondrial dysfunction, organ failure and mortality (Brealey et al. 2002).

Although the initial response to sepsis may be one of mitochondrial 'hibernation' with a reduction in O_2 utilization, the recovery phase involves a rebound increase in oxygen consumption and resting energy expenditure (Kreymann et al. 1993). This is likely to reflect the creation of new, healthy and active mitochondria (biogenesis) to meet cellular metabolic energy demands and to fulfill other roles including calcium homeostasis, maintenance of cellular redox state, and cell signaling. The onset of mitochondrial biogenesis in sepsis corresponds with the restoration of normal mitochondrial oxidative respiration (Haden et al. 2007). The course of sepsis and recovery is characterized by an increment in markers of mitochondrial biogenesis with increased mitochondrial number and density (Carchman et al. 2013).

Understanding the time course of changes in mitochondrial function in sepsis, and how these changes relate to recovery is important when considering any potential therapeutic intervention. Alterations to respiratory protein subunits and transcripts occur within the first 24 hours of admission to ICU and correlate to eventual outcome (Brealey et al. 2002). Skeletal muscle antioxidant reserves are reduced within 48 hours of admission to critical care, and are also associated with mortality risk (Carre et al. 2010).

At present, monitoring of mitochondrial function is limited to experimental work. Promising real-time *in vivo* techniques include NADH fluorometry, magnetic resonance spectroscopy (MRS) and near infrared spectroscopy (Ekbal et al. 2013). Such techniques have shown promise in animal models of different shock states and warrant further investigations in sepsis.

1.5 Immunology

Sepsis is defined as a dysregulated host response to an infection. Excessive inflammation is integral. The innate immune system is the first line defence against pathogens, and is involved in initiating and propagating inflammation. It is activated by a

series of pattern recognition receptors (PRRs) that enables discrimination of 'self' from 'non-self' antigens. PRRs recognize conserved pathogen-associated molecular patterns (PAMPs) on invading organisms, or respond to host-derived damage associated molecular patterns (DAMPs) released in response to stress, tissue injury or cell death. Several classes of PRRs have been identified, including transmembrane Toll-like receptors (TLR), C-type lectin receptors (CLRs), the retinoic acid inducible gene-I (RIG-I) receptors, intracellular Nod-like receptors (NLRs), and the recently identified HIN-200 receptors (Ferrari et al. 1997, Kahlenberg et al. 2005, Wewers and Sarkar 2009). Extracellular PAMPs and DAMPs are recognised by TLRs and CLRs, whereas NLRs and RIGs recognize intracellular molecular patterns.

PRRs are expressed primarily by innate immune cells, but also by endothelial and epithelial cells. The innate immune system is 'primed' by activation of PRRs by PAMPs and/or DAMPs, which leads to activation of numerous proinflammatory transcription factors, the best characterized being nuclear factor kappa-B (NF-κB), with subsequent transcription of multiple mediators (including cytokines and chemokines) and receptors.

An excessively dysregulated host response results in detriment to the host ('critical illness'). In many circumstances it remains unclear why some patients develop such a response to infection. Some bacterial toxins, including *Staphylococcus aureus* enterotoxin A, may result in a life-threatening 'toxic shock syndrome' secondary to non-specific polyclonal T-cell activation (Tilahun et al. 2014). However, in the vast majority of septic patients, there is no single identifiable cause. High levels of circulating plasma cytokines result in a cascade of events including enhanced neutrophil chemotaxis and phagocytic activity, increased capillary leak, complement activation, cellular stress, and activated coagulation factors, and these are associated with organ dysfunction in sepsis (Cinel and Opal 2009).

Genome-wide transcription profiling in human sepsis has demonstrated pro- and anti-inflammatory mechanisms occur concurrently (Cinel and Opal 2009). There is no distinct pro- or anti-inflammatory phase nor any clear transition point during sepsis. Most of the

research on immunomodulation in sepsis has focused on attenuating the pro-inflammatory phase. This includes the use of monoclonal antibodies against IL-1 (Opal et al. 1997) and tumor necrosis factor-α (TNF-α) (Abraham et al. 2001), TLR4 antagonists (Rice et al. 2010), inducible nitric oxide synthase (iNOS) inhibitors (Bakker et al. 2004, Lopez et al. 2004), antioxidants (Staubach et al. 1998) and modulation of the coagulation system (Ranieri et al. 2012). Despite initial promise in pre-clinical studies and early clinical studies, no immunomodulatory therapy to date has yet conclusively demonstrated any benefit in sepsis.

A significant subset of patients with critical illness do not die in the early pro-inflammatory phase of an acute infection. Ongoing immune dysfunction affecting T-cells, monocytes, and neutrophils predisposes the patient to the acquisition of nosocomial infections and subsequent renewed deterioration (Boomer et al. 2011, Conway Morris et al. 2013). There is a growing interest in immunostimulatory therapy in the latter stages of sepsis, including GM-CSF and interferon gamma, and more recently IL-7 and anti-PD1 therapy (Boomer et al. 2014). It remains likely that future immunotherapy will be individualized, guided by biomarkers of the immunological phenotype.

1.6 Animal models of sepsis

Improvements in survival over the past few decades have not been attributable to any single intervention or discovery, but have been achieved in a series of steps. Due diligence and attention to basic care is seen as a keystone in patient management.

The focus of treatment has historically been placed on the supposed benefits they provide. More recently, greater insight has been gained into the harm associated with therapies prescribed in our well-intentioned attempts to treat and cure. Aggressive diseases often require aggressive treatment, with serious side-effects perhaps being an inevitable consequence. *Primum non nocere*. As such, we are now faced with the realization that more is not necessarily better, and attempts to restore 'normal' physiology in critical illness are not necessarily logical or beneficial.

Another increasingly recognized problem area is that of long-term morbidity in survivors of critical illness. Severe muscle weakness, neuropathy, cognitive dysfunction and secondary infections are some of the long-term conditions that can afflict these patients. We are becoming ever aware of the iatrogenic contributions to such problems.

1.6.1 Adjuvant therapies

An area of sepsis research that has been highly disappointing has been the failure to develop any effective therapeutic agent for sepsis. Multiple phase II and phase III clinical trials of adjuvant therapies have been performed, ranging from specific immunomodulatory agents (such as monoclonal antibodies directed against a pro-inflammatory cytokine such as TNFalpha or IL-1), to semi-specific (e.g. activated protein C) or general anti-inflammatory therapies (e.g. corticosteroids), to extracorporeal techniques such as plasmapheresis (that non-specifically removes 'evil humours') or polymyxin B absorption columns (that binds and remove endotoxin and excess circulating inflammatory mediators). Unfortunately, none have shown consistent benefit.

Understanding the natural history of sepsis is a fundamental part of designing trials to evaluate potential therapeutic agents. Evolution has ensured that we can adapt to adverse situations, such as mounting an appropriate immunological and physiological response to survive an infection. However, if the insult is prolonged and severe, the same host response – albeit exaggerated - may have a detrimental effect. There is likely to be a complex interplay between the multiple interventions required for immediate life saving treatment and intrinsic adaptive changes. As medical interventions have evolved far quicker than biology, critical illness is no longer an adaptive state determined by evolution alone. This makes it very challenging to extrapolate findings from a simplistic animal model of sepsis to the complex clinical setting.

While many animal models of sepsis make some attempt to provide fluid resuscitation (discussed later), therapies that alter physiology and immunology including mechanical

ventilation, catecholamines, sedatives, steroids, and antibiotics are routinely used in clinical practice but rarely so in animal models of sepsis. To control for all these variables in a preclinical model would be impractical, given the number of permutations of different treatment conditions and the timing of their initiation.

1.6.2 Species differences - immunology and metabolism

Species differences clearly exist in both health and disease. The changes in gene expression profiling of leukocytes in response to three commonly studied inflammatory conditions (trauma, endotoxaemia, and burns) were compared in mice and humans (Seok et al. 2013). No correlation was seen between mouse and human genomic responses in any of the three conditions. Furthermore, although there was reasonable similarity between the genomic responses in the three inflammatory conditions among humans, this was not seen in mice. The authors concluded that their *"study supports higher priority for translational medical research to focus on the more complex human conditions rather than relying on mouse models to study human inflammatory diseases"*. While this study raises important questions, it is by no means conclusive (Perlman et al. 2013).

The circulating leukocyte pool in humans predominantly consists of neutrophils whereas that of mice predominantly consists of lymphocytes; direct comparisons may not be valid. Circulating immune cells may also be non-representative of the immune cell phenotype at the site of injury. Several genes and proteins in humans also do not have direct homologs in mice and *vice versa* (Mestas and Hughes 2004). Despite this, the genetic analysis was limited to human genes with identified murine orthologs. Some of the arguments cited against the validity of the Seok study in fact strengthen the argument that the immunophenotype of mice and humans are not directly comparable. Yet, this disparity has not hampered several important scientific discoveries.

The dose of endotoxin (lipopolysaccharide, LPS) required to induce the septic phenotype differs vastly between different species, with mice requiring several log orders more than humans (Suffredini et al. 1995) (Reynolds et al. 2002) (Nezic et al. 2009),(Taveira da Silva et al. 1993). Even non-human primates display significant differences in their immune response. Baboons and other monkey species display more resilience to LPS and live bacteria than humans (Hinshaw et al. 1981, Taylor et al. 1987). Blood cultures from septic baboons reveal bacterial counts in the range of 10^7 *E.Coli* per ml after infusion, far higher that that seen in critically ill septic patients. There are even variances in immune response across different species of mice. BALB/c mice injected with LPS were protected when pre-treated with anti-TNF sera, whereas CD-1 mice were not protected (Remick et al. 1995).

In addition to differences in mouse and human septic immunophenotypes (Mestas and Hughes 2004) there are significant differences in their metabolic profiles (Zolfaghari et al. 2013). In mice, sepsis resulted in severity-dependent reductions in core temperature and global metabolism with significant myocardial dysfunction. On the other hand, rats maintained body temperature and did not decrease their oxygen consumption.

1.6.3   Method of sepsis induction

In addition to the vastly different doses of LPS required to simulate sepsis in rodents, there are fundamental differences in the immmunophenotype of endotoxaemia compared to faecal peritonitis or pneumonia. Endotoxic animal models are characterized by hypotension, lactic acidosis, myocardial depression and elevated proinflammatory cytokines. While LPS has been used as a convenient mainstay of inducing an inflammatory phenotype, it primarily activates one arm of the immune system via TLR4. It is therefore not surprising that mice strains with different LPS sensitivity were equally susceptible to mortality from caecal ligation and puncture (CLP) (Echtenacher et al. 2001). Furthermore, the magnitude and temporal change of cytokines varies between

mice subjected to CLP or LPS, with earlier and more severe cytokine responses seen after LPS (Remick et al. 2000).

1.6.4   Fluid resuscitation

Intravenous fluid therapy is the cornerstone of resuscitation in sepsis to correct the intravascular volume depletion resulting from vasodilation and increased capillary leak (Coletta et al. 2014, Dormehl et al. 1992). Although the best type of fluid, the ideal volume, and the best means of assessing fluid status remain hotly debated, to omit fluid resuscitation in the acute phase of sepsis would be deemed clinically negligent. Despite this, several preclinical models of sepsis do not even attempt fluid resuscitation.

A systematic review of preclinical studies investigating renal blood flow (RBF) in sepsis revealed that 20 of 159 did not administer any fluid resuscitation and a further 34 did not mention whether they had done so (Langenberg et al. 2005). Sixteen of the 20 studies (80%) that did not administer fluid resuscitation demonstrated a reduction in RBF in contrast to 63 of the 106 studies (59%) where fluid was given. Nonetheless, studies specifically investigating responses with and without fluid resuscitation in the same model have shown important differences, with fluid resuscitation being associated with improved survival (Smith et al. 1993). The lack of fluid resuscitation in sepsis is associated with marked reductions in microvascular perfusion, and increased leukocyte-endothelium interactions and sequestration (Villela et al. 2014).

1.6.5   Timing of therapeutic intervention

It stands to reason that any therapeutic agent should be commenced soon after the induction of sepsis to maximize tis chances of success. However, septic patients presenting to the emergency department have invariably been unwell for some time beforehand. The exact time from onset of infection to clinical presentation is often

uncertain but may vary from hours to days. Many animal studies of putative therapeutic agents are often designed to administer the therapy before, at or soon after the time of infection/inoculation; any success is not likely to be representative of delayed therapy in a septic patient.

1.6.6   Age and co-morbidity

Sepsis primarily affects people above the age of 60 (Yealy et al. 2014), while those with pre-existing chronic co-morbidity have an age-independent increased risk of mortality (Huddle et al. 2013). Preclinical animal studies typically use mice aged 6-16 weeks, equivalent to a human age of 10-17 years (Turnbull et al. 2003). Not surprisingly, stepwise increases in mortality (20%, 70%, and 75%) were seen in more aged mice (4, 12, and 24 months, respectively) after CLP. Others have demonstrated increased sensitivity of older mice to sepsis (Hyde et al. 1990). Older mice produce more TNF-alpha, IL-6 and IL-10 (Saito et al. 2003, Turnbull et al. 2003), but benefit less from antibiotic treatment compared to young mice (Turnbull et al. 2003). Older mice also have different endothelial responses, with more extensive increase in expression of P- and E-selectin and increased polymorphonuclear cell influx (Wulfert et al. 2012). This may contribute to increased organ failure (Maddens et al. 2012).

1.6.7   Risk of death

The efficacy of any therapeutic intervention may only be evident for a given severity of illness. A drug aimed at improving survival will not demonstrate any benefit if the baseline mortality in the control arm is 0% (or too low). In contrast, when severity is so great, inhibition of an excessive inflammatory response may provide some benefit independent of the drug's mechanism of action. This was described by Eichacker *et al* in a meta-regression analysis of preclinical studies (Eichacker et al. 2002). The treatment effects of anti-inflammatory agents were highly dependent on risk of death ($p = 0.0001$), with

animals being studied at significantly higher control mortality rates than humans (88% vs. 39%, p = 0.0001) Anti-inflammatory agents studied in animal models with a similar risk of death to clinical studies demonstrated lack of benefit. Additionally, among the clinical trials included in the analysis, patients at greatest risk of death were most likely to benefit, whereas harm was seen following treatment in patients at low risk of death. Targeting treatment at a heterogeneous population may mask benefits seen within a specific subgroup of patients.

To stand the best chance of successful translation of preclinical studies to clinical utility, preclinical studies need to be rigorously designed. However, it may not be pragmatic to overcome all of the limitations highlighted, and the results of preclinical studies need to be interpreted in context of the limitations of the experimental model used.

2 Sepsis induced acute kidney injury

2.1 Epidemiology and definitions

Acute kidney injury (AKI) is a common problem associated with a significant human and financial cost. The annual incidence varies from 17-620 per million in adults <60 and 80-89 years, respectively (Pisoni et al. 2008). Although AKI accounts for just 1% of hospital admissions in the USA, the incidence of in-patient AKI is estimated at 5-7% (Lameire et al. 2006). Within the intensive care unit (ICU) up to 5% of critically ill patients require renal replacement therapy (RRT) (Bagshaw et al. 2005, Uchino et al. 2005), and sepsis is implicated in half the cases of AKI (Uchino et al. 2005).

Historically, AKI has been variously defined, resulting in marked variations in quoted rates of incidence and associated mortality from AKI (Ricci et al. 2006). To unify definitions, the Acute Dialysis Quality Initiative (ADQI) created the Risk-Injury-Failure-Loss-Endstage (RIFLE) criteria to diagnose and severity-stratify AKI (Appendix) (Bellomo et al. 2004). The RIFLE criteria uses urine output and either a rise in serum creatinine or fall in estimated glomerular filtration rate (eGFR) to define AKI. The Acute Kidney Injury Network (AKIN) modified the RIFLE criteria to further refine the AKI definition (Appendix) (Mehta et al. 2007). Most recently, the Kidney Disease: Improving Global Outcomes (KDIGO) group amalgamated the RIFLE and AKIN criteria, staging AKI severity on serum creatinine and urine output (KDIGO 2012). Though not intended to prognosticate for individuals, it does allow within-study comparisons. Importantly, these criteria are not designed to address aetiologies nor pathophysiological processes underlying AKI.

Table 2 KDIGO staging of AKI

Stage	Serum Creatinine	Urine output
1	1.5- 1.9 times baseline OR ≥0.3mg/dl (≥26.5 μmol/l) rise	<0.5 ml/kg/h for 6-12 h
2	2.0 – 2.9 times baseline	<0.5 ml/kg/h for ≥12h
3	3.0 times baseline OR Rise in serum creatinine >4 mg/dl (>353.6 μmol/l) OR Initiation of renal replacement therapy, OR In patients <18 years, decrease in eGFR to <35 ml/min per 1.73m^2	<0.3 ml/kg/h for ≥24h, OR anuria for ≥12h

The impact of AKI on immediate and long- term morbidity, mortality and financial resources is significant. Hospital mortality increases from RIFLE category R (17.9%) to F (33.2%) (Bagshaw et al. 2008), and the relative risk (RR) of mortality among patients with or without AKI increases progressively from Risk (RR=2.40), to Injury (RR=4.15), to Failure (RR=6.37) (Ricci et al. 2008). Five year survival in ICU patients who leave hospital following AKI was reported as 65-70% (Bagshaw 2006). Approximately 1 in 5 patients who requires RRT has residual renal impairment at 1 year (Bagshaw et al. 2005), while progression to CKD is related to AKI severity (Chawla et al. 2011). The estimated cost per quality-adjusted life-year saved by initiating dialysis and continuing care is $128,200 (Hamel et al. 1997). Despite the relative frequency of the condition and its impact on morbidity and mortality, therapy is limited to supportive measures. This relates in part to the continued lack of understanding of the pathophysiology of sepsis-induced AKI.

2.2 Serum creatinine and urine output

Glomerular filtration rate (GFR) is widely accepted as a marker of renal function but it is impractical to measure GFR routinely. Serum creatinine is used as a surrogate of GFR as creatinine is freely and non-selectively filtered by the kidneys. While serum creatinine may be a pragmatic tool to estimate GFR during stable renal function, there are significant limitations with its use in the diagnosis and monitoring of AKI:

1. A rise in serum creatinine is a relatively insensitive marker of early AKI as it may occur only after appreciable structural damage (Ronco and Rosner 2012). This may also explain why small rises in serum creatinine (26.5 μmol/l) are associated with increased mortality (Chertow et al. 2005).

2. Assuming the rate of creatinine production remains constant, intravenous fluid therapy may have a dilutional effect so a fall in GFR measured by a rise in serum creatinine may not be evident for several hours (Waikar and Bonventre 2009).

3. Creatinine production may fall in early sepsis, so concurrent reductions in GFR may not be evident (Doi et al. 2009). Creatinine is produced from creatine by non-enzymatic cyclization. This occurs throughout the body but especially in muscles where creatine concentrations are high. Creatine production itself occurs in the liver (Cocchetto et al. 1983). Creatinine production can therefore fall as lean muscle mass falls, or during liver disease; both of which are commonplace in the critically ill.

4. Creatinine kinetics depend upon the baseline creatinine value. The percentage change in serum creatinine after severe AKI is highly dependent upon baseline kidney function (Waikar and Bonventre 2009).

5. The modification of diet in renal disease (MDRD) formula used to calculate estimated GFR (eGFR) was designed for use in a population with stable GFR. GFR is not linearly associated with serum creatinine and estimation of GFR using this formula is less accurate at extreme values of serum creatinine (Levey et al. 1999, Levey et al. 2006). The CKD-epi formula (Levey et al. 2009) also performs poorly when estimating GFR in patients with AKI, with high biases and errors (Kirwan et al. 2013).

Creatinine clearance (CrCl) has been used as a measure of 'nephron number' with stable GFR. However, there are confounders to interpretation of CrCl in acute illness.

1. CrCl systematically overestimates actual GFR due to tubular creatinine secretion.

2. The method itself is prone to large inherent variation between serial measurements (Bragadottir et al. 2013) and may be unreliable in the critically ill (Bouchard et al. 2010).

3. CrCl as a measure of GFR assumes stable creatinine production and volume of distribution, both which may be altered in sepsis.

4. Creatinine clearance may be stable despite tubular injury.

The use of urine output to define AKI also has a number of limitations:

1. Oliguria does not always result in renal injury as defined by a change in serum creatinine. Oliguria may occur more frequently compared to the number of patients developing AKI as defined by the change in serum creatinine (Prowle et al. 2011).

2. A fall in urine output may occur only after significant renal injury

3. Urine output may not fall despite clinically significant changes in serum creatinine

4. Urine output may be modified by diuretic use

5. Urine output prior to ICU admission is not always recorded

Despite these limitations, the use of oliguria in addition to a rise in serum creatinine significantly improves the predictive value for mortality (Ricci et al. 2008).

2.3 Histology

As renal biopsies are rarely performed in critically ill septic patients with AKI, there is a relative paucity of histological data to aid understanding of the mechanisms underlying septic AKI at the tissue level. Only a few studies have been performed in humans (Rosenberg et al. 1971, Zappacosta and Ashby 1977), some being post-mortem (Diaz de Leon et al. 2006, Hotchkiss et al. 1999, Sato et al. 1978), or from biopsies performed a few days after the onset of AKI (Diaz de Leon et al. 2006). These findings were described in a systematic review of renal histopathology in septic AKI (Langenberg et al. 2008) in which marked heterogeneity was demonstrated. Acute tubular necrosis (ATN) was demonstrated in only 22% of renal histopathological specimens, with other findings

including acute tubulointerstitial nephropathy, acute glomerulonephritis, and completely normal histology in some cases These studies suggest that ATN is not the predominant histological feature in septic AKI, and that other mechanisms occur.

A more recent study has shed additional light on renal histopathological changes seen during septic AKI (Lerolle et al. 2010). Percutaneous renal biopsies were performed in 19 patients with septic AKI within 30 minutes of their death. As a control group, 9 patients without severe AKI who died from causes other than septic shock were biopsied. Compared to the control group, the patients who died from septic AKI had significantly greater renal monocyte/macrophage infiltration, polymorphonuclear leucocyte infiltration, and tubular apoptotic bodies, suggesting that immunological mechanisms may operate in addition to haemodynamic insults. As the degree of tubular cell injury is disproportionately low compared to functional impairment (Langenberg et al. 2008, Lerolle et al. 2010, Lipcsey and Bellomo 2011, Takasu et al. 2013), oliguria may reflect adaptive mechanisms during critical illness.

2.4 Renal blood flow

The haemodynamic instability associated with sepsis has led to the dogma that sepsis-induced AKI is primarily a consequence of renal ischaemia and ensuing acute tubular necrosis (ATN) (Schrier and Wang 2004). Profound and rapid alterations in blood pressure and regional blood flow during septic shock may lead to loss of autoregulatory ability of the kidneys, renal hypoperfusion, and ischaemia. The lack of an accurate non-invasive method to measure renal blood flow (RBF) on the ICU has limited our understanding. Early studies using indwelling renal vein catheters to measure renal blood flow in septic patients with AKI revealed preserved or even elevated RBF (Brenner et al. 1990, Lucas et al. 1973, Rector et al. 1973). Recent experimental work has confirmed this. Renal blood flow may change over time, with an early rise in response to an infusion of *E. Coli* (Wan et al. 2009). A three-fold increase in both CO and RBF occurred during experimental sepsis in ewes (Langenberg et al. 2006), the decrease in renal vascular resistance being proportional to the increase in RBF. A recent systematic review of 159

animal studies suggested that interpretation of experimental data should be viewed in the light of potential confounding factors, including the method of sepsis induction, the animal's size, consciousness level, time of measurement, use of fluid resuscitation, and systemic haemodynamics (Langenberg et al. 2005).

Glomerular filtration rate (GFR) and creatinine clearance are dependent on filtration pressure, which is partly dependent on RBF. GFR is also indirectly dependent on tubular cell function via feedback mechanisms (tubular glomerular feedback; TGF). Despite an increase in global RBF, a reduction in glomerular filtration pressure may occur as a result of efferent renal artery vasodilatation or afferent artery vasoconstriction (renal microcirculation). The reduction in urine output and rise in serum creatinine commonly seen in critically ill septic patients may therefore occur despite normal or elevated global renal blood flow. In fact, oliguria may occur in the presence of adequate glomerular filtration and intact tubular function as tubular cells may effectively reabsorb filtered plasma. Experimental models of sepsis have confirmed that creatinine clearance and RBF may not correlate (Prowle et al. 2012, Wan et al. 2009). Oliguria may occur with a fall in creatinine clearance despite an increase in RBF during sepsis (Langenberg et al. 2007). This suggests that changes in intra-renal circulation subsequent to modification in efferent arteriolar function and intra-renal shunting are much more likely to be responsible for septic AKI (Wan et al. 2009) than a global reduction in RBF.

2.5 Renal Microcirculation

Renal microvascular dysfunction has been characterized in preclinical models by a decrease in those vessels with continuous flow and an increase in vessels with intermittent or no flow (Holthoff et al. 2012, Seely et al. 2011, Tiwari et al. 2005). These changes are heterogeneous and may result in areas of hypoxia and normoxia, possibly explaining the patchy and sporadic histological changes. It is unclear if regions of hypoxia result in shutdown of cellular metabolism in an attempt to preserve cellular integrity

('oxygen conformance'), a phenomenon described in hepatocytes (Schumacker et al. 1993, Subramanian et al. 2007). This may explain the loss of function with relatively well-preserved histology.

Inducible nitric oxide synthase (iNOS) has been implicated in sepsis-induced renal microcirculatory dysfunction. Activation of iNOS by LPS increases the influence of nitric oxide on afferent and efferent arteriolar tone and impairs endothelium-dependent nitric oxide effects (Ichihara et al. 2000). Increased renal nitric oxide (NO) in sepsis may contribute to the heterogeneous microcirculation by shunting. Inhibition of iNOS improved renal microcirculatory dysfunction in experimental sepsis (Wu et al. 2007, Wu and Mayeux 2007).

Intra-renal shunting mediated by angiotensin may explain the findings of decreased renal vascular resistance and increased RBF yet oliguria and decreased creatinine clearance in fluid-resuscitated endotoxaemic sheep (Langenberg et al. 2007). Dilatation of the efferent artery relative to the afferent artery, thus decreasing filtration pressure and reducing GFR and urine output was considered a likely explanation. To test this hypothesis, they administered the potent vasoconstrictor, angiotensin II, to septic animals (Wan et al. 2009).. This drug has a preferential action on the efferent arteriole (Denton et al. 2000), whereas norepinephrine acts on both afferent and efferent arterioles (Myers et al. 1975). Angiotensin II also has constrictor effects on glomerular mesangial cells (Ausiello et al. 1980). Angiotensin II administration restored systemic arterial pressure but reduced global renal blood flow. Despite this, urine output and creatinine clearance increased significantly This observation is unlikely to be explained by the increase in MAP, as norepinephrine produced similar increments but had a less profound effect on creatinine clearance (Di Giantomasso et al. 2005, Di Giantomasso et al. 2003).

Consistent with these experimental data, a *post hoc* analysis of the VASST study revealed that use of vasopressin (compared to norepinephrine alone) was associated with a trend to a lower rate of progression of AKI from RIFLE stage R to stage F or L, a lower rate of use of renal replacement therapy, and a trend towards lower mortality in

patients in the "Risk" category (Gordon et al. 2010). The mechanism underlying the relative reduction in glomerular filtration pressure is unlikely to be due to an absolute deficiency of circulating vasopressin, as vasopressin levels are often elevated, at least in the early stages, in patients with septic shock (Sharshar et al. 2003). Reduced sensitivity of vasopressin receptors due to circulating pro-inflammatory cytokines or impaired vasopressin release due to high circulating levels of noradrenaline may account for this (Bucher et al. 2002, Day et al. 1985). Local mechanisms may operate concurrently to regulate GFR (i.e.: tubular glomerular feedback).

2.6 Tubular glomerular feedback

Tubular glomerular feedback (TGF) enables the kidney to regulate GFR in accordance to the capacity of the renal proximal tubular epithelial cell (PTEC) at the level of the individual nephron. TGF allows compensatory reductions in GFR and thus tubular workload. TGF is a negative feedback mechanism that senses changes in luminal chloride (Cl^-) delivery and reabsorption at the macula densa in the juxtaglomerular apparatus (JGA) and adjusts the vascular tone of the afferent arteriole accordingly (Schnermann et al. 1973).

During states of hypovolaemia, RBF and perfusion fall. A decrease in renal perfusion pressure results in a decrease in GFR. Proximal tubular cells then reabsorb a greater proportion of filtered solute via the epithelial sodium channel, ENaC, resulting in decreased macula densa NaCl delivery (Salomonsson et al. 1993). The macula densa apical Na-K-2Cl (NKCC2) co-transporter senses this reduction in NaCl delivery (Vallon 2003) with resulting renin release and activation of the renin-angiotensin system (Salomonsson et al. 1993). Increased angiotensin results in increased efferent arteriolar vasoconstriction relative to the afferent arteriole. The net effect is to maintain GFR to counter the decrease in renal perfusion pressure.

In addition to Cl⁻ delivery to the macula densa, renal interstitial adenosine is a potent regulator of GFR. (Le Hir and Kaissling 1993). Extracellular adenosine activates A1 receptors on vascular afferent arteriolar smooth muscle cells, resulting in vasoconstriction and a reduction in GFR (Schnermann et al. 1990). Renal adenosine concentrations are elevated in response to local ischaemia or endotoxic shock (Beach et al. 1991, Miller et al. 1978, Nishiyama et al. 1999). Antagonism of the A1 receptor attenuated reductions in MAP and RBF, suggesting that adenosine may mediate renal haemodynamic changes during endotoxin shock (Nishiyama et al. 1999).

Adenosine may also modulate immune function via A2 receptors on antigen presenting cells (APCs) and lymphocytes. A2 receptor activation results in diminished phagocytosis, anti-inflammatory cytokine production, and lymphocyte apoptosis. In a CLP model of sepsis selective A2 receptor antagonism reduced lymphocyte apoptosis, lowered IL-6 and IL-10 levels, and improved survival (Nemeth et al. 2006). Major actions of adenosine are summarized in (Figure 1).
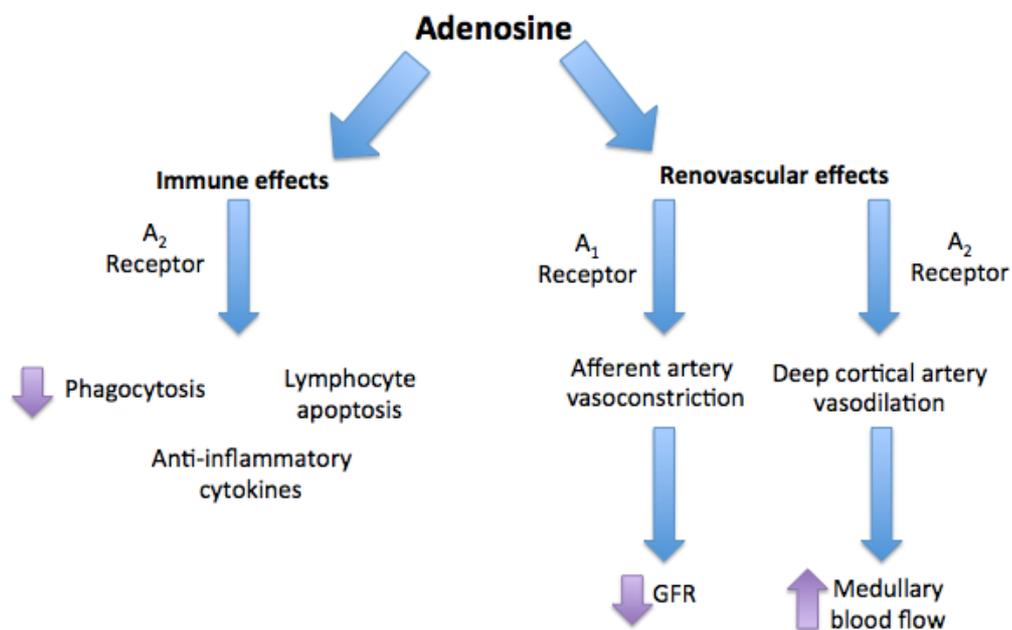
Figure 1 Major actions of adenosine are mediated via the A1 and A2 receptors. The main actions of adenosine are on immune function and vascular function. Adenosine results in

an anti-inflammatory phenotype, with decreased phagocytosis and anti-inflammatory cytokine production. In addition to systemic hypotension, adenosine results in a fall in GFR via afferent arteriolar constriction whilst maintaining deep cortical and medullary blood flow via A2 receptors.

2.7 Bioenergetics and mitochondria

The majority of renal ATP utilization is within the PTECs to enable reabsorption of filtered plasma solutes and water. The increased density of mitochondria within PTECs reflects the high metabolic demand of these cells (Hall et al. 2009). Given the paucity of histological damage and cell death in septic AKI, it is unlikely that any reduction in metabolism/function is a consequent to a significant and persisting fall in oxygenation. It is a reasonable assumption that PTEC workload and energy demand will be lowered by a reduction in GFR, and that local mediators may also play a role in the 'metabolic shutdown'.

Experimental studies investigating changes in renal oxidative phosphorylation during sepsis and endotoxaemia report variable results. Some demonstrated a reduction in renal oxidative phosphorylation (Tran et al. 2011), increased glycolysis (Smith et al. 2014) and decreased fatty acid oxidation (Kozlov et al. 2010). Even in the presence of hypotension and decreased RBF, total renal ATP and ATP/inorganic phosphate ratio remained unchanged during hyperdynamic sepsis implying a matched decrease in both oxygen supply and demand (May et al. 2007). Other investigators however found no difference in renal mitochondrial oxidative phosphorylation (Porta et al. 2006), renal gluconeogenesis (Caton et al. 2009), or state 3 or 4 respiratory control indices (Garrison et al. 1982). These differences may relate to the marked heterogeneity of the experimental and measurement techniques, the type and degree of the septic insult, the use of different species, duration, fluid resuscitation, etc

2.8 Immunology and Inflammation

Damage associated molecular patterns (DAMPs) and pathogen associated molecular patterns (PAMPs) result in inflammasome activation, chemokine release and immune cell infiltration. Intrinsic renal cells, especially tubular epithelial cells, express components of the inflammasome pathway, including TLRs (El-Achkar et al. 2006, Wolfs et al. 2002) that are upregulated in sepsis. Renal tubular epithelial cells produce various proinflammatory cytokines and chemokines, e.g. IL-6, IL-18 and monocyte chemotactic protein (MCP-1) (de Haij et al. 2002).

The kidney also contains resident antigen presenting cells (dendritic cells and macrophages) that modulate the local immune response to DAMPs and PAMPs filtered from the circulation (Rogers et al. 2014). The roles of resident immune cells include cell recruitment, regeneration and repair, and fibrosis. Resident renal macrophages assume a proinflammatory M1 phenotype (classically activated) or an anti-inflammatory M2 phenotype (alternatively activated) (Rees 2010) depending on the local environment. In the early stages of sepsis, resident macrophages and dendritic cells may have important pro-inflammatory roles in antigen presentation and phagocytosis. During the resolution phase of sepsis, renal macrophages may play a different role. Endotoxin exposure confers renal protection from subsequent damage (preconditioning), mediated via the anti-inflammatory (M2) effect of renal macrophages (Hato et al. 2014). In renal tubules, preconditioning resulted in increased macrophage number and trafficking within the kidney, clustering of macrophages around S1 proximal tubules, and amelioration of peroxisomal damage, oxidative stress and injury to S2 and S3 tubules.

TLR4 receptors may have an adaptive role in sepsis induced-AKI by internalizing filtered endotoxin through fluid-phase endocytosis (Kalakeche et al. 2011). MD2 and CD14, important co-effectors that participate in endotoxin-induced stimulation of TLR4, are detected in isolated murine tubular epithelial cells (Tsuboi et al. 2002). The levels of the soluble form of CD14 are increased in the urine of patients with sepsis and inflammation (Bussolati et al. 2002). S1 segments have evolved a protective mechanism of

upregulation of cytoprotective heme oxygenase-1 and sirtuin-1 (SIRT1) and showed no oxidative stress. In contrast, S2 segments did not upregulate SIRT1 and exhibited severe structural and functional peroxisomal damage (Kalakeche et al. 2011).

Studies investigating the expression and activity of channels responsible for solute reabsorption are downregulated during inflammation. TNF-α downregulates the renal Na^+-K^+ pump and the Na^+-K^+2Cl^- cotransporter *in vivo* (Kreydiyyeh and Markossian 2006), while IL-1β inhibited, in a dose-dependent manner, Na^+/K^+-ATPase activity in both medullary and cortical renal cells (Kreydiyyeh and Al-Sadi 2002). LPS significantly downregulated ion transporters including the Na^+/H^+ exchanger 3 (NHE3), Na^+/K^+-ATPase, renal outer medullary K^+ channel (ROMK), epithelial Na^+ channel (ENaC), Na^+–$K^+,2Cl^-$-cotransporter 2 (NKCC2), Na^+–Cl^--cotransporter (NCC), and kidney-specific chloride channels -1 and -2 (CLCK-1 and -2) (Olesen et al. 2009, Schmidt et al. 2007). This effect was also seen in mice given lower doses of LPS where blood pressure was maintained. Similar effects were seen with injection of pro-inflammatory cytokines (IL-1β, TNF-α, INF-γ), and ischaemia-reperfusion injury but not with hypoperfusion (Schmidt et al. 2007). Alteration of renal sodium transporters during LPS-induced AKI thus appears mediated by cytokines rather than ischaemia. Of note, studies using knockout (KO) mice for TNF-α, IL-1β, and INF-γ show that even in the absence of these cytokines, renal tubular epithelial cells can still down-regulate ion transport channels in response to LPS. This suggests that multiple pathways are present (Schmidt et al. 2007).

In sepsis and ischaemia, downregulation of sodium channel transporters such as ENaC decreases tubular reabsorption and therefore may reduce the metabolic demand of the kidney. Polyuria (due to decreased sodium and water reabsorption in the proximal collecting tubule) would be prevented by increased distal tubular Cl^- delivery, which, has the direct effect of decreasing GFR (TGF) (Wilcox 1983).

2.9 Renal biomarkers

A biomarker is a "*characteristic that is objectively measured and evaluated as an indicator of normal biological processes, pathogenic processes, or pharmacologic responses to a therapeutic intervention*" (Biomarkers Definitions Working 2001). Unlike traditional risk factors, biomarkers may provide a real-time picture of the underlying process- in addition to improving the diagnostic accuracy.

As discussed, serum creatinine has several limitations as a biomarker for AKI. Serum creatinine rises late and it is relatively insensitive - even a relatively small rise is related to a worse prognosis (Tian et al. 2009). The ability to intervene early in the course of AKI may alter prognosis (Schrier 2004). Several biomarkers have been investigated as potential candidates for the diagnosis and monitoring of AKI.

2.9.1 Neutrophil gelatinase-associated lipocalin

Neutrophil gelatinase-associated lipocalin (NGAL) was first identified as a 25kDa protein found within granules of human neutrophils (Kjeldsen et al. 1993). It is released into the bloodstream in response to bacterial infections (Xu et al. 1994). Bacteria produce siderophores to acquire iron for growth. NGAL can bind to these siderophores, thereby preventing bacterial growth (Goetz et al. 2002). The presence of NGAL was subsequently described in epithelial cells of other tissues, including lung, colon, stomach, and kidneys (Cowland and Borregaard 1997). NGAL was first described as a biomarker for ischaemic AKI (Mishra et al. 2003). NGAL may facilitate repair and regeneration processes in injured tubular cells by inducing differentiation of renal progenitor cells (Mori et al. 2005).

Its monomeric (25kD) form is the predominant form secreted by tubular epithelial cells, while the dimeric (45kD) form is predominantly secreted by neutrophils. NGAL is covalently conjugated with gelatinase (matrix metalloproteinase 9) as a 135-kD heterodimeric form (Cai et al. 2010). NGAL is dependent on renal clearance and undergoes glomerular filtration due to its low molecular weight and positive charge.

Filtered NGAL is captured and degraded to a 14-kDa fragment in PTEC lysosomes (Hvidberg et al. 2005).

A recent systematic review of NGAL as a biomarker of AKI (Hjortrup et al. 2013).included 11 studies with a total of 2,875 participants. The heterogeneity in study design and results made it difficult to evaluate the value of NGAL to predict AKI in critically ill patients (area under the receiver operated characteristic curve (AuROC) ranged from 0.54 to 0.98). Reasons cited included variations in study design, period from NGAL sampling to AKI follow-up (12 hours to 7 days), definition of baseline creatinine value, and urinary NGAL quantification method (normalizing to urinary creatinine or absolute concentration).

2.9.2 Interleukin-18

Mononuclear cells, macrophages and non-immune cells including proximal tubule cells, produce interleukin-18 (IL-18). IL-18 is a member of the IL-1 cytokine superfamily with a molecular weight of 18kDa. IL-18 has a major role in the Th1 response by stimulating the production of interferon-γ from T-cells and natural killer cells. Fas ligand-mediated cell death is also IL-18-dependent (Dao et al. 1996, Zhang et al. 2011). Mesangial cells express IL-18, and this increased significantly after LPS (Hardy et al. 2010). IL-18 is also expressed *de novo* within the distal convoluted and the connecting tubule and parts of the collecting duct (Gauer et al. 2007).

In a meta-analysis of 18 studies the odds ratio for urinary IL-18 to predict AKI was 4.22, with sensitivity and specificity of 0.58 and 0.75, respectively, and an AUROC of 0.70. IL-18 had better diagnostic accuracy in children and adolescents and also had better predictive value in cardiac surgical compared to general ICU patients. There was no significant difference in predictive performance of urinary IL-18 at various sampling times (Liu et al. 2013).

2.9.3 Kidney injury molecule -1

Kidney injury molecule -1 (KIM-1) is a 90kDa type I membrane glycoprotein (Ichimura et al. 1998) expressed on non-differentiated renal PTEC undergoing regeneration after toxic or ischaemic injury (Bailly et al. 2002). Its structural homology to several known adhesion proteins points to a possible role in cell adhesion during regeneration.

A recent meta-analysis of KIM-1 in a heterogeneous cohort of intensive care patients incorporated 2979 patients from 11 studies (Shao et al. 2014). This revealed that the sensitivity of urinary KIM-1 for the diagnosis of AKI was 0.74. (95% CI, 0.61-0.84), and specificity was 0.86 (95% CI, 0.74 -0.93%). Subgroup analysis suggested that population settings and detection time were the key factors affecting the efficiency of KIM-1 for AKI diagnosis

2.9.4 Cystatin C

Cystatin C is a 13kDa proteinase inhibitor produced by most nucleated cells. In humans, cystatins are the most important endogenous inhibitor of cysteine proteinases (Brzin et al. 1984). Due to its small size, it is freely filtered in the urine. Once filtered, it is reabsorbed and degraded in the renal proximal tubule by the endocytic receptor, megalin (Kaseda et al. 2007). Urine cystatin C levels increase when the reabsorptive capacity of the proximal tubule is exceeded. Urine cystatin C is therefore undetectable unless proximal tubular dysfunction is present. Microalbuminuria may increase levels of urine cystatin C as cystatin C absorption is reduced by competitive inhibition (Nejat et al. 2012). Serum cystatin C is dependent on GFR and may be a useful marker in critical illness as it is independent of muscle mass.

In a meta-analysis of studies involving intensive care patients (Zhang et al. 2011)., the estimated sensitivity and specificity of serum cystatin C for the diagnosis of AKI was 0.86 and 0.82 respectively, with an AuROC of 0.87. Urinary cystatin C excretion had sensitivity and specificity values of 0.61 and 0.67, respectively with an AuROC of 0.67 (95% CI

0.63-0.71) in predicting AKI. Some studies suggested that urine cystatin C may be an earlier and more sensitive marker of AKI compared to serum cystatin C (Sasaki et al. 2011, Togashi et al. 2012). This may relate to the timing of measurement as it was of less value after 24 hours of ICU admission (Zhang et al. 2011).

2.9.5   Clusterin

Clusterin is a secreted glycoprotein with cytoprotective functions. PTEC clusterin expression in renal ischaemia reperfusion injury (IRI) is associated with upregulation of genes that may induce cell cycle progression and DNA damage repair, promoting cell proliferation (Nguan et al. 2014). Absence of clusterin renders mice susceptible to IRI (Zhou et al. 2010). Urine clusterin was elevated in experimental drug-induced AKI (Zhou et al. 2014) The utility of urine clusterin has not been investigated in sepsis-induced AKI.

2.9.6   Osteopontin

Osteopontin (OPN) is an extracellular structural protein present predominantly in bone and epithelial tissues. Within the normal kidney, OPN is mainly present in the loop of Henle and distal nephrons (Xie et al. 2001). Its intimate role in the regulation of calcification is crucial for the prevention of calcium stone formation within the kidney (Wesson et al. 2003). However, OPN may be upregulated in response to a number of insults including renal ischaemia, lupus nephritis, and ureteric obstruction (Xie et al. 2001). OPN has been found in tissues with high cell turnover suggesting a possible role in tissue remodeling and repair (Persy et al. 1999).

OPN is present to lesser degrees in macrophages, activated T cells, and smooth muscle cells (Mazzali et al. 2002). It is integral for macrophage migration into sites of inflammation, and T cell chemotaxis and co-stimulation (Giachelli et al. 1998, O'Regan et al. 1999). OPN expression correlates with the degree of macrophage infiltration in various models of acute and chronic kidney injury (Panzer et al. 2001, Pichler et al. 1995).

Causality has been shown by administering anti-OPN neutralizing antibodies that reduced macrophage recruitment (Panzer et al. 2001, Yu et al. 1998). OPN also has a direct effect on renal tubular cells by inhibition of iNOS and promotion of survival in renal tubular epithelial cells (Hwang et al. 1994, Ophascharoensuk et al. 1999). In a model of gentamicin-induced AKI, OPN was related to the proliferation and regeneration of tubular epithelial cells after tubular damage (Xie et al. 2001). In a model of IRI, differences were seen in the distribution of OPN in PTECs and distal tubular epithelial cells (DTECs). DTECs showed an early and persistent increase in OPN staining in the absence of major morphological injury, whereas staining in PTECs was delayed and mostly associated with morphological regeneration (Persy et al. 1999). Osteopontin promoted early interstitial macrophage influx, proximal tubular cell survival, and interstitial fibrosis in a mouse model of unilateral ureteral obstruction (Ophascharoensuk et al. 1999).

The functional significance of these changes in sepsis is unclear, although it seems reasonable that OPN may promote recovery mediated via modulation of infiltrating cells and local responses by the proximal tubular epithelial cell. The utility of urine OPN as a biomarker in sepsis-induced AKI has not been previously investigated.

2.9.7 Calbindin

Calbindin-D28k is a cytoplasmic calcium-binding protein with high affinity for calcium. Renal calbindin-D28k is localized in the distal tubule and the proximal part of the collecting ducts. Functionally, it is thought to be involved in the regulation of reabsorption of calcium and possibly magnesium in the distal nephron. Urine calbindin was elevated in subacute drug-induced nephrotoxicity (Hoffmann et al. 2010). Its utility as a biomarker in sepsis-induced AKI has not been previously investigated.

2.9.8 Monocyte chemoattractant protein -1

Monocyte chemotactic protein-1 (MCP-1), also known as C-C motif ligand 2 (CCL2) is a 13kDa chemokine that recruits monocytes, dendritic cells and T cells into sites of

inflammation (Carr et al. 1994, Xu et al. 1996). MCP-1 is detectable in the urine in various aetiologies of AKI including maleate-induced AKI (Munshi et al. 2011), and vasculitis (Ohlsson et al. 2009, Tam et al. 2004). Urine MCP-1 was elevated in a small subset of 5 patients with septic AKI (Munshi et al. 2011). Patients with urosepsis had elevated levels of MCP-1 on diagnosis, and levels fell with initiation of treatment and clinical recovery (Olszyna et al. 1999). To date, there has not been any study of urine MCP-1 as a biomarker of sepsis-induced AKI.

2.9.9   Limitation of biomarkers

Multiple studies emphasize the potential benefit of one biomarker over another. Most have focused on demonstrating that kidney biomarkers appear at earlier time points than serum creatinine. The current non-utilization of current biomarkers may be due to: (Murray et al. 2014):

1. poor integration with creatinine and urine output to enhance AKI management

2. many emerging biomarkers with different test characteristics (in serum and urine). Standardization of the multiple methods and platforms for measuring assay ranges, levels and thresholds exist is required

3. predictive models relating biomarker values to clinical outcomes on a continuous scale may enhance the practicality of biomarker measurements

Specific clinical recommendations for applying these emerging biomarkers to optimize patient management are required. A kidney biomarker panel may prove to be more useful (Martensson et al. 2012), while specific treatment algorithms in response to elevated biomarkers need to be validated. Depending on the time of measurement, different AKI biomarkers had different predictive values for RRT requirement and mortality (Endre et al. 2011). There is still no clear understanding of the time course of AKI biomarkers.

3 The Inflammasome

3.1 The Inflammasome

The innate immune system plays a crucial role in mediating the initial host response to infection by recognizing 'danger signals', including 'pathogen- associated molecular patterns (PAMPS) and 'damage- associated molecular patterns (DAMPS) (Thijs and Hack 1995). PAMPs and DAMPs bind to host cell pattern recognition receptors (PRRs) which exist in the extracellular and intracellular compartments. Activation of PRRs result in initiation of the inflammatory cascade, including cytokine production.

A key mechanism responsible for the post-transcriptional processing and release of mature cytokines is formation of the inflammasome complex. The inflammasome is a multiprotein cytosolic complex that oligomerizes to provide a platform for processing and release of cytokines such as IL-β and IL-18 via direct activation of caspase-1 (Strowig et al. 2012). The human genome encodes 23 NLR proteins broadly divided into NLRP (with a pyrin domain) and NLRC (with a caspase recruitment domain), a subset of which is capable of forming an inflammasome complex. Seven cytoplasmic receptors form an inflammasome complex: NLRP1 (NLR family, pyrin domain containing 1, NALP1), NLRP3 (also called NALP3 or cryopyrin), NLRP6, NLRP12, NLRC4 (NLR family, caspase recruitment domain (CARD) containing 4, also called IPAF), AIM2 (absent in melanoma-2) and RIG-1 (retinoic acid inducible gene 1). Of these receptors, the NLRP3 inflammasome is the best characterized.

3.2 NLRP3 inflammasome

This large mulltiprotein complex (>700KDa) forms in response to diverse PAMPs including lipopolysaccharide (LPS), peptidoglycan, bacterial DNA, viral RNA and fungi, and DAMPs such as monosodium urate crystals (MSU), calcium pyrophosphate

dehydrate, cholesterol crystals, amyloid β, hyaluronan and, possibly, glucose (Ferrari et al. 1997) (Table 3)

Table 3 Activators of the inflammasome

Sterile activators		Pathogen activators (PAMPS)			
DAMPs	**Environment derived**	**Bacteria derived**	**Virus-derived**	**Fungus - derived**	**Protozoa-derived**
ATP Cholesterol crystals MSU/CPPD crystals Amyloid β Hyaluronian	Alum Asbestos Silica Alloy particles UV radiation Skin irritants	Pore-forming toxins Lethal toxin Flagellin/rod proteins MDP RNA DNA	RNA M2 protein	β-glucans Hyphae Mannan Zymosan	Hemozoin

Abbreviations: CPPD, calcium pyrophosphate dehydrate; DAMP, danger-associated molecular pattern; MDP, muramyl dipeptide; MSU, monosodium urate; PAMP, pathogen associated molecular pattern

Activators of the inflammasome are divided into two categories: sterile activators include host-derived DAMPs and environment-derived molecules, and pathogen activators including PAMPs derived from bacteria, virus, fungi and protozoa.

Priming of the cell (signal 1) by activation of PRRs results in NFκB-dependent transcription of pro-IL-1β and upregulation of NLRP3. Assembly of the NLRP3 inflammasome relies on the adaptor molecule ASC (Apoptosis-associated Speck-like protein containing a C-terminal caspase recruitment domain (CARD)). The ASC protein is composed of PYD (N-terminal pyrin domain) and CARD domains. The N-terminus of NLRP3 also contains a PYD that mediates homotypic binding with ASC via a PYD-PYD interaction. Through its CARD, ASC interacts with procaspase-1 leading to autocatalytic activation of caspase-1. This results in processing of pro-IL-1β and pro-IL-18 to their active forms (IL-1 β and IL-18) and their release (Figure 2).
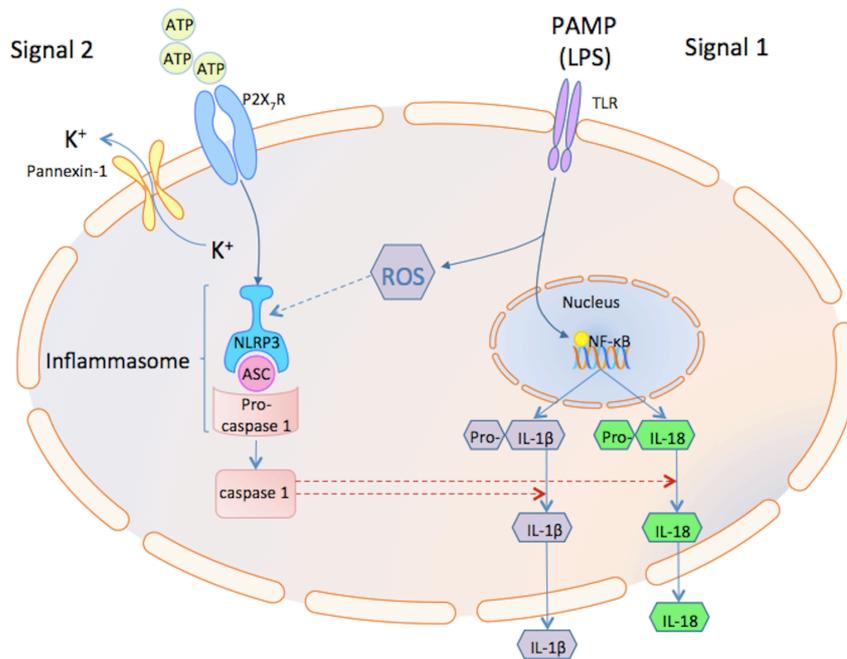
Figure 2: Model of NLRP3 inflammasome activation

NLRP3 is activated by a vast array of stimuli including extracellular pathogen PAMPs such as bacterial LPS via pattern recognition receptors (PRR) such as Toll-like receptors (TLR) and DAMPs. This comprises signal 1 and leads to synthesis of the cytokine precursor pro-IL-1β via NF-κB and other components of the inflammasome such as NLRP3 itself. Many of the known activators of the inflammasome generate ROS which can bind to NLRP3 and this appears necessary for its activation. Extracellular ATP binding to the $P2X_7$ comprises signal 2. This promotes the recruitment and opening of the pannexin-1 pore channel which causes rapid K^+ efflux, another event which appears necessary for NLRP3 activation. NLRP3 assembly occurs when, through its pyrin domain, NLRP3 binds to the pyrin domain on an ASC molecule which then binds to pro-caspase-1 via its CARD domain. This leads to cleavage of pro-caspase-1 and subsequent cleavage of pro-IL-1β and pro-IL-18 to their active forms.

Abbreviations: DAMP, damage-associated molecular pattern; LPS, lipopolysaccharide; ROS, reactive oxygen species; PAMP, pathogen-associated molecular pattern; PRR, pattern recognition receptor; TLR, toll-like receptor; PYD, pyrin domain.

NLRP3 is activated by many stimuli including PAMPs (e.g. LPS) and DAMPs. This comprises signal 1 and leads to synthesis of the cytokine precursor pro-IL-1β via NF-κB and other components of the inflammasome such as NLRP3 itself. Many known activators of the inflammasome generate ROS that bind to NLRP3; this appears necessary for its activation. Extracellular ATP binding to the $P2X_7$ comprises signal 2.

This promotes recruitment and opening of the pannexin-1 pore channel which causes rapid K^+ efflux, another event which appears necessary for NLRP3 activation. NLRP3 assembly occurs when NLRP3 binds to the pyrin domain on an ASC molecule which then binds to pro-caspase-1 via its CARD domain. This leads to cleavage of pro-caspase-1 and then cleavage of pro-IL-1β and pro-IL-18 to their active forms.

The cell surface P2X$_7$ receptor (P2X$_7$) facilitates assembly of the NLRP3 inflammasome (Bauernfeind et al. 2011, Bergsbaken et al. 2011, Miao et al. 2011). ATP released into the extracellular milieu during inflammation is a potent stimulus for P2X$_7$ activation (Bauernfeind et al. 2009, Fink and Cookson 2006, Shiohara et al. 2002). This results in formation of an ion pore and K^+ efflux, with reduction in intracellular K^+, a key step in inflammasome activation (Bryan et al. 2009). Activation of the P2X$_7$ by LPS and ATP results in MyD88-dependent NfκB activation (signal 2), and transcription of pro-IL-1β (Liu et al. 2011). Following LPS priming of monocytes, P2X$_7$ activation stimulates NADPH oxidase to generate superoxide anions, thereby facilitating NLRP3 activation (Bruey et al. 2007).

3.2.1 Processing of IL-1α, IL-1β, IL-18, and caspase-1

IL-1 is a central player in the inflammatory cascade. It is produced by many cells, including activated monocytes and macrophages. It has a variety of effects on its target cells by activation of signal transduction pathways, such as MAPK and NF-κB, resulting in upregulation of several gene products in the inflammatory cascade, such as cyclo-oxygenase (COX)-2, IL-6, chemokines, and cellular adhesion molecules. IL-1 has two isoforms, IL-1α and IL-1β, which bind to the same receptors and are both biologically active (Bevilacqua et al. 1989, Dinarello 2002).

Inflammatory stimuli, especially LPS, engage with the TLR4 receptor of T cells, resulting in synthesis of pro-IL-1β. Pro-IL-1α is constitutively expressed and does not require TLR stimulation (Dinarello 2009). Both isoforms are produced as 31 kDa precursors stored

within the cell cytosol. The pro- IL-1β precursor remains within the cytosol and is cleaved to its mature form through the action of caspase-1 (or interleukin 1β Converting enzyme; ICE). Pro-IL-1β is also cleaved into its active form by other enzymes such as serine proteases (e.g., proteinase 3) and metalloproteinases (MMP-2 and MMP-9). Caspase-1 is crucial for the processing of intracellular pro-IL-1β; although extracellular pro-IL-1β can be processed by a number of different proteases during inflammation (Ferrari et al. 2006, Thornberry et al. 1992).

Caspase-1 is itself produced from the constitutively expressed cytosolic 45 kDa pro-enzyme, pro-caspase; it requires post-translational processing to form 20 and 10k Da forms of active caspase-1 (Thornberry et al. 1992). Activation of caspase-1 occurs following assembly of the 'inflammasome'. The NALP3 inflammasome is a multiprotein complex containing NALP3, apoptosis-associated speck-like protein (ASC), and caspase-1, which oligomerise on cell activation (Ogura et al. 2006). Proteolytic activation of IL-1β occurs within the inflammasome complex. The exact mechanism of inflammasome formation and activation is not fully understood, and can be triggered by different mechanisms in different cell types.

In addition to IL-1, IL-18 is a key mediator in the host response to infection and the inflammatory response (Dinarello 2002, Dinarello 2007). IL-18 is also constitutively produced as a precursor, pro-IL-18 (Dinarello 2007). Pro-IL-18 is cleaved by either caspase-1 or proteinase-3 (cf. pro-IL-1β above) into its active form, which is released into the extracellular space along with mature IL-1β. Extracellular release of active IL-1β and IL-18 is dependent on ATP-sensitive P2X$_7$ activation. Contact with LPS alone is insufficient for extracellular release of IL-1β and IL-18; any one of a number of different stimuli, including extracellular ATP, nigericin, bacterial toxins, hypotonic stress, and T cells are usually required. The best-established stimulus to IL-1β and IL-18 post-translational processing and release is ATP acting via the P2X$_7$ (Dinarello 2007, Ferrari et al. 2006).

Experimental evidence supporting an attenuated inflammatory response with the use of P2X$_7$ antagonists, or in P2X$_7$ KO mice, may be directly related to inhibition of IL-1β release. However, the attenuated response may also be related to lack of induction of other inflammatory mediators. IL-1β may induce or release nitric oxide, COX-2, superoxide products, and other pro-inflammatory mediators (Dinarello 2009, Parvathenani et al. 2003).

3.2.2 Effects of IL-1α, IL-1β, IL-18

Il-1β has diverse functions relating to its unique ability to regulate inflammation at both the nuclear and membrane receptor levels. These include (i) induction of gene expression and synthesis of cyclooxygenase-1 (COX-2), prostaglandin-E2, platelet activating factor, NO, and IL-6 (Dinarello 2009, Parvathenani et al. 2003), (ii) expression of adhesion molecules on mesenchymal and endothelial cells (Myers et al. 1992, Ren et al. 2010, Wang et al. 1995, Yang et al. 2010) and (iii) angiogenesis via upregulation of VEGF (Sola-Villa et al. 2006) which may be an important protective mechanism in ischaemic injury. However, excessive IL-1 may be detrimental.

IL-1 knockout (KO) mice and antagonist-treated rats subjected to ischaemia-reperfusion injury developed significantly less infiltration of polymorphonuclear leukocytes and had less severe renal histological and biochemical derangement (Furuichi et al. 2006, Haq et al. 1998, Rusai et al. 2008). Deficiency or neutralization of IL-1 conferred a similar protective effect in experimental glomerulonephritis (GN) (Chen et al. 1997, Lichtnekert et al. 2011, Timoshanko et al. 2004).

Excessive tissue destruction may be mediated in part by IL-1α; the inflammation resulting from cell necrosis may be mediated by surface IL-1α (Chen et al. 2007). IL-1α is also expressed on the membrane of monocytes and B-lymphocytes (Kaplanski et al. 1994, Kurt-Jones et al. 1985). In addition, the induction of many genes by INF-γ, including HLA-DR, ICAM-1 and IL-18BP depends on basal IL-1α, but not IL-1β (Hurgin et al. 2007).

IL-18 is also a member of the IL-1 cytokine family. It is primarily expressed by macrophages and dendritic cells, but also by epithelial cells throughout the body (Perregaux et al. 2000, Takeuchi et al. 1999). One of its key features is its ability to induce INF-γ production (Takeuchi et al. 1999) and subsequent T cell polarisation (Takeda et al. 1998, Tomura et al. 1998). IL-18 plays an important role in the TH1 response, primarily by its ability to induce IFN-γ production in T cells and natural killer cells (Dinarello 1999). Fas ligand-mediated cell death is also IL-18-dependent (Dao et al. 1996, Zhang et al. 2011). IL-18 deficiency or neutralisation is associated with a reduction in renal tubular apoptosis in unilateral ureteric obstruction (UUO), I-R injury and glomerulonephritis (Bani-Hani et al. 2009, Sugiyama et al. 2008, Wang et al. 2012, Wu et al. 2008).

3.2.3 Cell death and pyroptosis

Caspase-1 activation with subsequent production of IL-1β and IL-18 has a biphasic effect; low levels cause cytokine production but, above a certain threshold, triggers pyroptosis (Bergsbaken and Cookson 2007).

This catastrophic form of cell death, commonly found in monocytes, macrophages and dendritic cells, has morphological characteristics of apoptosis and necrosis. Cell lysis occurs due to caspase-1-dependent pore formation in the cell membrane, disruption of the cellular ionic gradient, osmotic driven water influx, and cell swelling. (Fink and Cookson 2006, Miao et al. 2011). This leads to further inflammasome activation, release of proinflammatory cytokines, damaged DNA and, ultimately, cellular disruption releasing other DAMPs. Release of mitochondria into the extracellular space results in discharge of ATP and also acts as a DAMP.

An alternative mechanism of cell death relates to activation of the P2X$_7$. Here, irreversible pore formation allows non-selective passage of ions and hydrophilic solutes of up to 900 Da, resulting in colloido-osmotic cell lysis (Ferrari et al. 2006). P2X$_7$-induced shrinkage depends on K$^+$ efflux via K$_{Ca3.1}$, a voltage-independent potassium channel activated by

intracellular calcium, and a pathway of Cl⁻ efflux distinct from that implicated previously in apoptosis (Taylor et al. 2008).

3.2.4 Regulation of the inflammasome

Activation of the inflammasome results in a rapid and substantial inflammatory response. As such, the inflammasome is tightly regulated at both transcriptional and post-transcriptional levels. Basal expression of inflammasome components, in particular NLRP3, is relatively low (Bauernfeind et al. 2009); pro-apoptotic pathways, such as FAS ligand-receptor interactions, are required to induce ASC expression (Shiohara et al. 2002).. ASC is localized to the nucleus in quiescent cells, but recruited to the cytoplasm on activation (Bryan et al. 2009).

Alternatively, spliced inflammasome components generate protein variants with different activities. ASC has at least three different isoforms, one of which has an inhibitory effect on inflammasome activity (Bryan et al. 2010). Several proteins regulate inflammasome activity by sequestration of inflammasome components. Anti-apoptotic Bcl-2 proteins (e.g. Bcl-2, Bcl-x$_L$) interact with NLRP1 to prevent ATP binding and inflammasome activation (Bruey et al. 2007).

3.2.5 The NLRP3 inflammasome and host immunity in sepsis

The NLRP3 inflammasome pathway has profound and diverse effects. Tight regulation of its activity is therefore crucial in maintaining health. Genetic deficiencies in the inflammasome pathway highlight its importance in host immunity. Both MyD88 (myeloid differentiation factor 88) and IRAK-4 (IL-1 receptor-associated kinase 4) are key elements of the TLR-IL-1 pathway (Burns et al. 2003). Loss of function mutations in MyD88 and IRAK-4 are associated with increased susceptibility to life-threatening severe staphylococcal and invasive pneumococcal infections (Picard et al. 2010, Takeuchi et al. 2000, von Bernuth et al. 2008).

In addition to cytokine release, the NLRP3 inflammasome mediates host immunity by caspase-1 dependent pyroptotic cell death. This mechanism may be mediated by the P2X7 receptor (Taylor et al. 2008) which is crucial for destruction of intracellular pathogens including tuberculosis (Placido et al. 2006). Although pyroptosis and apoptosis are both programmed forms of cell death, unlike apoptosis, pyroptosis requires the activity of caspase-1 (Chen et al. 1996).

3.2.6 The Inflammasome and Renal Disease

Several primary renal diseases are associated with NLRP3 inflammasome activation, as are many systemic diseases affecting the kidneys (**Table 4**). These include I-R injury (Furuichi et al. 2006, Haq et al. 1998, Iyer et al. 2009, Rusai et al. 2008, Wang et al. 2012, Wu et al. 2008), glomerulonephritis (Chen et al. 1997, Kinoshita et al. 2004, Lichtnekert et al. 2011, Schorlemmer et al. 1993, Sugiyama et al. 2008, Taylor et al. 2008, Timoshanko et al. 2004, Turner et al. 2004), sepsis (Granfeldt et al. 2008, Hertting et al. 2003, Wang et al. 2005), CKD (Vilaysane et al. 2010, von Bernuth et al. 2008), and hypoxia (Edelstein et al. 2007). $P2X_7$, IL-1β, IL-18, caspase-1, ASC, and NLRP3 are all associated with renal inflammation and injury. Virtually every model using genetic deletions and/or receptor antagonists/antiserum against the NLRP3 inflammasome pathway has shown lower disease severity, though publication bias cannot be excluded.

Intrinsic renal cells express components of the inflammasome pathway. This is most prominent in tubular epithelial cells and, to a lesser degree, glomeruli. The precise mechanisms involving the NLRP3 inflammasome in disease relate to both systemic and local (renal) activation. Limited studies using global knockouts and bone marrow chimeras suggest that systemic production of cytokines may have a greater effect on renal injury (Wu et al. 2008). Genetic deletion or inhibition of the NLRP3 inflammasome pathway results in decreased local cytokines and chemokines, inflammatory cell infiltrate, and apoptosis. Locally released DAMPs result in inflammasome activation, resulting in chemokine release and immune cell infiltration. (Deplano et al. 2012).

The role of NLRP3 inflammasome activation in human renal disease remains uncertain. $P2X_7$ and NLRP3 are upregulated in lupus nephritis and non-diabetic CKD, respectively (Turner et al. 2004, Vilaysane et al. 2010). Elevated serum IL-18 correlates with the development of diabetic nephropathy (Fujita et al. 2012), while urine IL-18 is raised in AKI associated with critical illness (Siew et al. 2010), cardiac surgery (Parikh et al. 2006), and radiocontrast (Turkmen et al. 2012). These support the notion that the inflammasome is intimately involved in wider inflammatory renal disease.

Table 4 The inflammasome and inflammatory renal disease

P2X$_7$	Disease	Species	Antagonist/ genetic deletion	Effect	Renal localisation of inflammasome component
(Harada et al. 2000)	TNF-α stimulation	Rat	-	NA	Mesangial cells
(Goncalves et al. 2006)	Unilateral ureteric obstruction	Mouse	P2X$_7$ $^{-/-}$	Beneficial	PTEC
(Vonend et al. 2004)	Hypertension Diabetes mellitus	Rat	-	NA	Glomerular podocytes
(Turner et al. 2007)	Experimental glomerulonephritis	Mouse Rat	-	NA	Glomeruli and infiltrating macrophages Glomeruli
(Turner et al. 2007)	Lupus Nephritis	Humans	-	NA	Glomeruli PTEC
(Taylor et al. 2008)	Experimental Glomerulonephritis	Rat Mouse	Antagonist P2X$_7$ $^{-/-}$	Beneficial	-
NLRP3	Disease	Species	Antagonist/ genetic deletion	Effect	Renal localisation of inflammasome component
(Deplano et al. 2012)	Glomerulonephritis	Rat	Genetically susceptible strain	NA	Glomeruli and bone marrow derived macrophages
(Vilaysane et al. 2010)	Non-diabetic acute and chronic kidney diseases	Human	NA	NA	PTEC
(Vilaysane et al. 2010)	Unilateral ureteric obstruction	Mice	NLRP3$^{-/-}$	Beneficial	PTEC
(Iyer et al. 2009)	Ischaemia- reperfusion injury	Mice	NLRP3$^{-/-}$	Beneficial	-
(Jalilian et al. 2012)	None	Dog	NA	NA	Epithelial cells
IL-1	Disease	Species	Antagonist/ genetic deletion	Effect	Renal localisation of inflammasome component
(Yamagishi et al. 2001)	Unilateral ureteric obstruction	Mouse	IL-1 RA	Beneficial	PTEC
(Haq et al.	Ischaemia-	Mouse	IL-1 RA	Beneficial	-

1998)	reperfusion injury		IL-1R [-/-]		
(Chen et al. 1997)	IgA nephropathy	Mice	IL-1 RA	Beneficial	-
(Matsumoto et al. 1988)	Glomerulonephritis	Human	NA	NA	
(Tam et al. 1994)	Glomerulonephritis	Rat	NA	N/A	
(Lan et al. 1995)	Glomerulonephritis	Rat	IL-1RA	Beneficial	
(Karkar et al. 1992)	Glomerulonephritis	Rat	Antibody	Beneficial	
(Karkar et al. 1995) (Tam et al. 1996)	Glomerulonephritis	Rat	IL-1RA and soluble IL-1R	Beneficial	
(Timoshanko et al. 2004)	Crescentic glomerulonephritis	Mice	IL-1β [-/-] IL-1R [-/-]	Beneficial	-
(Lichtnekert et al. 2011)	Anti-GBM disease	Mice	NLRP3 [-/-] Caspase1 [-/-] ASC [-/-] IL-1R1 [-/-] Il-18 [-/-]	No effect No effect No effect Benefit Mild	Renal dendritic cells
(Schorlemmer et al. 1993)	SLE-like disease	Mice	IL-1 RA	Beneficial	-
(Furuichi et al. 2006)	Ischaemia- reperfusion injury	Mice	IL-1α/β [-/-] IL-1RA [-/-]	Beneficial	Glomeruli and cortical arterioles
(Rusai et al. 2008)	Ischaemia- reperfusion injury	Rats	IL-1 RA	Beneficial	-
(Granfeldt et al. 2008)	Endotoxaemia	Pigs	NA	NA	Endothelial cells of the cortical arterioles positive for IL-1β; IL-1ra detected in glomerulus and tubular cells

(Hertting et al. 2003)	E.Coli pyelonephritis	Mice	IL-1 β $^{-/-}$	Harmful	-
Caspase-1	Disease	Species	Antagonist/ genetic deletion	Effect	Renal localisation of inflammasome component
(Homsi et al. 2006)	Glycerol- induced AKI	Rats	Caspase-1 inhibitor	Beneficial	Constitutive tubular expression of IL-18 Induction of tubular IL-1β
(Wang et al. 2005)	Endotoxaemia	Mice	Caspase 1 $^{-/-}$ IL-1 Ra IL-18 antiserum	Beneficial No effect No effect	-
(Gauer et al. 2007)	None	Humans	NA	NA	Collecting duct alpha- and beta- intercalated cells express P2X$_7$, IL-18
(Edelstein et al. 2007)	Hypoxia	Mice	Caspase 1 $^{-/-}$ IL-18 BP	Beneficial No effect	IL-18 in PTEC
IL-18	Disease	Species	Antagonist/ genetic deletion	Effect	Renal localisation of inflammasome component
(Bani-Hani et al. 2009)	Unilateral ureteric obstruction	Mice	Transgenic mice overexpressing human IL-18-BP	Beneficial	TECs
(Wu et al. 2008)	Ischaemia- reperfusion injury	Mice	IL-18 $^{-/-}$ IL-18 $^{-/-}$ BM chimera IL-18-BP	Beneficial Beneficial Beneficial	TECs
(Sugiyama et al. 2008)	Bovine albumin- induced GN	Mice	IL-18R $^{-/-}$	Beneficial	-
(Kinoshita et al. 2004)	Autoimmune disease	Mice	IL-18R $^{-/-}$	Beneficial	-
(Wang et al. 2012)	Ischaemia- reperfusion injury	Rat	IL-18-binding protein	Beneficial	-
(Zhang et al. 2011)	Unilateral ureteric obstruction	Mice	Overexpresses human IL-18-BP	Beneficial	-
(VanderBrink et al. 2011)	Unilateral ureteric obstruction	Mice	IL-18 $^{-/-}$	NA	TECs
ASC	Disease	Species	Antagonist/	Effect	Renal localisation of

			genetic deletion		inflammasome component
(Iyer et al. 2009)	Ischaemia-reperfusion injury	Mice	ASC $^{-/-}$	Beneficial	-

Abbreviations: PTEC, proximal tubular epithelial cells, NLRP3, Nod-like receptor protein 3; IL-1RA, interleukin 1 receptor antagonist, ARF, acute renal failure; TEC, tubular epithelial cell; BM, bone marrow

3.2.7 Drugs modulating the NLRP3 inflammasome pathway

Growing evidence suggests that the inflammasome and the IL-1β/IL-18 axis play an integral part in the pathogenesis of many acute and chronic conditions, including gout, rheumatoid arthritis, atherosclerosis, Alzheimer's disease, diabetes mellitus and oxalate crystal nephropathy. Several components of the NLRP3 inflammasome are implicated in renal disease. Therapeutic interventions that modulate this pathway are being developed, e.g. inhibiting IL-1, $P2X_7$ or caspase-1, and the functional significance of the inflammasome and the IL-1β/IL-18 axis in renal disease is of growing interest. To date, only IL-1 inhibitors have been successful in clinical studies of rheumatoid arthritis (RA) and cryopyrin-associated periodic syndrome (CAPS).

3.2.7.1 IL-1 inhibitors

The clinical application of IL-1 inhibitors has been slow as the first generation of inhibitors, the recombinant IL-1 receptor antagonists, have a short circulatory half-life and limited affinity for the receptor. A large molar excess of recombinant IL-1ra is needed to antagonize endogenous IL-1 effectively. Drugs inhibiting the action of IL-1 include recombinant human IL-1ra (Anakinra), a humanised monoclonal IL-1β antibody (Canakinumab), and a neutralising antibody against IL-1α and IL-1β (Rilonacept). IL_1 antagonists may be beneficial in paediatric CPAS, systemic juvenile idiopathic arthritis, and type 2 diabetes mellitus (Hensen et al. 2013, Ruperto et al. 2012, Russo et al. 2014).

3.2.7.2 $P2X_7$ antagonists

Drugs inhibiting the $P2X_7$ are currently in Phase 1 and 2 clinical trials (Arulkumaran et al. 2011). At present there are no data to demonstrate a beneficial effect of $P2X_7$ antagonism, although trials are still at an early stage. Preclinical data suggest $P2X_7$ antagonists have a potential role in the treatment of inflammatory rheumatological (Dell'Antonio et al. 2002, Dell'Antonio et al. 2002), renal (Taylor et al. 2009, Turner et al. 2007), and pulmonary diseases (Fernando et al. 2007, Kolliputi et al. 2010, Wareham et

al. 2009). Although Phase 1 and 2 studies have demonstrated safety, preliminary studies have so far not shown clinical efficacy in the management of rheumatoid arthritis (Keystone et al. 2012).

3.2.7.3 Caspase-1 inhibitors

Small molecule inhibitors of caspase-1 have been used in experimental models. Only pralnacasan (VX-740) and VX-765 have been used so far in patients; however, concerns about liver toxicity with prolonged use of pralnacasan have resulted in discontinuation of clinical trials in RA, psoriasis, and osteoarthritis (Cornelis et al. 2007). A Phase 2 clinical trial of VX-765 has been completed, although results have yet to be published (Cornelis et al. 2007).

3.3 Other Inflammasomes

NLRP1 was the first inflammasome to be described (Levinsohn et al. 2012). It has its own CARD, so can bypass the requirement of the adapter molecule ASC for inflammasome activation (**Figure 3**). Cleavage by anthrax toxin directly activates CARD, leading to activation of caspase-1 (Levinsohn et al. 2012). An alternative mechanism of NLRP1 activation is by the toxin inhibiting p38 mitogen-activated protein kinase and Akt kinase, leading to opening of the connexion channel for ATP release, resulting in $P2X_7$ signalling (Ali et al. 2011). There are similarities with the mechanism of activation of the NLRP3 inflammasome.

A second class of inflammasomes contains members of the PYHIN family, rather than NLRs. Examples include AIM2 and Interferon-γ inducible protein 16 (IFI16) inflammasomes. These lack a CARD domain and require ASC for recruitment of pro-caspase-1 to form a stable inflammasome complex. Following detection of bacterial or viral dsDNA, AIM2 and IFI16 inflammasomes assemble with subsequent secretion of IL-1β and IL-18 (Roberts et al. 2009). AIM2 can recognise self-DNA, but this is limited under steady-state conditions because of its cytosolic location. In conditions where self-DNA is

not cleared from the extracellular compartment, it is likely that DNA can activate AIM2 and drive inflammation.

The NLRC4 inflammasome interacts directly with pro-caspase-1 via homotypic CARD interactions, leading to processing of caspase-1. This inflammasome complex plays an essential role in the innate immune response to the bacterial proteins flagellin and PrgJ (Zhao et al. 2011).

The NLRP6 inflammasome associates with ASC, inducing caspase-dependent processing and release of IL-1β. At the mRNA level NLRP6 is highly expressed in mouse liver, kidney and small intestine, and plays a central role in modulating inflammatory responses in the gut to allow recovery from intestinal epithelial damage, tumorigenesis, and in controlling the composition of the gut microflora to prevent colonization by harmful bacteria (Lech 2010(Chen et al. 2011, Lech et al. 2010). Data on NLRP6 and renal disease are limited and warrant further study.

The NLRP12 inflammasome is expressed in human myeloid cells. It acts as a negative regulator of inflammation by reducing Nf-κB activation and inhibiting chemokine expression through ATP hydrolysis (Ye et al. 2008). NLRP12 also reduces NFκB activation by TLR-signaling molecules (Williams et al. 2005).
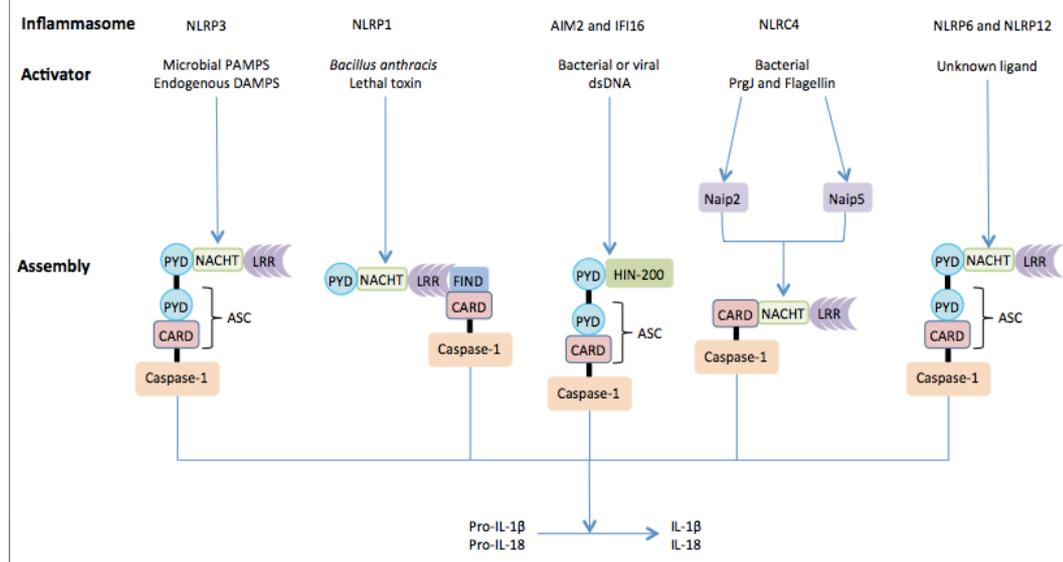
Figure 3 Models for inflammasome activation and assembly.

The NLR family members and the HIN-200 proteins, AIM2 and IFI16, assemble inflammasome complexes. NLRs are characterised by a NACHT domain with or without an N-terminal PYD domain and a variable number of LRRs. AIM2 and IFI16 contain an N-terminal PYD domain followed by a DNA binding HIN-200 domain. The PYD domain of NLRP3, 6 and 12, AIM2 and IFI16 recruit the adaptor protein ASC via homotypic binding to its PYD domain allowing indirect recruitment of caspase-1 through interaction with the CARD domain. NLRP1 and NLRC4 directly recruit caspase-1 through a CARD domain. NLRC4 is activated by NAIP proteins bound to specific ligands, NAIP 2 binds to the bacterial rod protein PrgJ whereas NAIP 5 and 6 bind to bacterial flagellin. Activation of the inflammasome leads to maturation and secretion of IL-1β and IL-18 aswell as inflammatory cell death by pyroptosis.

Abbreviations: AIM2, absent in melanoma 2; CARD, caspase recruitment domain; DAMP, danger-associated molecular pattern; FIND, domain with function to find; IFI16, Interferon-γ inducible protein 16; LRR, leucine rich repeat; NACHT, nucleotide-binding and oligomerization domain; NAIP, NLR family apoptosis inhibitor; NLR, Nod-like receptor, PAMP, pathogen associated molecular pattern; PYD, pyrin domain.

3.4 P2X$_7$ receptor

3.4.1 Purinergic receptors

in 1970 Burnstock proposed that adenosine triphosphate (ATP) may have an extracellular role as a signalling molecule and a neurotransmitter in so-called non-cholinergic, non-

adrenergic (NANC) neurotransmission. This role of ATP as an extracellular messenger (purinergic cell signaling) is now known to be not confined to the nervous system. Indeed, many roles for purinergic receptors in health and disease have now been identified.

In 1978, Burnstock sub-classified the purinergic receptors into P1 and P2 receptors: adenosine acts on P1 receptors, whereas ATP and its breakdown products, ADP and AMP, act on P2 receptors. Burnstock and Kennedy later proposed a further sub-classification of the P2 receptors, dividing them into P2X and P2Y receptors: P2X receptors are inotropic ligand-gated non-selective cation channel receptors and P2Y receptors are G protein coupled; there are currently seven P2X subtypes and eight P2Y subtypes (Burnstock 2006).

3.4.2   P2X$_7$ receptor

The P2X$_7$ receptor (P2X$_7$) is a distinct member of the P2X subclass, as its downstream signaling is coupled to pro-inflammatory cascades. It is a 595-amino acid polypeptide with two membrane-spanning domains and a long intracellular C-terminus compared with other P2X receptors (North 2002). It is expressed on many cell types, the most studied being macrophages and monocytes, and has a key role in regulating cell survival and release of mature IL-1β and IL-18 (Ferrari et al. 2006).

The P2X$_7$ receptor is a ligand-gated cation channel best characterized in immune cells (Di Virgilio et al. 2001). Expression and activity of the P2X$_7$ is significantly upregulated in response to inflammatory stimuli, including TNFα and LPS (Ferrari et al. 2006, Humphreys and Dubyak 1998, Mehta et al. 2001) P2X$_7$ channel activation results in release of mature IL-1β and IL-18 (Rassendren et al. 1997, Sluyter et al. 2004); prolonged activation results in irreversible pore formation and cell death (Sluyter et al. 2004, Taylor et al. 2008, Wilson et al. 2004).

During active inflammation, local concentrations of extracellular ATP are raised, which is thought to be mainly a consequence of cell damage and lysis. To activate the P2X$_7$ *in*

vitro, extracellular concentrations of ATP in the range of 1 mM are required, in contrast to concentrations of ≤ 100 μM needed to activate other P2 receptors. The ATP molecule binds to and activates $P2X_7$, resulting in pore formation. This leads to K^+ efflux from the cell, which is a crucial step in inflammasome assembly. In addition there is an influx of Ca^{2+}, which is also required for the release of active IL-1β (Ferrari et al. 2006, MacKenzie et al. 2001). Prolonged activation of the $P2X_7$ results in irreversible pore formation and allows non-selective passage of ions and hydrophilic solutes of up to 900Da; this can result in colloido-osmotic lysis and cell death by apoptosis or necrosis (Ferrari et al. 2006). Pore formation is thought to allow entry of bacterial products (PAMPs) and extracellular ATP into the cell, which drives inflammasome formation (Pelegrin and Surprenant 2009).

Oxidised ATP (oATP) is a potent, but non-selective, $P2X_7$ antagonist that can attenuate inflammatory responses independent of P2 receptor blockade (Beigi et al. 2003). This must considered when interpreting much of the experimental data referred to in this review as oATP has been one of the most widely used $P2X_7$ antagonists. In addition to blocking $P2X_7$, oATP is known to antagonise $P2X_1$ and $P2X_2$ receptors, and inhibit NFkB.

More selective $P2X_7$ antagonists exist and have been used successfully in *in vitro* experiments, and in Phase 1 and Phase 2 clinical trials (Arulkumaran et al. 2011).

3.4.3   The $P2X_7$ and cell survival

The $P2X_7$ has a role in cell survival and growth. Its growth-promoting function seems contradictory to its established role in apoptosis; however, this receptor is expressed at a high level in some malignancies, which may be consistent with its growth-promoting role (Adinolfi et al. 2002). The anti-apoptotic property of $P2X_7$ is based on studies using oATP (Adinolfi et al. 2009, Adinolfi et al. 2002) and KN-93 (Nagaoka et al. 2006). Basal activation of $P2X_7$ (via autocrine/paracrine release of extracellular ATP) promotes cell growth (Adinolfi et al. 2005).

3.4.4 LL-37

Although ATP is a $P2X_7$ agonist, causing IL-1β processing and release from LPS-primed macrophages and monocytes, the concentration of ATP (0.5-5mM) required to induce IL-1β release *in vitro* is believed to be far higher than is normally present in the extracellular space of tissues, at least under physiological conditions (North and Surprenant 2000).

Several studies suggest that human cathelicidin-derived peptide, LL-37, may be a $P2X_7$ agonist. Cathelicidins are an integral part of the innate immune system, with human cationic antimicrobial protein-18 (hCAP18) being the only known cathelicidin in humans (Gudmundsson et al. 1996). LL-37 has a well-established antimicrobial function, exerting direct antimicrobial activity against both Gram-positive and Gram-negative organisms, and neutralising LPS (Durr et al. 2006). In the presence of LL-37, the concentration of ATP required to activate $P2X_7$ was approximately 4000-fold lower than that usually needed to release the same amount of IL-1β (Elssner et al. 2004). LL-37 treatment of LPS-primed monocytes leads to caspase-1 activation and an increase in IL-1β release via $P2X_7$R in a dose-dependent manner (Elssner et al. 2004). LL-37 treatment of LPS-primed monocytes also results in transient release of ATP, peaking after 5-10 minutes at a concentration of ~150nM (Elssner et al. 2004)..

3.4.5 $P2X_7$ and antibody production

The role of $P2X_7$ in IL-1β and IL-18 release and in cell death is well established. The nephrotoxic nephritis model provides evidence that $P2X_7$ may affect antibody production. $P2X_7$ is primarily found on antigen-presenting cells, including dendritic cells and macrophages (Di Virgilio et al. 2001). In a nephrotoxic nephritis model there was a small decrease in the mouse anti-sheep IgG deposition in the glomeruli of $P2X_7$ KO mice (Taylor et al. 2009). This raises the possibility that $P2X_7$ may be involved in antibody production.

3.4.6 Current use of P2X$_7$ antagonists in clinical trials

Phase 1 and phase 2 clinical trials investigating the safety and efficacy of P2X$_7$ antagonists are currently underway (Arulkumaran et al. 2011). No serious safety concerns have been raised. Phase 2 clinical trials have investigated the use of P2X$_7$ antagonists in inflammatory bowel disease, rheumatoid arthritis, and chronic obstructive airway disease. Main side effects include gastrointestinal upset (diarrhoea and nausea), dizziness, and headaches.

Factors underlying the limited efficacy to date include pharmacokinetics and pharmacodynamics. P2X$_7$ polymorphisms may be another factor to consider. In future drug development, the affinity of P2X$_7$ antagonists for different polymorphic forms of P2X$_7$ may need investigation and correlation with efficacy. With better understanding the underlying disease processes and more drug development, the prospects for P2X$_7$ targeted therapy is encouraging.

3.4.7 P2X$_7$ receptor in sepsis

The importance of capase-1 and secretion of mature IL-1β in sepsis have been studied in rodent models (Mehta et al. 2001, Novogrodsky et al. 1994). Studies also suggest a key role for the regulation/inhibition of IL-1 β release as a therapeutic strategy (Li et al. 1995). However, a large Phase 3 randomised clinical trial failed to support the benefit of a recombinant human IL-1 receptor antagonist in patients with severe sepsis (Opal et al. 1997). However, this finding does not preclude the use of a P2X$_7$ antagonist in sepsis, as these have actions over and above IL-1β release that could be beneficial. An immunomodulatory agent that can interfere with more than one arm of the sepsis response, such as a P2X$_7$ receptor antagonist, may have promise if given to the right patient and at the right time.

Some experimental data suggests that P2X$_7$ receptor antagonism may be beneficial in sepsis. LL37 is a potent mediator of the P2X$_7$ pathway which reduces the ATP

concentration required to activate the $P2X_7$ by 4000-fold (Elssner et al. 2004). In an *in vivo* model of sepsis, LPS-induced $P2X_7$ activation, and subsequent IL-1β release, IL-1 β resulted in iNOS expression, increased levels of NO, and vascular smooth muscle hyporeactivity (Chiao et al. 2008). There is an association between sepsis severity, mitochondrial dysfunction, and outcome (Brealey et al. 2002). BzATP stimulation of $P2X_7$-transfected cell lines resulted in loss of the mitochondrial membrane potential with subsequent fragmentation of mitochondria and cell death (Adinolfi et al. 2005). Mitochondrial fragmentation was absent in cells lacking $P2X_7$. Thus, it is plausible that a $P2X_7$ antagonist could have a role in the preservation of mitochondrial function in sepsis. Apoptosis of lymphocytes is also associated with a worse outcome in sepsis (Hotchkiss et al. 1999, Hotchkiss et al. 2001) and blocking apoptosis has been improved survival in experimental models of sepsis (Chung et al. 2003, Hotchkiss et al. 2001). T lymphocytes express functional $P2X_7$ (Aswad and Dennert 2006); blocking these receptors with $P2X_7$ antagonists to prevent apoptosis may also confer a survival advantage in sepsis.

3.4.8 $P2X_7$ receptor and renal disease

Within the rat kidney, $P2X_7$ is expressed at very low levels under normal conditions (Turner et al. 2003). Several studies reported upregulation of renal $P2X_7$ expression under various pathological conditions *in vivo* and *in vitro* (**Table 5**). This was first described in a rat model of hypertension and diabetes mellitus (Vonend et al. 2004). Similarly, rats with streptozotocin-induced diabetes had significant $P2X_7$ detectable in their glomeruli at 6 and 9 weeks. At the mRNA level this corresponded to a ten-fold increase in expression of $P2X_7$. Immunohistochemistry and immuno-electron microscopy studies of diabetic rats showed that $P2X_7$ were expressed mainly in glomerular podocytes (also with some expression in endothelial cells and mesangial cells).

Turner et al demonstrated perhaps the most striking evidence for a pathogenic role of $P2X_7$ using a rodent model of experimental glomerulonephritis (GN) (Turner et al. 2007). Here, an increased glomerular expression of $P2X_7$ was demonstrated, co-existent with an

increase in glomerular apoptotic cells. These findings are consistent with clinical findings of increased glomerular, and some tubular, expression of $P2X_7$ in patients with lupus nephritis (Turner et al. 2007). $P2X_7$ KO mice exposed to nephrotoxic serum were significantly protected from antibody-mediated GN (Taylor et al. 2009), with reduced glomerular macrophage infiltration, fibrin deposition, glomerular thrombosis and reduction in proteinuria, and protection of overall renal function compared to wildtype controls. Renal IL-1β levels were too low for quantification, though CCL2 (MCP-1) levels were reduced in $P2X_7$ KO mice. In a rat model of antibody-mediated GN, the onset of glomerular $P2X_7$ expression coincided with the onset of proteinuria (Turner et al. 2007); treatment with a selective $P2X_7$ antagonist (A438079) reduced glomerular expression of CCL2, glomerular macrophage infiltration, severity of glomerular injury, and proteinuria. The $P2X_7$ gene polymorphisms may contribute to susceptibility to lupus nephritis in selected patient populations, and blockade of the $P2X_7$ has also been shown to be protective in murine lupus nephritis (Chen et al. 2013, Zhao et al. 2013).

$P2X_7$ is implicated in the pathogenesis of renal inflammation and fibrosis. In a mouse model of unilateral ureteral obstruction (UUO), immunohistochemistry demonstrated $P2X_7$ expression in the epithelial cells of the renal cortex in KO mice on day 7 only (Goncalves et al. 2006). Myofibroblast number and collagen deposition were significantly reduced in $P2X_7$ KO mice as were transforming growth factor-β (TGF-β) protein levels. By day 14, kidneys from the $P2X_7$ KO mice showed reduced numbers of infiltrating macrophages and less tubular cell apoptosis. The tubulo-interstitial damage and subsequent fibrosis associated with UUO were attenuated in $P2X_7$ KO mice, suggesting a role for tubular $P2X_7$ in renal inflammation and fibrosis.

Table 5: P2X$_7$ and inflammatory renal diseases

Reference	Disease	Species	Antagonist/ genetic deletion	Effect	Renal localisation of inflammasome component
(Harada et al. 2000)	TNF-α stimulation	Rat	-	NA	Mesangial cells
(Goncalves et al. 2006)	Unilateral ureteric obstruction	Mouse	P2X$_7$ -/-	Beneficial	PTEC
(Vonend et al. 2004)	Hypertension Diabetes mellitus	Rat	-	NA	Glomerular podocytes
(Turner et al. 2007)	Experimental glomerulonephritis	Mouse Rat	-	NA	Glomeruli and infiltrating macrophages Glomeruli
	Lupus Nephritis	Humans	-	NA	Glomeruli PTEC
(Taylor et al. 2008)	Experimental Glomerulonephritis	Rat Mouse	Antagonist P2X$_7$ -/-	Beneficial	-
(Zhao et al. 2013)	Murine lupus nephritis	Mouse	P2X$_7$ -targeted small interfering RNA (siRNA) BBG	Beneficial	-

4 Animal models of sepsis and recovery

4.1 Background

Despite the clinical significance of septic AKI, therapy is limited to supportive care. The complex interplay between global and renal haemodynamics, microcirculation, bioenergetic dysfunction, and the immune system underlie the pathophysiology of septic AKI and recovery (Chapter 2). The relative contribution of different mechanisms to the pathophysiology of septic AKI and recovery needs to be ascertained for the development of novel diagnostics, monitoring and therapeutics.

Animal models offer the advantage of knowing precisely when the septic insult commenced and allow control of volume status and other conditions in a relatively homogenous population. However, to be representative of the human condition, they have to simulate many of the physiological and pathological aspects of sepsis including a proper infectious insult, an adequate duration of study, and fluid resuscitation to avoid the consequences of untreated hypovolaemia leading to organ hypoperfusion (Chapter 1.6).

Over many years the Singer lab at University College London (UCL) has developed an increasingly sophisticated long-term (3 day) rat model of faecal peritonitis where the animals are conscious and instrumented with tunnelled arterial and venous lines (to enable continuous blood pressure monitoring, continuous fluid administration and intermittent blood sampling). Additional studies can be performed as needed, including intermittent echocardiography, and tissue oxygen measurements. In two studies from the lab, 6h echocardiographic measurements of stroke volume and heart rate could reproducibly differentiate between eventual survivors and non-survivors (Dyson et al. 2011, Rudiger et al. 2013).

The objective of this experiment was to characterize parallel changes in haemodynamic, biochemical, histological, and immunological parameters in a clinically relevant model of sepsis and recovery.

4.1.1   Characterization

Information from the characterization of the preclinical model was required prior to planning of further studies. The parameters that I characterized included:

1. Global haemodynamics

2. Biochemistry (renal and liver function tests, electrolytes)

3. Systemic cytokines including pro-inflammatory cytokines (IL-1β, IL-6, IL-18, INF-γ), anti-inflammatory cytokines (IL-10), and chemokines (MCP-1)

4. Renal cytokine release including pro-inflammatory cytokines (IL-1β, INF-γ), anti-inflammatory cytokines (IL-10, IL-4) and chemokines (MCP-1)

5. Renal histology (including tubular injury, cell death, and macrophage infiltration)

Additional studies were based on the results of this characterization study, including:

1. Temporal changes in a panel of renal biomarkers in septic AKI and recovery (described in this chapter)

2. Changes in renal haemodynamics and bioenergetics in sepsis (Chapter 5)

3. The role and potential therapeutic intervention of the inflammasome in sepsis and sepsis-induced AKI (Chapter 6)

4.1.2   Renal biomarkers in septic AKI

The current lack of a sensitive marker of early parenchymal kidney injury in sepsis reduces the window of opportunity for early effective intervention to prevent renal dysfunction and failure. Numerous novel blood and urine markers of renal injury/dysfunction are currently being promoted but, at present, remain poorly

characterized. Measuring a panel of renal injury/dysfunction markers will likely enhance interpretation of this dynamic process. However, studies in septic patients are confounded by an inability to precisely time the onset of sepsis. Thus, the temporal relationship of these biomarkers to the onset and progression of renal dysfunction and injury is unknown. Some clinical trials have investigated the utility of biomarkers in predicting recovery from AKI. Serial measurements of a panel of renal biomarkers in a well-characterized, clinically relevant and closely monitored animal model with a defined onset of polymicrobial sepsis may provide invaluable information that could be translatable to the patient.

We used a similar design to that described by Ozer *et al* who measured a panel of urinary biomarkers to monitor the reversibility of renal injury at different timepoints over 15 days following administration of nephrotoxic drugs such as gentamicin (Ozer et al. 2010). They compared changes in biomarkers against the degree of histological injury and standard measures of renal function, namely urea and creatinine. Using the fluid-resuscitated 3-day rat model of faecal peritonitis, we investigated a panel of biomarker changes across the septic process of inflammation and recovery and correlated these against changes in renal histology and standard measures of renal biochemical function. Characteristics of the biomarker panel are detailed in Chapter 2.9.

4.2 *In vivo Methods*

4.2.1 Instrumentation of animals

Male Wistar rats (Charles River, Margate, UK) weighing 300-375g were used throughout. All experiments were performed under a Home Office Project License (PPL 70/7029) and local UCL Ethics Committee approval. Before experimentation, the rats were housed in cages of six on a 12-12 h light–dark cycle. Six timepoints (3, 6, 12, 24, 48 and 72h) were selected to represent early, established and recovery phases of sepsis. Systemic haemodynamics were measured at these timepoints (Figure 4).
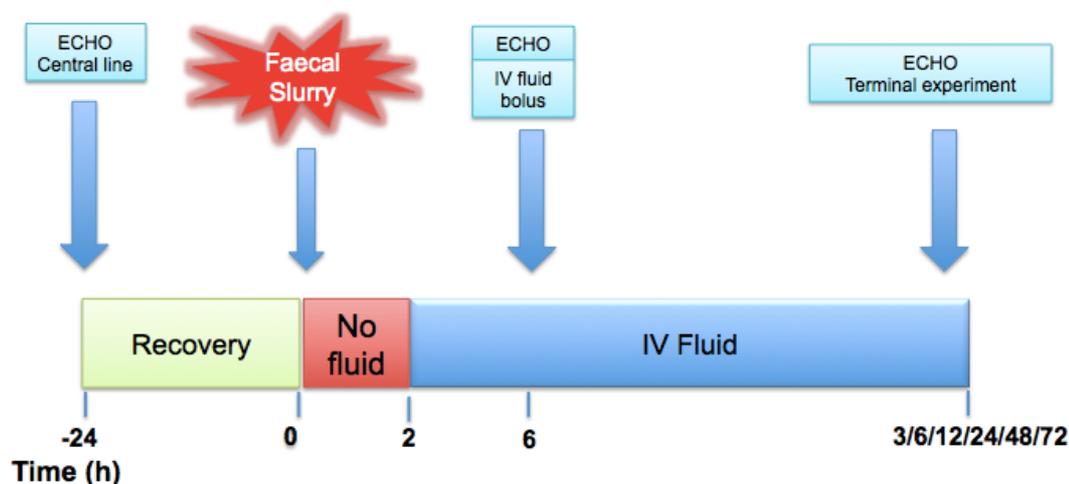
Figure 4 Diagrammatic representation of the time course of experiments. Animals are cannulated and allowed 24 h to recover. Intravenous fluid is commenced 2 h following induction of sepsis and a bolus is given at 6 h, and 24 h. Transthoracic echocardiography is performed at baseline, 6 h, and prior to the terminal experiment.

All invasive and imaging techniques were performed under general anaesthesia. Induction of anaesthesia was performed by placing an animal in a transparent plastic container filled with 5% isoflurane (Baxter Healthcare, Thetford, UK) in room air. A vaporiser (VetTech solutions, Congleton, UK) and a commercially available pump (Tetratec APS 400, Tetra GmbH, Melle, Germany) at a flow rate of 400 ml/min were used to administer the anaesthetic. Animals remained spontaneously breathing throughout.

Following loss of the righting reflex, animals were placed in the supine position on a heated mat. Core (rectal) temperature was monitored continuously using a TES 1319 thermometer (TES Electrical Electronic Corp, Taipei, Taiwan) and a heated lamp used to maintain core temperature between 36-37.5°C. Anaesthesia was maintained at a level (typically 2% isoflurane) that was adequate to abrogate the withdrawal reflex to pain.

Under strict aseptic technique, the neck, chest and left flank were shaved and sprayed with 70% ethanol. A 2cm vertical incision was made on the ventral aspect of the neck,

and the salivary glands separated by blunt dissection. The right internal jugular vein was isolated and cannulated using PVC tubing (outer diameter 0.96 mm) (Biocorp Ltd, Huntingdale, Australia). The central venous cannula (CVC) was secured with 2.0 silk sutures and flushed with 0.1 ml saline and a small quantity of blood drawn back to ensure correct placement and patency of the line. The line was tunneled subcutaneously to exit the skin at the nape of the neck. A swivel/tether system (InsTech, Plymouth Meeting, PA, USA) was secured to the neck by four 2-0 silk sutures (Ethicon Inc, Somerville, NJ, USA). Surgical incision sites were sutured using 3.0 silk sutures. N-saline was infused at 0.1 ml/hr to maintain patency. Prior to recovery from anaesthesia, 0.05mg/kg buprenorphine (Vetergesic, Reckitt Benckiser, York) was administered subcutaneously for ongoing pain relief.

Rats were then placed in individual cages mounted on the tether/swivel system to secure the intravenous catheter and allow unimpeded movement around the cage on awakening from anaesthesia. The animals had free access to food and water.and were scored at least four times daily. The clinical score has been previously validated in our lab (Table 6) (Brealey et al. 2004). A cumulative score was calculated and animals with a score of ≥4 or were culled to avoid excessive suffering. Animals culled prematurely, but which survived >90% of the predetermined time point, were included in the analysis. Peri-mortem animals were excluded from analysis (typically animals with a core body temperature <35°C).

Characteristic	Score*
Hunched	0- 1
Bloated	0- 1
Conjunctival injection	0- 1
Piloerection	0- 1
Lack of movement	0- 2
Lack of alertness	0- 2

* Score range from 0 (absent), 1 (present), and 2 (marked presence)

Table 6: Clinical scoring characteristics

4.2.2   Induction of sepsis

At 24 h post-CVC insertion, sepsis was induced by intraperitoneal injection of faecal slurry. Animals were re-anaesthetized briefly to received 3-5 μl/kg of fecal slurry (diluted 1-in-8 in 0.9% saline), injected using a 19-gauge needle into the right lower quadrant of the abdomen after raising a skin fold to avoid bowel perforation. A similar procedure was not carried out in sham animals to avoid inadvertent perforation of the bowel. Clinical scoring was performed at 2 h, and every 4 h thereafter.

4.2.3   Fluid therapy

Fluid resuscitation at 10 ml/kg/h was initiated from 2 hours' post-induction of sepsis. Sham animals received a similar fluid regimen. Starch-based solutions were avoided in view of potential nephrotoxicity. Similarly, chloride-rich solutions (0.9% saline) were avoided to avoid any adverse renal effects including reduced glomerular filtration rate (Wilcox 1983). Previous experience within the lab has shown that septic animals significantly reduce their oral food consumption and succumb to hypoglycaemia. A 1:1 mix of 5% glucose and a Hartmann's solution were used (

Table 7).

The optimal volume and rate of fluid administration to maintain intravascular volume based on echo parameters has been previously determined by the lab (Rudiger et al. 2013). To recreate a clinical scenario, intravenous fluid administration was started 2 hours following sepsis at 10 ml/kg/h. This was halved to 5 ml/kg/h at 24 h and to 2.5 ml/kg/h at 48 h. A 20 ml/kg fluid bolus was administered at 6 h, and 10 ml/kg fluid bolus at 24 h at a rate of 1 ml/min. Prior to each fluid bolus (and at the terminal timepoint), transthoracic echocardiography was performed.

	Serum	0.9% Saline	Hartmann's Solution	5% dextrose
Sodium (mmol/L)	135 - 147	154	131	0
Chloride (mmol/L)	98 - 106	154	111	0
Lactate (mmol/L)	< 2.0	0	29	0
Potassium (mmol/L)	3.5 – 5.5	0	5	0
Calcium (mmol/L)	2.1 – 2.8	0	2	0
Bicarbonate (mmol/L)	22 - 28	0	0	0
Glucose (mmol/L)	4 - 7	0	0	278
Osmolarity (mOsm/L)	280 - 195	300	279	272
pH (at room temperature)	7.35 – 7.45	5.5	6.5	4.3

Table 7 Composition and pH of different solutions compared to serum

Several rodent models of sepsis examining renal function have not given fluid, or included only a single bolus of subcutaneous fluid (Langenberg et al. 2007). This raises the possibility of hypovolaemia being a significant confounding factor in the pathogenesis of AKI. A separate experiment was therefore performed to ascertain the impact of this fluid resuscitation (a clinically relevant intervention) on the natural history of sepsis-induced AKI in my rat model. Septic animals without fluid resuscitation were culled at 6 hours (n=6 per group).

4.2.4 Slurry dose finding study

The dose of slurry producing a near-100% survival rate at 24h was determined to avoid a selection bias where only animals with a less profound septic response would be included in the analysis of renal haemodynamics. Doses ranged from 3-5 μl/Kg, based on previous

studies from the lab. I aimed to confirm a previous lab finding that a stroke volume <0.17 ml measured at 6 h could differentiate between eventual survivors and non-survivors with positive and negative predictive values of 93% and 80%, respectively (Rudiger et al. 2013). Cox-proportional regression analysis was performed to assess whether SV estimation at 6h could predict mortality at 24h.

4.2.5 Intermittent estimation of cardiac output and ventricular function

Prior to venous cannulation and at a subsequent timepoint (6 or 24 h post-induction of sepsis), transthoracic echocardiography was performed under a brief period of 1.2% isoflurane anaesthesia to determine global haemodynamics and left ventricular function. Scans were performed using a Vivid 7 Dimension™ device (GE Healthcare, Bedford, UK) with a 10 MHz probe recording at a depth of 2 cm. The parasternal long axis view (Figure 5) was used to obtain dimensions of the left ventricle at end-systole and end-diastole. Measurements were obtained from aortic annulus to apex. M-mode echocardiography (Figure 6) was used to obtain a parasternal short-axis view of the left ventricle (LV) in systole and diastole. Measurements were obtained from the internal dimension of the cavity. All images were recorded at 235.8 frames per second.
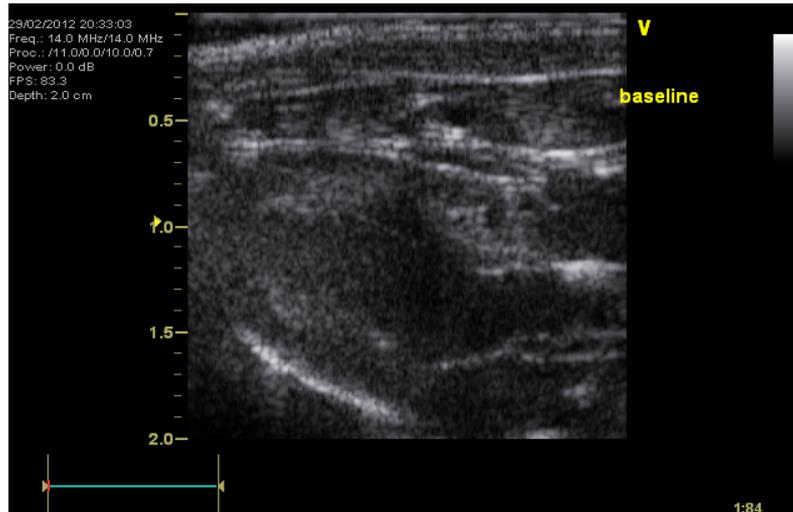
Figure 5 Parasternal long axis view for measuring ventricular length in systole and diastole. Measurements are taken from the aortic root to the apex of the heart at end systole and end diastole.
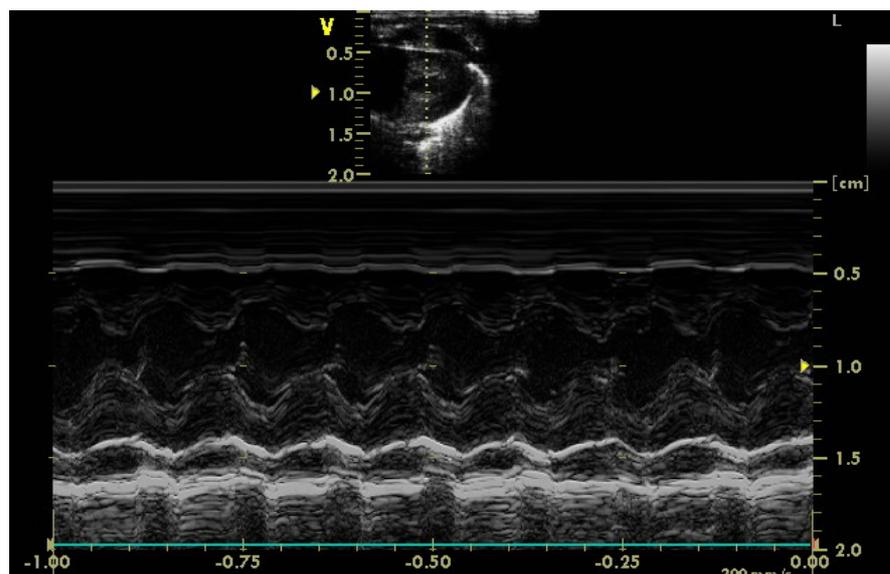
Figure 6 Parasternal short axis view for measuring ventricular width in systole and diastole. Measurements are taken at the origin of the papillary muscles at end systole and end diastole.

The volume of the left ventricle (v) in systole and diastole was calculated using the following formula for prolate spheroids:

$$V = 4/3 \, \pi * (w/2) * l/2$$

where w is ventricular width (parasternal short axis) and l is ventricular length (parasternal long axis).

Left ventricular ejection fraction (LVEF) was calculated according to the following formula:

$$LVEF = 100 * (EDV – ESV)/ EDV$$

where EDV is end-diastolic volume and ESV is end-systolic volume

Pulse wave Doppler (Figure 7) was used to measure stroke volume. Aortic blood flow was measured at the point the right carotid artery bifurcates from the aortic arch. The direction of blood flow was confirmed by colour Doppler.
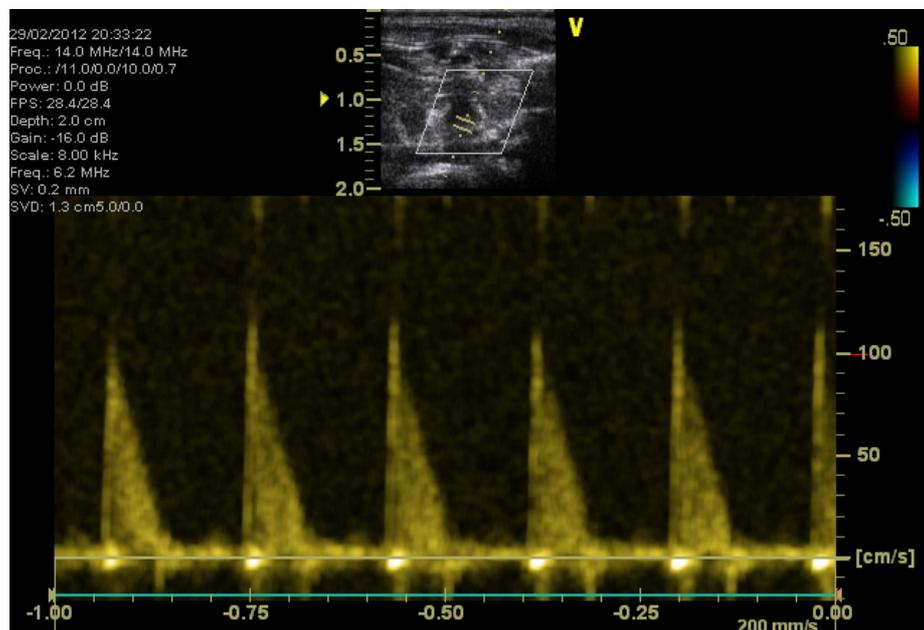
Figure 7: Blood flow measurements in the aortic arch. Colour Doppler was used to ensure correct probe placement. The waveform displays velocity (y-axis) over time (x-axis). The area under each waveform (velocity-time integral; VTI) is proportional to stroke volume.

Pulse wave Doppler was used to derive the velocity-time integral (VTI) of blood flowing through the aorta.

Stroke volume (SV) was derived from the following formula:

$$SV = VTI \times \{\pi \times (0.5 \times d)^2\}$$

where d is the aortic diameter, derived from measurements in a population of rats of similar size. The mean diameter of 0.26 cm has been previously calculated and a cross-sectional area of $(0.13)^2 \times \pi$ assumed in all calculations.

Heart rate was determined by measuring the time between six consecutive cycles from the start of each Doppler trace. Cardiac output was calculated as the product of stroke volume and heart rate. Previous work from our lab found that six consecutive cycles was sufficient to account for any respiration-induced variability of heart rate.

4.2.6 Blood pressure and blood gas analysis

Surgical tracheostomy was performed in anaesthetized, spontaneously breathing animals. The previous surgical incision was re-opened and salivary glands and muscle overlying the trachea were separated using blunt dissection. The trachea was identified and cannulated using 1.57 mm external diameter polythene tubing (Portex Ltd). The tracheal tube was attached to a T-piece through which the anaesthetic vapour was passed. The left common carotid artery was isolated, cannulated with PVC tubing with an outer diameter of 0.96mm (Biocorp Ltd, Huntingdale, NSW, Australia), and secured with 2.0 silk sutures. The arterial line was flushed with 0.1 ml n-saline and a small quantity of blood drawn back to ensure correct placement and line patency. The arterial line was connected to a pressure transducer (Powerlab, AD Instruments) for continuous monitoring of MAP and for intermittent blood sampling. The line was flushed with 0.5 ml n- saline after blood sampling.

The animal was then allowed 10-20 mins to stabilize to ensure normothermia, appropriate depth of anaesthesia, and adequate oxygenation and ventilation (Figure 8). Arterial blood gas analysis was performed with 0.2 ml taken into heparinized capillary tubes. Measurement was made of pH, sodium, potassium, ionized calcium, base excess, lactate, oxygen saturation (SaO_2), partial pressure of carbon dioxide ($PaCO_2$), and partial pressure of oxygen (PaO_2) (ABL-70 analyser, Radiometer, Copenhagen, Denmark).
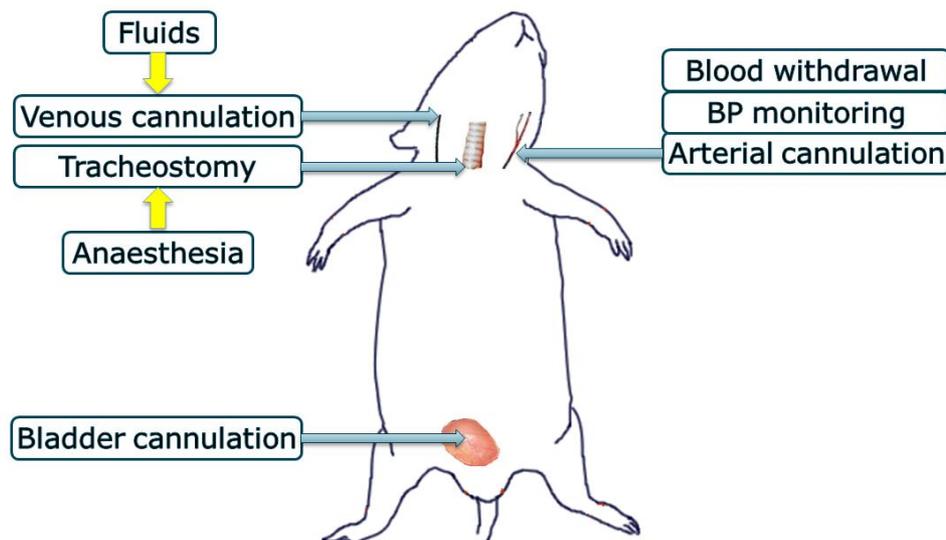
Figure 8 Model of anaesthetized rat. An arterial line is placed in the common carotid artery for invasive blood pressure monitoring and arterial blood gas sampling. A surgical tracheostomy is performed and the urinary bladder catheterized.

A lapatotomy incision was made from the lower abdomen in the midline extending to the left upper quadrant. A 22-gauge needle was used to aspirate urine via bladder puncture. The urine was snap-frozen in liquid nitrogen. The bladder apex was catheterized using polythene tubing (Portex Ltd, Hythe, Kent) of 1.57 mm external diameter inserted through a small incision at the apex and secured with 2.0 silk sutures. Moving overlying bowel to the right side of the abdominal cavity allowed access to the left kidney.

4.2.7   Organ collection and collection of serum

The left kidney was isolated from surrounding tissue by careful blunt dissection. The left renal vasculature was clamped and the kidney immediately resected. The renal capsule was stripped and the kidney divided into approximately equal thirds. The upper pole was placed into formalin and the mid and lower poles snap-frozen into liquid nitrogen. The thoracic cavity was opened and cardiac puncture performed to obtain blood. The blood was placed in a heparinized tube and centrifuged at 6500 rpm for 10 min. The serum was divided into aliquots and snap-frozen in liquid nitrogen.

4.3 In vitro techniques

4.3.1   Protein Extraction

Snap-frozen renal tissue was homogenized in radioimmunoprecipation assay homogenizing buffer (RIPA buffer; 50 mM NaCl, 1.0% IGEPAL (Octylphenyl-polyethylene glycol, Sigma Aldrich), 0.5% sodium deoxycholate, 0.1% SDS, and 50 mM Tris, pH 8.0) at an approximate ratio of 0.3g tissue with 1 ml buffer. Tissue was homogenized with a sonicator. The homogenate was centrifuged for 10 min at 14,000x g in a cold microfuge to remove tissue debris. The supernatant was pipetted and protein concentration determined using the bicinchoninic acid assay (BCA) kit (Pierce, Rockford, IL, USA) according to the manufacturer's protocol. Samples were stored at -80°C.

4.3.2   Enzyme linked immunosorbent assay (ELISA)

Serum samples were obtained during the experiment and centrifuged at 6500 g for 10 min in a lithium-heparin tube. The serum was siphoned off, snap-frozen in liquid nitrogen, and stored at -80°C. Sandwich ELISA was performed to assess serum levels of various cytokines. DuoSet ELISA kits (R&D Systems, Minneapolis, MN, USA and BD Biosciences, Oxford, UK) were used according to the manufacturer's instructions (

Analyte	Company	Units	Range-Minimum	Range Maximum	CV Intra-assay	CV inter-assay	Recovery (%) (Accuracy)
IL-1β	R&D	pg/ml	62.5	4000	N.S	N.S	40% decrease when incubated with IL-1R1
IL-4	BD	pg/ml	N.S	100	N.S	N.S	N.S
IL-6	BD	pg/ml	N.S	5000	N.S	N.S	N.S
IL-10	BD	pg/ml	N.S	1000	N.S	N.S	N.S
INF-γ	BD	pg/ml	N.S	2000	N.S	N.S	N.S
NGAL	R&D	pg/ml	78.1	5000	N.S	N.S	N.S
Cystatin C	R&D	pg/ml	125	8000	3.2	7.1	107 (98–113)
MCP-1	BD	pg/ml	N.S	2000	N.S	N.S	N.S

Table 8). ELISA was also performed to assess the presence of rat MCP-1, IL-10, IL-4, INF-γ and IL-1β in renal tissue homogenate. Tissue cytokine levels were expressed relative to the total protein content. Absorbance was read at 450 nm using a spectrophotometric ELISA plate reader (Anthos HTII; Anthos Labtec, Salzburg, Austria).

Analyte	Company	Units	Range-Minimum	Range Maximum	CV Intra-assay	CV inter-assay	Recovery (%) (Accuracy)
IL-1β	R&D	pg/ml	62.5	4000	N.S	N.S	40% decrease when

							incubated with IL-1R1
IL-4	BD	pg/ml	N.S	100	N.S	N.S	N.S
IL-6	BD	pg/ml	N.S	5000	N.S	N.S	N.S
IL-10	BD	pg/ml	N.S	1000	N.S	N.S	N.S
INF-γ	BD	pg/ml	N.S	2000	N.S	N.S	N.S
NGAL	R&D	pg/ml	78.1	5000	N.S	N.S	N.S
Cystatin C	R&D	pg/ml	125	8000	3.2	7.1	107 (98–113)
MCP-1	BD	pg/ml	N.S	2000	N.S	N.S	N.S

Table 8 ELISA analytes and specifications (N.S.: Not stated)

4.3.3 Multiplex

MILLIPLEX$^{®}_{MAP}$ multi-analyte panels (Merck Millipore, Watford, Hertfordshire, UK) were used for simultaneous detection and quantification of eight biomarkers and cytokines/chemokine in rat urine, including NGAL, cystatin C, IL-18, MCP-1, clusterin, calbindin, osteopontin, and KIM-1. The same technique was used to determine serum levels of IL-18 (**Table 9**).

MILLIPLEX$^{®}$ is a magnetic bead-based Luminex® assay that utilizes distinct sets of microspheres (fluorescent-coded beads) coated with a specific capture antibody to target the corresponding cytokine/chemokine/biomarker. Bound antigen is detected by biotinylated antibody. On addition of conjugated streptavidin-phycoerythrin (PE), the fluorescent reporter molecule, fluorescent signals from individual microspheres are quantified.

Assays were performed according to the manufacturer protocols. MILLIPEX$^{®}_{MAP}$ contains a filter plate and reagents (assay buffer, Standard, Quality Controls, 10x wash Buffer, and relevant antibody-bead vials). Briefly, 200 microlitres of well assay buffer was added to the plate and incubated at room temperature for 10 minutes. Assay buffer was removed gently by inverting the plate. 25µl of standards (serial dilution from stock) or Quality Controls were transferred into wells followed by an additional 25 µl matrix solution. 25 µl assay buffer and 25 µl rat urine were added into the sample wells. 60 µl of each antibody-bead was mixed together to a final volume of 3 ml with Bead Diluent. 25 µl of the mixed beads were transferred to each well and the plate incubated overnight at 4°C, or for 1hr at room temperature (depending on analytes). Contents apart from magnetic beads (with bound antigen) were removed and the plate washed twice. 25 µl detection antibody was added and incubated at room temperature for 2 hours. Following this, 25 µl Streptavidin-PE was added and incubated for 30 minutes. After removing the fluids and a further 2 washes, 150µl sheath fluid was added to resuspend the beads for 5 minutes. The plate

was read on a Bio-Plex 200 multiplex system (Bio-Rad, Hemel Hempstead, Hertfordshire, UK).

Analyte	Units	Minimum detectable level	Maximum detectable level	Precision: CV Intra-assay(%)	Precision: CV inter-assay(%)	Accuracy: Recovery (%)
IL-18	pg/ml	6.2	50,000	2.5	11.1	97.2
MCP-1	pg/ml	9.0	120,000	2.3	9.2	80.2
NGAL	ng/ml	0.002	10.0	<10	<10	100
Cystatin C	ng/ml	0.003	8.0	<10	<10	100
KIM-1	ng/ml	0.007	20.0	<10	<15	110
Osteopontin	ng/ml	0.008	20.0	<10	<15	92
Clusterin	ng/ml	0.307	1,500	<10	<15	126
Calbindin	ng/ml	0.079	250	<10	<15	70

Table 9 Multiplex analytes.

Recovery/ Accuracy: Represents mean percent recovery of spiked standards. *Minimum detectable concentration (MinDC)/ Sensitivity*: MinDC is calculated using MILLIPLEX Analyst. It measures the true limits of detection for an assay by mathematically determining what the empirical MinDC would be if an infinite number of standard concentrations were run for the assay under the same conditions

Intra-assay precision is generated from the mean of the %CV (coefficient of variation) from 8 reportable results across two different concentrations of analytes in a single assay

Inter-assay precision is generated from the mean of the %CVs across two different concentrations of analytes across 13 different assays

4.3.4 Biochemistry

Serum obtained at the end of each experiment was analyzed for renal function (serum urea and creatinine) and liver function (albumin, alkaline phosphatase (ALP), aspartame amino transferase (AST) and alanine amino transferase (ALT)). Samples were analyzed by the Clinical Pathology laboratory at the Royal Free Hospital, London.

4.3.5 Immunohistochemistry

Kidneys were fixed for 24-72 hours in formalin, transferred to 70% ethanol, and embedded in paraffin. Sections were then cut into 5 μm slices and mounted onto glass slides. Sections were examined using an Olympus BX4 microscope (Olympus Optical, London, UK) at x20 magnification. Ten random fields of view of the cortex were analyzed for each section. All analyses were performed blind.

4.3.5.1 Tubular injury

All sections were stained with Periodic acid-Schiff (PAS). Ten random fields of view of the cortex were analyzed for each section at x20 magnification under a light microscope. Sections were scored for acute tubular injury, glomerular injury, and interstitial infiltrate. Features of tubular injury included tubular dilatation, brush border loss, and tubular cast formation. Each feature was scored 0-3 (0- absent, 1- <33%, 2- 33- 67%, 3- >67%). The average score of the ten fields of view were totaled, the maximum tubular injury score being 9. Glomerular injury included collapsed glomeruli or glomerular thrombosis. Ten random glomeruli were examined and a score of 0 (absent) or 1 (present) assigned. The average score of the 10 fields of view were totaled. Interstitial infiltrate was scored as being absent (0) or present (1). The average score of the 10 fields of view were totaled. Two timepoints were chosen for tubular injury scoring - the early pro-inflammatory phase and the point at which serum creatinine was significantly elevated. Renal tissue from a rat that was subject to prolonged hypotension secondary to haemorrhage was used as a positive control.

4.3.5.2 Apoptosis

Apoptosis was detected by DNA fragments *in situ* using the terminal deoxyribonucleotidyl transferse (TdT)-mediated biotin-16-dUTP nick-end labelling (TUNEL assay). The commercially available TACS® TdT In Situ Apoptosis Detection Kit (R&D Systems) was used and recommended protocols followed. Briefly, slides were dewaxed and rehydrated through graded xylene and ethanol, respectively. Slides were immersed in 1x PBS for 10 min. Slides were covered with 50 µl of Proteinase K Solution for 30 minutes, then washed twice in deionized water for 2 min each time. Slides were immersed in Quenching Solution for 5 min, washed in 1x PBS for 1 min, then immersed in 1x TdT Labeling Buffer for 5 min before covering with 50 µl of Labeling Reaction Mix for 60 min at $37^{o}C$ in a humidity chamber. Placing slides in 1x TdT Stop Buffer for 5 min stopped the reaction. Slides were then washed twice in deionized H_2O for 5 min each, covered with 50 µl of Strep-HRP Solution and incubated for 10 min at $37^{o}C$ in a Humidity Chamber to avoid evaporation. Slides were washed twice more then immersed in DAB solution for 7 min, . washed twice in deionized H_2O, for 2 min each and finally immersed in 1% Methyl Green for up to 5 min. Each slide was dipped 10 times in two changes of deionized H_2O, followed by 95%, then 100% ethanol, and finally 2 changes of o-xylene. Glass coverslips were mounted using mounting medium Eukitt (VWR International). Sections were examined using an Olympus microscope (Model, Olympus Optical, London, UK) at x20 magnification. Ten random fields of view of the cortex were analyzed for each section. The total number of apoptotic bodies per x20 field were counted manually and an average taken for each group. A total of three slides for the septic groups (with at least one from the poor prognosis subgroup) and 2 from the naïve groups from timepoints 6, 12, 24, 48, and 72 hours were selected. All analyses were performed blind.

4.3.5.3 Macrophage infiltration

Sections were stained to assess macrophage infiltration. Slides were dewaxed and rehydrated through graded xylene and ethanol, respectively. Antigen retrieval was performed by placing slides in 0.01M sodium citrate buffer heated to $90^{o}C$ in a water bath

for 15 min. Following immersion in 50% methanol containing 0.3% H_2O_2 for 1 h to block endogenous peroxidase activity, non-specific binding was blocked by incubation with 20% normal goat serum (NGS) diluted in PBS. The primary antibody (mAb ED-1 CD68 mouse anti-rat, Serotec, Kidlington, Oxon) was diluted 1:500 in PBS and incubated for 1 h at room temperature. Slides were then incubated with biotinylated goat anti-mouse (Dako) for 45 min, then washed in PBS-tween to remove excessive, unbound antibody. Antibody binding was visualized using 3,3'-diaminobenzidene (Dako). Sections were counterstained with haematoxylin, then dehydrated, mounted with Eukitt (VWR International) and left to dry overnight. One section from each sample was incubated with antibody diluent instead of primary antibody and served as control. Sections were examined at x20 magnification. Ten random fields of view of the cortex were analyzed per section. The total number of macrophages per x20 field and the number of macrophages per glomerular cross-section were assessed semi-quantitatively using a Color Coolview camera (Photonic Sciences, Robertsbridge, East Sussex) and Image Pro Plus software (Media Cybernetics, Silver Spring, MD, USA). A total of six slides for the septic groups and from the naïve groups from timepoints 3, 6, 12, 24, 48, and 72 h were selected. All analyses were performed blind. Spleen tissue from a septic animal at 6 h was used as a positive control.

4.4 Statistics

All statistical analyses were performed using SPSS (IBM. Version 20) and graphs drawn using Graphpad Prism (GraphPad Software, Version 5.0d). Normality of continuous data was assessed using the Shapiro-Wilk test. Continuous variables are presented as means (standard deviation) where parametric, and median (interquartile range) where non-parametric. Parametric data were compared using unpaired Student's t-test, whereas non-parametric data were compared using the Mann Whitney U test for comparison of continuous data between 2 groups. For comparison of continuous variables between more than two groups, one-way analysis of variance (ANOVA) with post hoc Tukey's test is used. Cox-proportional regression was used to assess the sensitivity and specificity of

different haemodynamic parameters on survival. Pearson's correlation was performed to assess the degree of correlation between serum and urine levels of biomarkers (cystatin C, NGAL, IL-18, and MCP-1). A p-value <0.05 was taken as statistically significant.

4.5 Results

4.5.1 Dose finding study

Doses of slurry varied from 3 ml/kg (n=7), 4 ml/kg (n=7), 4.5 ml/kg (n=6), and 5 ml/kg (n=6). There was a stepwise dose-related decrease in 24 h survival, ranging from 100% with 3 ml/kg to 33% with a 5 ml/kg dose (**Table 10**). Cox-proportional regression revealed that a SV of 0.195 ml at 6 h predicted mortality at 24 h with a sensitivity of 60%, specificity of 90% and an area under the receiver operator curve of 0.84 (hazard ratio=6.6; p=0.008)**.** Based on these results, a faecal slurry dose of 4.5 ml/kg was used for the 72 hour characterization study.

Slurry dose (ml/kg)	Number	Survival at 24hrs
3	7	100%
4	7	71%
4.5	6	67%
5	6	33%

Table 10 Mortality associated with different faecal slurry doses

4.5.2 Systemic variables

There were no significant differences in baseline data (weight, temperature, HR, SV, and CO) between groups. By 3hrs post induction of sepsis, there was a significant fall in

stroke volume and cardiac output. Septic animals mounted a significant tachycardia by 6hrs, which persisted at 24hrs. This paralleled the increase in core body temperature. Mean arterial pressure remained relatively stable in the septic animals predicted to live but was higher at 6h and 12h in the septic animals predicted to die. This was associated with an increase systemic vascular resistance (SVR,) a lower global DO_2 and elevated arterial lactate.

The global DO_2 was significantly elevated at early time points (3hr and 6hr) in animals that were predicted to survive compared to animals that were predicted to die. Along with SV, global DO_2 and SVR were able to distinguish between septic animals that were predicted to live and those predicted to die (however SV and global DO_2 are coupled). By 48hrs, SV, CO, HR, and core temperature normalized among septic animals, and these remained stable till 72hrs (Figure 9).
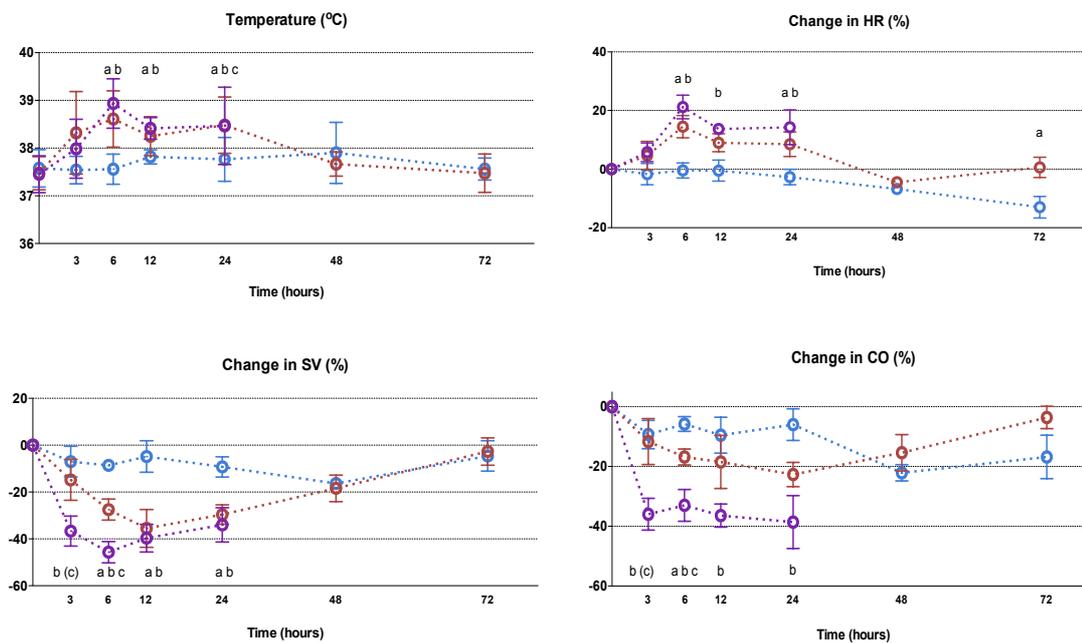
Figure 9 72hour characterization - Systemic variables following induction of experimental sepsis in Wistar rats (sham, sepsis good prognosis, sepsis poor prognosis). Septic animals develop a tachycardia, fall in stroke volume, increase in systemic vascular resistance, and fever early (3-6hr), which resolves from 24hr to reach baseline values at 72hr. Changes in global oxygen delivery and mean arterial pressure are smaller and more transient.

(a: $p < 0.05$ sham vs good prognosis; b: $p < 0.05$ sham vs poor prognosis; c: $p < 0.05$ good vs poor prognosis)

4.5.3 Biochemistry

Biochemistry data are shown below (Figure 10). Serum albumin was significantly lower in septic animals predicted to die from the 3 h time point with a progressive fall thereafter. Among septic animals predicted to live, serum albumin was lower from 12 – 48 h compared to sham animals. Serum glucose was also lower from 6h, likely to be due to decreased carbohydrate consumption and depletion of liver glycogen stores. The fall in base excess is seen early (from 3 h) and similar to the clinical scenario. This is due to an increase in inorganic acids being formed (e.g. ketoacids in starvation and lactate) along with the impaired ability of the kidney to excrete acids.

There was a very early peak (3 h) in serum urea in septic animals predicted to die compared to sham animals. This is consistent with urea as a marker of volume depletion and rising before serum creatinine rises. Once fluid resuscitation commenced (2 h) there was a progressive fall in urea that normalized by 12 h. However, once renal dysfunction (likely fall in GFR) ensues, serum urea rises but to a lesser amount. In contrast, serum creatinine, rises initially due to haemoconcentration/intravascular volume depletion (at 3 h), falls back to baseline once fluid resuscitation is commenced, and rises once again (at 24 h) likely due to a fall in GFR
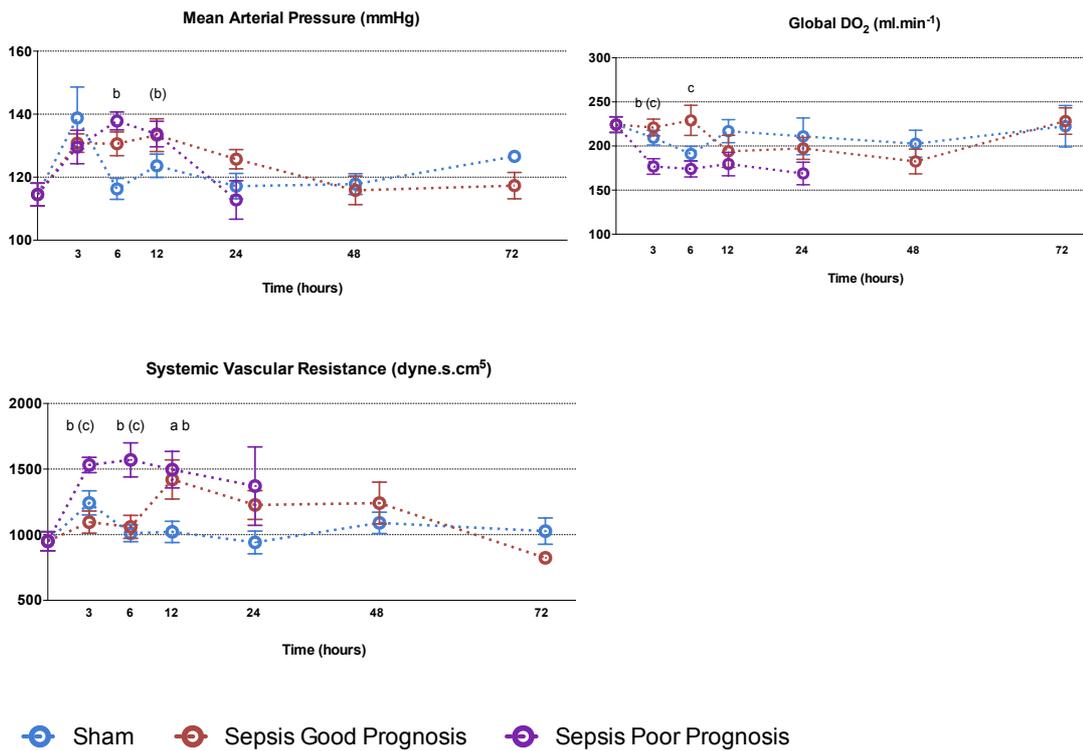
Figure 10 72 hour characterization- Biochemistry following induction of experimental sepsis in Wistar rats (sham, sepsis good prognosis, sepsis poor prognosis). Biochemical changes occur from 3hr. Apart from serum urea, changes are maximal at 24hrs followed by recovery to baseline values till 72hr. The early rise in urea, creatinine, and lactate fall promptly after fluid resuscitation is commenced, demonstrating early haemoconcentration.

(a: p<0.05 sham vs. good prognosis; b: p<0.05 sham vs. poor prognosis; c: p<0.05 good vs. poor prognosis)

4.5.4 Serum Cytokines

The pro-inflammatory serum cytokine IL-1β was significantly elevated by 3 h. This was maintained until 12 h, followed by a gradual fall to normal by 48 h. There was no difference in IL-1β levels between animals predicted to survive or die. Serum IL-6 levels were elevated at 3 h only in animals predicted to die. By 6 h, IL-6 levels peaked and were significantly elevated in all septic animals. IL-6 levels fell earlier than IL-1β (6 h). By 24 h, IL-6 levels had returned to baseline values in animals predicted to survive. There were no clear differences in IL-18 levels between sham and septic animals, which were widely variable between animals. Serum INF-γ was only detectable at 6 h, after the peak rise in IL-18. Serum MCP-1 levels followed a similar pattern to IL-1β. The anti-inflammatory cytokine IL-10 was elevated from 3 h in the animals predicted to die and in all septic animals by 6 h. IL-10 levels stayed elevated till 72 h compared to sham animals. Serum IL-4 levels could not be detected at any point while INF-γ levels were detected in only a few septic animals at 6 h. Therefore the overall balance of cytokines changed from a pro- to an anti-inflammatory profile in the acute and resolution phases of sepsis, respectively (Figure 11)
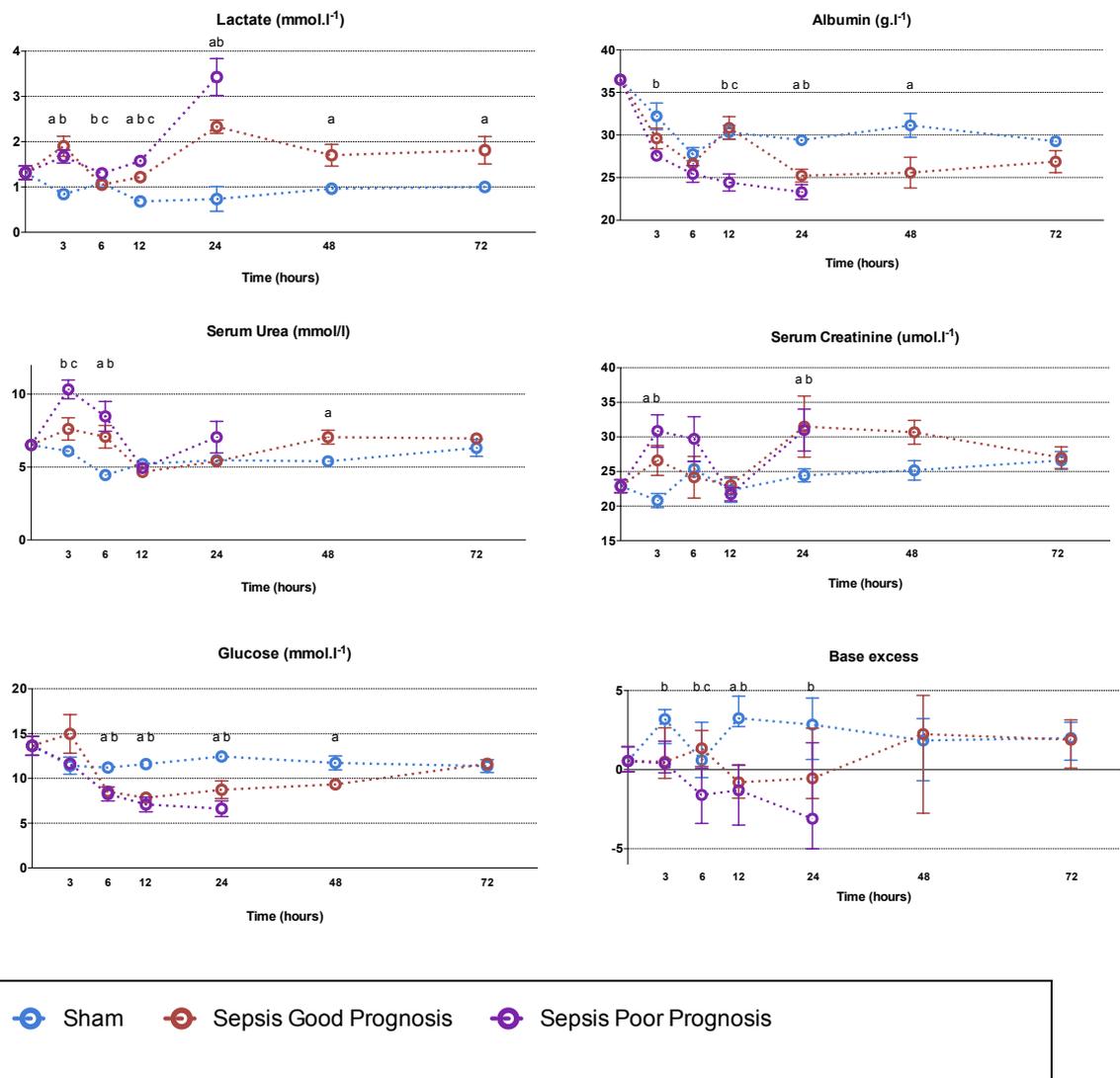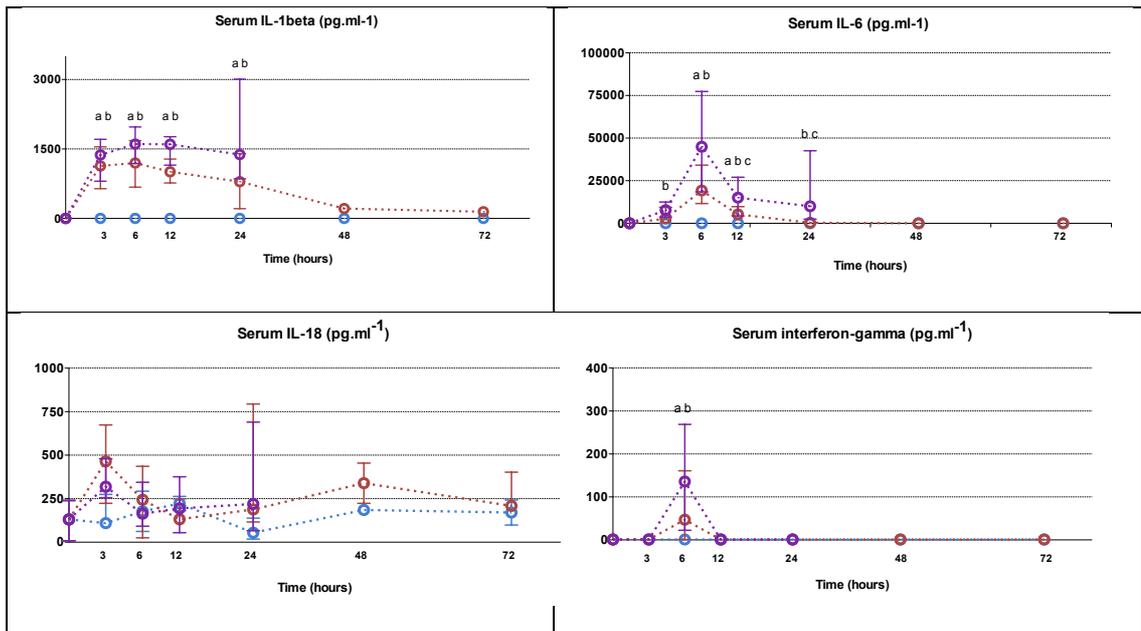
Figure 11 Characterization- Serum cytokines following induction of experimental sepsis in Wistar rats (sham, sepsis good prognosis, sepsis poor prognosis). There is a variable pattern of proinflammatory cytokine kinetics. IL-1β and IL-6 rise early (3 h) and remain elevated for 24 h. INF-γ is elevated only at 6 h, whereas IL-18 is not significantly elevated. Anti-inflammatory cytokine IL-10 begins to rise by 3 h but remains elevated through to resolution of sepsis at 72 h.

(a: p<0.05 sham vs good prognosis; b: p<0.05 sham vs poor prognosis; c: p<0.05 good vs poor prognosis)

4.5.5 Renal Cytokines

Renal IL-β was elevated by 3 h and 6 h in septic animals predicted to die and survive, respectively. From 12 h there was no difference in renal cytokine levels between septic and sham animals. Renal MCP-1 demonstrated a rise from baseline to peak at 24 h, when it was higher in septic predicted survivors compared to sham animals. Renal INF-γ, IL-4, and IL-10 demonstrated no convincing trends or differences between sham and septic animals. Sham animals demonstrated variability in these renal cytokine values (Figure 12).

Figure 12 72 hour characterization - Renal cytokines following induction of experimental sepsis in Wistar rats (sham, sepsis good prognosis, sepsis poor prognosis). Renal IL-β was elevated by 3 h and 6 h in septic animals predicted to die and survive, respectively. From 12 h there was no difference in renal cytokine levels between septic and sham animals. Renal INF-γ, IL-4, and IL-10 levels were variable.

(a: p<0.05 sham vs good prognosis; b: p<0.05 sham vs poor prognosis; c: p<0.05 good vs poor prognosis)

4.5.6 Biomarkers

Eight different urine biomarkers were measured in addition to urine Na$^+$ and creatinine concentrations (the latter two in fewer animals due to lack of urine volume) (**Figure 13**). All biomarkers related to PTEC injury were altered to varied degrees and with different kinetics. After a recovery period, all biomarkers returned to levels approaching those observed in sham animals. Apart from urine osteopontin and IL-18, all other urine biomarkers were elevated and at an earlier time point to serum creatinine (at 24 h).

Urine NGAL was the most sensitive marker amongst those studied, rising from 3 h to 24 h. Although other biomarkers were also elevated before the rise in serum creatinine, the magnitude of their rise was much less compared to NGAL. Urine NGAL was also the earliest biomarker to rise. Urine KIM-1 was the only biomarker to show a greater rise in animals predicted to die. This was seen at 12 h, when serum creatinine was identical between septic and sham animals. Urine IL-18 has been analyzed in septic AKI, but has been less promising than urine NGAL (Kashani et al. 2013). We demonstrated similar findings. The rise in urine IL-18 occurred at 12 h but did not reach significance. Urine cystatin C. a marker of GFR and intact tubular reabsorption, was raised between 12-48 h in septic animals.

I also measured two markers of distal tubular injury, namely calbindin and osteopontin. Neither have been previously evaluated in septic AKI. Interestingly, urine calbindin was elevated at 6-12 h whereas urine ostopontin did not differ between septic and sham animals. Although septic AKI is typically associated with PTEC injury, there may be some DTEC injury. Urine MCP-1 has also not been characterized in septic AKI. I found a rise in urine MCP-1 levels between 12-18 h.

A fall in urine KIM-1 and calbindin at 24 h may predict renal recovery. Although this timepoint coincided with the rise in serum creatinine, it was associated with improvement in clinical parameters (cardiovascular) and a fall in pro-inflammatory cytokines (Il-1β, IL-6, IL-18).

Urine NGAL (ng.ml^{-1})

Urine Cystatin C (microg.ml^{-1})

Urine IL-18 (pg.ml^{-1})

Urine MCP-1 (pg.ml^{-1})

Urine Calbindin (ng.ml^{-1})

Urine Osteopontin (ng.ml^{-1})

Urine Clusterin (ng.ml^{-1})
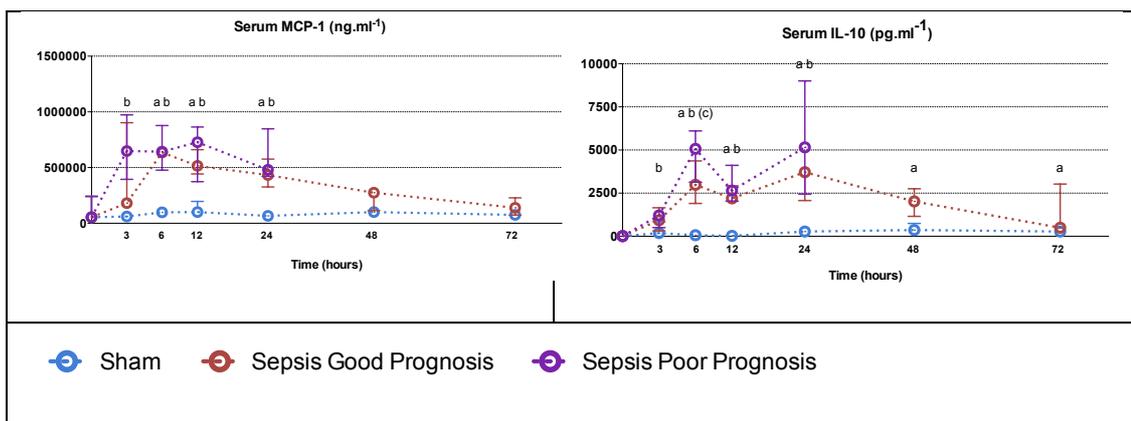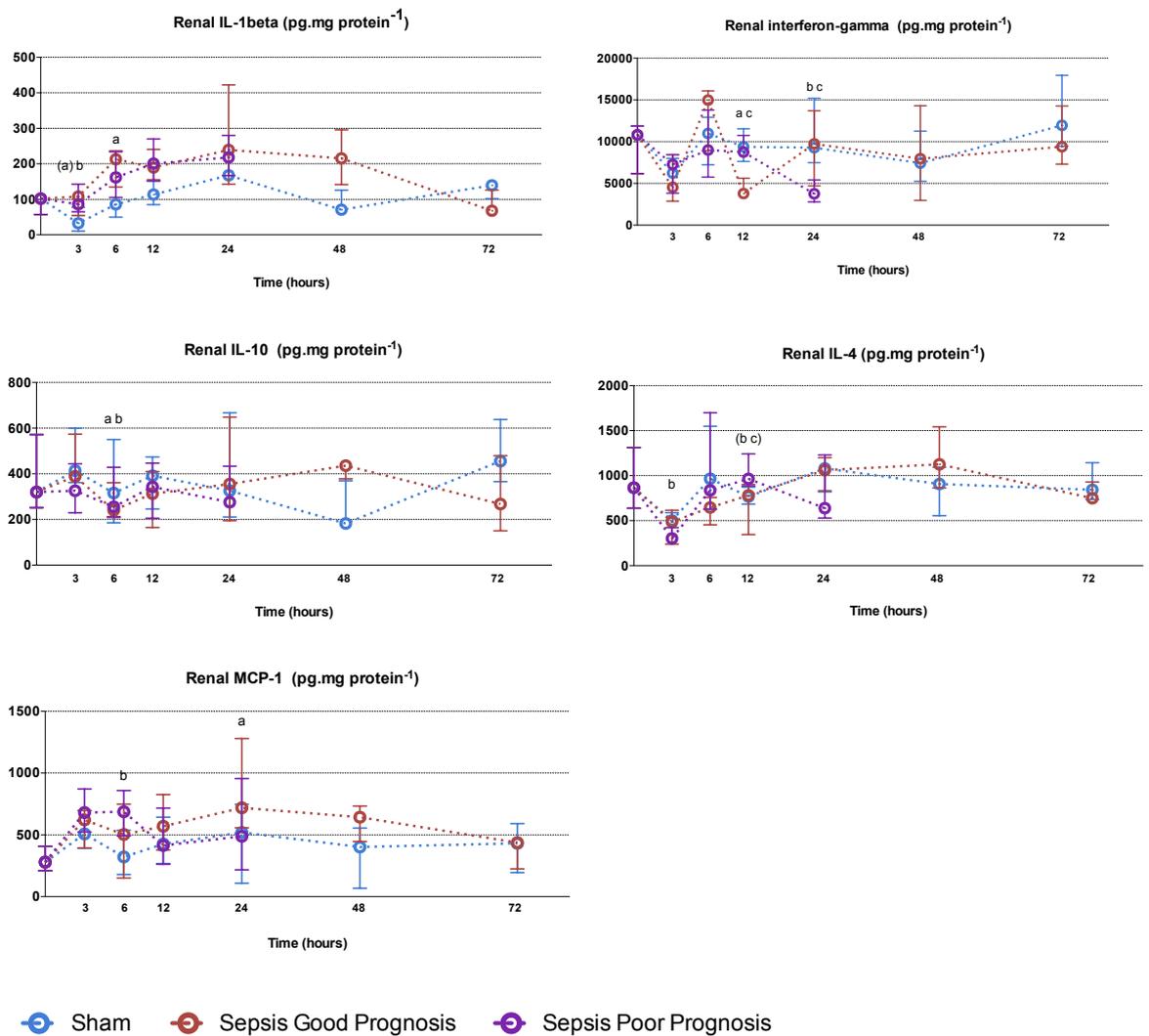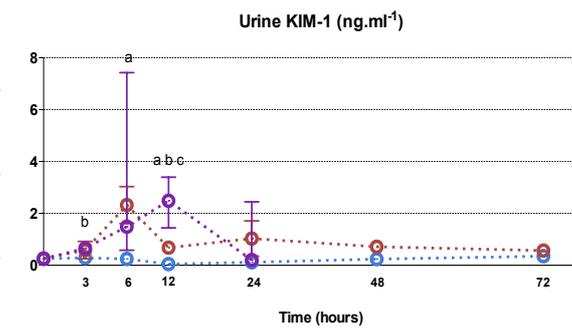
Urine KIM-1 (ng.ml^{-1})
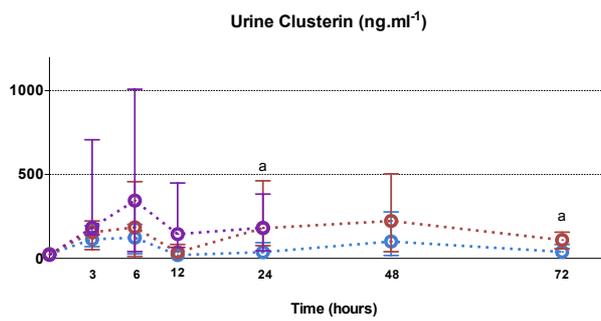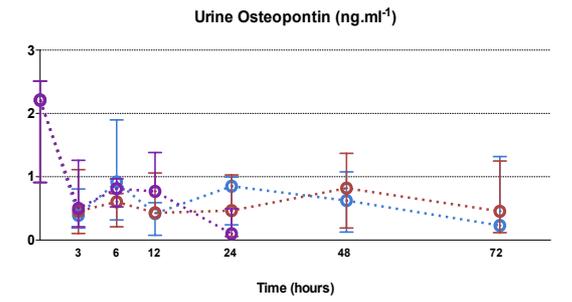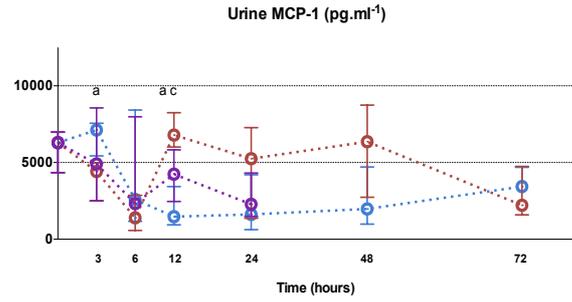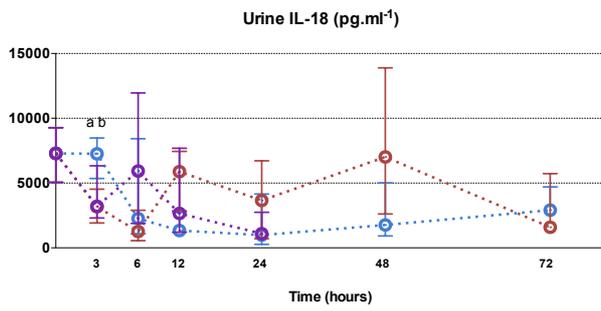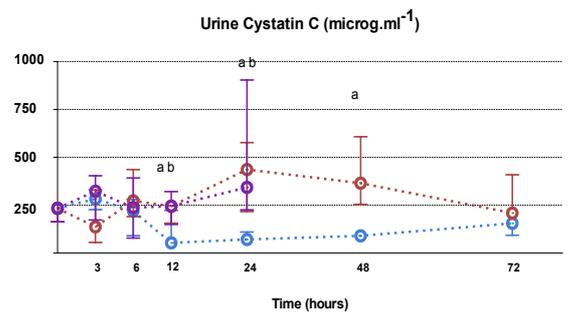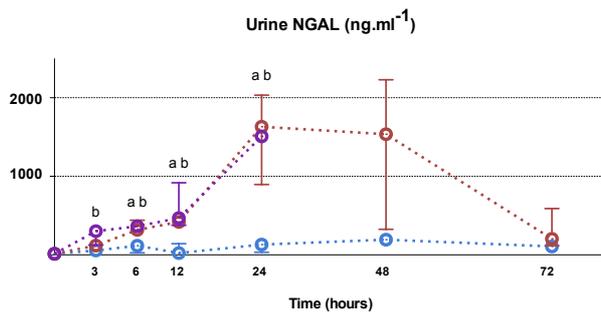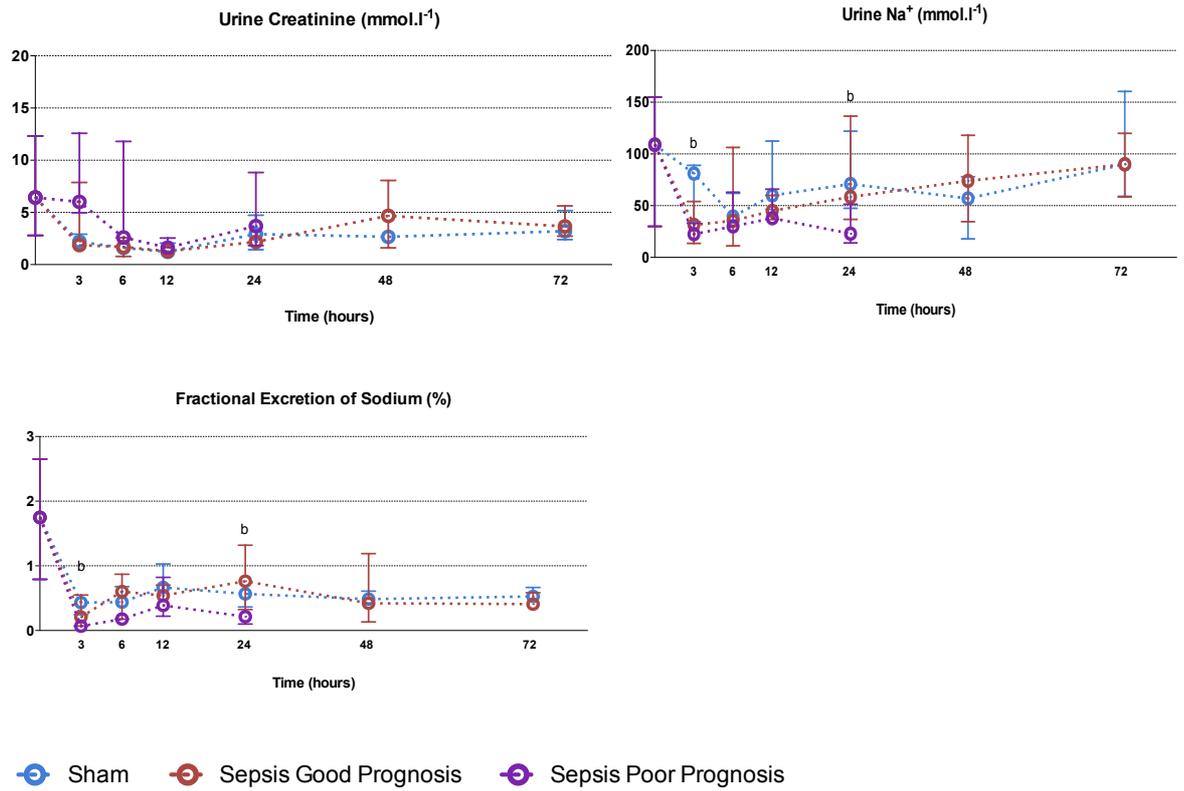
Figure 13 72 hour characterization - Urine biomarkers following induction of experimental sepsis in Wistar rats (sham, sepsis good prognosis, sepsis poor prognosis). Urine NGAL was the most sensitive marker, rising from 3 h to 24 h. Other biomarkers were also elevated before the rise in serum creatinine, though the magnitude of their rise was much less compared to NGAL. Urine KIM-1 was the only biomarker to show a greater rise in animals predicted to die. Urine IL-18 and osteopontin were not elevated in septic animals. (a: $p<0.05$ sham vs good prognosis; b: $p<0.05$ sham vs poor prognosis; c: $p<0.05$ good vs poor prognosis)

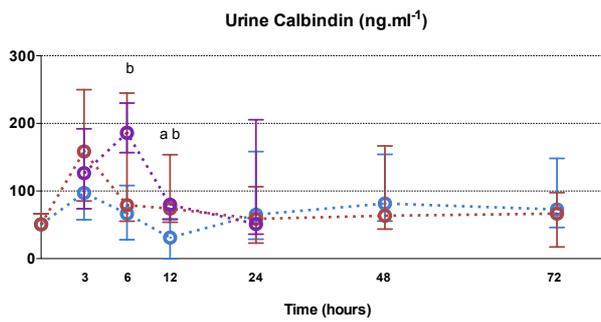### 4.5.7 Serum biomarkers
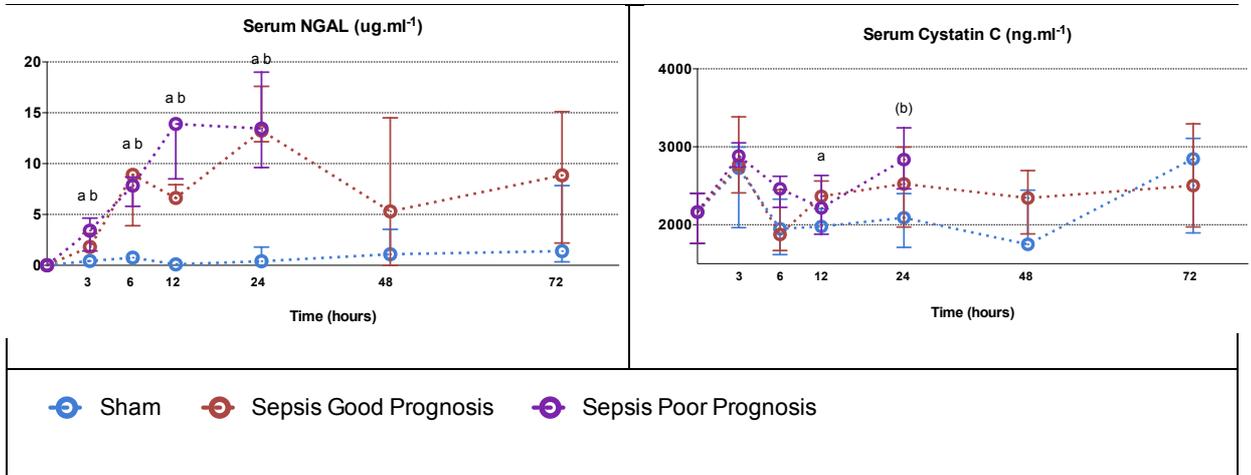
Figure 14 72 hour characterization - Serum biomarkers following induction of experimental sepsis in Wistar rats (sham, sepsis good prognosis, sepsis poor prognosis). Serum NGAL rose early at 3 h whereas serum cystatin C rises at 12 h. Both biomarkers were elevated till 24 h.

(a: $p < 0.05$ sham vs good prognosis; b: $p < 0.05$ sham vs poor prognosis; c: $p < 0.05$ good vs poor prognosis)

Serum NGAL rose early at 3 h (Figure 14). However, this may reflect neutrophil activation rather than tubular injury. Serum cystatin C rises at 12 h at a point when serum creatinine falls towards baseline. This interesting finding may reflect a fall in GFR (and hence rise in serum cystatin C) along with decreased creatinine production.

4.5.7.1 Correlation between urine and serum biomarkers

	All		Septic animals only	
	r^2	p- value	r^2	p- value
MCP-1	0.122	0.356	0.051	0.756
NGAL	0.713	<0.001	0.654	<0.001
IL-18	0.014	0.908	0.016	0.914
Cystatin C	0.059	0.655	0.072	0.660

Table 11 Correlations between paired urine and serum biomarkers

It is unclear to what extent the urine biomarkers reflect what is filtered from the circulation and eliminated in the urine, as opposed to *de novo* production within the kidney. There was no correlation between urine and serum levels of IL-18, MCP-1, and cystatin C (Table 11). There was, however, a positive correlation between urine and serum NGAL values, even when including only septic animals. Urine NGAL, Cystatin C, and Clusterin were the only biomarkers to correlate with serum creatinine. None of the urine biomarkers had a correlation defined as $r^2 > 0.5$ with serum creatinine (**Table 12**). Correlations between different urine biomarkers were assessed. Of 16 positive correlations between the urine biomarkers, only four were positive as defined by an r^2 value >0.5 (**Table 13**).

Urine biomarker	r^2	p- value
NGAL	0.318	0.008
Cystatin C	0.304	0.008
Clusterin	0.274	0.011

Table 12 Positive correlations with serum creatinine

Urine biomarker	r^2	p- value
Cystatin C vs. NGAL	0.766	< 0.001
Cystatin C vs. KIM-1	0.516	< 0.001
IL-18 vs. MCP-1	0.869	< 0.001
Clusterin vs. KIM-1	0.628	< 0.001

Table 13 Significantly positive correlations (r^2 > 0.5) between urine biomarkers

4.5.8 Renal Histology

4.5.8.1 Tubular injury

Histological sections were scored at two timepoints for assessment of tubular injury. The 6 h point was chosen as an early phase and the 24 h point taken as the point at which serum creatinine was significantly elevated. The tubular injury score was similar between septic and sham-operated animals at 6 h (1.10±0.46 vs. 0.63±0.52; p=0.26). A higher tubular injury score at 24 h was seen in septic animals compared to sham (1.97±0.83 vs. 0.63±0.52; p=0.001). Despite this higher score, the degree of injury was still relatively mild (the highest possible score being 9). Predominant findings included mild tubular dilatation and brush border loss. Tubular injury was patchy, among areas of normal histology. There was no evidence of tubular cell necrosis, interstitial cellular infiltrate, glomerular collapse, or glomerular thrombosis. Tubular cast formation, when present, was sporadic (Figure 15).
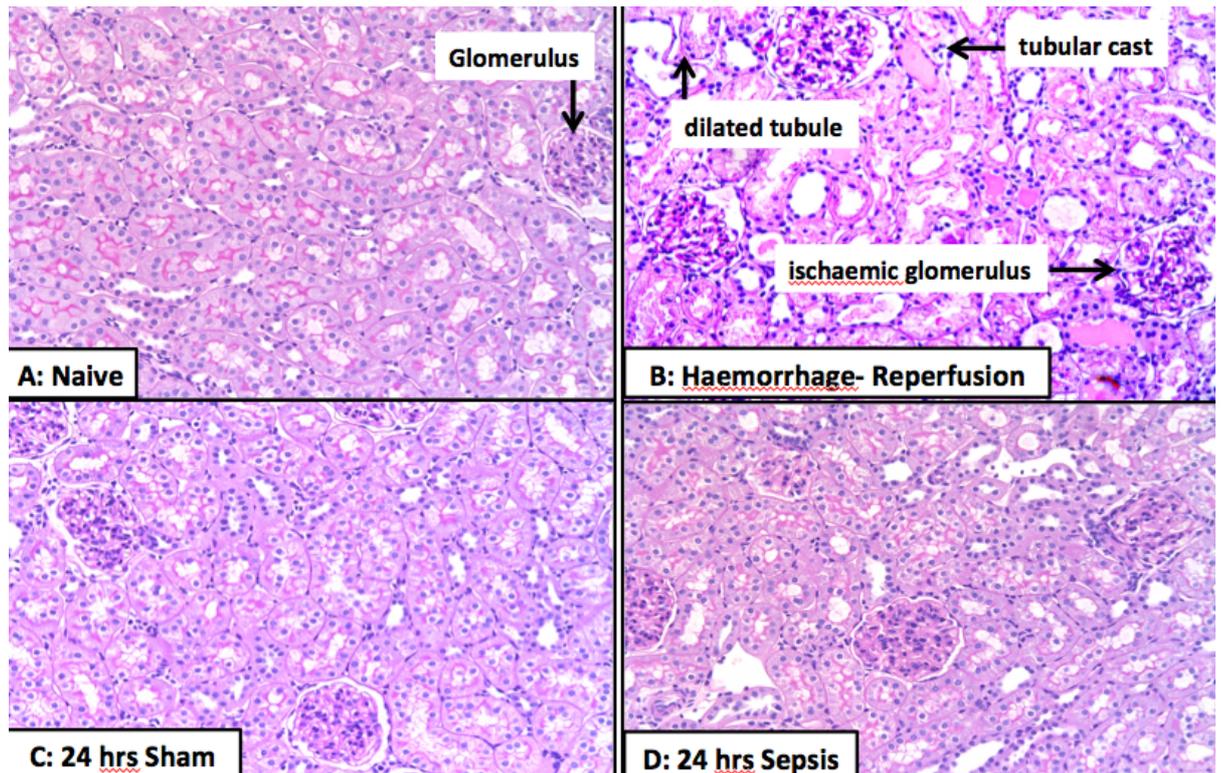
Figure 15 Histological assessment of rat kidneys for renal damage (PAS-staining, magnification x 20). A. Naive renal tissue without any significant damage. B. Renal tissue obtained from a haemorrhage-reperfusion model (A. Dyson, UCL), showing several characteristics of acute tubular injury including dilated tubules, ischemic glomeruli and tubular casts. C. Kidney section from a 24h sham-operated animal. D. Kidney section from a 24h septic rat.

4.5.8.2 Apoptosis

TUNEL stain revealed minimal presence of cell death, with an average of two TUNEL positive cells per 20x magnification field. Where present, TUNEL positive cells were within proximal tubular epithelial cells (Figure 16).
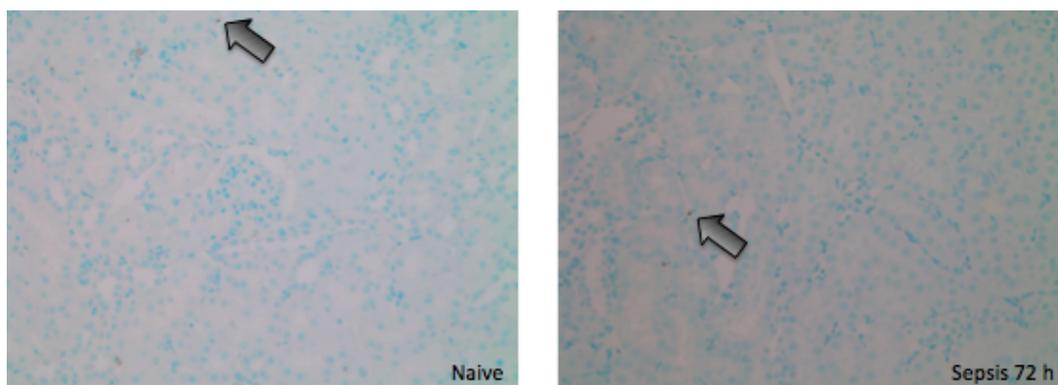
Figure 16 TUNEL stain of renal tissue. Apoptotic cells stain dark brown (arrow). Apoptotic bodies seen mainly in proximal tubular epithelial cells. No significant difference in apoptotic bodies seen between naïve and septic kidneys. (x20 magnification).

4.5.8.3 Macrophage infiltration

Naive kidneys revealed no or minimal staining of macrophages. When present, macrophages were found within the interstitium. There was significant infiltration of renal macrophages within the interstitium of septic animals at 72 h (Figure 17), though there was a trend towards an increase in renal macrophages from 24 h. Glomerular macrophages were significantly elevated at 72 h. There was wide variability in the presence of macrophages among septic animals. The rise in renal macrophages was associated with a fall in serum-renal MCP-1 ratio (ratio between serum MCP-1 (ng/ml) and renal MCP-1 (pg/mg protein) (Figure 18). This chemokine gradient may be responsible for local macrophage recruitment.
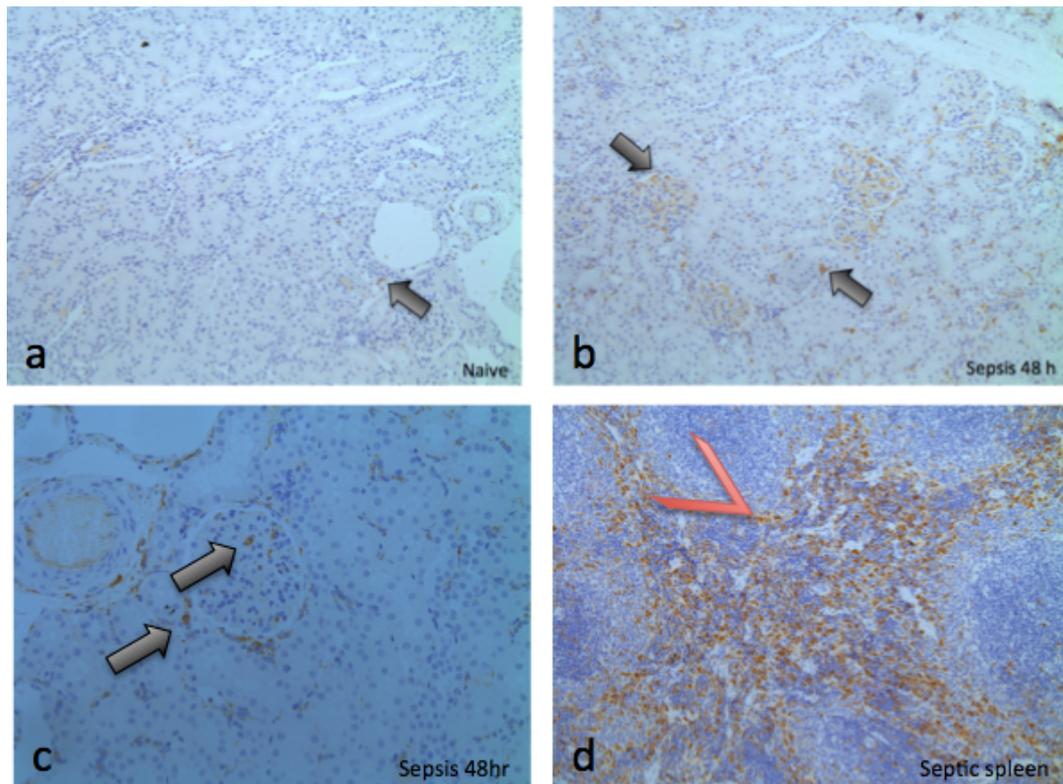
Figure 17 Macrophage infiltration. (a).Macrophages (stained brown colour) are seen within the renal interstitium and glomeruli of naïve and (b). septic animals (black arrows) (x10 magnification). The quantity and intensity of macrophage infiltration is much greater in the septic kidney. (c). Higher magnification of macrophages seen within the interstitium and glomeruli (x20 magnification). (d). Septic spleen used as a positive control (x10 magnification).
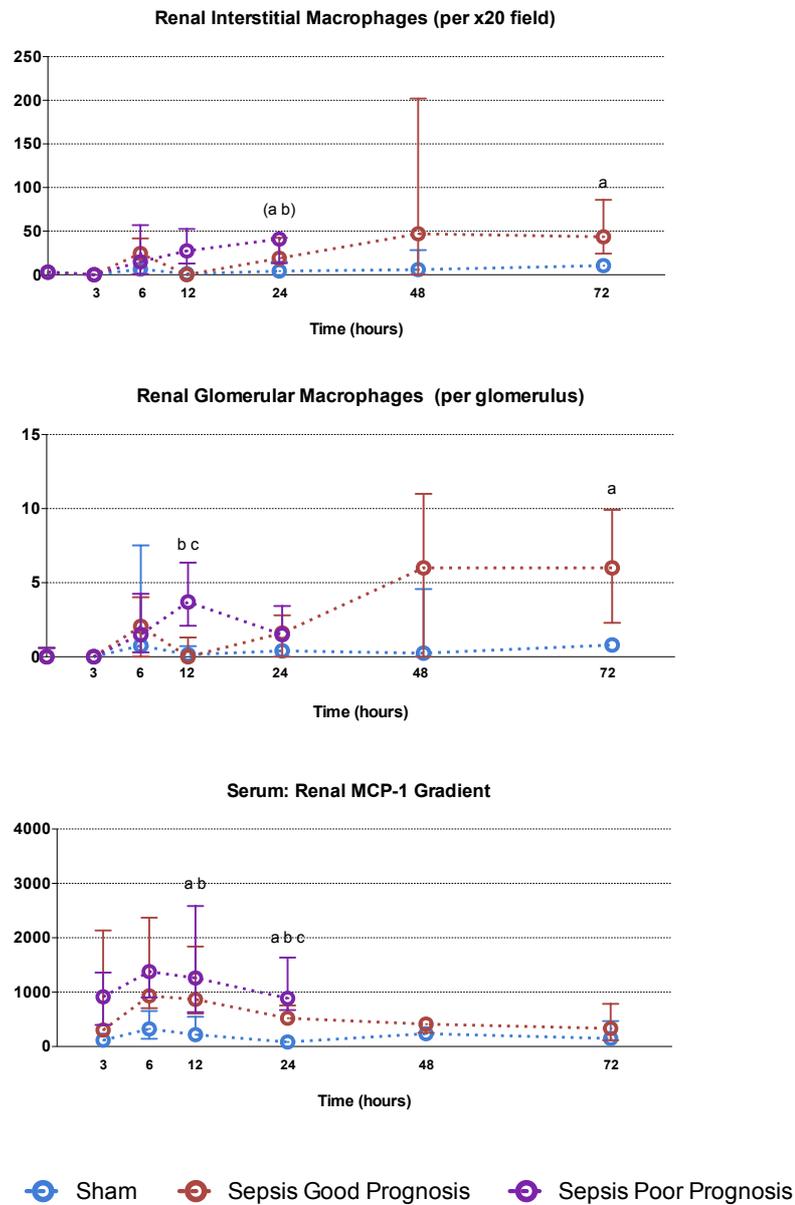
Figure 18 72 hour characterization - Renal macrophages and MCP-1 levels following induction of experimental sepsis in Wistar rats (sham, sepsis good prognosis, sepsis poor prognosis). Maximal renal macrophage infiltration is associated with clinical recovery. The amount of renal macrophage infiltration in inversely proportional to the gradient of MCP-1 between serum and renal tissue.

(a: $p < 0.05$ sham vs good prognosis; b: $p < 0.05$ sham vs poor prognosis; c: $p < 0.05$ good vs poor prognosis)

4.5.9 Effect of Fluid Resuscitation

A separate experiment was carried out in which fluid resuscitation was not given to a group of animals. Compared to the animals that received fluid resuscitation (as per protocol), animals without fluid resuscitation had a significantly higher urea, creatinine, and lactate (Figure 19). Despite this, there was no difference between groups in global haemodynamic parameters including change in cardiac output, change in stroke volume, change in heart rate, global oxygen delivery, and mean arterial pressure.

Core body temperature and the tubular injury score were higher in animals that did not receive fluid resuscitation, although this did not reach statistical significance.
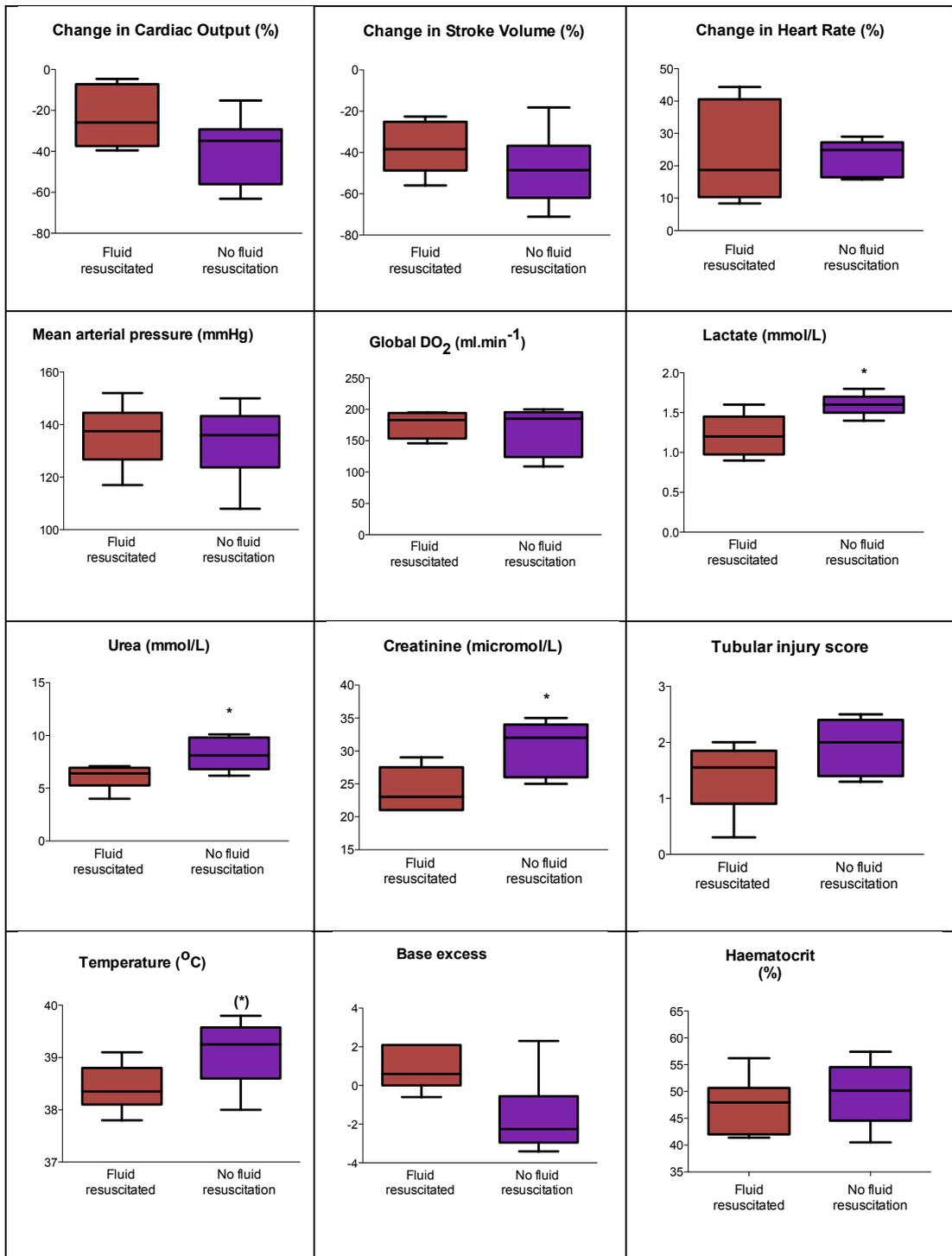
Figure 19 Effect of fluid resuscitation on haemodynamic and biochemical parameters at 6hrs following induction of experimental sepsis in Wistar rats. Septic rats that are fluid resuscitated have a lower serum urea and creatinine, arterial lactate, and core

temperature compared to septic rats without fluid resuscitation. Global haemodynamic variables do are not significantly different between groups.

(* p<0.05 compared to fluid resuscitated animals)

4.6 Discussion

4.6.1 **Characterization**

In this clinically relevant rat model of polymicrobial sepsis, features of inflammation such as temperature and tachycardia become evident from 3 h, although many parameters do not reach statistical significance at that early time point. By 6h, clinical features of sepsis were fairly evident and sustained until 24 h. From 24 h, there was clinical recovery (fall in temperature towards baseline, resolution of tachycardia and recovery of SV). Temperature and cardiac indices follow a similar temporal trend throughout sepsis and recovery.

Consistent with previous work in our laboratory, echocardiographic findings at 6 h could predict survival in the septic animals (Rudiger et al. 2013). Myocardial depression in early sepsis was associated with transcriptomic changes in pathways controlling JAK/STAT, TLR2/MYD88, β-adrenergic signaling and intracellular calcium cycling (Rudiger et al. 2013).

Despite significant volume fluid resuscitation, there is a significant reduction in SV between 3 and 24 h. This may be due to capillary leak and myocardial depression (Rudiger et al. 2013). In animals predicated to die, MAP is maintained for the initial 12 h due to a rise in SVR. This increase in SVR is likely to be a consequence of increased sympathetic drive. As MAP is maintained at the expense of intense vasoconstriction, flow is not maintained as evidenced by a fall in global DO_2 and a greater rise in serum lactate compared to septic animals predicted to live. Animals predicted to live have an early rise in global DO_2. This mirrors the clinical picture where septic patients often have a hyperdynamic circulation in early sepsis, unless peri-mortem (Groeneveld et al. 1988). However, in contrast to what is often seen clinically, patients who die from overwhelming sepsis often have significant vasoplegia rather than the increase in SVR seen in this rodent model of sepsis (Groeneveld et al. 1988). This may relate to the age of the

animals used and within-species differences. Older mice exposed to LPS treatment demonstrate excessive TNF-α and nitric oxide production compared to younger mice (Chorinchath et al. 1996). This has not been demonstrated in rats, but might explain why the relatively young rats used in my studies maintained mean arterial pressure until the hour or so pre-mortem. It would thus be also important to measure key markers and mediators of cardiovascular dysfunction in sepsis, including troponin, cateocholamines, vasopressin and nitric oxide.

4.6.2 Immunology (systemic)

Serum pro-inflammatory (IL-1β, IL-6, IL-18, INFγ) and anti-inflammatory (IL-10) cytokines were measured. Most pro-inflammatory cytokines were elevated early, with peaks in IL-1β and IL-18 as early as 3 h. Serum INF-γ was only detectable at 6 h. The peak in INF-γ followed the peak in IL-18 (a potent stimulant of INF-γ release previously known as INF-γ inducing factor) (Tomura et al. 1998). Furthermore, we demonstrated a correlation between peak serum IL-1β and IL-18 levels. Release of IL-1β and IL-18 is tightly coupled, supporting NLRP3 inflammasome activation early in sepsis. The pattern of temporal change in serum IL-10 was very similar to that seen with the pro-inflammatory cytokine profiles, though elevated IL-10 levels persisted throughout recovery. Animals predicted to die had higher pro- and anti-inflammatory cytokine levels compared to sham animals.

In a large cohort study of 1886 subjects hospitalized with community-acquired pneumonia, cytokine concentrations (IL-6, IL-10, TNF-α) were highest at presentation and declined rapidly over the first few days (Kellum et al. 2007). Temporal changes in cytokines were similar (early peak of both pro- and anti-inflammatory cytokines followed by decline). Furthermore, these levels were highest in those who were sicker and proceeded to eventually die, and lowest in those without severe sepsis. A similar pattern was seen in my animal model of sepsis. The pro-inflammatory cytokines mirrored illness severity, falling towards baseline as the animal recovered clinically. This was in contrast to the clinical study where cytokines remained elevated throughout the first week, beyond

resolution of the clinical signs of infection. However, the illness time in young rodent models of sepsis may not be directly comparable to that seen in generally elderly humans.

4.6.3 Renal Inflammation

I found an increase in renal IL-1β levels from 3 h that peaked at 24h. The source of IL-1β has not been determined. In a porcine model of endotoxaemia, renal IL-1β was expressed in renal arteriolar endothelial cells but not tubular epithelial cells (Granfeldt et al. 2008). IL-1β administered to mice resulted in decreased renal function and expression of functional renal transporters, including the epithelial sodium channel (ENaC), the renal outer medullary potassium channel (ROMK), and the Na$^+$/K$^+$-ATPase (Schmidt et al. 2007). LPS-induced downregulation of sodium transporters was unaltered in cytokine-deficient mice.

I measured renal levels of cytokines hypothesizing an increase in renal IL-4 and IL-10 during the resolution phase of AKI. IL-4-stimulated macrophages with an M2 phenotype promoted renal tubular cell proliferation (Lee et al. 2011). M2 macrophages produce IL-10 which decreases the local inflammatory profile and increases expression of pro-regenerative lipocalin-2 and its receptors in a model of renal ischaemia reperfusion (Jung et al. 2012). However, I could not find any convincing trend or difference between sham and septic rats.

4.6.4 Renal Histology

Despite a higher tubular injury score in septic compared to sham-operated animals at 24 h, the degree of tubular injury was mild (mean score of 1.9 out of a maximum of 9 in septic animals at 24 h). Consistent with other studies, our renal histology findings show that histological injury is disproportionately low for the degree of functional impairment, and with minimal apoptosis (Langenberg et al. 2008, Lerolle et al. 2010, Takasu et al.

2013). There was no evidence of interstitial hypercellularity at any point to suggest significant immune cell infiltration.

We demonstrated significant renal macrophage infiltration at 48 h, subsequent to a rise in renal MCP-1 at 24 h. This was coincident with clinical recovery. I speculate that the phenotype of this macrophage may be of the 'M2' pro-resolution phenotype. However, co-staining with ED-1 and markers of macrophage subtype is required to demonstrate this (iNOS and mannose receptor for M1 and M2 subtypes, respectively) (Lee et al. 2011). During the resolution phase of sepsis, renal macrophages may play a different role. Endotoxin exposure confers renal protection from subsequent damage (preconditioning), mediated via the anti-inflammatory (M2) effect of renal macrophages (Hato et al. 2014). In renal tubules, preconditioning resulted in increased macrophage number and trafficking within the kidney, clustering of macrophages around S1 proximal tubules, and amelioration of peroxisomal damage and oxidative stress and injury to S2 and S3 tubules.

Patients with septic AKI who died had significantly greater renal macrophage and polymorphonuclear leucocyte infiltration in addition to tubular apoptosis compared to patients without severe AKI who die from causes other than septic shock (Lerolle et al. 2010). The role of the renal macrophage in clinical AKI is difficult to entangle, as clinical data are often limited to post- mortem renal biopsies in patients with established septic AKI.

4.6.5   Renal function

Serum urea and creatinine are elevated at 3 and 6 h, and fell towards baseline values at 12 h with IV fluid resuscitation. This is consistent with early haemoconcentration followed by an dilution effect. A correction factor can be applied to measured serum creatinine to correct for the fluid bolus given using the following formula (Macedo et al. 2010):

Corrected pCr = pCr x <u>0.6 x (admission weight) + ε (daily cumulative fluid balance)</u>

0.6 x admission weight

(Where pCr = plasma creatinine)

Acute haemodilution may mask the creatinine rise in early AKI (Liu et al. 2011). Applying the correction factor for cumulative fluid balance over periods longer than a few hours after volume expansion lacks a physiological rationale or any objective evidence to support its accuracy (Prowle et al. 2015). The formula assumes all cumulative volume expansion occurs instantaneously at the point of serum creatinine measurement, failing to account for the actual kinetics of creatinine excretion. When volume expansion acutely reduces serum creatinine, the filtration of creatinine falls in parallel, and creatinine clearance will therefore also fall. Assuming that creatinine generation remains constant, creatinine will then accumulate in the body water until serum creatinine rises again to its baseline value. Modelling shows that after a large fluid bolus that increases circulating volume by 25%, 24 h serum creatinine is only 2% below expected (Prowle et al. 2015).

In addition to haemodilution, the fall in serum creatinine at 12 h may be due to reduced creatinine production. At 14 h in a mouse model of sepsis, creatinine production was decreased (Doi et al. 2009). Creatinine is produced from creatine by non-enzymatic cyclization. This occurs throughout the body but especially in muscles where creatine concentrations are high. Creatinine production itself occurs in the liver (Cocchetto et al. 1983). Creatinine production can therefore fall as lean muscle mass falls, or during liver disease/dysfunction. Loss of muscle mass and subclinical liver disease is common in critically ill septic patients. The rise in serum cystatin C (suggestive of decreased GFR) from 6 to 12 h with concurrent falls in serum creatinine may be a consequence of decreased creatinine production.

4.6.6   Renal Biomarkers

There are numerous studies investigating the utility of biomarkers to predict the onset of AKI prior to a rise in serum creatinine (Vanmassenhove et al. 2013). Several studies have

utilized more than one biomarker and have also looked at serial measures. However, a major limitation of clinical studies is that the exact timing of onset of illness is unclear. Furthermore, use of nephrotoxic drugs, significant hypovolaemia, comorbid illness, and heterogeneity in underlying diagnoses places limitations in interpretation of results. I have shown a clear trend in the kinetics of renal biomarkers. It needs to be determined if the same holds in the clinical setting where there are significant confounding factors (drug-induced AKI, hypovolaemia, etc.). The use of diuretics and pre-existing CKD may also confound the results. Furthermore, the time course of sepsis in individual patients can vary markedly.

Inducers of cell cycle arrest, TIPM-2 and IGFBP-7, have shown promise as novel AKI biomarkers (Kashani et al. 2013). Urine TIPM-2 and IGFBP-7 may be more sensitive and specific in diagnosing AKI than NGAL in critically ill patients, including patients with sepsis. The combined AUROC was 0.80 in prediction of KDIGO stage 2-3 AKI 12 h following ICU admission. Commercial Multiplex kits to measure rat TIMP-2 and IGFBP-7 are not available however, the University of Pittsburgh has an in–house version using ELISA kit (Professor Kellum's lab; personal communication). At the time of writing we are collaborating on order that he measure these analytes.

Novel biomarkers are often assessed to *predict* a subsequent rise in creatinine. The diagnostic performance of a biomarker depends on the disease prevalence, and the sensitivity and specificity of an often imperfect gold standard. It has therefore been argued that an inherent flaw in the analysis of biomarkers is that a rise in serum creatinine is used as a 'gold standard' for AKI and all other biomarkers are compared to this. Apparent diagnostic errors using a new biomarker may be a reflection of errors in the imperfect gold standard itself, rather than poor performance of the biomarker (Waikar et al. 2012).

To improve the assessment of the diagnostic performance of a novel biomarker, stricter criteria for the definition of AKI can be applied. Small changes in serum creatinine alone should not be used to define AKI in biomarker or interventional studies. A combination of

≥2 criteria may be a more appropriate standard. Although the KDIGO staging of AKI includes both serum creatinine and urine output, virtually all biomarker studies only use serum creatinine (KDIGO 2012). Furthermore, serum creatinine is a continuous variable but AKI is often categorized into absence/presence or ordinal stages.

The clinical utility of a biomarker may be demonstrated by improvements in clinical outcome from biomarker-guided therapy. However, there is no proven specific treatment nor treatment algorithm for septic AKI so it may be difficult to demonstrate that biomarker-guided treatment would result in a better outcome compared to creatinine.

4.6.7   Effect of Fluid Resuscitation

Haemodynamic instability during the early phase of septic shock is primarily the consequence of intravascular volume depletion and cardiac impairment. Pathophysiological changes are characterized by profound vasodilation due to relative deficiencies in vasoactive mediators and increased nitric oxide. This, results in a reduced venous return and cardiac output, often confounded by associated mitochondrial dysfunction in myocytes (Kumar et al. 2004, Pedoto et al. 1999). Tissue hypoxia may develop due to low blood flow and/or perfusion pressure. Fluid resuscitation is therefore the cornerstone of resuscitation in sepsis, and should be initiated promptly in patients with haemodynamic instability or evidence suggestive of tissue hypoperfusion, such as an elevated lactate, to achieve an adequate oxygen delivery. In critically ill patients, lactate is a surrogate marker of inadequate tissue oxygenation. Though not strictly accurate, a good relationship is nevertheless seen between hyperlactaemia and mortality (Aduen et al. 1994, Soliman and Vincent 2010).

I also demonstrated the importance of fluid resuscitation as evidenced by the elevated serum urea and creatinine at 6 h compared to the rise in serum creatinine occurring at 24 h when fluid resuscitation was administered. Fluid resuscitation is particularly important for studies assessing organ perfusion and renal function in sepsis, as renal ion

transporter expression in response to sepsis and hypotension are dissimilar (Schmidt et al. 2007).

Despite this , a significant proportion of preclinical studies investigating renal blood flow did not administer fluid (Langenberg et al. 2005). As would be expected, fluid resuscitation in endotoxin- or CLP-treated rats is associated with improved survival (Smith et al. 1993). A reduction in serum TNF-α levels was also seen, though dilution may have had an effect. The lack of fluid resuscitation is associated with markedly reduced microvascular perfusion, increased leukocyte-endothelium interactions and sequestration (Villela et al. 2014).

4.6.8 Limitations and future work

My findings are applicable to this 72 h rat model of acute sepsis that represents a two-hit model where animals are instrumented under general anaesthesia 24 h prior to the onset of sepsis. While I made every attempt to recapitulate clinical sepsis, there are several limitations. This model is performed in relatively young rats, whereas patients with sepsis are usually older with co-existing comorbid illness. Other than haemodynamics, I generally did not make serial measurements in the same animal. Each time point represents the terminal experiment. However, this was required so that I could analyze histology. The most unwell animals were anuric and therefore it was not possible to measure urine biomarkers.

The serum creatinine in the septic animals rose by only 30%, which is less than what is seen clinically. This raises potential questions as to the validity of the model to study AKI. However, in this fluid-resuscitated model of sepsis, animals with a >50% rise in serum creatinine at 24 h tended to not survive much longer. It is therefore not possible to study a recovery model of septic AKI with significant rises in serum creatinine. The creatinine rise seen at 24 h can be reached by 6 h in the absence of fluid resuscitation. However, this would not be clinically relevant and introduces the confounding variable of hypovolaemia.

The utility of biomarkers is dependent on their quantification; absolute concentration, biomarker normalized to urinary creatinine concentration, and biomarker excretion rate. In a prospective study of 529 critically ill patients, urine alkaline phosphatase, γ-glutamyl transpeptidase, cystatin C, NGAL, KIM-1, and IL-18 were measured on admission and after 12 and 24 h (Ralib et al. 2012). .Normalization to urinary creatinine concentration improved the prediction of developing AKI and outcome but provided no advantage in diagnosing established AKI. Similar findings were described in a rat model of drug-induced AKI (Tonomura et al. 2011). I attempted to correct biomarker levels to the urine creatinine concentration, however this was not possible in many samples as urine output was limited, particularly in the most severely affected animals.

Many cytokines are produced along with endogenous receptor inhibitors. IL-1β and IL-18 have endogenously occurring inhibitors, IL-1Ra (Lamacchia et al. 2010) and IL-18 binding protein (Novick et al. 1999) respectively. The techniques used to measure cytokines cannot differentiate between total and unbound cytokines. Furthermore, there may be inaccuracies in measuring the pro-form of the cytokines and also partially degraded cytokines. Other proteins, both cytokines and other proteins, may also interact to give false positive results. This appears to be a problem in the tissue homogenates, where sham animals had variable levels of detectable cytokines both at the same timepoint and also across different timepoints. This was particularly a problem with tissue IL-6 (data not shown), where results could not be replicated on two separate occasions.

I used a multiplex kit to measure urine NGAL and an ELISA based kit to measure serum NGAL. The monomeric (25kD) form is the predominant form secreted by tubular epithelial cells, and the dimeric (45kD) form is the predominant form secreted by neutrophils. NGAL is covalently conjugated with gelatinase (matrix metalloproteinase 9) via an intermolecular disulfide bridge as a 135-kD heterodimeric form. Western blot, but not ELISA based-techniquescan differentiate between the two. The development of molecular form-specific assays for NGAL may be a means to identify the origin of

HNL/NGAL in urine and construct more specific tools for the diagnosis of AKI (Cai et al. 2010).

The analysis of renal histology requires further work. This includes detailed histological characterization of the renal medulla and comparison to the renal cortex. Furthermore, the use of a control irrelevant isotype antibody in place of the primary antibody should be performed to demonstrate antibody specificity. Treatment of histology slices with DNase should be performed as a positive control for TUNEL stain.

4.6.9   Summary and conclusion

In this clinically relevant model of sepsis and recovery, I found many haemodynamic, biochemical, and immunological features consistent with clinical sepsis. Renal histology demonstrates minimal histological injury while renal recovery was associated with an increase in renal macrophages.

For the first time, the temporal profile of a panel of renal biomarkers in sepsis in the context of systemic and renal inflammation and recovery has been characterized. All biomarkers related to PTEC injury were altered to varied degrees and with different kinetics. After a recovery period, all biomarkers returned to levels approaching those observed in sham animals. Apart from urine osteopontin and IL-18, all other urine biomarkers were elevated and at an earlier timepoint to serum creatinine (raised at 24 h). Urine NGAL was the most sensitive marker among those studied, rising from 3 to 24 h. Urine KIM-1 was the only biomarker to show a greater rise in animals predicted to die. While serum creatinine fell at 12 h, serum cystatin C increased, suggestive of decreased creatinine production.

These clinically relevant findings could inform future clinical testing.

5 Renal haemodynamics and bioenergetics

5.1 Background

The haemodynamic instability associated with severe sepsis and septic shock has led to the dogma that sepsis-induced AKI is primarily a consequence of renal ischaemia and ensuing acute tubular necrosis (ATN) (Schrier and Wang 2004). Profound and rapid alterations in blood pressure and regional blood flow during septic shock may lead to loss of renal autoregulation, renal hypoperfusion and ischaemia. However, early studies using indwelling renal vein catheters to measure renal blood flow (RBF) in septic patients with AKI revealed preserved or even elevated renal blood flow (Brenner et al. 1990, Lucas et al. 1973, Rector et al. 1973). An early study using indwelling renal vein thermodilution catheters in septic patients with AKI demonstrated that RBF was maintained within normal limits (Brenner et al. 1990). A systematic review of RBF in experimental sepsis recorded 159 separate studies (Langenberg et al. 2005). The method of sepsis induction, size and conscious level of the animal, time of measurement, use of fluid resuscitation, and systemic haemodynamics were important covariates. Such models of sepsis have confirmed that creatinine clearance and RBF may not correlate (Prowle et al. 2012, Wan et al. 2009).

I have demonstrated in my clinically relevant fluid-resuscitated rat model of sepsis that systemic inflammation occurs as early as 6 h while renal dysfunction, as defined by elevated serum creatinine, occurs at 24 h. Renal histology remains relatively normal with mild acute tubular injury at 24 h.

I hypothesized that the rise in serum creatinine at 24 h is not secondary to a reduction in renal blood flow but rather to bioenergetic dysfunction. As data on mitochondrial dysfunction in sepsis are conflicting (Section 2.7), I investigated the effects of sepsis-induced inflammation on renal tubular mitochondria, without any

influence from renal blood flow or oxygen delivery, using multiphoton imaging of a live kidney slice.

5.2 Methods

5.2.1 Renal cortical oxygen tension

To ascertain renal blood flow and tissue oxygen tension within the kidney, I performed a laparotomy under anaesthesia (as described earlier) at either 6 or 24 h post-induction of sepsis with an echocardiogram and renal ultrasound scan performed beforehand. The fluid infusion of 10 ml/kg/h was continued until the abdominal cavity was opened, after which the infusion rate was increased to 20 ml/kg/h to compensate for evaporative losses.

A 22-gauge needle was used to puncture the renal capsule at the mid-pole. A fibreoptic optode ($250\mu m$ diameter) connected to an Oxylite tissue monitoring system (Oxford Optronix, Didcot, Oxon UK) was inserted into the kidney to a depth of 4-5 mm and subsequently withdrawn to a depth of 1-2 mm to prevent anomalous measurements due to any local haematoma (Figure 20). This sensor enabled continuous tissue oxygen tension (tPO_2) monitoring within the renal cortex (Whitehouse et al. 2006).

The oxygen sensors are pre-calibrated within the range 0- 26.7 kPa. Short excitatory pulses of light (475 nm) are emitted along the fibre-optic cable to a platinum-complex fluorophore situated at the sensor tip. Upon interaction with oxygen, the fluorophore emits light (600 nm) that is recorded at the detection unit. The lifetime of the returned light is inversely proportional to local PO_2, according to the Stern-Volmer equation:

$$\tau_0/\tau_1 = 1 + (\kappa_q \times \tau_0 \times \{O_2\})$$

where τ_0 is the decay time at zero oxygen, τ_1 is the decay time at a specific oxygen concentration (O_2) and κ_q is a quenching rate constant that denotes the probability of a

photoluminescent molecule and oxygen molecule colliding. As luminescence decay is longer at a lower PO_2, accurate measurements can be made within the physiological range (0-8 mmHg). Continuous tPO_2 measurements were recorded onto a computer using a 16-channel Powerlab system and Chart 5 acquisition software (AD Instruments, Chalgrove, Oxon, UK). At least five minutes were allowed prior to obtaining a reading to allow for any local oedema surrounding the sensor tip to resolve.

Figure 20 Picture taken at laparotomy demonstrating oxygen sensor *in situ*. The fibreoptic optode is inserted into the renal cortex at the level of the mid pole of the left kidney.

5.2.2 Renal Blood flow

The left renal artery was isolated by careful blunt dissection. An ultrasonic flow probe (Transonic Systems, Ithaca, NY, USA) of 1 mm diameter was coated in a water-soluble lubricant and placed around the left renal artery to measure renal blood flow (RBF) (Figure 21). Renal oxygen delivery (DO_2 renal) was calculated using the following formula:

$$DO_2 \text{ (renal)} = 1.34 \times RBF \text{ (L/min)} \times Hb \text{ (g/dl)} \times SaO_2$$
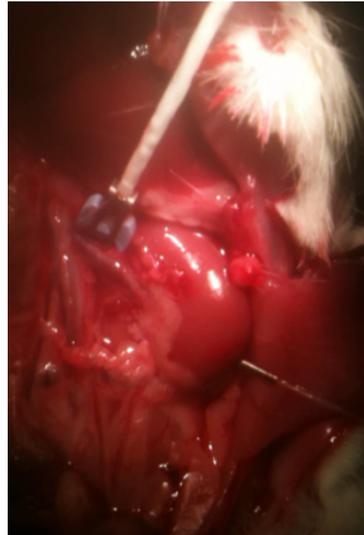
Figure 21: Picture taken at laparotomy demonstrating renal artery ultrasonic flow probe and large area oxygen sensor *in situ*. The ultrasonic flow probe of 1 mm diameter was coated in a water-soluble lubricant and placed around the left renal artery to measure renal blood flow.

5.2.3 Renal oxygen extraction ratio

The left renal vein was isolated from surrounding tissue by careful blunt dissection. One ligature was placed around the renal vein, and another around the renal artery and vein. The renal vein was kinked using the ligature, punctured with an 18-gauge needle, and approximately 0.3 ml of blood was aspirated. The renal vein and artery were then ligated to prevent blood loss. A simultaneous blood sample was taken from the arterial line. Both were analyzed in an ABL-70 blood gas analyser (Radiometer, Copenhagen, Denmark).

The renal oxygen extraction ratio (ERO_2) was calculated using the following formula:

$$ERO_2 = \frac{(SaO_2 - RVO_2)}{SaO_2} \times 100$$

where RVO_2 is renal vein oxygen saturation and SaO_2 the arterial blood oxygen saturation.

5.2.4 Electron microscopy

As the renal instrumentation methodologies described below are likely to affect serum creatinine and histology, samples for electron microscopy and biochemistry were taken in repeat experiments at 24h where instrumentation was not performed. A kidney was obtained from a septic and a sham animal under anaesthesia. The septic animal had significant renal dysfunction (serum creatinine 42 μmol/l) but was not conisdered peri-mortem. Renal tissue was cut into sections of approximately 1 x 1 x 1 mm using a surgical scalpel and placed immediately into glutaraldehyde fixative. The histopathology laboratory at the Royal Free Hospital, London performed electron microscopy. Analysis was qualitative and focused on mitochondrial structure within proximal tubular epithelial cells. Ten random fields were examined at x2,650 magnification in a blinded manner. Tubules at the cortico-medullary junction and within the cortex were assessed. Higher magnifications (x15,000) were used to evaluate changes within the mitochondria.

5.2.5 Ex-vivo assessment of mitochondrial function - confocal microscopy

Using dyes or natural flurophores, confocal microscopy allows detailed imaging of cellular physiological processes in intact renal tissue sections. Multiphoton imaging uses a long wavelength excitation laser that permits significantly greater tissue penetration compared to conventional single-laser confocal fluorescence microscopy. This results in less phototoxicity and is therefore a better technique for imaging live kidney sections. This technique can image live kidney slices in real-time in response to various insults or drugs. Multiphoton imaging of freshly prepared rat kidney slices has been previously used to investigate mitochondrial function in cells along the nephron, both at rest and in response to toxic stimuli, including chemical anoxia (Hall et al. 2009).

The left kidney was removed from an anaesthetized healthy male Wistar rat and immediately placed in oxygenated ice-cold HEPES-buffered solution (118mM NaCl,

10mM NaHCO$_3$, 4.7mM KCl, 1.44mM MgSO$_4$, 1.2mM KH$_2$ PO$_4$, 1.8mM CaCl$_2$, 10mM HEPES, 5mM glucose, 5 mM sodium butyrate, and 5mM pyruvate). The kidney was sliced in half along the transverse plane and mounted on a stage. Slices were cut at 200 μm in oxygenated ice-cold HEPES-buffered solution using a Microm 650V tissue slicer.

Slices were incubated in oxygenated HEPES-buffered solution at room temperature until used. Kidney slices were placed in an open bath chamber (Harvard Apparatus, Edenbridge, Kent, UK) and secured with a slice anchor. Dyes and reagents were loaded using an on-stage perfusion system, and changes in signal imaged in real-time in response to reagents. Kidney sections were studied up to 6 hours following resection. Structures were identified by their characteristic morphology and location.

Slices were imaged using a Zeiss LSM 510 NLO axiovert microscope coupled to a tunable Coherent Chameleon laser. For all probes used, the optimal excitation wavelength was based on two-photon excitation spectra (Hall et al. 2009). An internal detector captured emitted light. Image processing and analysis was performed using Zeiss LSM software (Carl Zeiss Ltd., Welwyn Garden City, Herts, UK) and Image J software (National Institutes of Health, Bethesda, MD, http://rsb.info.nih.gov/ij/). To quantify fluorescence signals, regions of interest were drawn around tubules in a minimum of three different fields (imaged using a x40 objective). All values are expressed as the mean fluorescence intensity, per image pixel (arbitrary units, AU), within the relevant region of interest.

The cationic lipophilic indicator tetramethyl rhodamine methyl ester (TMRM) was used to determine mitochondrial membrane potential, at a concentration of 50 nM. The greater the potential, the more dye that accumulates and the greater the signal intensity at any given pixel. ROS generation in tubules was measured using dihydroethidium (HEt), at a concentration of 5 μM. As HEt fluoresces on oxidization by superoxide, the fluorescence signal thus increases in proportion to the rate of ROS production. At 720 nm excitation, the autofluorescence signal emitted between 435-485 nm (cyan) arises predominantly

from mitochondrial NADH. The resulting image consists of striations of signal at the basal pole of the cell, matching the known distribution of mitochondria in the tubule and the signal seen with TMRM (**Table 14**) (Figure 22).

Fluorophore	Function	Final concentration	Excitation wavelength (nm)	Emission wavelength (nm)
Tetramethyl rhodamine methyl ester (TMRM)	Mitochondrial membrane potential	50nM	860	575-640
Dihydroethidium (HEt)	ROS generation	5μM	720	575-640
NADH autofluoresence	Redox state	N.A	720	435-485

Table 14 Mitochondrial fluorophores
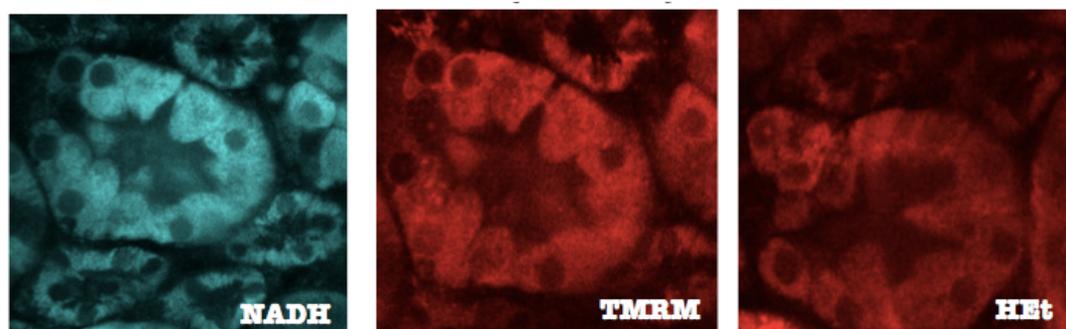
Figure 22 Confocal images of the proximal tubule NADH, TMRM and Het. NADH is auto-fluorescent at 720nm and emits a wavelength of 435- 485nm, appearing cyan. TMRM is excited at 860nm, and Het is excited at 720nm. Both TMRM and HEt emit wavelengths of 575- 640nm, appearing red.

I studied changes in mitochondrial membrane potential, reactive oxygen species (ROS) production, and the redox state of PCTs and DCTs. Images were obtained in

physiological saline solution (PSS), 24h sham serum, and 24h septic serum. I chose this timepoint to collect serum as it corresponded to measurement of significant differences in renal VO$_2$ *in vivo*. Serum was diluted to a 1:3 ratio in PSS to minimize the total amount of serum required. Images were taken every 5 min for a total of 45 min. A total of six sets of images were taken in PSS, three in sham serum, and three in septic serum.

Kidney slices were imaged up to 60 min. The mean fluorescent intensity at 60 min was expressed as a percentage of mean fluorescent intensity at baseline. Images were taken at 15-min intervals, focusing on different areas of the slice to avoid damage (bleaching) to the slice from repeated imaging of the same field.

5.2.6   Protein extraction and quantification

Snap-frozen renal tissue was homogenized in radioimmunoprecipitation assay homogenizing buffer (RIPA buffer; 50 mM NaCl, 1.0% IGEPAL (Octylphenyl-polyethylene glycol, Sigma Aldrich), 0.5% sodium deoxycholate, 0.1% SDS, and 50 mM Tris, pH 8.0) at an approximate ratio of 0.3g tissue with 1 ml buffer. Tissue was homogenized with a sonicator. The homogenate was centrifuged for 10 min at 14,000g in a cold microfuge to remove tissue debris. The supernatant was pipetted and protein concentration determined using the bicinchoninic acid assay kit (Pierce, Rockford, IL, USA) according to the manufacturer's protocol. Samples were stored at -80°C.

In preparation for Western blot analysis, samples were diluted to a concentration of 6 mg/ml in RIPA buffer and reduced by adding an equal volume of β-mercapthethanol and sodium dodecyl sulfate (SDS) buffer (50 μl β-mercapthethanol added to 950 μl SDS) buffer) and heated in a heating block for 5 min at 95°C. The final protein concentration used for Western blot was therefore 3 mg/ml. Samples were stored at -80°C.

5.2.7 **Western blot**

Protein was extracted and estimated from renal tissue as described. Samples (20 μg protein) were electrophoresed at 100V for 1 h through a 12% or 15% sodium dodecyl sulfate polyacrylamide gel electrophoresis (SDS-PAGE) gel under reducing conditions. Proteins were transferred to a polyvinylidine difluoride (PVDF) membrane (GE Healthcare) at 10V for 45 min, and then blocked for 1 h in 5% milk/1% TBST. This membrane was then incubated with goat anti-mouse IgG polyclonal UCP-2 antibody (Santa Cruz) at 1:250 in 5% bovine serum albumin (BSA; Sigma) in PBS overnight at 4°C. Following incubation with the primary antibody, HRP rabbit anti-goat IgG (Sigma) was added at 1:3000 in 5% milk for 1 h. Activity was detected using ECL Plus substrate (GE Healthcare). Two animals were randomly selected from each of the naïve, sham and sepsis (6, 12, and 24 h) groups for analysis. Naïve kidney was used as a relevant negative control.

5.3 Statistics

All statistical analyses were performed using SPSS (IBM. Version 20) and graphs drawn using Graphpad Prism (GraphPad Software, Version 5.0d). Normality of continuous data was assessed using the Shapiro-Wilk test. Continuous variables are presented as means (standard deviation) where parametric, and median (interquartile range) where non-parametric. Parametric data were compared using unpaired Student's t-test, whereas non-parametric data were compared using the Mann Whitney U test for comparison of continuous data between 2 groups. For comparison of continuous variables between more than two groups, one-way analysis of variance (ANOVA) with post hoc Tukey's test is used. A p-value <0.05 was taken as statistically significant.

5.4 Results

5.4.1 Baseline Variables

At baseline (before central venous catheter insertion), all variables including body weight, haemodynamics and renal resistive index of each study group were similar (p>0.05) (Appendix). All instrumented animals recovered fully prior to induction of faecal slurry. Sham-operated animals remained active throughout. All animals in the sham-operated groups survived the 6- and 24 h experiments. All animals in the septic group survived the 6 and 24 h experiments but two animals in the 24 h group were peri-mortem and excluded from analysis.

5.4.2 Systemic variables

At 6 and 24h, septic animals had a significantly higher core body temperature compared to sham-operated animals. Despite fluid replacement, there was a significant fall in SV and CO in septic animals at both 6 and 24 h compared to baseline values. Septic animals had a significant increase in HR at 6 h that returned to baseline values by 24 hr. Mean arterial pressure and global oxygen delivery were similar at 6 and 24 h compared to naïve and sham animals (Figure 23). Changes in systemic haemodynamics, biochemistry, acid-base balance, and systemic cytokines are described in detail in Chapter 4.
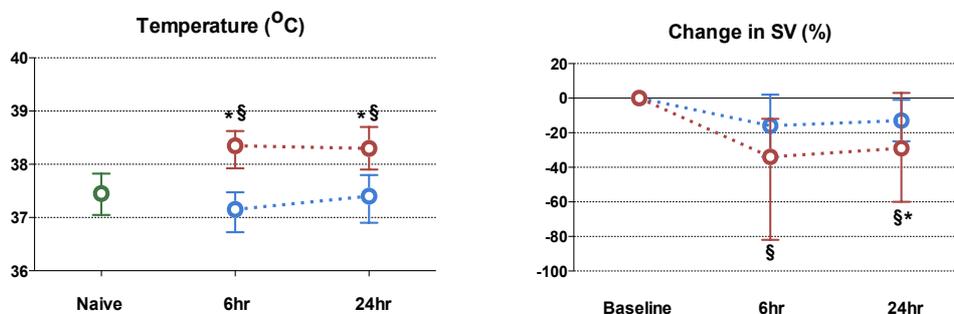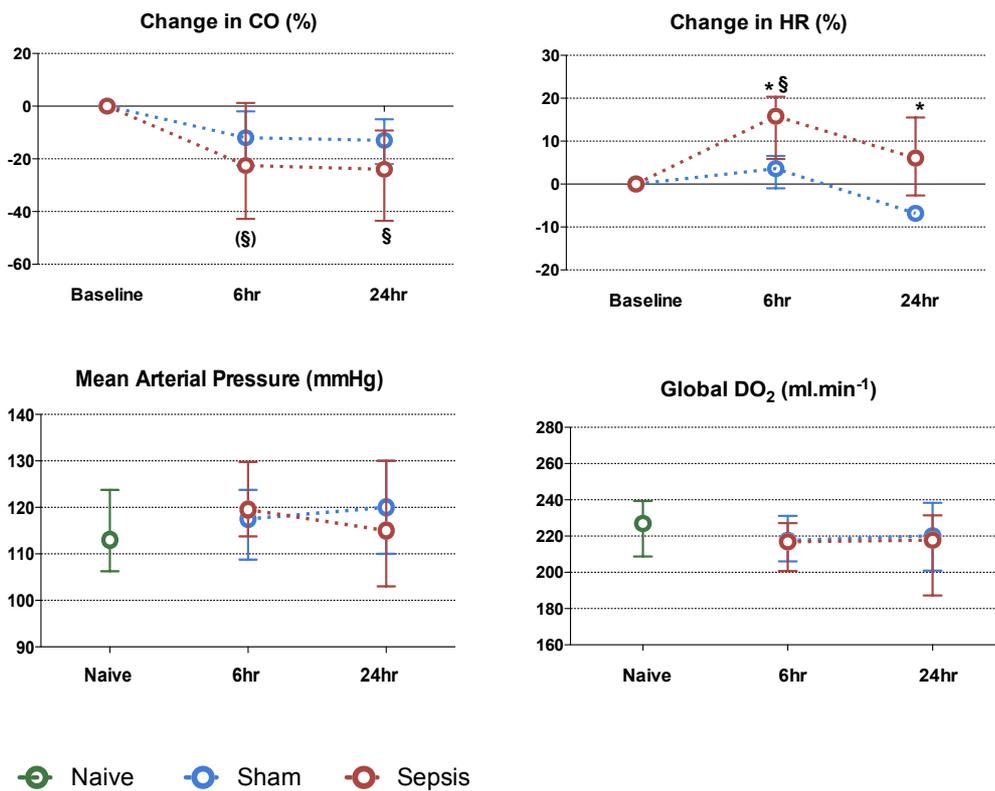
Figure 23 Systemic variables following induction of experimental sepsis in Wistar rats (at 6 h and 24 h) compared to naïve Wistar rats. Septic animals develop fever, tachycardia, and impaired SV by 6hrs, which persists through to 24 h. Mean arterial pressure and global oxygen delivery remain unchanged.

(* $p < 0.05$ for sham vs. sepsis (corresponding time points); § $p < 0.05$ for Naïve vs. sepsis)

5.4.3 Renal haemodynamic variables

Renal blood flow, renal oxygen delivery, and the proportion of global O_2 delivery to the kidneys remained unchanged in septic compared to naïve rats. Renal oxygen extraction ratio and consumption were significantly lower at 6 h and recovered by 24 h (septic vs. naïve animals) (Figure 24). At 24 h, there was a significant increase in lactate being produced by the kidneys, despite renal DO_2 and VO_2 being similar to naïve animals. This was associated with a significant fall in renal cortical oxygenation. The urinary fractional

excretion of sodium fell at 6 and 24 h, though serum creatinine was elevated only at 24 h in septic animals compared to naïve animals (Figure 25). (See Appendix for tables).
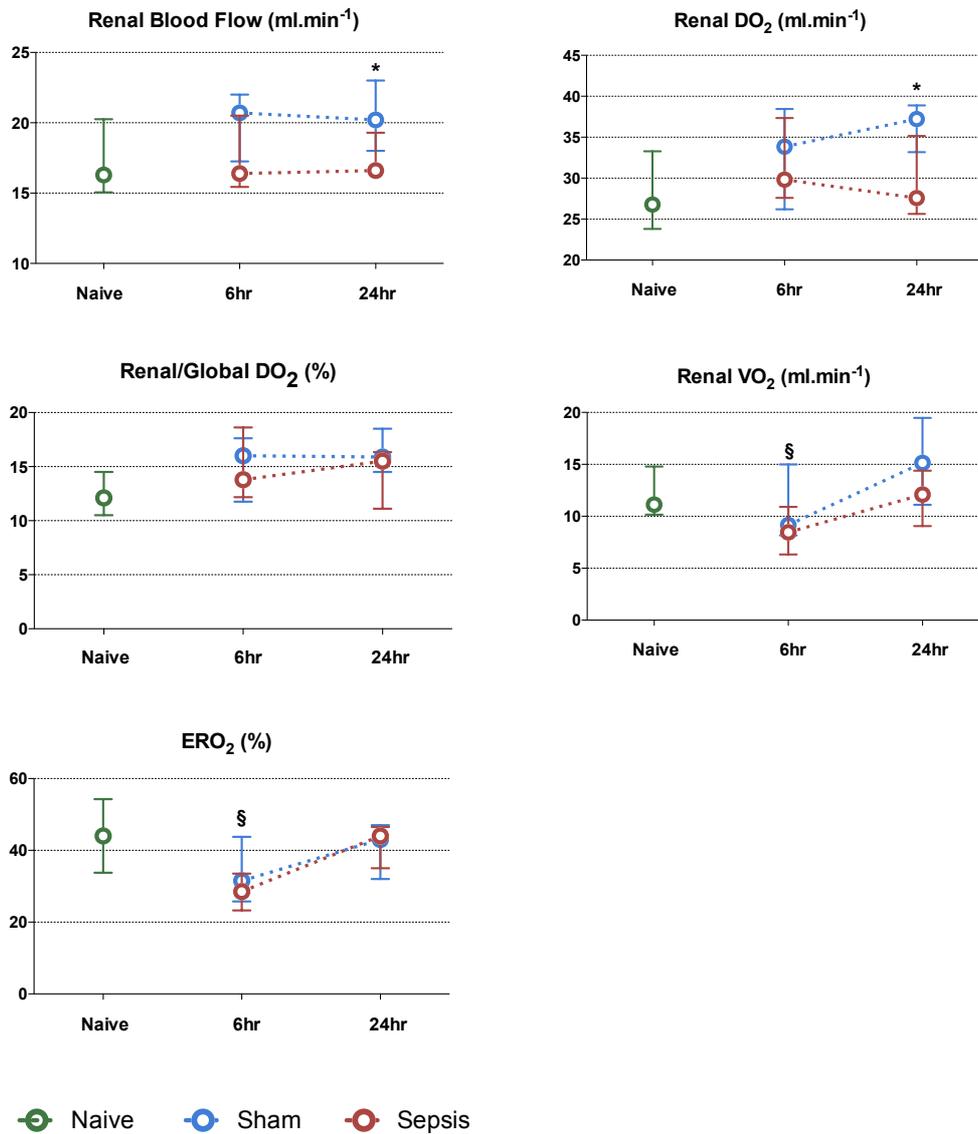
Figure 24 Renal haemodynamics following induction of experimental sepsis in Wistar rats (at 6 hr and 24hr) compared to naïve Wistar rats. Compared to naïve animals, renal blood flow and oxygen delivery is maintained in sepsis. Despite this, there is an early fall in renal oxygen consumption which recovers to baseline by 24 h.

(* $p < 0.05$ for sham vs. sepsis (corresponding time points); § $p < 0.05$ for Naïve vs. sepsis)
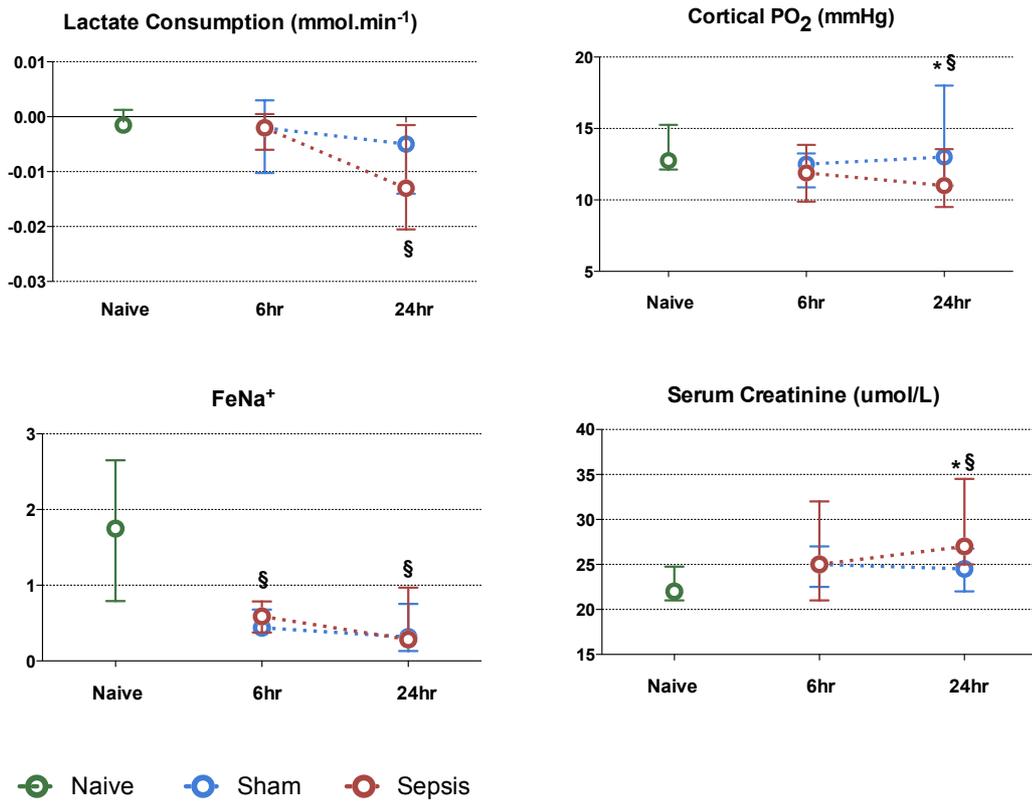
Figure 25 Renal metabolism and function following induction of experimental sepsis in Wistar rats (at 6 hr and 24hr) compared to naïve Wistar rats. At 24 h, lactate clearance falls in septic animals. This is associated with a fall in cortical oxygen tension and a rise in serum creatinine. Fractional excretion of sodium falls at 6 h and remains low at 24 h.

(* $p < 0.05$ for sham vs. sepsis (corresponding time points); § $p < 0.05$ for Naïve vs. sepsis)

5.4.4 Mitochondrial ultrastructure
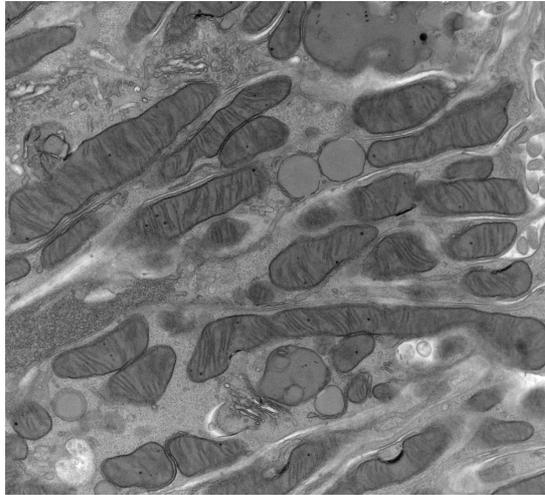
Figure 26 Electron microscopy of proximal tubule epithelial cell mitochondria (obtained from septic animal at 24 h) reveals normal mitochondrial ultrastructure (x15,000).

Mitochondria within the septic kidney appeared normal (Figure 26). There were no features of isometric vacuolization, hydropic mitochondria, or structural loss of mitochondrial cristae.

5.4.5 Confocal Microscopy

Mitochondrial NADH redox state, membrane potential, and tubular reactive oxygen species levels remained stable over the 60 min time period in both PSS and sham serum (Figure 27). There was a significant drop in NADH redox state in the proximal tubules when incubated in septic serum, which was abrogated by pre-incubation with 4-OH-TEMPO.
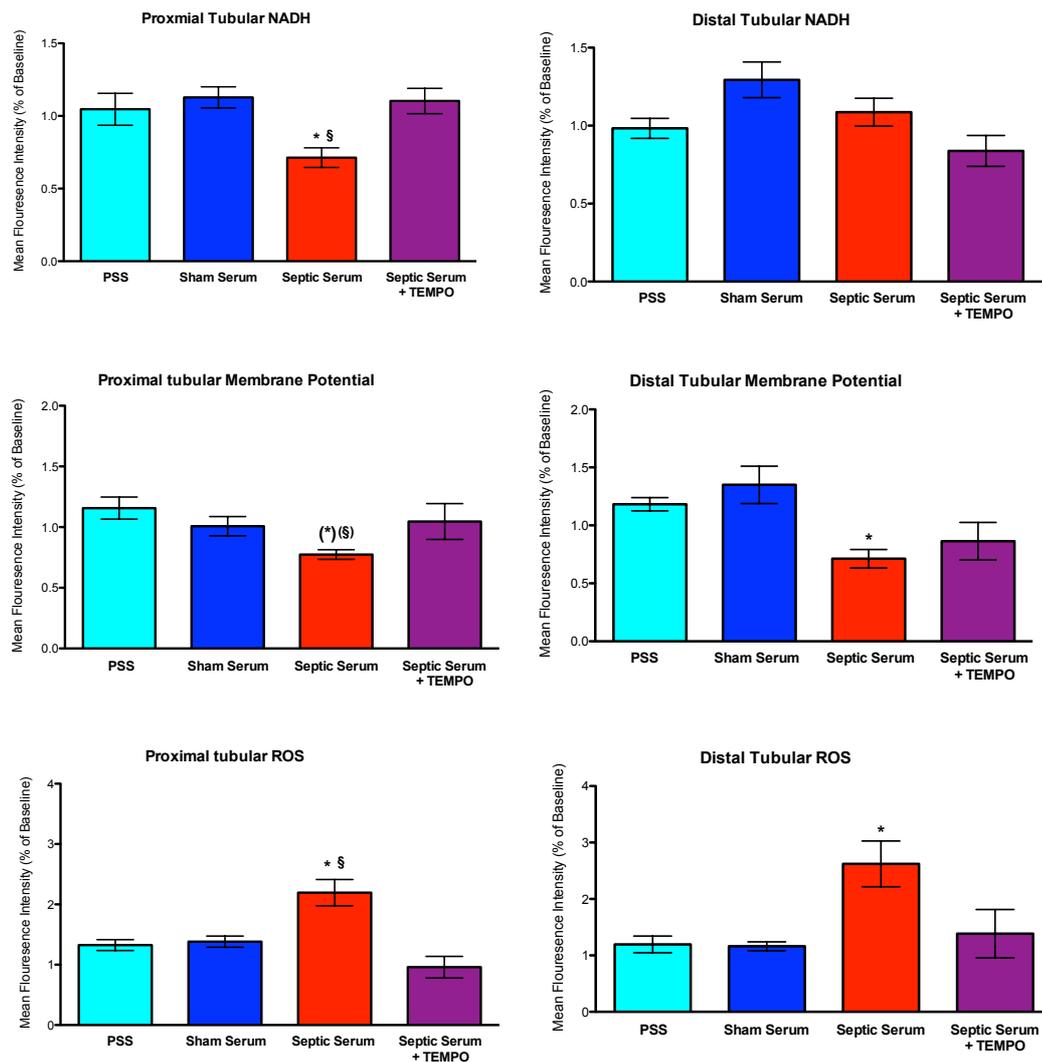
Figure 27 Changes to mitochondrial redox state, reactive oxygen species (ROS), and membrane potential in response to physiological saline solution (PSS) sham serum, septic serum, and pre-treatment with 4-OH-TEMPO and septic serum. Exposure to septic serum results in an increase in proximal tubular reactive oxygen species and a concurrent fall in NADH and mitochondrial membrane potential compared to incubation in PSS for 45min. Similar changes are seen in the distal tubules, apart from the fall in NADH. These changes are abrogated with 4-OH-TEMPO pre-treatment. Bar graphs and error bars represent mean and standard deviation respectively of > 6 replicates.

(* $p < 0.05$ sham serum vs. septic serum. § $p < 0.05$ septic serum vs. septic serum + TEMPO.)

The change in redox state was not evident in distal tubular cells. The fall in mitochondrial membrane potential when incubated in septic serum approached statistical significance in the PTECs and was significantly reduced in DTECs. This change was not prevented by 4-OH-TEMPO. Both PTEC and DTEC ROS levels were significantly increased in kidney slices incubated in septic serum, and were completely prevented by pre-incubation with 4-OH-TEMPO (Figure 27).

5.4.6 Western blot for UCP-2
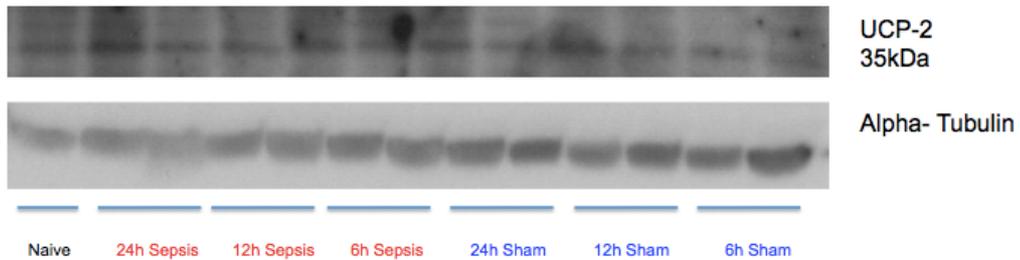
Figure 28 Western blot for Uncoupling Protein (UCP-2) in renal homogenate. Expression of UCP-2 (35kDa) and alpha-tubulin (55kDa).
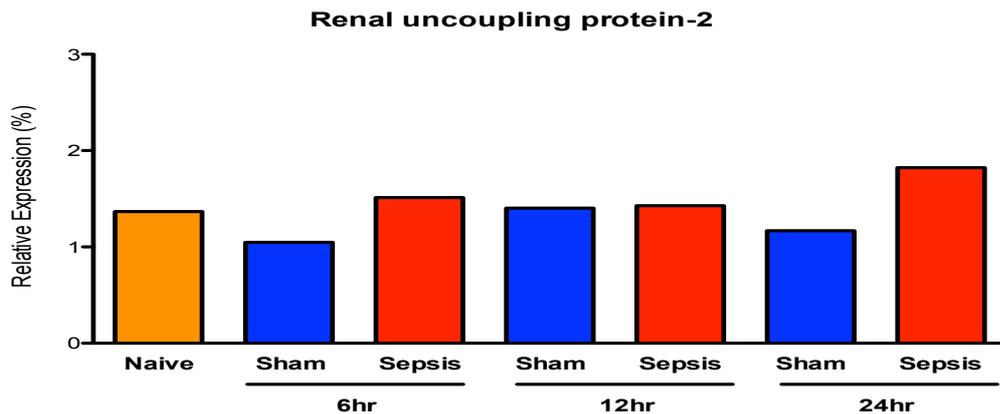
Figure 29 Relative expression of renal uncoupling protein-2 (n=2 per group). There was a trend towards an increase in renal UCP-2 expressed in septic compared to sham animals at 24 h.

The relative expression of UCP-2 was increased in kidney homogenates from septic animals at 24 h compared to sham-operated animals and naïve animals (Figure 28). There was no differences in UCP-2 levels at either 6 or 12 h. At 24 h, there was a trend towards an increase in renal UCP-2 expressed in septic compared to sham animals (Figure 29). However, as only n=2 per group was performed, it was not possible to assess for statistical significance.

5.5 Discussion

5.5.1 Systemic features

Blood pressure remained relatively constant throughout the 24 h study period. Despite the similar MAP, lactate was elevated at 24 h, suggestive of tissue hypoperfusion and/or mitochondrial dysfunction. Despite a higher tubular injury score in septic animals at 24 h, the degree of tubular injury was mild with a mean score 1.9 (maximum of 9). Renal histology was consistent with other septic AKI studies (Langenberg et al. 2008, Lerolle et al. 2010, Takasu et al. 2013), being disproportionately low for the degree of functional impairment. RBF remained stable in this model of sepsis. My results suggest that structural tubular injury or falls in RBF are not the predominant pathological process underlying septic AKI.

5.5.2 Renal haemodynamics

GFR, tubular sodium transport and renal VO_2 are closely linked. Tubular reabsorption of filtered sodium is the major determinant of renal VO_2 (Kiil et al. 1961), and tubular transport processes are dependent upon the filtered load (Sward et al. 2005, Torelli et al. 1966). At 6 h there was no alteration in serum creatinine, possibly because creatinine would take some time to rise from the point of a decreased GFR. Furthermore, in early sepsis, there is a decreased production of creatinine (Doi et al. 2009). At 6 h, renal DO_2 and cortical oxygenation are maintained but renal VO_2 falls. The fall in $FeNa^+$ suggests

that tubular workload and VO_2 should be increased. I therefore postulate that GFR falls and the (absolute) amount of solute reabsorbed by the tubules falls, though the proportion of filtered solute reabsorbed is increased, as reflected by the fall in $FeNa^+$.

Tubuloglomerular feedback (TGF) allows each nephron to regulate its GFR in accordance with the capacity of its proximal tubule to reabsorb NaCl. Extracellular adenosine contributes to the regulation of GFR. Renal interstitial adenosine is mainly derived from dephosphorylation of released ATP, AMP, or cAMP by the enzyme ecto-5'-nucleotidase (Le Hir and Kaissling). This enzyme is located primarily on external membranes and on mitochondria of proximal tubule cells (Miller et al. 1978). Extracellular adenosine activates A1AR adenosine receptors on vascular afferent arteriolar smooth muscle cells, resulting in vasoconstriction, reduced GFR, a reduced need for tubular reabsorption and preservation of renal bioenergetics (Schnermann et al. 1990). I speculate that the increased workload of the PTECs from 6 h results in ATP depletion and accumulation of adenosine.

At 24 h, serum creatinine rose in septic animals despite a stable RBF. This suggests intra-renal shunting, with either less blood flowing through the glomerulus and/or dilatation of the efferent arteriole to reduce glomerular filtration. Selective augmentation of adenosine around afferent arterioles causes persistent vasoconstriction and a reduction in glomerular blood flow. Concurrent global elevation of renal adenosine causes steady-state vasodilatation resulting from A2AR-mediated generation of nitric oxide (NO) (Hansen et al. 2005). The A2AR mediates vasodilatation in deep cortical glomerular vessels, increasing medullary blood flow and oxygenation (Vallon and Osswald 2009). Therefore, adenosine may maintain renal perfusion via A2 generation of NO, while allowing a compensatory reduction in tubular workload mediated by a reduction in A1 receptor activation. Antagonism of the A1AR decreased renal blood flow during endotoxic shock (Nishiyama et al. 1999).

Renal oxygenation depends on the balance between renal DO_2 and VO_2. In health, renal VO_2 depends on renal DO_2, and oxygen extraction remains stable over a wide range of

RBF (Levy 1960). Any reduction in renal DO_2 should be accompanied by a corresponding fall in renal VO_2 to maintain renal cortical PO_2. At 24 h, cortical PO_2 fell in the septic animals despite renal DO_2 and VO_2 values that were similar to baseline. The rise in serum creatinine at 24 h implies a reduction in GFR. Tubular workload and renal VO_2 should therefore be reduced. However, during hypovolaemic states, the proportion of filtered solute reabsorbed by the tubules is increased in an effort to conserve fluid. This will increase renal VO_2 which, when combined with a stable renal DO_2, results in a fall in cortical oxygenation. This may be compounded by the diversion of oxygen from ATP production as a consequence of uncoupling (Crouser et al. 2002).

5.5.3   Mitochondrial structure and function
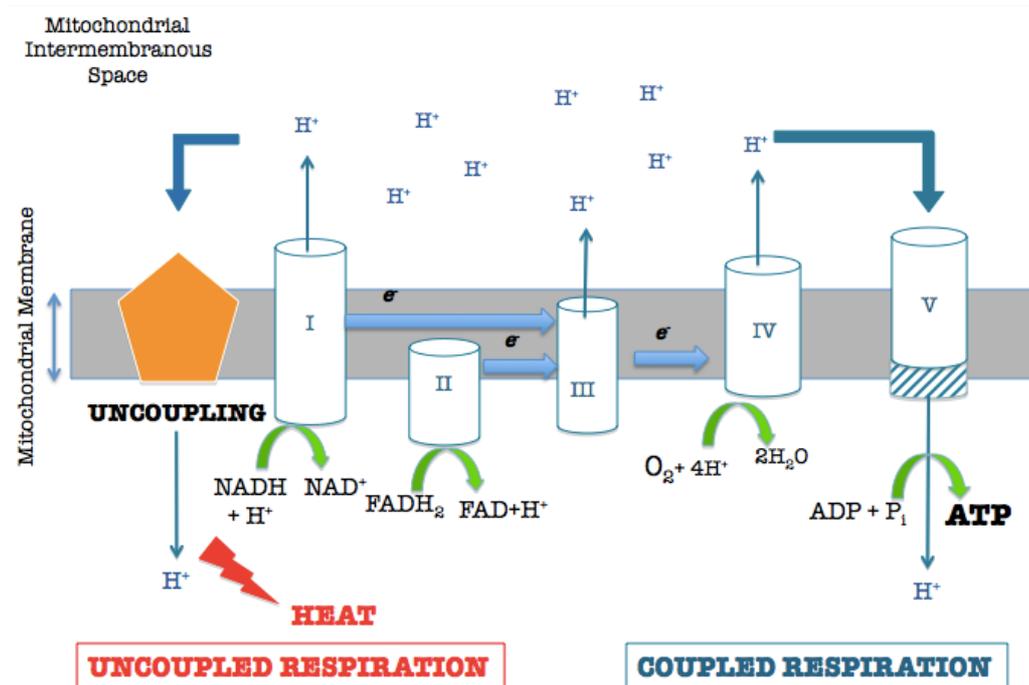
Figure 30 Electron transport chain and oxidative phosphorylation. During oxidative phosphorylation, the main process of ATP production in most body cell types, electrons are donated from the Krebs' cycle to NADH and $FADH_2$, and then pass down the electron transport chain (ETC). O_2 is the terminal electron acceptor at Complex IV. As electrons move down the ETC, H^+ ions are driven into the intermembrane space, generating a chemiosmotic proton gradient to generate ATP from ADP and inorganic phosphate at complex V (ATP synthase). The use of O_2 to drive ATP production is known as coupled respiration.

Superoxide is the primary reactive oxygen species produced by mitochondria; this arises from respiratory complexes I and III (semiubiquinone pathway). In health, the small amount of superoxide generated has a signaling role. These levels are kept low by mitochondrial antioxidants such as manganese superoxide dismutase (MnSOD). Relatively low levels of ROS may also be beneficial with important signaling (hypoxic

pulmonary vasoconctriction), biosynthetic (HIF-1 production) and immune functions (TLR signaling and post-transcriptional modifications in TNF signaling).

During sepsis, harmful levels of ROS and reactive nitrogen species (RNS) are produced and these can overwhelm the antioxidant capacity. The reaction of NO with superoxide generates peroxynitrite, a potent oxidizing agent that causes protein nitration, DNA damage and mitochondrial dysfunction (Cuzzocrea et al. 2006). Features of hydropic mitochondria and increased autophagosomes in critically ill septic patients are more prevalent in septic than in non-septic patients (Takasu et al. 2013). Furthermore, mitochondria exposed to non-mitochondrial ROS become a source of ROS themselves. Renal tubular cells increase their expression of inducible nitric oxide synthase (iNOS) and NADPH oxidase 4 (NOX-4) in response to LPS. This culminates in cytosolic overexpression of NO and superoxide,,respectively (Quoilin et al. 2014). This positive feedback loop of ROS-induced-ROS is likely to culminate in inhibition, dysregulation and damage to mitochondria.

Uncoupling can occur in various physiological states such as heat production in brown fat. Protons pumped across the mitochondrial membrane can 'leak' back into the mitochondrial matrix and the energy is dissipated as heat. In this situation, NADH is oxidized, the mitochondrial membrane potential falls, and O_2 is used but ATP is not produced (**Figure 30**). The reduction in mitochondrial membrane potential limits the amount of electrons passing along the mitochondrial membrane, and thus the amount of ROS produced, however, this is at the expense of ATP production.

I speculate that a decrease in ATP synthesis (mediated in part via mitochondrial uncoupling) would increase the relative amount of renal adenosine. Extracellular adenosine activates A1 receptors on afferent arteriolar smooth muscle cells, resulting in vasoconstriction and a reduction in GFR (thereby conserving circulating volume). Concurrent activation of A2 receptors maintains renal perfusion and facilitates blood shunting from the glomeruli. Renal inflammation in sepsis (detailed in section 2.8) decreases PTEC ion transporters. This 'functional shut down' of GFR, tubular function

and ATP production triggers various protective mechanisms, though at the expense of renal function. These include conservation of circulating volume, reduction in ROS, and 'energy conservation'. This also explains the relatively well-preserved renal histology seen in sepsis despite an increase in serum creatinine,

Treatment with antioxidants ameliorates organ injury in experimental models of sepsis. Several therapeutic agents have been tried, including n-acetyl cysteine (NAC) to reduce hepatic oxidative stress (Zapelini et al. 2008), MITO-Tempo to reduce renal injury (Patil et al. 2014), and inhibiting peroxynitrite with MnTMPyP or inducible nitric oxide synthase with aminoguanidine and to prevent renal injury (Seija et al. 2012).The lack of clear clinical benefit of antioxidants in sepsis may be due to late initiation (preventative therapies have greater benefit), inadequate dosing (particularly with respect to tissue levels), and the need to target mitochondrial ROS.

By incubating fresh kidney slices with septic serum, I demonstrated that "circulating humors" rather than RBF or oxygen delivery could induce mitochondrial dysfunction. As such, therapies using extracorporeal blood purification may be beneficial. Methods of extracorporeal blood purification include high volume haemofiltration, combined plasma filtration and absorption, haemoabsorption (using polymyxin B or Cytosorb columns), plasma exchange, and now selective removal of cytokines using the biospleen (Zhou et al. 2013). Trials of high volume haemofiltration have not shown clinical benefit and blood purification strategies may also remove useful molecules including amino acids and drugs. Promising results were seen from a pilot study of polymyxin haemoabsorption in septic patients (Cruz et al. 2009) and a larger trial is ongoing.

5.5.4   Limitations and future work

All BP recordings were obtained in anaesthetized animals and the severity of sepsis was relatively modest (100% survival). Increasing severity to include peri-mortem animals was not possible, as they deteriorated and sometimes died during invasive measurements.

The interpretation of experimental results requires appropriate sham animals. I conducted

parallel experiments in animals without faecal peritonitis, but which had received a similar volume of intravenous fluid. This increased RBF, renal DO_2, and cortical oxygenation at 24 h. The workload of the PTECs would have increased in view of the need to eliminate the large volume of free water and to reabsorb a significant proportion of filtered sodium (animals were given solutions with low Na^+ concentrations).

High-volume resuscitation itself is associated with renal impairment. The kidney lies within a capsule and increased venous pressures may result in a 'renal compartment syndrome' (Cruces et al. 2014). Clinical data suggest that critically ill patients with increased positive fluid balance are at greater risk of AKI (Payen et al. 2008). However, causality is difficult to prove as sicker patients are more likely to require fluid resuscitation and develop AKI from the underlying disease. I therefore compared values of septic to sham animals without any intravenous fluid (but the other invasive procedures were performed).

The invasive nature of the techniques places limitations on data interpretation. Instrumentation of the kidney and its vasculature is highly invasive and, in itself, was associated with a rise in serum creatinine (data not shown). The model was repeated without renal instrumentation to obtain histology and measurement of serum urea and electrolytes. The methodology cannot offer information on specific functional anatomical structures (e.g., glomerulus, peritubular area, outer versus inner medulla). The renal microvascular anatomy of the rat differs from large animals. Thus, observed distributive effects of sepsis on renal oxygenation may differ in humans.

Mitochondrial work was performed at levels of oxygen that are 'non-physiological'. Although differences were seen between kidney slices incubated with either septic or sham serum, it is yet to be determined whether the same hold true in physiological levels of oxygen. I demonstrated an upregulation in UCP-2 protein in the kidney. However, I have not demonstrated the functional significance of this, e.g. a reduction in ATP production. The role of uncoupling within the kidney needs to be better characterized with knowledge of the time course and the impact on of ATP turnover. The effect of

uncoupling can be determined either by inhibiting uncoupling (e.g. with genipin or siRNA) or by augmenting it (e.g. with dinitrophenol). Inhibition of uncoupling may result in greater ROS formation, the by-products of which could be measured.

5.6 Conclusion

Renal blood flow is maintained in fluid-resuscitated experimental sepsis. Renal cortical oxygenation falls despite similar renal oxygen delivery and utilization at 24 h. The presence of UCP-2 in the kidney at this timepoint suggests that mitochondrial uncoupling may account for the similar renal oxygen consumption despite less tubular workload (as reflected by a rise in GFR). I used multiphoton imaging of the live kidney slice to investigate the effect of systemically produced circulating factors on renal tubular bioenergetics. This resulted in a fall in tubular NADH and mitochondrial membrane potential that are consistent with mitochondrial uncoupling. Furthermore, the amount of tubular ROS production is increased. These changes may be driven by ROS as *in vivo* treatment with the ROS scavenger TEMPO abrogated the changes. Mitochondrial uncoupling itself may be an adaptive mechanism in which ROS production is limited. I have demonstrated that "circulating humors" and not RBF/ DO_2, may be causative in inducing mitochondrial dysfunction. If renal dysfunction (reduction in GFR) and decreased oxidative phosphorylation are adaptive phenomena to decrease reactive oxygen species production, then targeting global or renal DO_2 may not ameliorate organ injury.

6 The role of the NLRP3 inflammasome in sepsis-induced acute kidney injury

6.1 Background

The NLRP3 inflammasome has been best characterized in immune cells including monocytes and macrophages. However, intrinsic renal cells also demonstrate components of the inflammasome in various pro-inflammatory diseases, while pharmacological inhibition and/or genetic deletion have shown protective effects in many preclinical models of AKI.

The presence of inflammasome components in epithelial cells in closer proximity to the ureters and bladder suggests that the renal tubular epithelial inflammasome may have evolved to deal with local (ascending) Gram-negative infections. The late distal convoluted tubule, the connecting tubule, and the collecting duct epithelial cells express $P2X_7$, IL-18 and caspase-1 under basal conditions (Gauer et al. 2007). Similarly, medullary collecting ducts express TLR4 and its accessory molecules MD2, MyD88, and CD14 in response to LPS (Chassin et al. 2006). Uropathogenic *E coli* strains bind preferentially to intercalated cells of the collecting duct (Chassin et al. 2006) that can mount an appropriate immune response. A deficient TLR4/ inflammasome response, as seen in patients with TLR4 polymorphisms associated with hyporeactivity to LPS, predisposes to Gram-negative sepsis (Lorenz et al. 2002).

While the NLRP3 inflammasome is crucial for host immunity, it is unclear if excessive activation of the inflammasome in sepsis may have detrimental effects on organ function and survival. Several preclinical and clinical studies have investigated the role of inhibiting the inflammasome pathway in endotoxaemia and sepsis. There are clear benefits from preclinical models demonstrating the protective effect of Caspase-1 (ICE)

deficiency in a mouse model of endotoxic shock (Li et al. 1995). Similarly, NLRP3 deficient mice had markedly better survival compared to wildtype mice and produced significantly less IL-1β and IL-18 (Mariathasan et al. 2006). Pharmacological agents with inhibitory effects on the NLRP3 inflammasome, including dimethylsulphoxide, have also demonstrated survival benefit when mice were pre-treated (Ahn et al. 2014).

The effect of IL-1β blockade in sepsis has been evaluated in humans. A series of multicentre randomized clinical trials (RCT) in the 1990s investigated the therapeutic effect of human recombinant IL-1 receptor antagonist (IL-1ra) in sepsis. A dose-dependent 28- day survival benefit was seen in patients with septic shock due to Gram-negative infection (Fisher et al. 1994). *Post- hoc* analysis revealed an increased survival time in patients with sepsis and secondary organ dysfunction and a predicted mortality ≥24%. However, interim analysis of a subsequent multicentre RCT suggested it was unlikely that the primary efficacy endpoints would be met, so the study was terminated early (Opal et al. 1997).

The functional significance of *de novo* organ-specific inflammasome expression in systemic inflammatory diseases such as sepsis is unclear. The notion that NLRP3 inhibition may be beneficial in sepsis-induced AKI was demonstrated by caspase-1 deficiency in a LPS model of endotoxaemia (Wang et al. 2005). With the use of global KOs and receptor antagonists, it is difficult to ascertain the relative contribution of systemic versus renal inflammasome activation in sepsis-induced AKI. The role of TLR4 signaling in sepsis-induced AKI has been investigated in mice with functional TLR4 deficiency (C3H/HeJ mice). These mice transplanted with wild-type kidneys were protected from LPS-induced AKI, whereas wild-type mice transplanted with C3H/HeJ kidneys developed severe LPS-induced AKI. This suggests that TLR4 expression in circulating cells propagates injury in septic AKI rather than intra-renal TLR4 (Cunningham et al. 2004). However, in a murine model of UUO, use of bone marrow chimeras revealed that NLRP3 mediates injurious/inflammatory processes in both hematopoietic and non-hematopoietic cellular compartments (Vilaysane et al. 2010).

In another murine model of UUO, P2X$_7$ was upregulated in cortical tubular epithelial cells; genetic deletion protected against macrophage infiltration, collagen deposition and apoptosis (Goncalves et al. 2006). This contrasts with the predominant *glomerular* P2X$_7$ expression seen in a glomerulonephritis model, which was also protected by genetic deletion or by P2X$_7$ receptor antagonism (Taylor et al. 2009). The close association between the site of renal injury in and the presence of P2X$_7$, along with the protective effect of a P2X$_7$ antagonist or genetic deletion, strongly supports a role for P2X$_7$ in AKI pathogenesis.

A similar relationship may hold for sepsis-induced AKI. Pilot data from the rat sepsis model showed upregulation of proximal tubular epithelial P2X$_7$ at 6 hours, associated with (mild) acute tubular injury, while glomerular P2X$_7$ expression and damage were minimal (Figure 31).
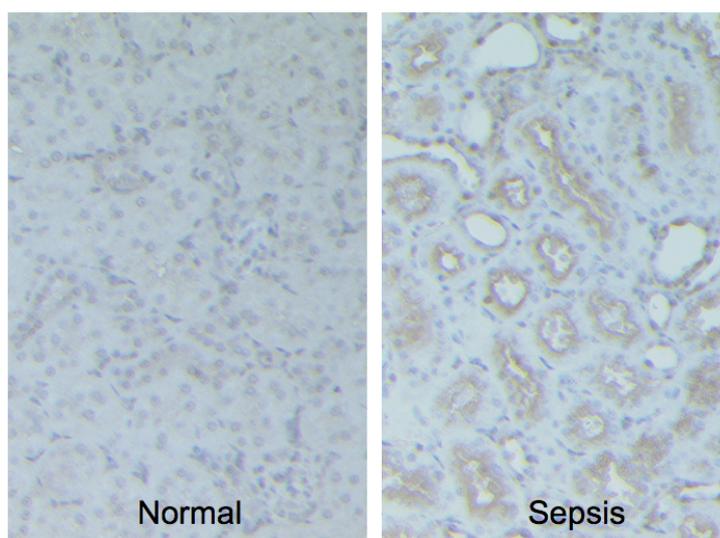
Figure 31 Renal tissues sampled at 6 h post-induction of faecal peritonitis (or control) were stained for the presence of the P2X$_7$. Significant acute tubular injury was seen in rats subjected to sepsis; this correlated with increased P2X$_7$ expression in the renal tubules. (x20 magnification)**.** On PAS sections there was little evidence of infiltrating cells while staining for macrophages (CD68) was negative at this early timepoint (Chapter 4).

I therefore hypothesized that upregulation of the ATP-sensitive $P2X_7$ receptor causes renal injury in sepsis through local production of cytokines and chemokines, and cell death. The aim of the work in this chapter was to define the role of the $P2X_7$ in septic AKI, specifically to:

1. *Define patterns of expression of this receptor within the kidney, its relationship to inflammasome expression within the kidney, and to histological changes;*

2. *Assess effects of $P2X_7$ antagonism in a rat model of sepsis-induced AKI*

6.2 Methods

6.2.1 Natural history of the renal inflammasome in sepsis

6.2.1.1 Live kidney slice incubation and immunoflurosence

The left kidney was removed from anaesthetized healthy male Wistar rats and immediately placed in oxygenated ice-cold HEPES-buffered solution (118mM NaCl, 10mM $NaHCO_3$, 4.7mM KCl, 1.44mM $MgSO_4$, 1.2mM $KH_2 PO_4$, 1.8mM $CaCl_2$, 10mM HEPES, 5mM glucose, 5 mM sodium butyrate, and 5mM pyruvate). The kidney was sliced in half along the transverse plane and mounted on a stage. Slices were cut at 200 μm in oxygenated ice-cold HEPES-buffered solution using a Microm 650V tissue slicer (OTS 5000 tissue slicer, Electron microscopy sciences, Hatfield, UK).

The slices were then placed in each well of a 6-well cell culture plate. (6-well Corning® Costar® cell culture plate (VWR, Lutterworth, Leicestershire, UK). Slices were washed 3 times with 1x PBS (1 ml per well). Slices were incubated in either sham serum (1:3 sham serum and 2:3 PSS) or septic serum sampled at the 24 h timepoint (1:3 septic serum and 2:3 PSS). Slices were then incubated in 5% CO_2/ 95% O_2 at $37^{\circ}C$ for 90 mins.

Live kidney slices were fixed with 4% methanol free PFA (about 500 µl per well) in 1x PBS for 15 min at room temperature. Slices were washed 3 times with 1x PBS (1 ml PBS

added per slice and washed for 1 min each time). Kidney slices were permeablized with 0.5% Triton-x 100 in 1x PBS (about 500 µl per well) at room temperature for 10 min on a plate shaker. Slices were washed three times as described. Slices were blocked with 10% BSA in 1x PBS for 2 h at room temperature followed by another three washes. Slices were incubated with primary antibody rabbit anti-mouse caspase-1 (Santa Cruz Biotechnology) diluted 1:500 in 1% BSA overnight at 4°C (1ml per well). The next day, slices were washed three times and the secondary antibody (Alexa Fluor® 568 goat anti-rabbit with excitation/emission wavelengths of 578⁄603nM, ThermoFisher Scientific. Waltham, MA USA) diluted 1:500 in 1% BSA in 1xPBS was added and slices incubated for 2 h incubation at room temperature in the dark. Slices were washed and nuclei were stained using DAPI (4',6-Diamidino-2-Phenylindole, Dilactate) with excitation/emission wavelengths of 360⁄460nM (ThermoFisher). Two drops of DAPI were added per ml of 1x PBS and slices incubated for 5 min at room temperature in the dark. Slices were washed three times and then washed with ddH$_2$O. Slices were mounted on glass slides and excess water removed using a pipette. 50µL of Mowiol mounting medium (made in laboratory using Chemicals from Sigma Aldrich) was added as a droplet to cover the slice and a coverslip was placed over the slices. The Mowiol mounting medium was allowed to dry at room temperature for 30 min. Slides were stored at 4°C.

All procedures following addition of the secondary antibody were performed in a room with minimal light so as to avoid bleaching of the fluorescent probes. All steps with incubations and washing were performed with the cell culture plate on a plate shaker with gentle agitation. One ml of reagent or wash solution was added per well to ensure the slice was covered adequately.

Slices were imaged using a Zeiss LSM 510 NLO axiovert microscope coupled to a tunable Coherent Chameleon laser. An internal detector captured emitted light. Image processing and analysis were performed using LSM software (Carl Zeiss, Welwyn Garden City, Herts).

6.2.1.2   Immunohistochemistry (Paraffin embedded sections)

Sections from the *in vivo* experiments (Chapter 4: Animal models of sepsis and recovery) were fixed in 10% formalin and embedded in paraffin. Sections were cut 5μm thick and then mounted on glass slides (performed by histopathology lab at Imperial College, London).

For detection of P2X$_7$, slides were dewaxed and rehydrated through graded xylene and ethanol, respectively. Antigen retrieval was performed by placing slides in 0.01M sodium citrate buffer heated to 90°C in a water bath for 15 min. Slides were then immersed in 50% methanol containing 0.3% H$_2$O$_2$ for 1 h to block endogenous peroxidase activity. Slides were washed with PBS then incubated with 20% normal goat serum for 30 min to prevent non-specific binding. The primary antibody (mAb P2X$_7$, APR-004, Alamone, Jerusalem, Israel) was diluted in 1% BSA/0.05M Tris-HCL (pH 7.2) and incubated at room temperature for 1 h. Slides were rinsed in PBS for 15 min and incubated with peroxidase-labelled polymer conjugated to goat anti-mouse immunoglobulins (Dako, Ely, Cambs) for 1 h. Antibody binding was visualized using 3,3'-diaminobenzidene (Dako) and counterstained with hematoxylin. Spleen tissue from a septic animal at 6 h was used as a positive control.

Sections were examined using a light microscope (Olympus Optical, London, UK) at x20 magnification. All sections were scored in a blinded manner. Ten random fields of view of the cortex were analyzed for each section at x20 magnification. P2X$_7$ staining was assessed semi-quantitatively using a Color Coolview camera (Photonic Sciences, Robertsbridge, UK) and analyzed using Image Pro Plus software (Media Cybernetics, Silver Spring, MD, USA). For each section, ten random fields of view were analyzed and mean fluorescence intensity calculated (Figure 32). One section from each sample was incubated with antibody diluent instead of primary antibody and served as control.

$$\text{ImagePro Score:} \quad \frac{\text{Area of P2X}_7 \text{ Expression x Density of P2X}_7 \text{ staining}}{\text{Total Area}}$$
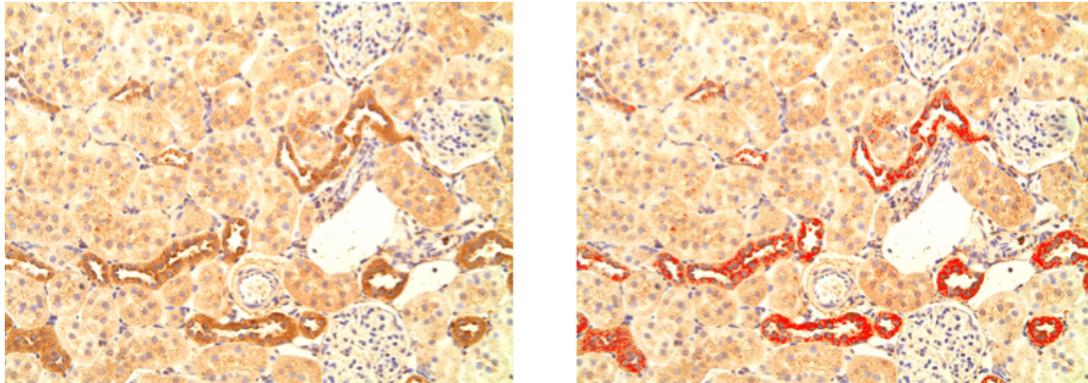
Figure 32: Localization of P2X$_7$ by Image Pro software. Increased P2X$_7$ is seen in cortical distal tubules and occasional proximal tubular cells, (x20 magnification).

6.2.1.3 Proximal tubular cell culture

NRK 52E rat tubular epithelial cells (Sigma Aldrich), derived from a primary cell line, were cultured in DMEM medium (Invitrogen, Paisley UK) supplemented with 10% fetal calf serum (FCS), 2 mM glutamine, 0.1 mM non-essential amino acids, 100 U/ml penicillin and 100 mg streptomycin. Cells were cultured in T75 flasks (TPP Techno Plastic Products AG, Trasadingen, Switzerland) at 37°C in 5% CO$_2$ / 95% O$_2$. Once confluent, cells were re-suspended (by adding 5 ml trypsin and placing in 5% CO$_2$ / 95% O$_2$ at 37°C for up to 5 min). The cells were then washed in Hank's buffered saline solution (HBSS; Invitrogen), counted using a haematocytometer (Bright-Line Hemacytometer, Sigma-Aldrich, Gillingham, Dorset, UK), and transferred to 6-well Corning$^®$ Costar$^®$ cell culture plates to achieve a concentration of half a million cells per well. Once confluent, complete medium was changed to serum-free medium for 24 h. Before stimulation, cells were washed with HBSS.

Two wells of cells were used as controls. Control cells were not exposed to lipopolysaccharide (from *Escherichia coli* 0111:B4, Sigma Aldrich) or the P2X$_7$ partial

agonist 2′(3′)-O-(4-Benzoylbenzoyl)adenosine 5′-triphosphate triethylammonium (BzATP; Sigma Aldrich). The four remaining wells of cells were primed with LPS (1 µg/ml) for 5.5 hours. Two wells had BzATP added at a concentration of 200 ng/ml for 30 minutes. At the end of this period, the supernatant was collected. Cells were treated with 0.5 ml 2-Mercaptoethanol (Sigma) and collected. The cells were stored at -80°C and supernatant stored at -20°C. Cells were analyzed for expression of IL-1β and P2X$_7$ protein using Western blot. IL-1β and MCP-1 were quantified in the supernatant using ELISA.

6.2.1.4   Monocyte isolation and culture

Naïve male Wistar rats were given 1000 units heparin intraperitoneally 30 min prior to culling. Animals were anaesthetized as described and blood obtained via cardiac puncture. Blood was stored in a sterile Falcon tube on ice. Fifteen ml blood was added to 30 ml volume of sterile PBS and mixed. Twenty ml was transferred onto 15 ml of Ficoll very slowly using a 1ml pipette to ensure the Ficoll-blood layer was not broken. The suspension was centrifuged for 30 min at 1400 rpm at room temperature ensuring the centrifuge break was off (to avoid disrupting the layer). Three layers were formed - the lowermost Ficoll layer, followed by the thin layer of monocytes, and the layer of PBS. Cells were re-suspended in 30 ml complete culture medium (RPMI with 10% FBS and 1% Pen/Strep) and centrifuged at 1200 rpm for 8 min at room temperature. The monocyte pellet was re-suspended once again and placed in 30 ml complete medium at 37°C in 5% CO_2 / 95% O_2 for 24 h. The next day, cells were centrifuged at 1200 rpm for 8 min at room temperature, re-suspended in 2 ml serum-free culture medium, and counted. Serum-free medium was added to give a total cell count of 4 x 10^6 cells per 1 ml. One ml was added per well in a 6 well plate and left overnight at 37°C in 5% CO_2/ 95% O_2.

The next day, cell culture was started. Macrophages and monocytes require priming with LPS (signal 1) prior to release of IL-1β by co-stimulation with LPS (signal 2). The duration of LPS-priming is variable, though 4 h has been shown to be adequate (Qu et al. 2007). Stimulation by ATP is only required for 30 min after LPS priming (Mehta et al. 2001).

The following conditions were used:

- control (unstimulated)

- LPS: 1 μg/ml LPS per well for 6 h

- LPS + ATP: 1 μg/ml LPS per well incubated for 5.5 h followed by 5 nM ATP for 30 min

- LPS + ATP + DMSO/P2X$_7$A: 1μg/ml LPS per well incubated for 5.5 h followed by 10 μM P2X$_7$ antagonist dissolved in DMSO (final concentration 2%) followed by 5 nM ATP for 30 min

- LPS + ATP + DMSO: 1 μg/ml LPS per well was incubated for 5.5 h followed by DMSO (final concentration 2%) followed by 5 nM ATP for 30 min

- Positive control BBG: 1 μg/ml LPS per well incubated for 5.5 h followed by 5 μM BBG and then 5 nM ATP for 30min

Cell suspension was collected in a 1.5 ml tube and centrifuged at 1200g for 5 min at room temperature. Medium was transferred to new tubes and the pellets dissolved in 50 μl RIPA. Samples were stored at -80°C.

6.2.1.5 Western Blot

Protein was extracted and estimated from cultured cells or from whole kidney tissue as described (sections 4.3.1, 6.2.1.3). Samples (20 μg protein) were electrophoresed at 100 V for 1 h through a 12% or 15% SDS-PAGE gel under reducing conditions. Proteins were transferred to a polyvinylidine difluoride (PVDF) membrane (GE Healthcare, Amersham, Bucks) at 10V for 45 min, and then blocked for 1 h in 5% milk/1% TBST. This membrane was then incubated with goat anti-mouse IL-1β (Santa Cruz Biotechnology) at 1:1000 overnight at 4°C. Following incubation with the primary antibody, HRP rabbit anti-goat IgG (Sigma) was added at 1:3000 in 5% milk for 1 h. Activity was detected using ECL Plus substrate (GE Healthcare).

6.2.1.6 ELISA

Serum samples were obtained during the experiment and centrifuged at 6500 rpm for 10 min in a lithium-heparin tube. The serum was siphoned off, snap-frozen in liquid nitrogen, and stored at -80°C. Supernatants from cell culture experiments were collected and stored in -80°C freezer. Sandwich ELISA was performed to assess serum levels of IL-1β and MCP-1 from cell culture experiments. DuoSet ELISA kits (R&D Systems, Minneapolis, MN, USA) were used according to the manufacturer's instructions. The antibody supplied in the IL-1β kit does not cross-react with pro–IL-1β. ELISA was also performed to assess the presence of cytokines within renal tissue homogenate. Tissue cytokine levels were expressed relative to the total protein content. Absorbance was read at 450 nm using a spectrophotometric ELISA plate reader (Anthos HTII; Anthos Labtec, Salzburg, Austria).

6.3 Statistics

All statistical analyses were performed using SPSS (IBM. Version 20) and graphs drawn using Graphpad Prism (GraphPad Software, Version 5.0d). Normality of continuous data was assessed using the Shapiro-Wilk test. Continuous variables are presented as means (standard deviation) where parametric, and median (interquartile range) where non-parametric. Parametric data were compared using unpaired Student's t-test, whereas non-parametric data were compared using the Mann Whitney U test for comparison of continuous data between 2 groups. For comparison of continuous variables between more than two groups, one-way analysis of variance (ANOVA) with post hoc Tukey's test is used. A p-value <0.05 was taken as statistically significant.

6.4 In vivo study

6.4.1 P2X$_7$ receptor antagonist
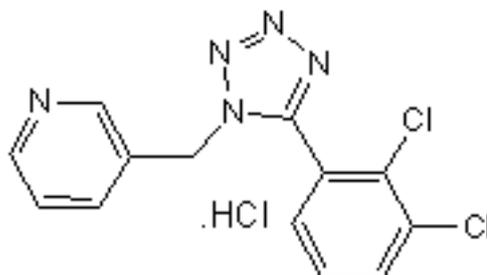
Figure 33 Chemical structure of P2X$_7$ antagonist (A-438079)

The P2X$_7$ antagonist (A-438079) (Figure 33) was kindly donated by Abbvie (Abbott Park, IL, USA). Based on previously published data and personal communication with Abbvie, the pharmacokinetic profile of the P2X$_7$ antagonist (A-438079) was determined. A 3 μM concentration of A-438079 has been shown to block 75% of IL-1β release from cultured peritoneal macrophages stimulated with LPS and BzATP (3 μg/ml LPS priming for 2 h followed by 30 min stimulation with 0.3 – 3.0μM BzATP) (Figure 34) (McGaraughty et al. 2007).

a. A-438079: P2X$_7$ Selectivity   b. A-438079 inhibition of IL-1β release
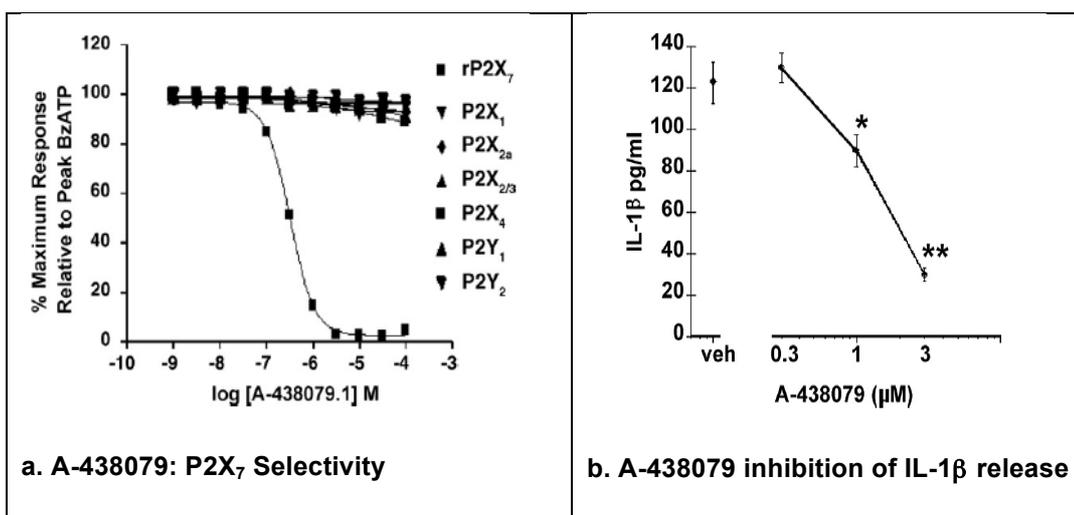
Figure 34 $P2X_7$ selectivity and effect on IL-1β release ($P2X_7$-related modulation of pathological nociception in rats (McGaraughty et al. 2007). (a). A-438079 blocked BzATP (10μM)–mediated changes in intracellular Ca^{++} concentrations at rat $P2X_7$ receptors but not at other P2 receptors. (b). A-438079 (0.3–3μM) attenuated the release of IL-1β from peritoneal macrophage cells following the application of 3μM BzATP.

6.4.2 Selection of time points

My aim was to study the *in vivo* activity of the drug and the clinical impact. The 72- hour characterization study informed timepoints for the antagonist study.

The main pharmacological action of the $P2X_7$ antagonist is to inhibit the NLRP3 inflammasome activity and therefore reduce IL-1β and IL-18. *In vivo* activity was therefore defined as the ability of the $P2X_7$ antagonist to reduce IL-1β and IL-18 release in the rat model of sepsis. As renal IL-1β is elevated at 6 h in this model, I therefore used this as the first predetermined timepoint. Serum IL-1β and IL-18 were elevated by 3 h and IL-1β remained elevated for 48 h. Therefore, one group of animals were given low dose DMSO/$P2X_7$ antagonist at the same time as sepsis was induced (pre-treatment group) to evaluate if the drug could decrease serum IL-1β in vivo at 24 h. As urinary IL-18 was only elevated after a rise in serum creatinine, this was therefore not used as an endpoint as the aim was to prevent the onset of AKI in sepsis.

The primary aim of this study was to evaluate the effect of $P2X_7$ antagonism on preventing renal dysfunction (as defined by an elevated serum creatinine) in sepsis (i.e. the clinical impact). Serum creatinine was elevated at 3 h in septic animals compared to sham animals. However, this primarily reflects hypovolaemia as creatinine (and urea) promptly fell after fluid resuscitation was started. Serum creatinine was subsequently significantly elevated at 24 h in septic animals compared to sham animals. Thus, 24 h was therefore used as the second predetermined time point.

6.4.3 Dose calculation

Unpublished data from Abbvie Pharmaceuticals demonstrates that the half-life of IV A-438079 is 0.69 h (41 min) (Figure 35, **Table 15**). An intravenous dose of 10 μg/kg can achieve a peak serum concentration of 4000 ng/ml. I intended to give a dose of $P2X_7$ antagonist sufficient to inhibit IL-1β release. I was therefore aiming for a peak concentration of at least 3 μM which would blocked 75% of IL-1β release from macrophages *in vitro*) (Figure 34).

A concentration of 3 μM A-438079 is equivalent to 1029 ng/ml (MW = 342.6). Therefore I chose an intravenous bolus of 10 μg/kg (giving a peak concentration of 4000 ng/ml) as the lower dose. As this drug was used to inhibit activity of tissue macrophages, a 'high dose' (20 μg/kg) was also chosen to achieve adequate tissue levels.
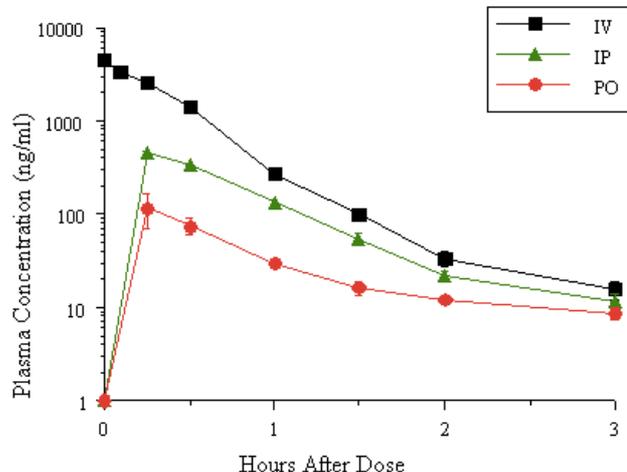
Figure 35 Pharmakokinetics of A-438079 (Data supplied by Steve McGaraughty, Abbvie USA. Personal communication). The half-life of IV A-438079 is 0.69 h (41 min). An intravenous dose of 10 μg/kg can achieve a peak serum concentration of 4000 ng/ml.

Vb$_p$ (L/kg)	Cl$_p$ (L/hr-kg)	T$_{1/2}$ (hr)
1.7	1.6	0.69

Table 15 Pharmakokinetics of A-438079 (10µmol/kg IV dose)

The antagonist was given as a single bolus to achieve a peak (therapeutic) concentration, followed by 4x the dose (i.e.: 40 µg/kg for the low-dose experiments) for the first half-life, followed by 2x the dose for the second half life, followed by 10 µg/kg/hr thereafter. For the 24 h experiments, a bolus dose of IV fluids was given at 6hrs as per protocol. In order to avoid dilution of the drug, the IV bolus contained 10µg/kg A-438079 (or twice as much for high-dose experiments) (Figure 36).
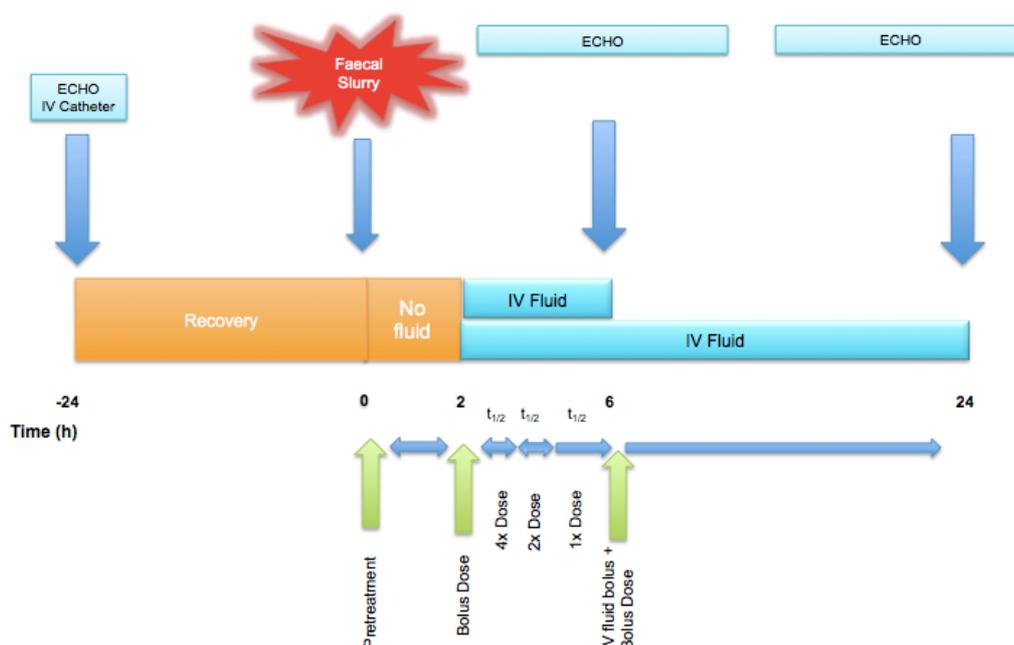
Figure 36 Study protocol. As renal IL-1β is elevated at 6 h in this model, this time point was chosen as the first timepoint. Serum creatinine was significantly elevated at 24 h in septic animals. Thus, 24 h was therefore used as the second time point. The carrier ± antagonist was started at 2 h post sepsis induction- at either high dose (n=10- 12 per

group) or low dose (n=6 per group). In a separate experiment, the carrier and antagonist was started at the induction of sepsis at a low dose.

6.4.4 Preparation of drug

On dissolving the drug in water for a final concentration of 20μM, the pH at room temperature fell to 2.2, and at $38^{o}C$ was 1.6. Higher concentrations of the drug produced even more acidic solutions. A stock solution of 80 μM had a pH of 1.4 at room temperature and 0.9 at $38^{o}C$. On addition of sodium hydroxide to neutralize the drug solution, the drug crystalized once the pH was >3. Preliminary experiments (data not shown) were carried out in which animals (n=7) received the low concentration of the drug. This however caused a significant metabolic acidosis and a raised anion gap compared to untreated septic animals.

I then selected dimethylsulfoxide (DMSO) as a drug solvent. This is a commonly used drug solvent however itself has biological activity (see below). I therefore compared DMSO-treated septic animals to DMSO / $P2X_7$ treated septic animals. The strength of DMSO used varied from 3-15% depending on the concentration of $P2X_7$ required (

, **Table 17**).

Time of infusion	$P2X_7$ concentration (μM)	$P2X_7$ (mg)	H_2O (ml)	DMSO (ml)	Total vol. (ml)	DMSO (%)
Initial bolus	10	2.25	0.9	0.1	1	10.0
Continuous infusion	10	2.25	3.2	0.1	3.3	3.0
Second $t_{1/2}$	20	4.5	3.15	0.15	3.3	4.5
First $t_{1/2}$	40	9	2.8	0.5	3.3	15

Table 16 Example calculation for 330g rat in low dose experiment

Time of infusion	P2X$_7$ concentration (μM)	P2X$_7$ (mg)	H$_2$O (ml)	DMSO (ml)	Total vol. (ml)	DMSO (%)
Initial bolus	20	4.5	3.15	0.15	3.3	4.5
Continuous infusion	20	4.5	3.15	0.15	3.3	4.5
Second t$_{1/2}$	40	9	2.8	0.5	3.3	15
First t$_{1/2}$	80	18	2.8	0.5	3.3	15

Table 17 Example calculation for 330g rat in high dose experiment

6.4.5 DMSO

Due to its amphipathic properties, DMSO is an effective solvent for water-insoluble compounds and is a hydrogen-bound disrupter. As such it is a commonly used solvent for many drugs in pharmacological studies. However, DMSO decreases IL-1β mRNA transcription and therefore reduces inflammation (Ahn et al. 2014). DMSO also inhibited NLRP3 inflammasome activity and attenuated IL-1β maturation, caspase-1 activity and ASC pyroptosome formation, but had no effect on NLRC4 and AIM2 inflammasomes. Pre-treatment with 10% DMSO resulted in a significant survival benefit in mice (Ahn et al. 2014). However, there are also isolated reports of the pro-inflammatory action of DMSO in human PBMCs (Xing and Remick 2005) and low-dose toxicity in a retinal neuronal cell line (Galvao et al. 2014). The action of DMSO needs to be evaluated further before any firm conclusions are determined. Differences may be related to the dose of DMSO, cell/species type, and duration of stimulation.

DMSO also exerts anti-inflammatory effects as a hydroxyl radical scavenger. In cardiac myocytes, DMSO can increase heme-oxygenase-1 (HO-1) mediated via activation of p38 MAPK and Nrf2 translocation (Man et al. 2014). Furthermore, mitochondrial reactive

174

oxygen species can induce IL-1β and NLRP3 activity, and this was inhibited by DMSO (Ahn et al. 2014).

Alternatives to DMSO as a solvent include ethanol and MF59. MF59 is an oil-in-water emulsion made of squalene, emulsified with two surfactants, polysorbate 80 and sorbitan trioleate (commercially known as Tween 80). Although MF59 does not act on the NLRP3 inflammasome, it activates MyD88 for a Toll-like receptor-independent signaling pathway (Seubert et al. 2011). Ethanol also has immunomodulatory effects on the NLRP3 inflammasome. The effects may depend on the cell type. In macrophages, ethanol decreased NLRP3 activation (Nurmi et al. 2013). In contrast, ethanol up-regulates NLRP3 expression and inflammasome activation in astrocyte supernatant (Alfonso-Loeches et al. 2014, Lippai et al. 2013). This is mediated by mitochondrial ROS generation and can be reversed by a specific mitochondria ROS scavenger (Alfonso-Loeches et al. 2014). As the purpose of this experiment was to investigate the potential role of NLRP3 inhibition in a clinically relevant model of sepsis, I chose to use DMSO.

6.4.6 Sample size calculation

The number of antagonist-treated animals and placebo-treated controls was calculated based on previous lab experience. I regarded a 20% change in a tested variable as an important biological effect. The sample size (n) was estimated according to the formula $n=2f(\alpha, P)\sigma^2/()^2$, where $f(\alpha, P)$ is a function of the power and significance level of the study, σ is the standard deviation of the measured variable, and $\mu1$ and $\mu2$ are the mean values in the two groups for comparison. The study was designed to have a power of 90% and a significance level of 5%. In these circumstances $f(\alpha, P)$ has a value of 10.5. Substituting the above values gives $n= 2 \times 10.5 \times 34.7/(54.5-(08 \times 54.5))^2$, i.e. n=6.1. Therefore I included at least 6 replicate animals per group per timepoint (**Table 18**).

		Treatment 2 h post- sepsis				Pre-treatment
Time	Untreated	Low dose DMSO	Low dose DMSO/ P2X$_7$	High dose DMSO	High dose DMSO/ P2X$_7$	Low dose DMSO/ P2X$_7$
6hr	7	-	-	6	6	-
24h	12	6	6	10	10	6

Table 18 Antagonist treatment groups and numbers of animals per group

Results

6.4.7   Natural history of renal inflammasome expression

6.4.7.1 $P2X_7$ expression

Naïve and sham-operated animals demonstrated minimal $P2X_7$ presence on immunohistochemistry. $P2X_7$ was present at a low level in distal tubular epithelial cells, and was predominantly localized to the basolateral membrane.

There was variable expression of $P2X_7$ in septic rats at 6h, and no significant difference in the expression of renal $P2X_7$ at 6 hours between sham-operated and septic rats as quantified by ImagePro software. Expression of $P2X_7$ in septic animals at 24h was present in both proximal tubules and distal tubules and was localized to the cytoplasm. In peri-mortem animals (excluded from statistical analyses) there was evidence of intraluminal debris, which stained intensely for $P2X_7$ (Figure 37). At 24h, renal $P2X_7$ expression in septic compared to sham-operated animals (0.015 ± 0.002 vs. 0.007 ± 0.003; p=0.003) was significantly increased (**Table 19**), (Figure 38).

	6hr			24hr		
	Sham	Septic	p	Sham	Septic	p
$P2X_7$ score	$0.009 \pm$ 0.006	$0.018 \pm$ 0.011	0.310	$0.007 \pm$ 0.003	$0.015 \pm$ 0.002	0.003*

Table 19 Renal histology $P2X_7$ quantification (Arbitrary units)
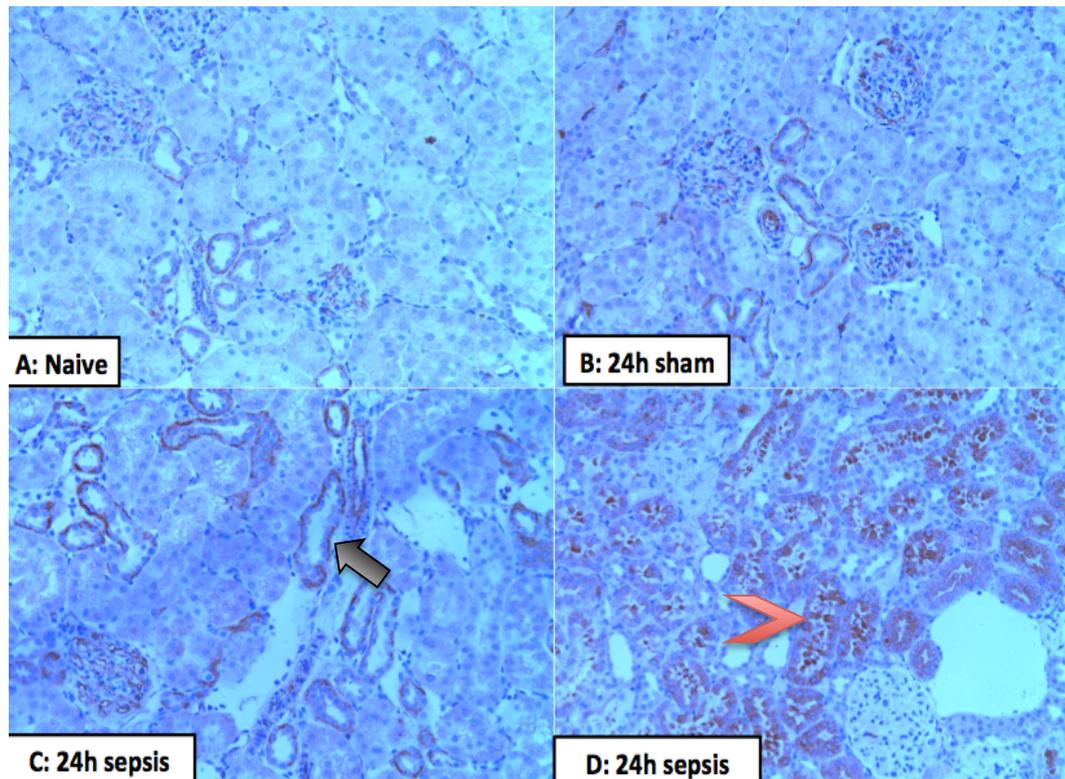
Figure 37: Histological assessment of renal $P2X_7$ (20x magnification)

A: Naive kidney with minimal $P2X_7$;

B: Kidney from a 24 h sham animal with minimal $P2X_7$, mainly within the capillary loops of the glomeruli and at the basolateral regions of tubules (black arrow);

C: Kidney from a 24 h septic animal with a similar pattern as the 24 h shams but greater intensity and wider distribution;

D: Kidney from a severe septic animal at 24 h with intense staining for $P2X_7$ of intraluminal debris (red arrowhead)
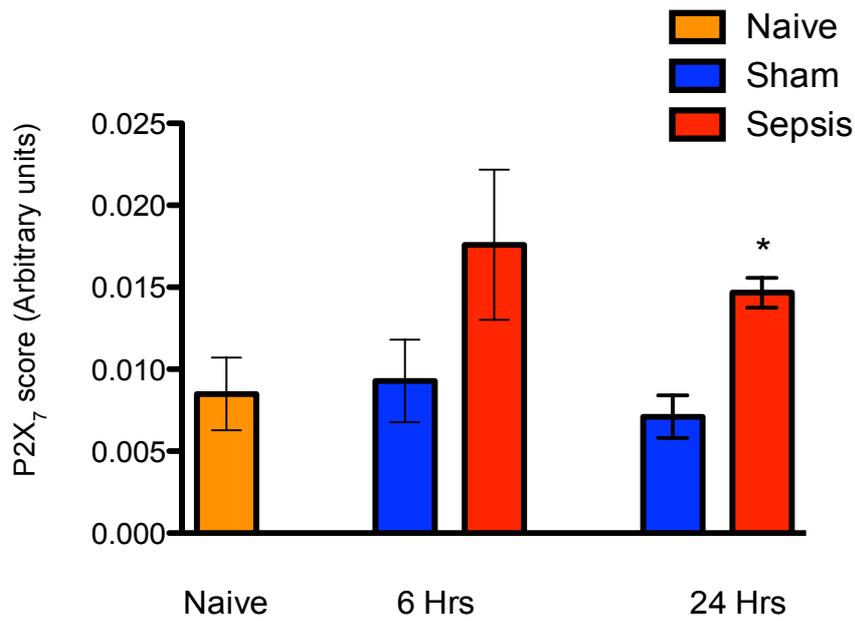
Figure 38 Immunohistochemistry scores for $P2X_7$ expression in naïve, sham and septic animals (n=6-8 per group). There is significantly increased renal tubular $P2X_7$ expression at 24h in septic animals compared to sham animals. Bar graphs and error bars represent mean and standard deviation respectively of ≥ 6 replicates (* $p<0.05$ sham serum vs. septic animals).

Cultured NRK52E cells did not express pro-IL-1β or $P2X_7$ protein under basal conditions. Cells treated with LPS showed significant increases in $P2X_7$ and pro-IL-1β protein in LPS-primed cells. There was no increase in pro-IL-1β or $P2X_7$ protein when NRK52E cells were co-incubated with BzATP (**Figure 39**).

Western blot

Rat tubular epithelial cells

75—		P2X7
37—		pro-IL1β
37—		β actin

LPS	-	+	+
BZ ATP	-	-	+
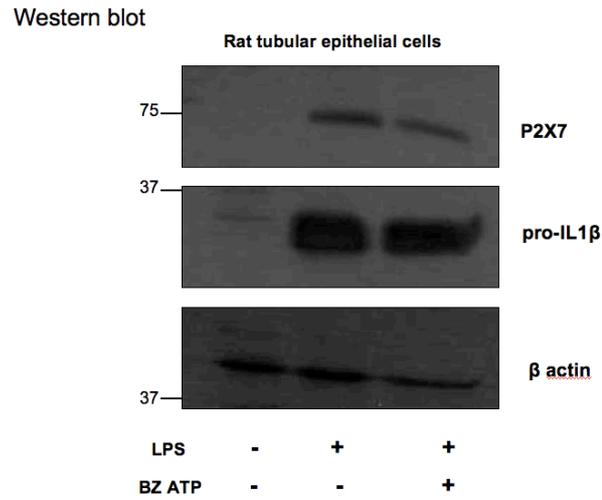
Figure 39 The presence of P2X$_7$ and pro-IL-1β protein in LPS-primed NRK 52E rat tubular epithelial cells is demonstrated by Western blotting. P2X$_7$ and pro-IL-1β protein were not detected under basal conditions. Experiment conducted once.

6.4.7.2   Caspase-1 expression
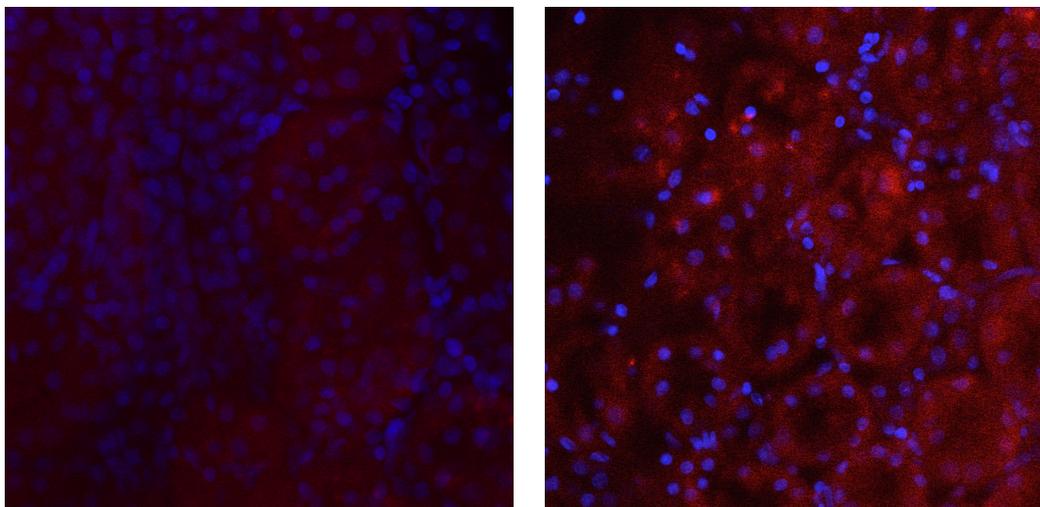
Figure 40 Immunofluoresence for caspase-1 of live kidney slice incubated in sham serum (left panel) and septic serum (right panel). Experiment conducted twice, each in triplicates

The live slice of the naïve rat kidney incubated in sham serum did not reveal any caspase-1 on immunofluroscence. When incubated in septic serum for 90 min, immunofluorescence revealed caspase-1 in proximal tubular cells (

Figure 40).

6.4.7.3 IL-1β expression
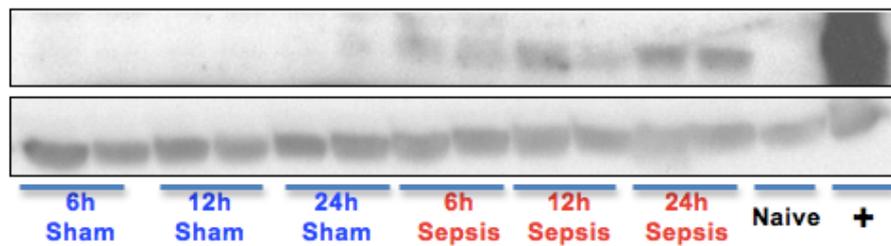
Figure 41 IL-1β Western blot of kidney homogenate from sham and septic animals at 6 h, 12 h, and 24 h. Positive control (+) is a spleen from a septic animal. Loading control is alpha-tubulin (55kDa). Pro-Il1β (31kDa) is present in septic kidney homogenates only. The quantity of IL-1β expressed in septic kidneys increases from 6h to 24h. Active (cleaved) IL-1 β was not detected in kidney homogenate. n=2 per group. Experiment conducted once.

There was no pro-IL-1β or active (cleaved) IL-1β expression in kidneys of sham-operated animals. Pro-IL-1 β was expressed in the kidneys of septic animals with an increment in the relative expression over time (from 6 to 24 h) (Figure 41). Active IL-1β was not detected. The results of the Western blot are consistent with the ELISA (Section 4.5.5).

Cultured NRK52E cells did not release IL-1β into the supernatant as detected by ELISA on stimulation with LPS or LPS and BzATP (despite expression of pro-IL-1β in the homogenate of cells exposed to LPS (**Figure 39**). There was a significant amount of MCP-1 detected in the supernatant of cultured NRK52E cells stimulated with LPS (Figure 42).

MCP-1 (pg/mL)
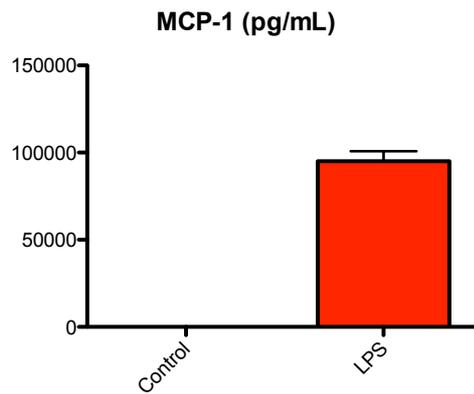
Figure 42 MCP-1 production by renal tubular epithelial cells. NRK52E cells produce MCP-1 on exposure to LPS. Experiments were conducted twice, in triplicates. Bar graphs and error bars represent mean and standard deviation respectively of 6 replicates (p<0.001)

Effect of DMSO and P2X$_7$ antagonist on IL-1β production

IL-1β (pg.ml^{-1})
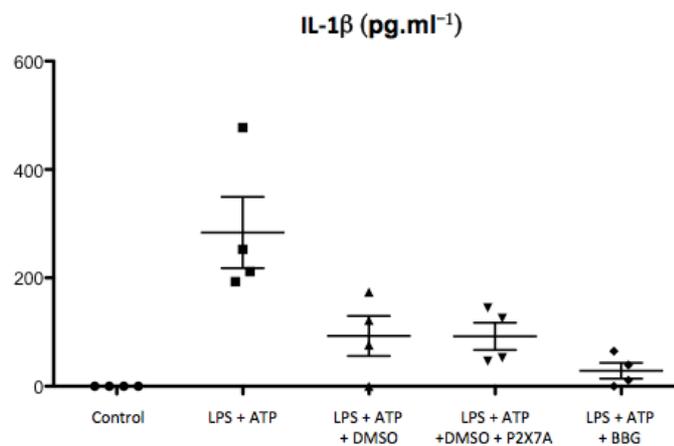
Figure 43 Effect of DMSO and P2X$_7$ antagonist on monocyte IL-1β release. LPS priming followed by ATP stimulation resulted in significant IL-1β release from PBMCs. 2% IL-1β release was inhibited by the addition of 2% DMSO prior to ATP exposure. Addition of 10 μM P2X$_7$ antagonist had no added effect on the reduction of IL-1β release. 5 μM BBG had a significant inhibitory effect on monocyte IL-1β release**.** Experiments were

conducted twice, with each condition in duplicate. Data plotted represents mean and standard deviation.

LPS and ATP together resulted in significant IL-1β production. Addition of 2% DMSO significantly inhibited the release of IL-1β. Addition of 10 μM P2X$_7$ antagonist had no added effect on the reduction of IL-1β release. 5 μM BBG had a significant inhibitory effect on monocyte IL-1β release.

6.4.8   Effect of P2X$_7$ antagonist in sepsis

One animal (untreated) in the 24 h study died prematurely. When treatment was commenced 2 h after the onset of sepsis, there were no clear benefits of treatment with low-dose DMSO or low-dose DMSO/P2X$_7$ (data not shown in figures but tabulated in the appendix). However, if treatment with low-dose DMSO/P2X$_7$ was commenced at the initiation of sepsis, there was an improvement in haemodynamics (tachycardia and stroke volume) at 6 and 24 h. At 24 h, MAP and global DO$_2$ were higher, and serum creatinine was lower in pre-treated animals compared to untreated animals. There was also a trend for a lower serum IL-1β value (p=0.07) at 24 h in low dose pre-treated animals.

Compared to untreated animals, high-dose DMSO treated animals showed no significant improvement in clinical parameters (Figure 44). At 6 h, animals treated with high dose DMSO had lower values of creatinine and lactate, compared to untreated animals. However, all animals had biochemical parameters within the normal clinical range and so the differences in creatinine and lactate are of doubtful clinical significance (Figure 45). The 24 h serum MCP-1 was higher in high dose DMSO treated animals (Figure 46). The mechanism and clinical significance behind these are unclear, as previous reports mention DMSO inhibition of MCP-1 transcription in response to LPS or IL-1β (Xing and Remick 2007, Xing and Remick 2007).

The combination of high dose P2X$_7$ antagonist and DMSO had several beneficial effects. At 6 h, animals treated with high dose DMSO/P2X$_7$ had a lower temperature and higher SaO$_2$ compared to untreated animals (Figure 44). The 6 h renal IL-1β and IL-10 were significantly lower in DMSO/P2X$_7$ treated animals, although this did not translate to a lower serum creatinine at 24 h (Figure 45). There was a *trend* to a lower serum IL-1β, creatinine, and urine NGAL at 24 h in DMSO/P2X$_7$ treated animals, though none reached statistical significance.

At 24 h, there was a significant improvement in cardiac function (stroke volume and heart rate) associated with DMSO/P2X$_7$ treatment. The 24 h serum lactate was lower and albumin higher with DMSO/P2X$_7$ treatment compared to untreated and DMSO-treated animals. Only serum lactate, albumin, and anion gap were significantly improved in high dose DMSO/P2X$_7$ treated animals compared to high dose DMSO-treated animals at 24 h.

6.4.8.1 Systemic variables

6hr Change in SV (%)

24hr Change in SV (%)

6hr MAP (mmHg)

24hr MAP (mmHg)

6hr Global DO$_2$ (ml.min^{-1})

24hr Global DO$_2$ (ml.min^{-1})

6hr SVR (ml/min/mmHg)

24hr SVR (ml/min/mmHg)

6hr SaO$_2$(%)

24hr SaO$_2$(%)
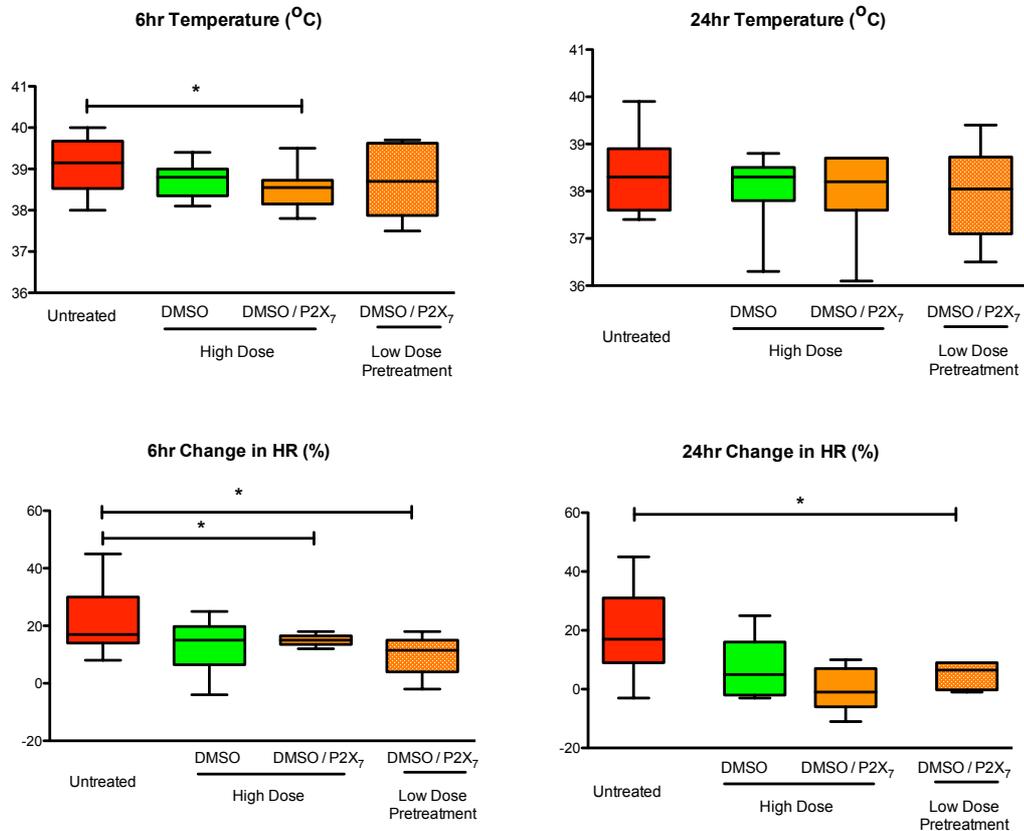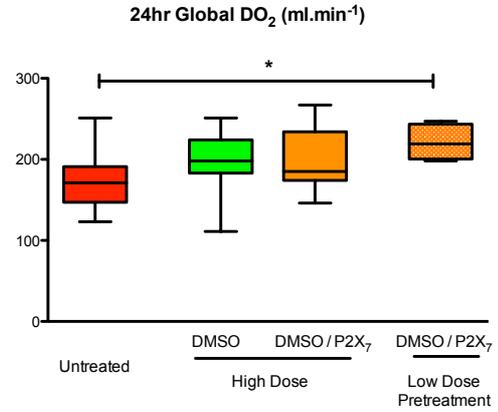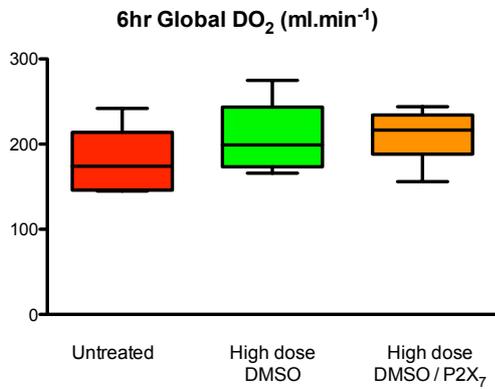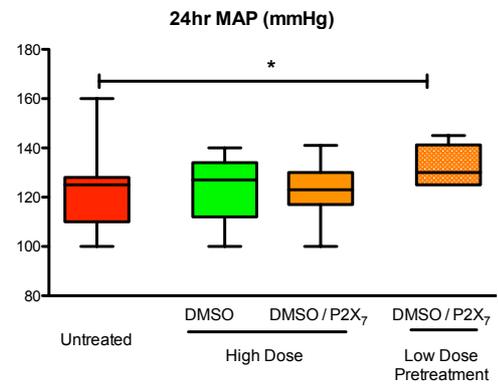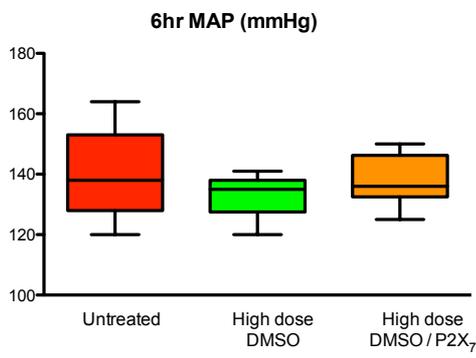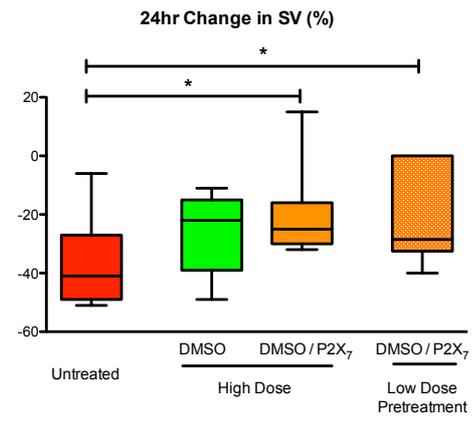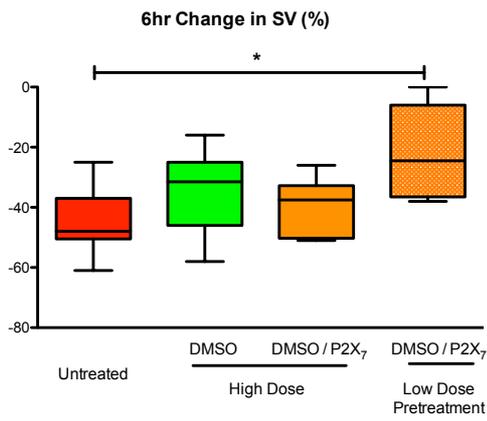
Figure 44 P2X$_7$ antagonist experiment- Systemic variables following induction of experimental sepsis in Wistar rats (that received no drug, DMSO carrier, or P2X$_7$ antagonist in DMSO). At 6 h, the combination of P2X$_7$ antagonist in DMSO blunted the increase in core body temperature, and tachycardia compared to untreated septic animals. At 24 h, the combination of P2X$_7$ antagonist in DMSO was associated with a higher stroke volume than untreated septic animals. Box and whisker plots represent mean and standard deviation respectively. Experiments included 6 animals per group for 6 h time point and 10 -12 animals per group for 24 h time point. (* $p < 0.05$).

6.4.8.2   Biochemistry

6hr Lactate (mmol/L)

24hr Lactate (mmol/L)

6hr Urea (mmol.l^{-1})

24hr Urea (mmol.l^{-1})

6hr Creatinine (umol.l^{-1})

24hr Creatinine (umol.l^{-1})

Figure 45 $P2X_7$ antagonist experiment- Biochemistry following induction of experimental sepsis in Wistar rats (that received no drug, DMSO carrier, or $P2X_7$ antagonist in DMSO). Serum lactate and creatinine were statistically higher in the $P2X_7$ antagonist/DMSO treated group compared to the DMSO treated group- though the clinical significance of the marginally elevated creatinine and lactate is unclear. Animals in the $P2X_7$ antagonist/DMSO treated group had a lower arterial lactate and higher serum albumin than the DMSO treated group and the untreated group. Only the pre-treated ($P2X_7$

antagonist/DMSO) animals had a lower serum creatinine, despite a half of the dose. Box and whisker plots represent mean and standard deviation respectively. Experiments included 6 animals per group for 6 h time point and 10 -12 animals per group for 24 h time point. (* $p<0.05$).

6.4.8.3 Systemic cytokines

6hr Serum IL-1beta (pg.mL^{-1})

24hr Serum IL-1beta (pg.mL^{-1})

6hr Serum IL-6 (pg.ml^{-1})

24hr Serum IL-6 (pg.ml^{-1})

6hr Serum MCP-1 (pg.ml^{-1})

24hr Serum MCP-1 (pg.ml^{-1})

6hr Serum IL-10 (pg.ml^{-1})

24hr Serum IL-10 (pg.ml^{-1})
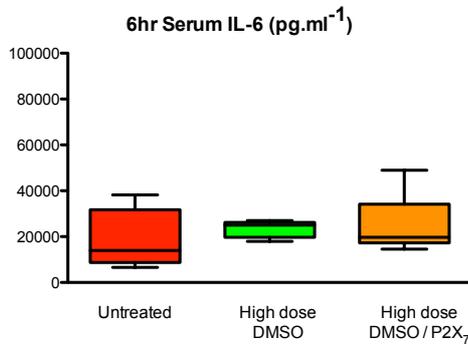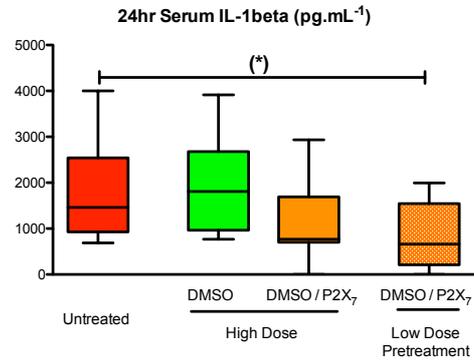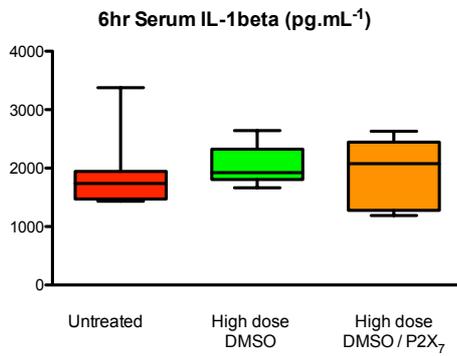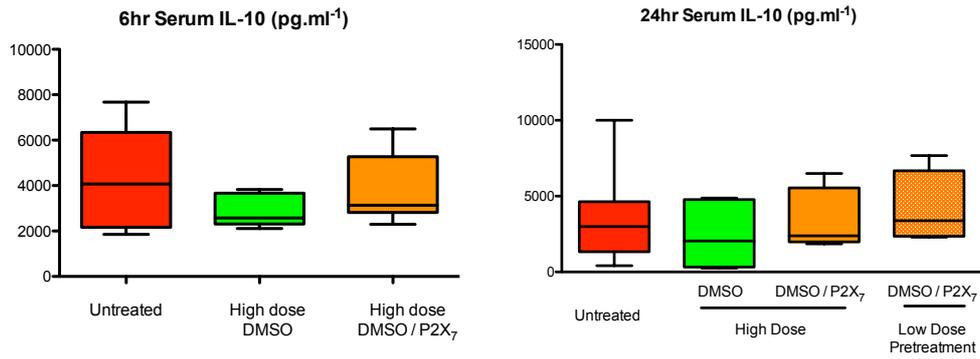
Figure 46 P2X$_7$ antagonist experiment- Systemic cytokines following induction of experimental sepsis in Wistar rats (that received no drug, DMSO carrier, or P2X$_7$ antagonist in DMSO). Serum cytokines were not different between groups at 6 h. At 24 h, only the pretreatment group had a lower serum IL-1β compared to the untreated group. Box and whisker plots represent mean and standard deviation respectively. Experiments included 6 animals per group for 6 h time point and 10 -12 animals per group for 24 h time point. (* p<0.05)

Renal cytokines

6hr Renal IL-1beta (pg/mg protein)

24hr Renal IL-1beta (pg/mg protein)

6hr renal MCP-1 (pg.mg protein^{-1})

24hr renal MCP-1 (pg.mg protein^{-1})
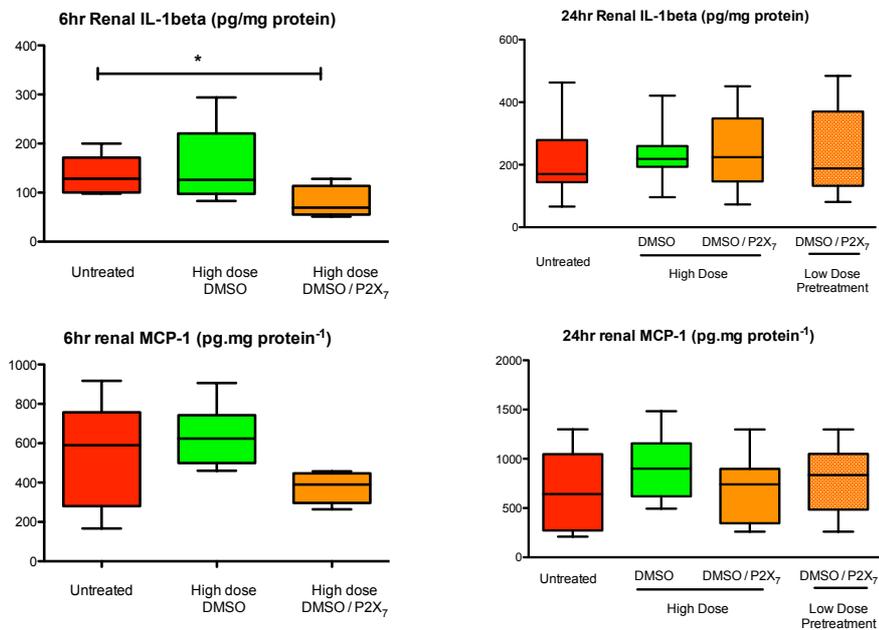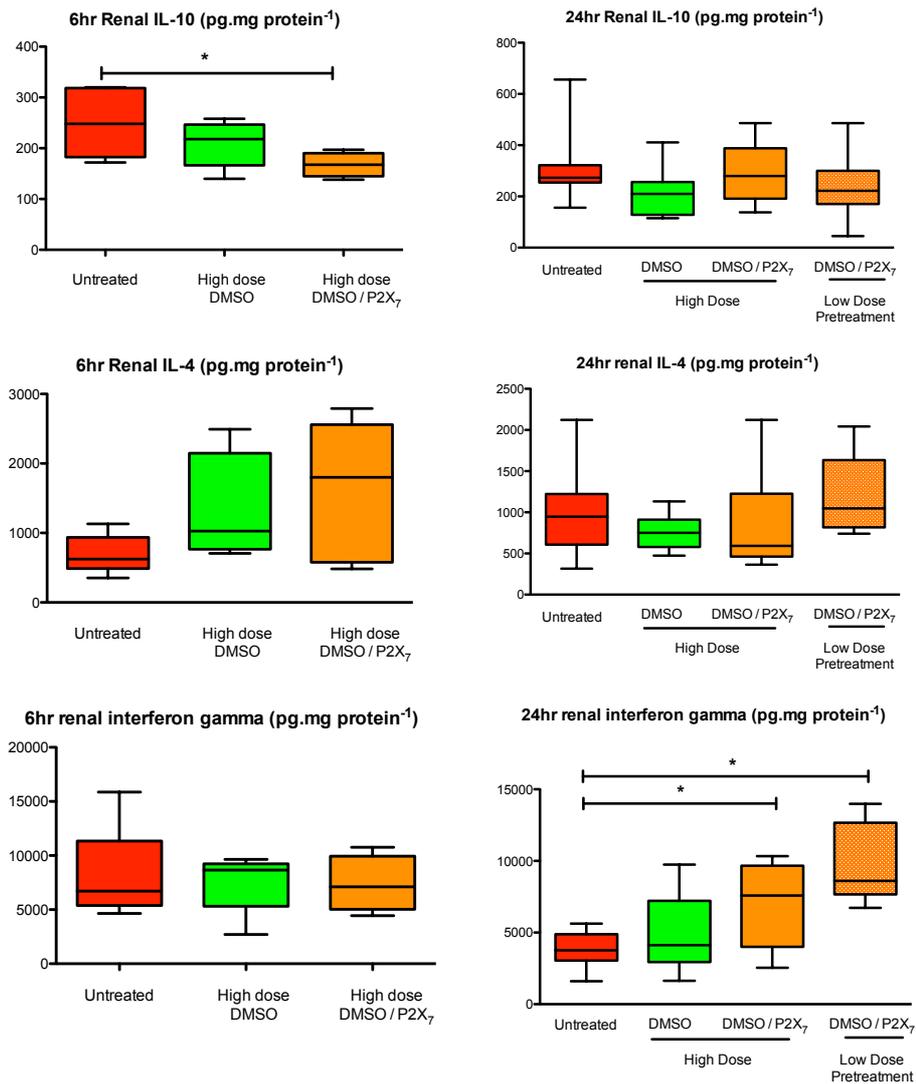
Figure 47 P2X$_7$ antagonist experiment- Renal cytokines following induction of experimental sepsis in Wistar rats (that received no drug, DMSO carrier, or P2X$_7$ antagonist in DMSO). At 6 h, the animals in the P2X$_7$ antagonist/DMSO treated group had a lower renal IL-10 and IL-1b compared to untreated animals. At 24 h, this difference did not persist. Renal INF-g was significantly higher in the P2X$_7$ antagonist/DMSO treated animals and the pretreated low dose P2X$_7$ antagonist/DMSO compared to the untreated animals. Box and whisker plots represent mean and standard deviation respectively. Experiments included 6 animals per group for 6 h time point and 10 -12 animals per group for 24 h time point. (* $p < 0.05$)

6.4.8.4 Urine Biomarkers

6hr Urine NGAL (ug/mL)

24hr Urine NGAL (ug/mL)

6hr Urine IL-18 (pg/ml)

24hr Urine IL-18 (pg/ml)

6hr Urine MCP-1 (pg/ml^{-1})

24hr Urine MCP-1 (pg.ml^{-1})

6hr Urine KIM-1 (pg.ml$_{-1}$)
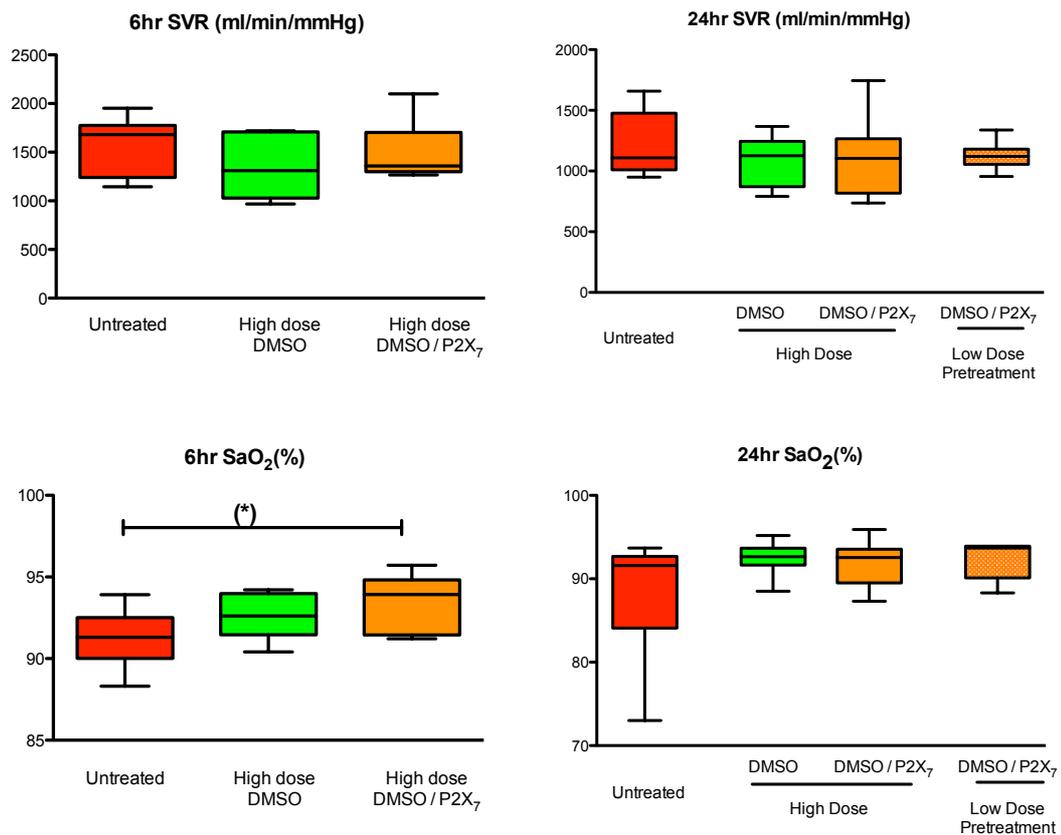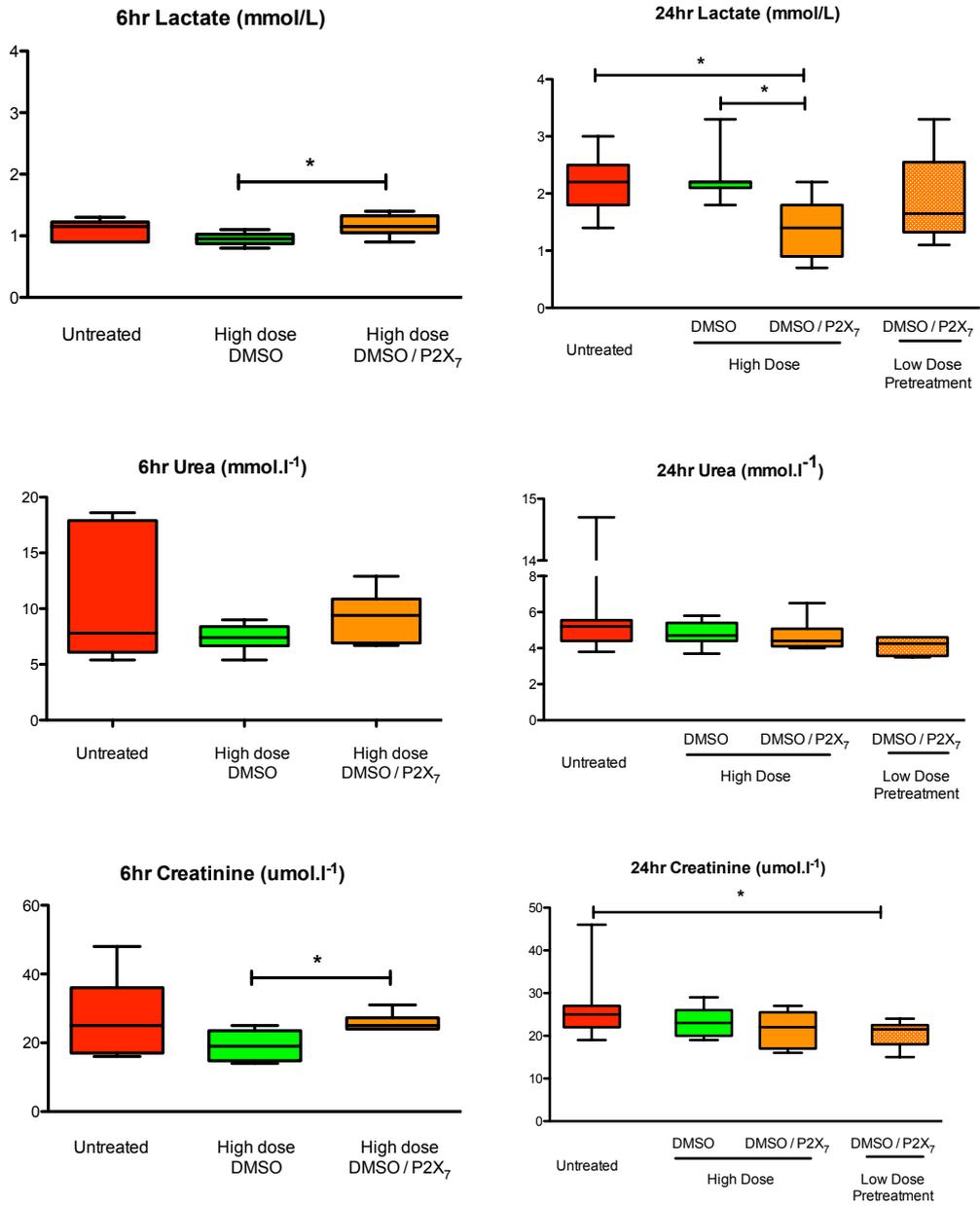

24hr renal KIM-1 (pg.ml^{-1})
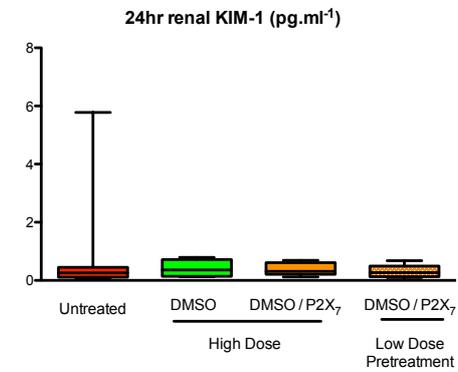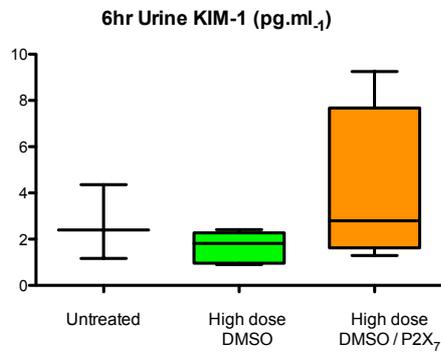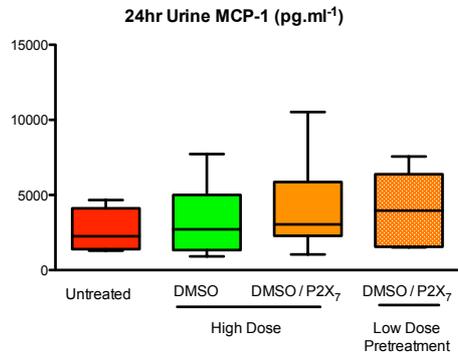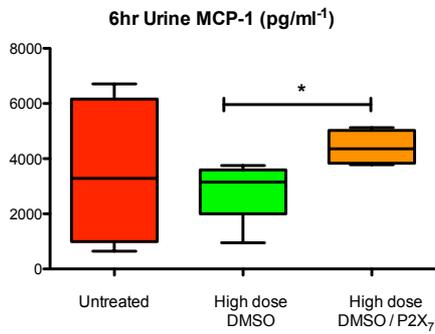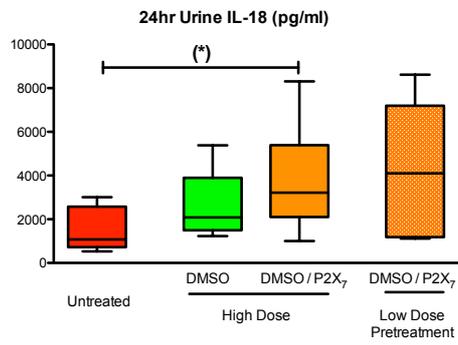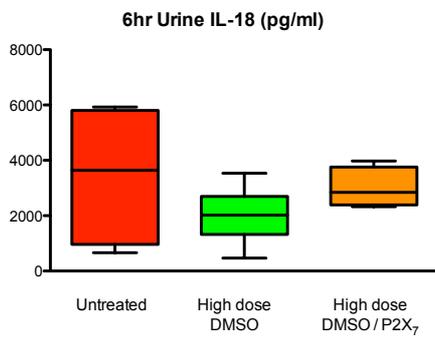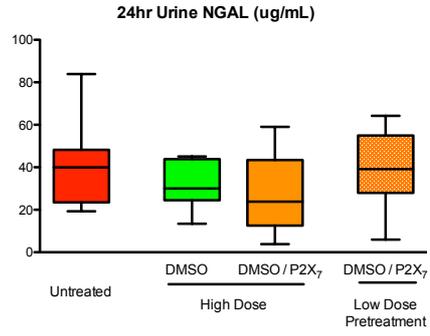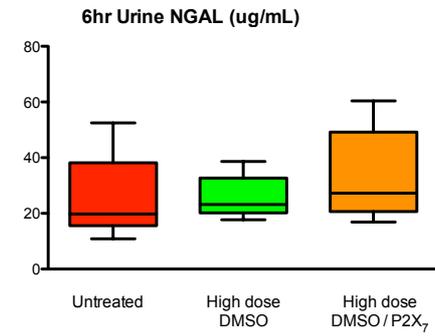
Figure 48 P2X$_7$ antagonist experiment- Urine biomarkers following induction of experimental sepsis in Wistar rats (that received no drug, DMSO carrier, or P2X$_7$ antagonist in DMSO). Apart for a higher urine MCP-1 at 6 h in the P2X$_7$ antagonist/DMSO treated animals compared to the DMSO treated animals, there were no difference in urine biomarkers between groups at 6 h or 24 h. Box and whisker plots represent mean and standard deviation respectively. Experiments included 6 animals per group for 6 h time point and 10 -12 animals per group for 24 h time point. (* $p < 0.05$)
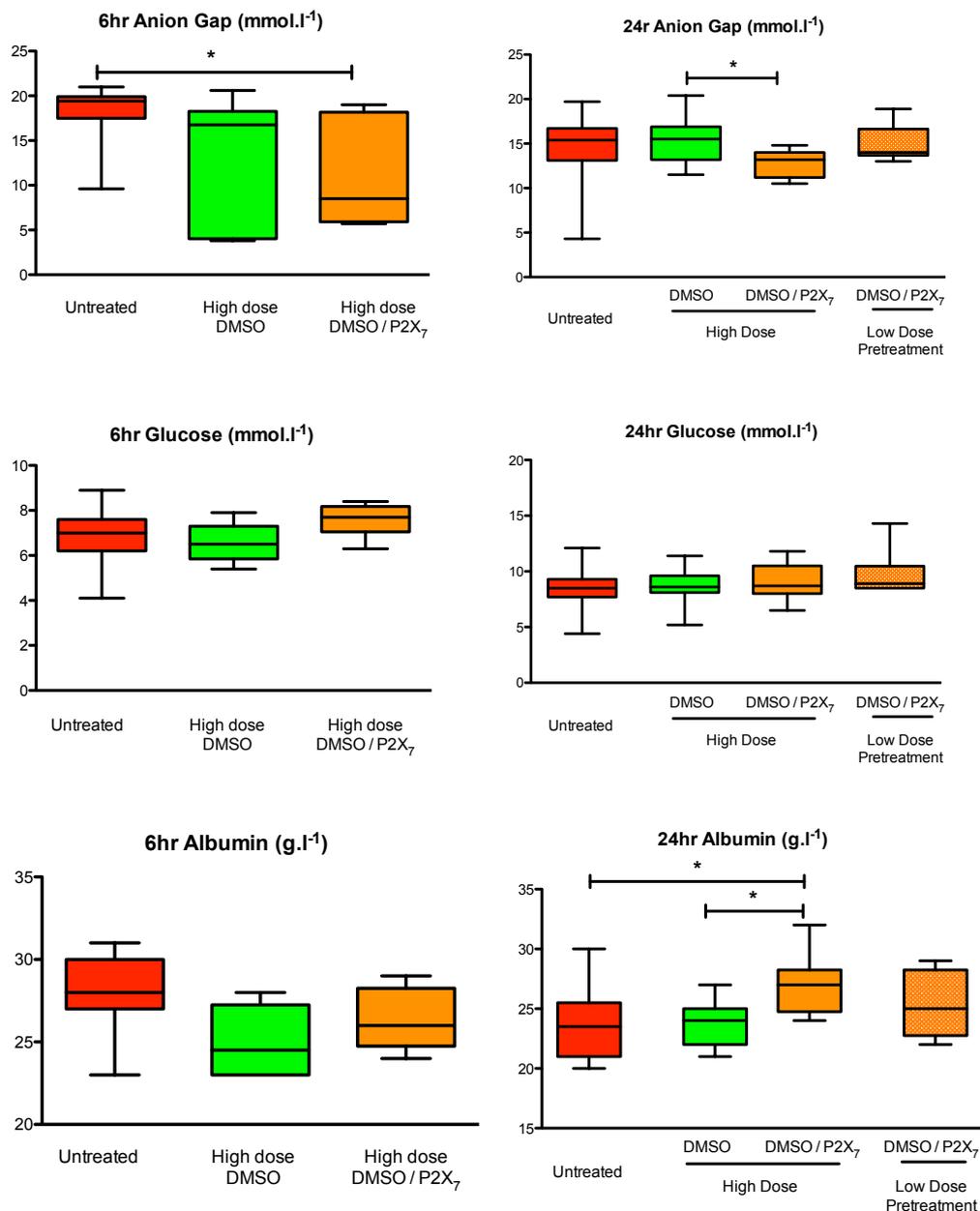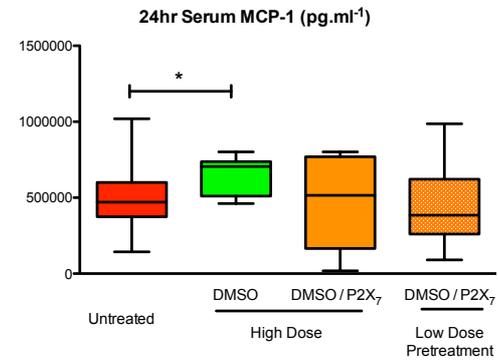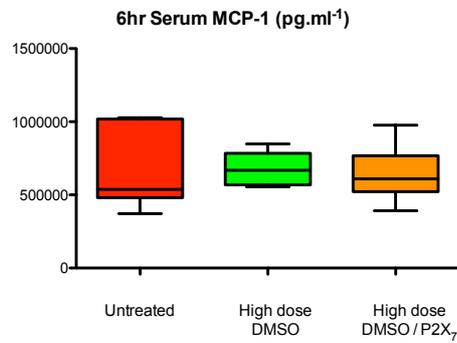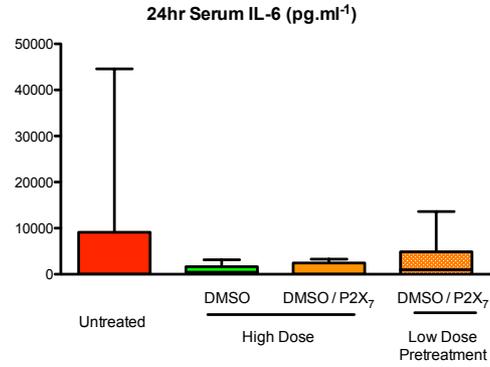
6.5 Discussion

6.5.1 Natural history of the inflammasome within intrinsic renal cells

Using different techniques, I have demonstrated expression of various components of the NLRP3 inflammasome in this septic model. My findings are consistent with published data showing that LPS-primed Madin–Darby canine kidney (MDCK) renal tubular epithelial cells express Toll-like receptor 4, NLRP3, caspase-1, interleukin-1β and interleukin-18 mRNA (Jalilian et al. 2012).

I found using both renal immunohistochemistry and cell culture techniques that renal tubular epithelial cells express $P2X_7$ in response to sepsis and LPS, respectively. Immunohistochemistry revealed positive $P2X_7$ staining of intraluminal debris. It is likely that the debris represents mucoprotein rather than shed tubular cells, as a TUNEL stain would be positive if the latter were the case. Increased staining is likely to represent non-specific binding of protenaceous material to the $P2X_7$ antibody. Nevertheless, Western blot of LPS-stimulated NRK52E renal tubular cells demonstrated expression of $P2X_7$, confirming the positive staining of proximal tubules I visualized on immunohistochemistry (experiment repeated twice). Furthermore, tubular cells express caspase-1 on incubation of a live kidney slice in septic serum. The use of the live kidney slice experiment allows examination of the effect of circulating mediators on renal inflammation, independent of renal perfusion/blood flow. The latter experiment was performed on three slices incubated in pooled septic serum from 6 animals.

In my 72 h model of sepsis and recovery, serum IL-1β was significantly elevated by 3 h. This was maintained for 24 h, followed by a gradual fall to normal levels by 48 h. Renal levels of IL-1β started to rise by 3 h but peaked at 24 h. Neither renal nor serum IL-β levels could differentiate between animals predicted to survive or die. There were no clear differences between IL-18 levels in sham and septic animals, with large inter-

individual variations in levels. A non-significant increase in serum IL-18 was seen at 3 h. One would expect a significant correlation between serum IL-1β and IL-18 levels as their release is tightly coupled. The peak in IL-1β and IL-18 did coincide, lending evidence to the role of early inflammasome activation in sepsis. Urine IL-18 fell in septic animals compared to sham animals at 3 h. Urine IL-18 levels started to rise from 12 h in septic animals predicted to live, and peaked at 48 h. The peak in urine IL-18 coincided with clinical recovery. Urine IL-1β was not detectable in the urine of septic animals at either 6 or 24 h.

6.5.2 Effect of P2X$_7$ antagonist in sepsis

I hypothesized that P2X$_7$ receptor antagonism ameliorates renal dysfunction in sepsis (as defined as a rise in serum creatinine). I did not find any difference in serum creatinine levels between P2X$_7$ receptor antagonist-treated animals and untreated animals when treatment was initiated after the onset of sepsis. However, it is not possible to come to any firm conclusion, as I could not demonstrate a significant rise in serum creatinine in the untreated animals. In the 72 h characterization study (Chapter 4), there was a statistically significant rise in serum creatinine, though only 30% above baseline. The lack of rise in creatinine in the experiments repeated for the antagonist study is a reflection of the limitations of serum creatinine as a biomarker in AKI and also a limitation of this animal model of sepsis, where serum creatinine rise is not clinically significant. I therefore measured urine NGAL, a more sensitive biomarker of AKI than serum creatinine. Although urine NGAL was lower in animals treated with high dose DMSO/P2X$_7$ compared to untreated animals (23 (15 – 40) vs. 40 (24-47) μg/ml respectively), this did not reach statistical significance so a Type II error may exist.

DMSO/P2X$_7$ reduced renal inflammation as indicated by lower renal IL-1β levels at 6 h. Treatment was initiated early enough (at 2 h), before renal IL-1β levels had peaked. The reduction in renal IL-1β was not sustained at 24 h, which may relate to the dosing

regimen used. In contrast to renal IL-1β, serum IL-1β peaked by 3 h in untreated animals. Therefore treatment initiated at 2 h did not significantly reduce either serum IL-1β or IL-18 (see Appendix) at 24 h.

Despite a trend towards a lower serum creatinine and urine NGAL at 24 h in DMSO/P2X$_7$ –treated animals, there was an increase in urine IL-18 that approached statistical significance (p=0.06) in DMSO/P2X$_7$-treated animals compared to untreated animals. This was associated with a significant increase in renal INF-γ. Elevated urine IL-18 and NGAL are both markers of AKI. Yet, a fall in NGAL was associated with a rise in urine IL-18 with P2X$_7$ antagonist treatment. This was also associated with an increase in renal INF-γ expression. INF-γ is a potent modulator of P2X$_7$ expression and activity in epithelial cells (Welter-Stahl et al. 2009). I hypothesize that inhibition of P2X$_7$ receptor may have increased INF-γ expression by negative feedback, mediated via IL-18 production (a potent inducer of INF-γ). The increase in IL-18 may have been via P2X$_7$-independent but TLR4-dependent pathways (Gupta et al. 2006).

As would be predicted, there would be systemic effects of inhibition of the inflammasome in sepsis over and above renal-specific effects. The reduction in heart rate, and improved stroke volume, lactate and albumin at 24 h associated with high dose DMSO/P2X$_7$ treatment may be possibly explained by a reduction in systemic or cardiac inflammatory mediator levels. This needs to be evaluated further. Alternatively, DMSO increases heme-oxygenase-1 (HO-1) levels, mediated via p38 MAPK activation and Nrf2 translocation in cardiac myocytes (Man et al. 2014). HO-1 is a potent anti-oxidant and improves cardiac myocyte survival.

It seems unlikely that IL1-β and IL-18 are released by only one mechanism in polymicrobial sepsis, as redundancy is integral to the innate immune system. The inability of DMSO/P2X$_7$ to reduce serum IL-1β levels may be explained by P2X$_7$-independent mechanisms of IL-1β release. Monocytes are capable of IL-1β release independent of P2X$_7$ receptor activation (e.g. via TLR 7/8 ligands), though P2X$_7$ activation accelerates

mature IL-1β release from monocytes (Ward et al. 2010). Splenic dendritic cells are able to release mature IL-1β in the absence of P2X$_7$ activation, but require the NLRP3 inflammasome. Intraperitoneal administration of LPS induced IL-1β production in serum, which was abrogated in Nlrp3-null mice but was unaffected in P2X$_7$-deficient mice (He et al. 2013). IL-18 is also released by P2X7-independent pathways (Gupta et al. 2006). IL-1β and IL-18 may be released independently of NLRP3 activity. NLRP3-deficient mice had detectable (but significantly reduced) levels of these cytokines (Mariathasan et al. 2006). Accordingly, pre-treatment at time 0 with low dose DMSO/P2X$_7$ lowered (but did not abrogate) serum IL-1β at 24 h.

The number of improved parameters seen with combination treatment compared to DMSO and A-438079 alone suggests a synergistic effect. This is evident in that many of the parameters demonstrate a trend to improvement with DMSO alone that reaches statistical significance with combination treatment (haemodynamics at 6 and 24 h, 6 h temperature, 24 h reduction in renal IL-1β, and renal IL-10).

DMSO/P2X$_7$ receptor antagonist use was associated with a significant reduction in arterial lactate and improvement in serum albumin compared to DMSO-treated animals at 24 h. Basal expression of P2X$_7$ promotes cell growth in P2X$_7$-transfected HEK293 (Adinolfi et al. 2005). However, an ATP challenge resulted in mitochondrial fragmentation mediated by increases in ER Ca^{2+} concentration and subsequent cell death (Adinolfi et al. 2009). Therefore, prevention of excessive P2X$_7$ activation may have promoted mitochondrial health associated with improved oxidative phosphorylation and lower lactate. The improvement in serum albumin is likely to relate to reduced capillary leak from decreased systemic inflammation rather than increased albumin synthesis by the liver. Reduced capillary leak is likely due to less microvascular inflammation, although I did not quantify this.

6.6 Limitations and further work

The main limitation was the lack of significant rise in serum creatinine in untreated septic animals, as discussed above. The effects of $P2X_7$ receptor blockade in this experimental model of sepsis is difficult to ascertain, as there is likely to be synergy with DMSO. However, in a clinically relevant model of sepsis, the potential role of NLRP3 inhibition (via the synergistic effect of DMSO and $P2X_7$ receptor antagonism) warrants further investigation. I recognize that DMSO may have had beneficial effects in addition to NLRP3 inhibition (anti-oxidant), however I was unable to find another suitable diluent that also had no inflammation-modulating effects. Furthermore, in the pretreatment group, I did not perform an experiment with DMSO treatment alone. I cannot therefore conclude which changes seen in the treatment are attributable to $P2X_7$ receptor blockade and which are due to DMSO.

I performed ELISA and Western blots on whole kidney homogenate for cytokine measurement. Neither of these methods allows localization to specific cell types. $P2X_7$ immunohistochemistry, caspase-1 expression in the live kidney slice, and results from cell culture of NRK52E cells are consistent with PTEC expression of IL-1β, although I have not demonstrated this conclusively. NRK52E cells also produced MCP-1. Immunohistochemistry would enable localization of these cytokines. The effect of $P2X_7$ antagonism on renal tubular epithelial cells also needs to be investigated.

The methods I used to measure cytokines have inherent limitations. ELISA and Multiplex are subject to error from endogenous binding protein and antibodies against cytokines (total and unbound cytokines), the pro-forms of the cytokines, partially degraded cytokines. Monocyte cell purity and phenotype were not ascertained and should be performed in future experiments.

I found a progressive increase in renal IL-1β in septic animals from 6 to 24 h on whole tissue homogenate detected by Western blot and ELISA. It is not possible to differentiate between the IL-1β precursor and active IL-1β on ELISA. Western blot of whole kidney

homogenate revealed pro-IL-1β. Furthermore, I did not detect IL-1β in cell culture supernatant of LPS-stimulated NRK52E renal tubular cells despite the presence of pro-IL-1β and $P2X_7$ in cell lysates. The experiment was repeated twice but yielded similar results. There are a number of possibilities for this observation. Unlike IL-1β processing, the upregulation of pro-IL-1β is dependent on signaling via NF-κB and not the inflammasome per se (Martinon et al. 2009). I cannot therefore conclude that there has been inflammasome activity, although there is evidence of the inflammasome components. Alternatively, cells that are immortalized (cell lines) may have altered inflammatory pathways, as cell death pathways and inflammation pathways overlap. Active (cleaved) IL-1β was also not detected in tissue homogenates of kidneys from septic animals. IL-1β activation and release are closely coupled, and any active IL-1β may have been released into the circulation or urine. I could not detect any urinary IL-1β on ELISA. An alternative explanation would be that there is endogenous soluble IL-1R within the renal tissue, though this needs to be evaluated in the model.

Although I have provided some insights into renal expression of the inflammasome and the $P2X_7$ in sepsis, the expression of the $P2X_7$ in other organs and on immune cells needs to be evaluated. Polymerase chain reaction (PCR) was not performed in any of the experiments, which may have differences at the transcriptional level.

6.7 Conclusion

The NLRP3 inflammasome has an important role in pro-inflammatory cytokine production and cell death. NLRP3 inflammasome inhibition has been shown to attenuate immune-mediated injury in several *in vivo* models. Both DMSO and $P2X_7$ antagonism inhibited NLRP3-mediated pro-inflammatory cytokine IL-1β production by peripheral blood monocytes *in vitro*. Combination drug therapies may be more efficacious than single drug therapies. Preliminary studies using knockout mice and endotoxin treatment have demonstrated a potential benefit of NLRP3 inflammasome inhibition in sepsis. However,

the role of the NLRP3 inflammasome has not been evaluated in a clinically relevant model of sepsis. I therefore studied the effect of NLRP3 inhibition in experimental sepsis using a fluid-resuscitated rodent model of faecal peritonitis, looking at both pre- and post-treatment.

I found that tubular $P2X_7$ and caspase-1 expression and activation occured both *in vivo* and *ex vivo*. Combined treatment with DMSO and a $P2X_7$ antagonist after the onset of sepsis reduced renal IL-1β expression early (6 h), with a trend towards a lower urine NGAL at 24 h. In addition, this DMSO/$P2X_7$ antagonist combination reduced fever at 6 h, and improved haemodynamics (HR and SV) at 24 h. The $P2X_7$ receptor antagonist had additional benefits of improving serum levels of albumin and lactate. Given these encouraging results in an in *vivo* model that is applicable to human disease, I believe further studies targeting the NLRP3 inflammasome in sepsis are warranted

Final overview

Summary of findings, limitations, and future work

The clinical problem

Sepsis is a major global problem, with a high mortality and morbidity. Organ dysfunction is a hallmark of sepsis and AKI is a part of this spectrum. Despite the significant clinical and financial burden, we are only just beginning to understand the complexities that underlie this heterogeneous condition. Several changes observed in the process may be adaptive. However, if prolonged or excessive, these changes may become maladaptive and detrimental. The interplay between changes in global and intrarenal haemodynamics, local bioenergetics and metabolism, and immunological processes need to be dissected out in context to the acute inflammatory, established, and resolution phases of sepsis.

There are several limitations that hinder the investigation of AKI in clinical practice, including the lack of access to histological specimens, the often uncertain timing of the onset of illness, the heterogeneity of AKI (drugs, hypovolaemia), and pre-existing CKD. It is therefore useful to have a clinically relevant model to investigate the pathophysiology and potential tools for diagnosis, monitoring, and management of sepsis-induced AKI.

I have demonstrated that septic AKI can happen with very mild morphological renal changes, and that haemodynamic factors cannot fully explain the development of AKI. As such, I investigated more specific mechanisms including mitochondrial and immunological pathways.

Laboratory model of sepsis-induced AKI and recovery

I used a fluid resuscitated model of faecal peritonitis with intermittent non-invasive haemodynamic monitoring to investigate the pathophysiology of septic AKI and recovery. Serum creatinine was only elevated relatively late (24 h) after the onset of sepsis, with changes in serum IL-1β occurring as early as 3 h. Renal histology demonstrated minimal histological injury and renal recovery was associated with an increase in renal macrophages. An acute increment in serum creatinine and/or fall in urine output are currently used criteria for the diagnosis of AKI. These however lack sensitivity and specificity. A better biomarker for the early diagnosis of AKI is required. Several have been investigated yet none have been validated and confirmed suitable for routine clinical use. Using an animal model of sepsis, I demonstrated the temporal changes of a panel of biomarkers in context to systemic inflammation and renal histology. The exact timing of insult along with the access to histological samples is a clear advantage of the animal model for this purpose. I demonstrated that urine NGAL was the most sensitive biomarker for renal inflammation, rising the earliest of those tested. A fall in urine KIM-1 and calbindin at 24 h may predict renal recovery. Future work should focus on obtaining serial samples of urine from patients and normalization to urinary creatinine concentration. The utility of novel biomarkers including TIMP-2 and IGFBP-7 needs to be investigated.

Renal haemodynamics and bioenergetics

Much emphasis is placed on the correction of global haemodynamic factors in sepsis. Yet, regional blood flow and microvascular perfusion may be altered in sepsis, and may not reflect global haemodynamics. The dogma that septic AKI is primarily a disorder of renal hypoperfusion has been challenged by studies demonstrating preserved or even elevated renal blood flow in sepsis and a relatively unchanged renal histology. Furthermore, 'normal' organ blood flow may not prevent the onset of organ dysfunction, as there may be a defect with cellular energetics. I demonstrated a fall in renal cortical oxygenation despite similar renal oxygen delivery and utilization at 24 h. The presence of

UCP-2 in the kidney was consistent with findings on multiphoton imaging of the live kidney slice. In these studies, incubation with septic serum containing circulating inflammatory factors resulted in a fall in tubular NADH, and mitochondrial membrane potential that are consistent with mitochondrial uncoupling. Furthermore, the amount of tubular ROS production was increased. These changes were prevented by pre-treatment with the ROS scavenger TEMPO. Mitochondrial uncoupling itself may be an adaptive mechanism to limit ROS production.

Future work should determine if the same changes hold in physiological levels of oxygen. I have demonstrated an upregulation in UCP-2 protein within the kidney. The role of uncoupling in this organ needs to be better characterized with knowledge of the time course and the effect on ATP/ADP turnover. The effect of uncoupling can be determined either by inhibiting uncoupling (e.g. with genipin or siRNA) or by augmenting it (e.g. with dinitrophenol). Inhibition of uncoupling may result in greater ROS formation, the byproducts of which could be measured.

The role of the NLRP3 inflammasome in sepsis-induced acute kidney injury

Intrinsic renal cells demonstrate components of the inflammasome in various pro-inflammatory diseases. Pharmacological inhibition and/or genetic deletion has demonstrated a protective effect in many preclinical models of AKI.

Using a variety of techniques, I demonstrated expression of various components of the NLRP3 inflammasome in this long-term septic model, including upregulation of proximal tubular epithelial $P2X_7$ at 6 h. The functional significance of *de novo* renal-specific inflammasome expression in sepsis is unclear. I could not demonstrate any difference in serum creatinine between $P2X_7$ receptor antagonist-treated animals and untreated animals when treatment was initiated after the onset of sepsis. However, it is not possible to come to any firm conclusion as I did not demonstrate a significant rise in serum creatinine in the untreated animals. Nonetheless, there were beneficial effects of NLRP3 inhibition on recovery of haemodynamics, lactate, and serum albumin.

Future work should focus on the effects of sepsis on renal tubular epithelial cells and the effect of NLRP3 inhibition. The experiments need to be conducted in a reliable model of septic AKI. The effects of inhibition of the NLRP3 inflammasome on survival also need to be ascertained using a more severe model.

.

7 List of Figures

8 List of Tables

9 References

Abraham, E., P. F. Laterre, J. Garbino, *et al.* Lenercept (p55 tumor necrosis factor receptor fusion protein) in severe sepsis and early septic shock: a randomized, double-blind, placebo-controlled, multicenter phase III trial with 1,342 patients. Crit Care Med. Mar 2001;29(3):503-510.

Adinolfi, E., M. G. Callegari, M. Cirillo, *et al.* Expression of the P2X7 receptor increases the Ca2+ content of the endoplasmic reticulum, activates NFATc1, and protects from apoptosis. J Biol Chem. Apr 10 2009;284(15):10120-10128.

Adinolfi, E., M. G. Callegari, D. Ferrari, *et al.* Basal activation of the P2X7 ATP receptor elevates mitochondrial calcium and potential, increases cellular ATP levels, and promotes serum-independent growth. Mol Biol Cell. Jul 2005;16(7):3260-3272.

Adinolfi, E., L. Melchiorri, S. Falzoni, *et al.* P2X7 receptor expression in evolutive and indolent forms of chronic B lymphocytic leukemia. Blood. Jan 15 2002;99(2):706-708.

Aduen, J., W. K. Bernstein, T. Khastgir, *et al.* The use and clinical importance of a substrate-specific electrode for rapid determination of blood lactate concentrations. JAMA. Dec 7 1994;272(21):1678-1685.

Ahn, H., J. Kim, E. B. Jeung, *et al.* Dimethyl sulfoxide inhibits NLRP3 inflammasome activation. Immunobiology. Apr 2014;219(4):315-322.

Ahn, H., J. Kim, M. J. Lee, *et al.* Methylsulfonylmethane inhibits NLRP3 inflammasome activation. Cytokine. Nov 21 2014;71(2):223-231.

Alfonso-Loeches, S., J. R. Urena-Peralta, M. J. Morillo-Bargues, *et al.* Role of mitochondria ROS generation in ethanol-induced NLRP3 inflammasome activation and cell death in astroglial cells. Front Cell Neurosci. 2014;8:216.

Ali, S. R., A. M. Timmer, S. Bilgrami, *et al.* Anthrax toxin induces macrophage death by p38 MAPK inhibition but leads to inflammasome activation via ATP leakage. Immunity. Jul 22 2011;35(1):34-44.

Angus, D. C., W. T. Linde-Zwirble, J. Lidicker, *et al.* Epidemiology of severe sepsis in the United States: analysis of incidence, outcome, and associated costs of care. Crit Care Med. Jul 2001;29(7):1303-1310.

Arulkumaran, N., R. J. Unwin and F. W. Tam. A potential therapeutic role for P2X7 receptor (P2X7) antagonists in the treatment of inflammatory diseases. Expert Opin Investig Drugs. Jul 2011;20(7):897-915.

Asfar, P., F. Meziani, J. F. Hamel, *et al.* High versus low blood-pressure target in patients with septic shock. N Engl J Med. Apr 24 2014;370(17):1583-1593.

Aswad, F. and G. Dennert. P2X7 receptor expression levels determine lethal effects of a purine based danger signal in T lymphocytes. Cell Immunol. Sep 2006;243(1):58-65.

Ausiello, D. A., J. I. Kreisberg, C. Roy, *et al.* Contraction of cultured rat glomerular cells of apparent mesangial origin after stimulation with angiotensin II and arginine vasopressin. J Clin Invest. Mar 1980;65(3):754-760.

Bagshaw, S. M. The long-term outcome after acute renal failure. Curr Opin Crit Care. Dec 2006;12(6):561-566.

Bagshaw, S. M., C. George and R. Bellomo. A comparison of the RIFLE and AKIN criteria for acute kidney injury in critically ill patients. Nephrol Dial Transplant. May 2008;23(5):1569-1574.

Bagshaw, S. M., K. B. Laupland, C. J. Doig, *et al.* Prognosis for long-term survival and renal recovery in critically ill patients with severe acute renal failure: a population-based study. Crit Care. 2005;9(6):R700-709.

Bailly, V., Z. Zhang, W. Meier, *et al.* Shedding of kidney injury molecule-1, a putative adhesion protein involved in renal regeneration. J Biol Chem. Oct 18 2002;277(42):39739-39748.

Bakker, J., R. Grover, A. McLuckie, *et al.* Administration of the nitric oxide synthase inhibitor NG-methyl-L-arginine hydrochloride (546C88) by intravenous infusion for up to 72 hours can promote the resolution of shock in patients with severe sepsis: results of a randomized, double-blind, placebo-controlled multicenter study (study no. 144-002). Crit Care Med. Jan 2004;32(1):1-12.

Bani-Hani, A. H., J. A. Leslie, H. Asanuma, *et al.* IL-18 neutralization ameliorates obstruction-induced epithelial-mesenchymal transition and renal fibrosis. Kidney Int. Sep 2009;76(5):500-511.

Bauernfeind, F., E. Bartok, A. Rieger, *et al.* Cutting edge: reactive oxygen species inhibitors block priming, but not activation, of the NLRP3 inflammasome. J Immunol. Jul 15 2011;187(2):613-617.

Bauernfeind, F. G., G. Horvath, A. Stutz, *et al.* Cutting edge: NF-kappaB activating pattern recognition and cytokine receptors license NLRP3 inflammasome activation by regulating NLRP3 expression. J Immunol. Jul 15 2009;183(2):787-791.

Beach, R. E., B. A. Watts, 3rd, D. W. Good, *et al.* Effects of graded oxygen tension on adenosine release by renal medullary and thick ascending limb suspensions. Kidney Int. May 1991;39(5):836-842.

Beigi, R. D., S. B. Kertesy, G. Aquilina, *et al.* Oxidized ATP (oATP) attenuates proinflammatory signaling via P2 receptor-independent mechanisms. Br J Pharmacol. Oct 2003;140(3):507-519.

Bellomo, R., C. Ronco, J. A. Kellum, *et al.* Acute renal failure - definition, outcome measures, animal models, fluid therapy and information technology needs: the Second International Consensus Conference of the Acute Dialysis Quality Initiative (ADQI) Group. Crit Care. Aug 2004;8(4):R204-212.

Bergsbaken, T. and B. T. Cookson. Macrophage activation redirects yersinia-infected host cell death from apoptosis to caspase-1-dependent pyroptosis. PLoS Pathog. Nov 2007;3(11):e161.

Bergsbaken, T., S. L. Fink, A. B. den Hartigh, *et al.* Coordinated host responses during pyroptosis: caspase-1-dependent lysosome exocytosis and inflammatory cytokine maturation. J Immunol. Sep 1 2011;187(5):2748-2754.

Bevilacqua, M. P., S. Stengelin, M. A. Gimbrone, Jr., *et al.* Endothelial leukocyte adhesion molecule 1: an inducible receptor for neutrophils related to complement regulatory proteins and lectins. Science. Mar 3 1989;243(4895):1160-1165.

Biomarkers Definitions Working, G. Biomarkers and surrogate endpoints: preferred definitions and conceptual framework. Clin Pharmacol Ther. Mar 2001;69(3):89-95.

Boekstegers, P., S. Weidenhofer, G. Pilz, *et al.* Peripheral oxygen availability within skeletal muscle in sepsis and septic shock: comparison to limited infection and cardiogenic shock. Infection. Sep-Oct 1991;19(5):317-323.

Boomer, J. S., J. M. Green and R. S. Hotchkiss. The changing immune system in sepsis: is individualized immuno-modulatory therapy the answer? Virulence. Jan 1 2014;5(1):45-56.

Boomer, J. S., K. To, K. C. Chang, *et al.* Immunosuppression in patients who die of sepsis and multiple organ failure. JAMA. Dec 21 2011;306(23):2594-2605.

Bouchard, J., E. Macedo, S. Soroko, *et al.* Comparison of methods for estimating glomerular filtration rate in critically ill patients with acute kidney injury. Nephrol Dial Transplant. Jan 2010;25(1):102-107.

Bragadottir, G., B. Redfors and S. E. Ricksten. Assessing glomerular filtration rate (GFR) in critically ill patients with acute kidney injury--true GFR versus urinary creatinine clearance and estimating equations. Crit Care. 2013;17(3):R108.

Brealey, D., M. Brand, I. Hargreaves, *et al.* Association between mitochondrial dysfunction and severity and outcome of septic shock. Lancet. Jul 20 2002;360(9328):219-223.

Brealey, D., S. Karyampudi, T. S. Jacques, *et al.* Mitochondrial dysfunction in a long-term rodent model of sepsis and organ failure. Am J Physiol Regul Integr Comp Physiol. Mar 2004;286(3):R491-497.

Brenner, M., G. L. Schaer, D. L. Mallory, *et al.* Detection of renal blood flow abnormalities in septic and critically ill patients using a newly designed indwelling thermodilution renal vein catheter. Chest. Jul 1990;98(1):170-179.

Bruey, J. M., N. Bruey-Sedano, F. Luciano, *et al.* Bcl-2 and Bcl-XL regulate proinflammatory caspase-1 activation by interaction with NALP1. Cell. Apr 6 2007;129(1):45-56.

Bryan, N. B., A. Dorfleutner, S. J. Kramer, *et al.* Differential splicing of the apoptosis-associated speck like protein containing a caspase recruitment domain (ASC) regulates inflammasomes. J Inflamm (Lond). 2010;7:23.

Bryan, N. B., A. Dorfleutner, Y. Rojanasakul, *et al.* Activation of inflammasomes requires intracellular redistribution of the apoptotic speck-like protein containing a caspase recruitment domain. J Immunol. Mar 1 2009;182(5):3173-3182.

Brzin, J., T. Popovic, V. Turk, *et al.* Human cystatin, a new protein inhibitor of cysteine proteinases. Biochem Biophys Res Commun. Jan 13 1984;118(1):103-109.

Bucher, M., J. Hobbhahn, K. Taeger, *et al.* Cytokine-mediated downregulation of vasopressin V(1A) receptors during acute endotoxemia in rats. Am J Physiol Regul Integr Comp Physiol. Apr 2002;282(4):R979-984.

Burns, K., S. Janssens, B. Brissoni, *et al.* Inhibition of interleukin 1 receptor/Toll-like receptor signaling through the alternatively spliced, short form of MyD88 is due to its failure to recruit IRAK-4. J Exp Med. Jan 20 2003;197(2):263-268.

Burnstock, G. Pathophysiology and therapeutic potential of purinergic signaling. Pharmacol Rev. Mar 2006;58(1):58-86.

Bussolati, B., S. David, V. Cambi, *et al.* Urinary soluble CD14 mediates human proximal tubular epithelial cell injury induced by LPS. Int J Mol Med. Oct 2002;10(4):441-449.

Cai, L., J. Rubin, W. Han, *et al.* The origin of multiple molecular forms in urine of HNL/NGAL. Clin J Am Soc Nephrol. Dec 2010;5(12):2229-2235.

Carchman, E. H., S. Whelan, P. Loughran, *et al.* Experimental sepsis-induced mitochondrial biogenesis is dependent on autophagy, TLR4, and TLR9 signaling in liver. FASEB J. Dec 2013;27(12):4703-4711.

Carr, M. W., S. J. Roth, E. Luther, *et al.* Monocyte chemoattractant protein 1 acts as a T-lymphocyte chemoattractant. Proc Natl Acad Sci U S A. Apr 26 1994;91(9):3652-3656.

Carre, J. E., J. C. Orban, L. Re, *et al.* Survival in critical illness is associated with early activation of mitochondrial biogenesis. Am J Respir Crit Care Med. Sep 15 2010;182(6):745-751.

Caton, P. W., N. K. Nayuni, O. Murch, *et al.* Endotoxin induced hyperlactatemia and hypoglycemia is linked to decreased mitochondrial phosphoenolpyruvate carboxykinase. Life Sci. May 22 2009;84(21-22):738-744.

Chassin, C., J. M. Goujon, S. Darche, *et al.* Renal collecting duct epithelial cells react to pyelonephritis-associated Escherichia coli by activating distinct TLR4-dependent and -independent inflammatory pathways. J Immunol. Oct 1 2006;177(7):4773-4784.

Chawla, L. S., R. L. Amdur, S. Amodeo, *et al.* The severity of acute kidney injury predicts progression to chronic kidney disease. Kidney Int. Jun 2011;79(12):1361-1369.

Chen, A., L. F. Sheu, W. Y. Chou, *et al.* Interleukin-1 receptor antagonist modulates the progression of a spontaneously occurring IgA nephropathy in mice. Am J Kidney Dis. Nov 1997;30(5):693-702.

Chen, C. J., H. Kono, D. Golenbock, *et al.* Identification of a key pathway required for the sterile inflammatory response triggered by dying cells. Nat Med. Jul 2007;13(7):851-856.

Chen, G. M., C. C. Feng, Q. L. Ye, *et al.* Association of P2X7R gene polymorphisms with systemic lupus erythematosus in a Chinese population. Mutagenesis. May 2013;28(3):351-355.

Chen, G. Y., M. Liu, F. Wang, *et al.* A functional role for Nlrp6 in intestinal inflammation and tumorigenesis. J Immunol. Jun 15 2011;186(12):7187-7194.

Chen, Y., M. R. Smith, K. Thirumalai, *et al.* A bacterial invasin induces macrophage apoptosis by binding directly to ICE. EMBO J. Aug 1 1996;15(15):3853-3860.

Chertow, G. M., E. Burdick, M. Honour, *et al.* Acute kidney injury, mortality, length of stay, and costs in hospitalized patients. J Am Soc Nephrol. Nov 2005;16(11):3365-3370.

Chiao, C. W., R. C. Tostes and R. C. Webb. P2X7 receptor activation amplifies lipopolysaccharide-induced vascular hyporeactivity via interleukin-1 beta release. J Pharmacol Exp Ther. Sep 2008;326(3):864-870.

Chorinchath, B. B., L. Y. Kong, L. Mao, *et al.* Age-associated differences in TNF-alpha and nitric oxide production in endotoxic mice. J Immunol. Feb 15 1996;156(4):1525-1530.

Chung, C. S., G. Y. Song, J. Lomas, *et al.* Inhibition of Fas/Fas ligand signaling improves septic survival: differential effects on macrophage apoptotic and functional capacity. J Leukoc Biol. Sep 2003;74(3):344-351.

Cinel, I. and S. M. Opal. Molecular biology of inflammation and sepsis: a primer. Crit Care Med. Jan 2009;37(1):291-304.

Cocchetto, D. M., C. Tschanz and T. D. Bjornsson. Decreased rate of creatinine production in patients with hepatic disease: implications for estimation of creatinine clearance. Ther Drug Monit. Jun 1983;5(2):161-168.

Coletta, C., K. Modis, G. Olah, *et al.* Endothelial dysfunction is a potential contributor to multiple organ failure and mortality in aged mice subjected to septic shock: preclinical studies in a murine model of cecal ligation and puncture. Crit Care. Sep 16 2014;18(5):511.

Conway Morris, A., N. Anderson, M. Brittan, *et al.* Combined dysfunctions of immune cells predict nosocomial infection in critically ill patients. Br J Anaesth. Nov 2013;111(5):778-787.

Cornelis, S., K. Kersse, N. Festjens, *et al.* Inflammatory caspases: targets for novel therapies. Curr Pharm Des. 2007;13(4):367-385.

Cowland, J. B. and N. Borregaard. Molecular characterization and pattern of tissue expression of the gene for neutrophil gelatinase-associated lipocalin from humans. Genomics. Oct 1 1997;45(1):17-23.

Creteur, J., T. Carollo, G. Soldati, *et al.* The prognostic value of muscle StO2 in septic patients. Intensive Care Med. Sep 2007;33(9):1549-1556.

Crouser, E. D., M. W. Julian, D. V. Blaho, *et al.* Endotoxin-induced mitochondrial damage correlates with impaired respiratory activity. Crit Care Med. Feb 2002;30(2):276-284.

Cruces, P., C. Salas, P. Lilo, *et al.* The renal compartment: a hydraulic view. ICM Experimental. 2014;2(26).

Cruz, D. N., M. Antonelli, R. Fumagalli, *et al.* Early use of polymyxin B hemoperfusion in abdominal septic shock: the EUPHAS randomized controlled trial. JAMA. Jun 17 2009;301(23):2445-2452.

Cunningham, P. N., Y. Wang, R. Guo*, et al.* Role of Toll-like receptor 4 in endotoxin-induced acute renal failure. J Immunol. Feb 15 2004;172(4):2629-2635.

Cuzzocrea, S., E. Mazzon, R. Di Paola*, et al.* A role for nitric oxide-mediated peroxynitrite formation in a model of endotoxin-induced shock. J Pharmacol Exp Ther. Oct 2006;319(1):73-81.

Dao, T., K. Ohashi, T. Kayano*, et al.* Interferon-gamma-inducing factor, a novel cytokine, enhances Fas ligand-mediated cytotoxicity of murine T helper 1 cells. Cell Immunol. Nov 1 1996;173(2):230-235.

Day, T. A., J. C. Randle and L. P. Renaud. Opposing alpha- and beta-adrenergic mechanisms mediate dose-dependent actions of noradrenaline on supraoptic vasopressin neurones in vivo. Brain Res. Dec 9 1985;358(1-2):171-179.

De Backer, D., J. Creteur, J. C. Preiser*, et al.* Microvascular blood flow is altered in patients with sepsis. Am J Respir Crit Care Med. Jul 1 2002;166(1):98-104.

de Haij, S., A. M. Woltman, A. C. Bakker*, et al.* Production of inflammatory mediators by renal epithelial cells is insensitive to glucocorticoids. Br J Pharmacol. Sep 2002;137(2):197-204.

Dell'Antonio, G., A. Quattrini, E. D. Cin*, et al.* Relief of inflammatory pain in rats by local use of the selective P2X7 ATP receptor inhibitor, oxidized ATP. Arthritis Rheum. Dec 2002;46(12):3378-3385.

Dell'Antonio, G., A. Quattrini, E. Dal Cin*, et al.* Antinociceptive effect of a new P(2Z)/P2X7 antagonist, oxidized ATP, in arthritic rats. Neurosci Lett. Jul 19 2002;327(2):87-90.

Dellinger, R. P., M. M. Levy, A. Rhodes*, et al.* Surviving sepsis campaign: international guidelines for management of severe sepsis and septic shock, 2012. Intensive Care Med. Feb 2013;39(2):165-228.

Denton, K. M., W. P. Anderson and R. Sinniah. Effects of angiotensin II on regional afferent and efferent arteriole dimensions and the glomerular pole. Am J Physiol Regul Integr Comp Physiol. Aug 2000;279(2):R629-638.

Deplano, S., H. T. Cook, R. Russell, *et al.* P2X7 receptor-mediated Nlrp3-inflammasome activation is a genetic determinant of macrophage-dependent crescentic glomerulonephritis. J Leukoc Biol. Oct 22 2012.

Di Giantomasso, D., R. Bellomo and C. N. May. The haemodynamic and metabolic effects of epinephrine in experimental hyperdynamic septic shock. Intensive Care Med. Mar 2005;31(3):454-462.

Di Giantomasso, D., C. N. May and R. Bellomo. Norepinephrine and vital organ blood flow during experimental hyperdynamic sepsis. Intensive Care Med. Oct 2003;29(10):1774-1781.

Di Virgilio, F., P. Chiozzi, D. Ferrari, *et al.* Nucleotide receptors: an emerging family of regulatory molecules in blood cells. Blood. Feb 1 2001;97(3):587-600.

Diaz de Leon, M., S. A. Moreno, D. J. Gonzalez Diaz, *et al.* [Severe sepsis as a cause of acute renal failure]. Nefrologia. 2006;26(4):439-444.

Dinarello, C. A. IL-18: A TH1-inducing, proinflammatory cytokine and new member of the IL-1 family. J Allergy Clin Immunol. Jan 1999;103(1 Pt 1):11-24.

Dinarello, C. A. The IL-1 family and inflammatory diseases. Clin Exp Rheumatol. Sep-Oct 2002;20(5 Suppl 27):S1-13.

Dinarello, C. A. Interleukin-18 and the pathogenesis of inflammatory diseases. Semin Nephrol. Jan 2007;27(1):98-114.

Dinarello, C. A. Immunological and inflammatory functions of the interleukin-1 family. Annu Rev Immunol. 2009;27:519-550.

Doerschug, K. C., A. S. Delsing, G. A. Schmidt, *et al.* Impairments in microvascular reactivity are related to organ failure in human sepsis. Am J Physiol Heart Circ Physiol. Aug 2007;293(2):H1065-1071.

Doi, K., P. S. Yuen, C. Eisner, *et al.* Reduced production of creatinine limits its use as marker of kidney injury in sepsis. J Am Soc Nephrol. Jun 2009;20(6):1217-1221.

Dormehl, I. C., N. Hugo, J. P. Pretorius, *et al.* In vivo assessment of regional microvascular albumin leakage during E. coli septic shock in the baboon model. Circ Shock. Sep 1992;38(1):9-13.

Dunser, M. W., E. Ruokonen, V. Pettila, *et al.* Association of arterial blood pressure and vasopressor load with septic shock mortality: a post hoc analysis of a multicenter trial. Crit Care. 2009;13(6):R181.

Durr, U. H., U. S. Sudheendra and A. Ramamoorthy. LL-37, the only human member of the cathelicidin family of antimicrobial peptides. Biochim Biophys Acta. Sep 2006;1758(9):1408-1425.

Dyson, A., A. Rudiger and M. Singer. Temporal changes in tissue cardiorespiratory function during faecal peritonitis. Intensive Care Med. Jul 2011;37(7):1192-1200.

Echtenacher, B., M. A. Freudenberg, R. S. Jack, *et al.* Differences in innate defense mechanisms in endotoxemia and polymicrobial septic peritonitis. Infect Immun. Dec 2001;69(12):7271-7276.

Edelstein, C. L., T. S. Hoke, H. Somerset, *et al.* Proximal tubules from caspase-1-deficient mice are protected against hypoxia-induced membrane injury. Nephrol Dial Transplant. Apr 2007;22(4):1052-1061.

Eichacker, P. Q., C. Parent, A. Kalil, *et al.* Risk and the efficacy of antiinflammatory agents: retrospective and confirmatory studies of sepsis. Am J Respir Crit Care Med. Nov 1 2002;166(9):1197-1205.

Ekbal, N. J., A. Dyson, C. Black, *et al.* Monitoring tissue perfusion, oxygenation, and metabolism in critically ill patients. Chest. Jun 2013;143(6):1799-1808.

El-Achkar, T. M., X. Huang, Z. Plotkin, *et al.* Sepsis induces changes in the expression and distribution of Toll-like receptor 4 in the rat kidney. Am J Physiol Renal Physiol. May 2006;290(5):F1034-1043.

Elssner, A., M. Duncan, M. Gavrilin, *et al.* A novel P2X7 receptor activator, the human cathelicidin-derived peptide LL37, induces IL-1 beta processing and release. J Immunol. Apr 15 2004;172(8):4987-4994.

Endre, Z. H., J. W. Pickering, R. J. Walker, *et al.* Improved performance of urinary biomarkers of acute kidney injury in the critically ill by stratification for injury duration and baseline renal function. Kidney Int. May 2011;79(10):1119-1130.

Fernando, S. L., B. M. Saunders, R. Sluyter*, et al.* A polymorphism in the P2X7 gene increases susceptibility to extrapulmonary tuberculosis. Am J Respir Crit Care Med. Feb 15 2007;175(4):360-366.

Ferrari, D., C. Pizzirani, E. Adinolfi*, et al.* The P2X7 receptor: a key player in IL-1 processing and release. J Immunol. Apr 1 2006;176(7):3877-3883.

Ferrari, D., S. Wesselborg, M. K. Bauer*, et al.* Extracellular ATP activates transcription factor NF-kappaB through the P2Z purinoreceptor by selectively targeting NF-kappaB p65. J Cell Biol. Dec 29 1997;139(7):1635-1643.

Fink, S. L. and B. T. Cookson. Caspase-1-dependent pore formation during pyroptosis leads to osmotic lysis of infected host macrophages. Cell Microbiol. Nov 2006;8(11):1812-1825.

Fisher, C. J., Jr., G. J. Slotman, S. M. Opal*, et al.* Initial evaluation of human recombinant interleukin-1 receptor antagonist in the treatment of sepsis syndrome: a randomized, open-label, placebo-controlled multicenter trial. Crit Care Med. Jan 1994;22(1):12-21.

Fujita, T., N. Ogihara, Y. Kamura*, et al.* Interleukin-18 contributes more closely to the progression of diabetic nephropathy than other diabetic complications. Acta Diabetol. Apr 2012;49(2):111-117.

Furuichi, K., T. Wada, Y. Iwata*, et al.* Interleukin-1-dependent sequential chemokine expression and inflammatory cell infiltration in ischemia-reperfusion injury. Crit Care Med. Sep 2006;34(9):2447-2455.

Galvao, J., B. Davis, M. Tilley*, et al.* Unexpected low-dose toxicity of the universal solvent DMSO. FASEB J. Mar 2014;28(3):1317-1330.

Garrison, R. N., D. J. Ratcliffe and D. E. Fry. The effects of peritonitis on murine renal mitochondria. Adv Shock Res. 1982;7:71-76.

Gattinoni, L., L. Brazzi, P. Pelosi*, et al.* A trial of goal-oriented hemodynamic therapy in critically ill patients. SvO2 Collaborative Group. N Engl J Med. Oct 19 1995;333(16):1025-1032.

Gauer, S., O. Sichler, N. Obermuller*, et al.* IL-18 is expressed in the intercalated cell of human kidney. Kidney Int. Nov 2007;72(9):1081-1087.

Georger, J. F., O. Hamzaoui, A. Chaari, *et al.* Restoring arterial pressure with norepinephrine improves muscle tissue oxygenation assessed by near-infrared spectroscopy in severely hypotensive septic patients. Intensive Care Med. Nov 2010;36(11):1882-1889.

Giachelli, C. M., D. Lombardi, R. J. Johnson, *et al.* Evidence for a role of osteopontin in macrophage infiltration in response to pathological stimuli in vivo. Am J Pathol. Feb 1998;152(2):353-358.

Goetz, D. H., M. A. Holmes, N. Borregaard, *et al.* The neutrophil lipocalin NGAL is a bacteriostatic agent that interferes with siderophore-mediated iron acquisition. Mol Cell. Nov 2002;10(5):1033-1043.

Goncalves, R. G., L. Gabrich, A. Rosario, Jr., *et al.* The role of purinergic P2X7 receptors in the inflammation and fibrosis of unilateral ureteral obstruction in mice. Kidney Int. Nov 2006;70(9):1599-1606.

Gordon, A. C., J. A. Russell, K. R. Walley, *et al.* The effects of vasopressin on acute kidney injury in septic shock. Intensive Care Med. Jan 2010;36(1):83-91.

Granfeldt, A., L. Ebdrup, E. Tonnesen, *et al.* Renal cytokine profile in an endotoxemic porcine model. Acta Anaesthesiol Scand. May 2008;52(5):614-620.

Groeneveld, A. B., J. J. Nauta and L. G. Thijs. Peripheral vascular resistance in septic shock: its relation to outcome. Intensive Care Med. 1988;14(2):141-147.

Gudmundsson, G. H., B. Agerberth, J. Odeberg, *et al.* The human gene FALL39 and processing of the cathelin precursor to the antibacterial peptide LL-37 in granulocytes. Eur J Biochem. Jun 1 1996;238(2):325-332.

Gupta, S., M. P. Gould, J. DeVecchio, *et al.* CpG-induced IFNgamma expands TLR4-specific IL-18 responses in vivo. Cell Immunol. Oct 2006;243(2):75-82.

Haden, D. W., H. B. Suliman, M. S. Carraway, *et al.* Mitochondrial biogenesis restores oxidative metabolism during Staphylococcus aureus sepsis. Am J Respir Crit Care Med. Oct 15 2007;176(8):768-777.

Hall, A. M., R. J. Unwin, N. Parker, *et al.* Multiphoton imaging reveals differences in mitochondrial function between nephron segments. J Am Soc Nephrol. Jun 2009;20(6):1293-1302.

Hamel, M. B., R. S. Phillips, R. B. Davis, *et al.* Outcomes and cost-effectiveness of initiating dialysis and continuing aggressive care in seriously ill hospitalized adults. SUPPORT Investigators. Study to Understand Prognoses and Preferences for Outcomes and Risks of Treatments. Ann Intern Med. Aug 1 1997;127(3):195-202.

Hansen, P. B., S. Hashimoto, M. Oppermann, *et al.* Vasoconstrictor and vasodilator effects of adenosine in the mouse kidney due to preferential activation of A1 or A2 adenosine receptors. J Pharmacol Exp Ther. Dec 2005;315(3):1150-1157.

Haq, M., J. Norman, S. R. Saba, *et al.* Role of IL-1 in renal ischemic reperfusion injury. J Am Soc Nephrol. Apr 1998;9(4):614-619.

Harada, H., C. M. Chan, A. Loesch, *et al.* Induction of proliferation and apoptotic cell death via P2Y and P2X receptors, respectively, in rat glomerular mesangial cells. Kidney Int. Mar 2000;57(3):949-958.

Hardy, J., B. Hambly, H. Ko, *et al.* Stimulation of mesangial cells by angiotensin II and lipopolysaccharide increases expression of interleukin-18, but not IL-18 receptor. Nephron Exp Nephrol. 2010;116(4):e63-71.

Hato, T., S. Winfree, R. Kalakeche, *et al.* The Macrophage Mediates the Renoprotective Effects of Endotoxin Preconditioning. J Am Soc Nephrol. Nov 14 2014.

Hayes, M. A., A. C. Timmins, E. H. Yau, *et al.* Elevation of systemic oxygen delivery in the treatment of critically ill patients. N Engl J Med. Jun 16 1994;330(24):1717-1722.

He, Y., L. Franchi and G. Nunez. TLR agonists stimulate Nlrp3-dependent IL-1beta production independently of the purinergic P2X7 receptor in dendritic cells and in vivo. J Immunol. Jan 1 2013;190(1):334-339.

Hensen, J., C. P. Howard, V. Walter, *et al.* Impact of interleukin-1beta antibody (canakinumab) on glycaemic indicators in patients with type 2 diabetes mellitus: results of secondary endpoints from a randomized, placebo-controlled trial. Diabetes Metab. Dec 2013;39(6):524-531.

Hertting, O., A. Khalil, G. Jaremko, *et al.* Enhanced chemokine response in experimental acute Escherichia coli pyelonephritis in IL-1beta-deficient mice. Clin Exp Immunol. Feb 2003;131(2):225-233.

Hinshaw, L. B., B. K. Beller-Todd, L. T. Archer, *et al.* Effectiveness of steroid/antibiotic treatment in primates administered LD100 Escherichia coli. Ann Surg. Jul 1981;194(1):51-56.

Hjortrup, P. B., N. Haase, M. Wetterslev, *et al.* Clinical review: Predictive value of neutrophil gelatinase-associated lipocalin for acute kidney injury in intensive care patients. Crit Care. 2013;17(2):211.

Hoffmann, D., T. C. Fuchs, T. Henzler, *et al.* Evaluation of a urinary kidney biomarker panel in rat models of acute and subchronic nephrotoxicity. Toxicology. Nov 9 2010;277(1-3):49-58.

Holthoff, J. H., Z. Wang, K. A. Seely, *et al.* Resveratrol improves renal microcirculation, protects the tubular epithelium, and prolongs survival in a mouse model of sepsis-induced acute kidney injury. Kidney Int. Feb 2012;81(4):370-378.

Homsi, E., P. Janino and J. B. de Faria. Role of caspases on cell death, inflammation, and cell cycle in glycerol-induced acute renal failure. Kidney Int. Apr 2006;69(8):1385-1392.

Hotchkiss, R. S., P. E. Swanson, B. D. Freeman, *et al.* Apoptotic cell death in patients with sepsis, shock, and multiple organ dysfunction. Crit Care Med. Jul 1999;27(7):1230-1251.

Hotchkiss, R. S., P. E. Swanson, C. M. Knudson, *et al.* Overexpression of Bcl-2 in transgenic mice decreases apoptosis and improves survival in sepsis. J Immunol. Apr 1 1999;162(7):4148-4156.

Hotchkiss, R. S., K. W. Tinsley, P. E. Swanson, *et al.* Sepsis-induced apoptosis causes progressive profound depletion of B and CD4+ T lymphocytes in humans. J Immunol. Jun 1 2001;166(11):6952-6963.

Howell, M. D., M. Donnino, P. Clardy, *et al.* Occult hypoperfusion and mortality in patients with suspected infection. Intensive Care Med. Nov 2007;33(11):1892-1899.

Huddle, N., G. Arendts, S. P. Macdonald, *et al.* Is comorbid status the best predictor of one-year mortality in patients with severe sepsis and sepsis with shock? Anaesth Intensive Care. Jul 2013;41(4):482-489.

Humphreys, B. D. and G. R. Dubyak. Modulation of P2X7 nucleotide receptor expression by pro- and anti-inflammatory stimuli in THP-1 monocytes. J Leukoc Biol. Aug 1998;64(2):265-273.

Hurgin, V., D. Novick, A. Werman, *et al.* Antiviral and immunoregulatory activities of IFN-gamma depend on constitutively expressed IL-1alpha. Proc Natl Acad Sci U S A. Mar 20 2007;104(12):5044-5049.

Hvidberg, V., C. Jacobsen, R. K. Strong, *et al.* The endocytic receptor megalin binds the iron transporting neutrophil-gelatinase-associated lipocalin with high affinity and mediates its cellular uptake. FEBS Lett. Jan 31 2005;579(3):773-777.

Hwang, S. M., C. A. Lopez, D. E. Heck, *et al.* Osteopontin inhibits induction of nitric oxide synthase gene expression by inflammatory mediators in mouse kidney epithelial cells. J Biol Chem. Jan 7 1994;269(1):711-715.

Hyde, S. R., R. D. Stith and R. E. McCallum. Mortality and bacteriology of sepsis following cecal ligation and puncture in aged mice. Infect Immun. Mar 1990;58(3):619-624.

Ichihara, A., M. Hayashi, L. G. Navar, *et al.* Inducible nitric oxide synthase attenuates endothelium-dependent renal microvascular vasodilation. J Am Soc Nephrol. Oct 2000;11(10):1807-1812.

Ichimura, T., J. V. Bonventre, V. Bailly, *et al.* Kidney injury molecule-1 (KIM-1), a putative epithelial cell adhesion molecule containing a novel immunoglobulin domain, is up-regulated in renal cells after injury. J Biol Chem. Feb 13 1998;273(7):4135-4142.

Iyer, S. S., W. P. Pulskens, J. J. Sadler, *et al.* Necrotic cells trigger a sterile inflammatory response through the Nlrp3 inflammasome. Proc Natl Acad Sci U S A. Dec 1 2009;106(48):20388-20393.

Jalilian, I., M. Spildrejorde, A. Seavers*, et al.* Functional expression of the damage-associated molecular pattern receptor P2X7 on canine kidney epithelial cells. Vet Immunol Immunopathol. Oct 4 2012.

Jalilian, I., M. Spildrejorde, A. Seavers*, et al.* Functional expression of the damage-associated molecular pattern receptor P2X7 on canine kidney epithelial cells. Vet Immunol Immunopathol*.* Dec 15 2012;150(3-4):228-233.

Jones, A. E. and M. A. Puskarich. Sepsis-induced tissue hypoperfusion. Crit Care Clin. Oct 2009;25(4):769-779, ix.

Jung, M., A. Sola, J. Hughes*, et al.* Infusion of IL-10-expressing cells protects against renal ischemia through induction of lipocalin-2. Kidney Int. May 2012;81(10):969-982.

Kahlenberg, J. M., K. C. Lundberg, S. B. Kertesy*, et al.* Potentiation of caspase-1 activation by the P2X7 receptor is dependent on TLR signals and requires NF-kappaB-driven protein synthesis. J Immunol. Dec 1 2005;175(11):7611-7622.

Kalakeche, R., T. Hato, G. Rhodes*, et al.* Endotoxin uptake by S1 proximal tubular segment causes oxidative stress in the downstream S2 segment. J Am Soc Nephrol. Aug 2011;22(8):1505-1516.

Kaplanski, G., C. Farnarier, S. Kaplanski*, et al.* Interleukin-1 induces interleukin-8 secretion from endothelial cells by a juxtacrine mechanism. Blood. Dec 15 1994;84(12):4242-4248.

Karkar, A. M., Y. Koshino, S. J. Cashman*, et al.* Passive immunization against tumour necrosis factor-alpha (TNF-alpha) and IL-1 beta protects from LPS enhancing glomerular injury in nephrotoxic nephritis in rats. Clin Exp Immunol. Nov 1992;90(2):312-318.

Karkar, A. M., F. W. Tam, A. Steinkasserer*, et al.* Modulation of antibody-mediated glomerular injury in vivo by IL-1ra, soluble IL-1 receptor, and soluble TNF receptor. Kidney Int. Dec 1995;48(6):1738-1746.

Kaseda, R., N. Iino, M. Hosojima*, et al.* Megalin-mediated endocytosis of cystatin C in proximal tubule cells. Biochem Biophys Res Commun. Jun 15 2007;357(4):1130-1134.

Kashani, K., A. Al-Khafaji, T. Ardiles*, et al.* Discovery and validation of cell cycle arrest biomarkers in human acute kidney injury. Crit Care. 2013;17(1):R25.

KDIGO. Kidney Disease: Improving Global Outcomes (KDIGO) Acute Kidney Injury Work Group. KDIGO Clinical Practice Guideline for Acute Kidney Injury. Summary of recommendations. Kidney inter. 2012;Suppl. 2:1–138.

Kellum, J. A., L. Kong, M. P. Fink, *et al.* Understanding the inflammatory cytokine response in pneumonia and sepsis: results of the Genetic and Inflammatory Markers of Sepsis (GenIMS) Study. Arch Intern Med. Aug 13-27 2007;167(15):1655-1663.

Keystone, E. C., M. M. Wang, M. Layton, *et al.* Clinical evaluation of the efficacy of the P2X7 purinergic receptor antagonist AZD9056 on the signs and symptoms of rheumatoid arthritis in patients with active disease despite treatment with methotrexate or sulphasalazine. Ann Rheum Dis. Oct 2012;71(10):1630-1635.

Kiil, F., K. Aukland and H. E. Refsum. Renal sodium transport and oxygen consumption. Am J Physiol. Sep 1961;201:511-516.

Kinoshita, K., T. Yamagata, Y. Nozaki, *et al.* Blockade of IL-18 receptor signaling delays the onset of autoimmune disease in MRL-Faslpr mice. J Immunol. Oct 15 2004;173(8):5312-5318.

Kirwan, C. J., B. J. Philips and I. A. Macphee. Estimated glomerular filtration rate correlates poorly with four-hour creatinine clearance in critically ill patients with acute kidney injury. Crit Care Res Pract. 2013;2013:406075.

Kjeldsen, L., A. H. Johnsen, H. Sengelov, *et al.* Isolation and primary structure of NGAL, a novel protein associated with human neutrophil gelatinase. J Biol Chem. May 15 1993;268(14):10425-10432.

Kolliputi, N., R. S. Shaik and A. B. Waxman. The inflammasome mediates hyperoxia-induced alveolar cell permeability. J Immunol. May 15 2010;184(10):5819-5826.

Kozlov, A. V., M. van Griensven, S. Haindl, *et al.* Peritoneal inflammation in pigs is associated with early mitochondrial dysfunction in liver and kidney. Inflammation. Oct 2010;33(5):295-305.

Kreydiyyeh, S. I. and R. Al-Sadi. Interleukin-1beta increases urine flow rate and inhibits protein expression of Na(+)/K(+)-ATPase in the rat jejunum and kidney. J Interferon Cytokine Res. Oct 2002;22(10):1041-1048.

Kreydiyyeh, S. I. and S. Markossian. Tumor necrosis factor alpha down-regulates the Na+-K+ ATPase and the Na+-K+2Cl- cotransporter in the kidney cortex and medulla. Cytokine. Feb 7 2006;33(3):138-144.

Kreymann, G., S. Grosser, P. Buggisch, et al. Oxygen consumption and resting metabolic rate in sepsis, sepsis syndrome, and septic shock. Crit Care Med. Jul 1993;21(7):1012-1019.

Kumar, A., R. Anel, E. Bunnell, et al. Pulmonary artery occlusion pressure and central venous pressure fail to predict ventricular filling volume, cardiac performance, or the response to volume infusion in normal subjects. Crit Care Med. Mar 2004;32(3):691-699.

Kurt-Jones, E. A., D. I. Beller, S. B. Mizel, et al. Identification of a membrane-associated interleukin 1 in macrophages. Proc Natl Acad Sci U S A. Feb 1985;82(4):1204-1208.

Lamacchia, C., G. Palmer, L. Bischoff, et al. Distinct roles of hepatocyte- and myeloid cell-derived IL-1 receptor antagonist during endotoxemia and sterile inflammation in mice. J Immunol. Aug 15 2010;185(4):2516-2524.

Lameire, N., W. Van Biesen and R. Vanholder. The changing epidemiology of acute renal failure. Nat Clin Pract Nephrol. Jul 2006;2(7):364-377.

Lan, H. Y., D. J. Nikolic-Paterson, W. Mu, et al. Interleukin-1 receptor antagonist halts the progression of established crescentic glomerulonephritis in the rat. Kidney Int. May 1995;47(5):1303-1309.

Langenberg, C., S. M. Bagshaw, C. N. May, et al. The histopathology of septic acute kidney injury: a systematic review. Crit Care. 2008;12(2):R38.

Langenberg, C., R. Bellomo, C. May, et al. Renal blood flow in sepsis. Crit Care. Aug 2005;9(4):R363-374.

Langenberg, C., L. Wan, M. Egi, et al. Renal blood flow in experimental septic acute renal failure. Kidney Int. Jun 2006;69(11):1996-2002.

Langenberg, C., L. Wan, M. Egi, et al. Renal blood flow and function during recovery from experimental septic acute kidney injury. Intensive Care Med. Sep 2007;33(9):1614-1618.

Le Hir, M. and B. Kaissling <u>Distribution and regulation of renal ecto-5'-nucleotidase: implications for physiological functions of adenosine</u>, Am J Physiol. 1993 Mar;264(3 Pt 2):F377-87.

Le Hir, M. and B. Kaissling. Distribution and regulation of renal ecto-5'-nucleotidase: implications for physiological functions of adenosine. Am J Physiol. Mar 1993;264(3 Pt 2):F377-387.

Lech, M., A. Avila-Ferrufino, V. Skuginna*, et al.* Quantitative expression of RIG-like helicase, NOD-like receptor and inflammasome-related mRNAs in humans and mice. Int Immunol. Sep 2010;22(9):717-728.

Lee, S., S. Huen, H. Nishio*, et al.* Distinct macrophage phenotypes contribute to kidney injury and repair. J Am Soc Nephrol. Feb 2011;22(2):317-326.

Lerolle, N., D. Nochy, E. Guerot*, et al.* Histopathology of septic shock induced acute kidney injury: apoptosis and leukocytic infiltration. Intensive Care Med. Mar 2010;36(3):471-478.

Levey, A. S., J. P. Bosch, J. B. Lewis*, et al.* A more accurate method to estimate glomerular filtration rate from serum creatinine: a new prediction equation. Modification of Diet in Renal Disease Study Group. Ann Intern Med. Mar 16 1999;130(6):461-470.

Levey, A. S., J. Coresh, T. Greene*, et al.* Using standardized serum creatinine values in the modification of diet in renal disease study equation for estimating glomerular filtration rate. Ann Intern Med. Aug 15 2006;145(4):247-254.

Levey, A. S., L. A. Stevens, C. H. Schmid*, et al.* A new equation to estimate glomerular filtration rate. Ann Intern Med. May 5 2009;150(9):604-612.

Levinsohn, J. L., Z. L. Newman, K. A. Hellmich*, et al.* Anthrax lethal factor cleavage of Nlrp1 is required for activation of the inflammasome. PLoS Pathog. 2012;8(3):e1002638.

Levy, M. M., R. P. Dellinger, S. R. Townsend*, et al.* The Surviving Sepsis Campaign: results of an international guideline-based performance improvement program targeting severe sepsis. Crit Care Med. Feb 2010;38(2):367-374.

Levy, M. M., M. P. Fink, J. C. Marshall*, et al.* 2001 SCCM/ESICM/ACCP/ATS/SIS International Sepsis Definitions Conference. Crit Care Med. Apr 2003;31(4):1250-1256.

Levy, M. N. Effect of variations of blood flow on renal oxygen extraction. Am J Physiol. Jul 1960;199:13-18.

Li, P., H. Allen, S. Banerjee, et al. Mice deficient in IL-1 beta-converting enzyme are defective in production of mature IL-1 beta and resistant to endotoxic shock. Cell. Feb 10 1995;80(3):401-411.

Lichtenstern, C., C. Koch, R. Rohrig, et al. [Near-infrared spectroscopy in sepsis therapy : predictor of a low central venous oxygen saturation]. Anaesthesist. Oct 2012;61(10):883-891.

Lichtnekert, J., O. P. Kulkarni, S. R. Mulay, et al. Anti-GBM glomerulonephritis involves IL-1 but is independent of NLRP3/ASC inflammasome-mediated activation of caspase-1. PLoS One. 2011;6(10):e26778.

Lipcsey, M. and R. Bellomo. Septic acute kidney injury: hemodynamic syndrome, inflammatory disorder, or both? Crit Care. 2011;15(6):1008.

Lippai, D., S. Bala, J. Petrasek, et al. Alcohol-induced IL-1beta in the brain is mediated by NLRP3/ASC inflammasome activation that amplifies neuroinflammation. J Leukoc Biol. Jul 2013;94(1):171-182.

Liu, K. D., B. T. Thompson, M. Ancukiewicz, et al. Acute kidney injury in patients with acute lung injury: impact of fluid accumulation on classification of acute kidney injury and associated outcomes. Crit Care Med. Dec 2011;39(12):2665-2671.

Liu, Y., W. Guo, J. Zhang, et al. Urinary interleukin 18 for detection of acute kidney injury: a meta-analysis. Am J Kidney Dis. Dec 2013;62(6):1058-1067.

Liu, Y., Y. Xiao and Z. Li. P2X7 receptor positively regulates MyD88-dependent NF-kappaB activation. Cytokine. Aug 2011;55(2):229-236.

Lopez, A., J. A. Lorente, J. Steingrub, et al. Multiple-center, randomized, placebo-controlled, double-blind study of the nitric oxide synthase inhibitor 546C88: effect on survival in patients with septic shock. Crit Care Med. Jan 2004;32(1):21-30.

Lorenz, E., J. P. Mira, K. L. Frees, et al. Relevance of mutations in the TLR4 receptor in patients with gram-negative septic shock. Arch Intern Med. May 13 2002;162(9):1028-1032.

Lucas, C. E., F. E. Rector, M. Werner, *et al.* Altered renal homeostasis with acute sepsis. Clinical significance. Arch Surg. Apr 1973;106(4):444-449.

Macedo, E., J. Bouchard, S. H. Soroko, *et al.* Fluid accumulation, recognition and staging of acute kidney injury in critically-ill patients. Crit Care. 2010;14(3):R82.

MacKenzie, A., H. L. Wilson, E. Kiss-Toth, *et al.* Rapid secretion of interleukin-1beta by microvesicle shedding. Immunity. Nov 2001;15(5):825-835.

Maddens, B., B. Vandendriessche, D. Demon, *et al.* Severity of sepsis-induced acute kidney injury in a novel mouse model is age dependent. Crit Care Med. Sep 2012;40(9):2638-2646.

Man, W., D. Ming, D. Fang, *et al.* Dimethyl sulfoxide attenuates hydrogen peroxide-induced injury in cardiomyocytes via heme oxygenase-1. J Cell Biochem. Jun 2014;115(6):1159-1165.

Mariathasan, S., D. S. Weiss, K. Newton, *et al.* Cryopyrin activates the inflammasome in response to toxins and ATP. Nature. Mar 9 2006;440(7081):228-232.

Marik, P. E., M. Baram and B. Vahid. Does central venous pressure predict fluid responsiveness? A systematic review of the literature and the tale of seven mares. Chest. Jul 2008;134(1):172-178.

Martensson, J., C. R. Martling and M. Bell. Novel biomarkers of acute kidney injury and failure: clinical applicability. Br J Anaesth. Dec 2012;109(6):843-850.

Martinon, F., A. Mayor and J. Tschopp. The inflammasomes: guardians of the body. Annu Rev Immunol. 2009;27:229-265.

Matsumoto, K., J. Dowling and R. C. Atkins. Production of interleukin 1 in glomerular cell cultures from patients with rapidly progressive crescentic glomerulonephritis. Am J Nephrol. 1988;8(6):463-470.

May, C., L. Wan, J. Williams, *et al.* A technique for the simultaneous measurement of renal ATP, blood flow and pH in a large animal model of septic shock. Crit Care Resusc. Mar 2007;9(1):30-33.

Mazzali, M., T. Kipari, V. Ophascharoensuk, *et al.* Osteopontin--a molecule for all seasons. QJM. Jan 2002;95(1):3-13.

McGaraughty, S., K. L. Chu, M. T. Namovic, *et al.* P2X7-related modulation of pathological nociception in rats. Neuroscience. Jun 8 2007;146(4):1817-1828.

Mehta, R. L., J. A. Kellum, S. V. Shah, *et al.* Acute Kidney Injury Network: report of an initiative to improve outcomes in acute kidney injury. Crit Care. 2007;11(2):R31.

Mehta, V. B., J. Hart and M. D. Wewers. ATP-stimulated release of interleukin (IL)-1beta and IL-18 requires priming by lipopolysaccharide and is independent of caspase-1 cleavage. J Biol Chem. Feb 9 2001;276(6):3820-3826.

Mestas, J. and C. C. Hughes. Of mice and not men: differences between mouse and human immunology. J Immunol. Mar 1 2004;172(5):2731-2738.

Miao, E. A., J. V. Rajan and A. Aderem. Caspase-1-induced pyroptotic cell death. Immunol Rev. Sep 2011;243(1):206-214.

Michard, F., S. Boussat, D. Chemla, *et al.* Relation between respiratory changes in arterial pulse pressure and fluid responsiveness in septic patients with acute circulatory failure. Am J Respir Crit Care Med. Jul 2000;162(1):134-138.

Miller, W. L., R. A. Thomas, R. M. Berne, *et al.* Adenosine production in the ischemic kidney. Circ Res. 1978;43(3):390-397.

Mishra, J., Q. Ma, A. Prada, *et al.* Identification of neutrophil gelatinase-associated lipocalin as a novel early urinary biomarker for ischemic renal injury. J Am Soc Nephrol. Oct 2003;14(10):2534-2543.

Mongardon, N., A. Dyson and M. Singer. Is MOF an outcome parameter or a transient, adaptive state in critical illness? Curr Opin Crit Care. Oct 2009;15(5):431-436.

Mori, K., H. T. Lee, D. Rapoport, *et al.* Endocytic delivery of lipocalin-siderophore-iron complex rescues the kidney from ischemia-reperfusion injury. J Clin Invest. Mar 2005;115(3):610-621.

Munshi, R., A. Johnson, E. D. Siew, *et al.* MCP-1 gene activation marks acute kidney injury. J Am Soc Nephrol. Jan 2011;22(1):165-175.

Murray, P. T., R. L. Mehta, A. Shaw, *et al.* Potential use of biomarkers in acute kidney injury: report and summary of recommendations from the 10th Acute Dialysis Quality Initiative consensus conference. Kidney Int. Mar 2014;85(3):513-521.

Myers, B. D., W. M. Deen and B. M. Brenner. Effects of norepinephrine and angiotensin II on the determinants of glomerular ultrafiltration and proximal tubule fluid reabsorption in the rat. Circ Res. Jul 1975;37(1):101-110.

Myers, C. L., S. J. Wertheimer, J. Schembri-King, *et al.* Induction of ICAM-1 by TNF-alpha, IL-1 beta, and LPS in human endothelial cells after downregulation of PKC. Am J Physiol. Oct 1992;263(4 Pt 1):C767-772.

Nagaoka, I., H. Tamura and M. Hirata. An antimicrobial cathelicidin peptide, human CAP18/LL-37, suppresses neutrophil apoptosis via the activation of formyl-peptide receptor-like 1 and P2X7. J Immunol. Mar 1 2006;176(5):3044-3052.

Nejat, M., J. V. Hill, J. W. Pickering, *et al.* Albuminuria increases cystatin C excretion: implications for urinary biomarkers. Nephrol Dial Transplant. Oct 2012;27 Suppl 3:iii96-103.

Nemeth, Z. H., B. Csoka, J. Wilmanski, *et al.* Adenosine A2A receptor inactivation increases survival in polymicrobial sepsis. J Immunol. May 1 2006;176(9):5616-5626.

Nezic, L., R. Skrbic, S. Dobric, *et al.* Effect of simvastatin on proinflammatory cytokines production during lipopolysaccharide-induced inflammation in rats. Gen Physiol Biophys. 2009;28 Spec No:119-126.

Nguan, C. Y., Q. Guan, M. E. Gleave, *et al.* Promotion of cell proliferation by clusterin in the renal tissue repair phase after ischemia-reperfusion injury. Am J Physiol Renal Physiol. Apr 1 2014;306(7):F724-733.

Nishiyama, A., K. Miura, A. Miyatake, *et al.* Renal interstitial concentration of adenosine during endotoxin shock. Eur J Pharmacol. Dec 3 1999;385(2-3):209-216.

North, R. A. Molecular physiology of P2X receptors. Physiol Rev. Oct 2002;82(4):1013-1067.

North, R. A. and A. Surprenant. Pharmacology of cloned P2X receptors. Annu Rev Pharmacol Toxicol. 2000;40:563-580.

Novick, D., S. H. Kim, G. Fantuzzi, *et al.* Interleukin-18 binding protein: a novel modulator of the Th1 cytokine response. Immunity. Jan 1999;10(1):127-136.

Novogrodsky, A., A. Vanichkin, M. Patya, *et al.* Prevention of lipopolysaccharide-induced lethal toxicity by tyrosine kinase inhibitors. Science. May 27 1994;264(5163):1319-1322.

Nurmi, K., J. Virkanen, K. Rajamaki, *et al.* Ethanol inhibits activation of NLRP3 and AIM2 inflammasomes in human macrophages--a novel anti-inflammatory action of alcohol. PLoS One. 2013;8(11):e78537.

O'Regan, A. W., G. L. Chupp, J. A. Lowry, *et al.* Osteopontin is associated with T cells in sarcoid granulomas and has T cell adhesive and cytokine-like properties in vitro. J Immunol. Jan 15 1999;162(2):1024-1031.

Ogura, Y., F. S. Sutterwala and R. A. Flavell. The inflammasome: first line of the immune response to cell stress. Cell. Aug 25 2006;126(4):659-662.

Ohlsson, S., O. Bakoush, J. Tencer, *et al.* Monocyte chemoattractant protein 1 is a prognostic marker in ANCA-associated small vessel vasculitis. Mediators Inflamm. 2009;2009:584916.

Olesen, E. T., S. de Seigneux, G. Wang, *et al.* Rapid and segmental specific dysregulation of AQP2, S256-pAQP2 and renal sodium transporters in rats with LPS-induced endotoxaemia. Nephrol Dial Transplant. Aug 2009;24(8):2338-2349.

Olszyna, D. P., J. M. Prins, P. E. Dekkers, *et al.* Sequential measurements of chemokines in urosepsis and experimental endotoxemia. J Clin Immunol. Nov 1999;19(6):399-405.

Opal, S. M., C. J. Fisher, Jr., J. F. Dhainaut, *et al.* Confirmatory interleukin-1 receptor antagonist trial in severe sepsis: a phase III, randomized, double-blind, placebo-controlled, multicenter trial. The Interleukin-1 Receptor Antagonist Sepsis Investigator Group. Crit Care Med. Jul 1997;25(7):1115-1124.

Ophascharoensuk, V., C. M. Giachelli, K. Gordon, *et al.* Obstructive uropathy in the mouse: role of osteopontin in interstitial fibrosis and apoptosis. Kidney Int. Aug 1999;56(2):571-580.

Ospina-Tascon, G., A. P. Neves, G. Occhipinti, *et al.* Effects of fluids on microvascular perfusion in patients with severe sepsis. Intensive Care Med. Jun 2010;36(6):949-955.

Ozer, J. S., F. Dieterle, S. Troth, *et al.* A panel of urinary biomarkers to monitor reversibility of renal injury and a serum marker with improved potential to assess renal function. Nat Biotechnol. May 2010;28(5):486-494.

Panzer, U., F. Thaiss, G. Zahner, *et al.* Monocyte chemoattractant protein-1 and osteopontin differentially regulate monocytes recruitment in experimental glomerulonephritis. Kidney Int. May 2001;59(5):1762-1769.

Parikh, C. R., J. Mishra, H. Thiessen-Philbrook, *et al.* Urinary IL-18 is an early predictive biomarker of acute kidney injury after cardiac surgery. Kidney Int. Jul 2006;70(1):199-203.

Parvathenani, L. K., S. Tertyshnikova, C. R. Greco, *et al.* P2X7 mediates superoxide production in primary microglia and is up-regulated in a transgenic mouse model of Alzheimer's disease. J Biol Chem. Apr 11 2003;278(15):13309-13317.

Patil, N. K., N. Parajuli, L. A. MacMillan-Crow, *et al.* Inactivation of renal mitochondrial respiratory complexes and manganese superoxide dismutase during sepsis: mitochondria-targeted antioxidant mitigates injury. Am J Physiol Renal Physiol. Apr 1 2014;306(7):F734-743.

Payen, D., A. C. de Pont, Y. Sakr, *et al.* A positive fluid balance is associated with a worse outcome in patients with acute renal failure. Crit Care. 2008;12(3):R74.

Peake, S. L., A. Delaney, M. Bailey, *et al.* Goal-directed resuscitation for patients with early septic shock. N Engl J Med. Oct 16 2014;371(16):1496-1506.

Pedoto, A., J. E. Caruso, J. Nandi, *et al.* Acidosis stimulates nitric oxide production and lung damage in rats. Am J Respir Crit Care Med. Feb 1999;159(2):397-402.

Pelegrin, P. and A. Surprenant. The P2X(7) receptor-pannexin connection to dye uptake and IL-1beta release. Purinergic Signal. Jun 2009;5(2):129-137.

Perlman, H., G. R. Budinger and P. A. Ward. Humanizing the mouse: in defense of murine models of critical illness. Am J Respir Crit Care Med. May 1 2013;187(9):898-900.

Perregaux, D. G., P. McNiff, R. Laliberte, *et al.* ATP acts as an agonist to promote stimulus-induced secretion of IL-1 beta and IL-18 in human blood. J Immunol. Oct 15 2000;165(8):4615-4623.

Persy, V. P., W. A. Verstrepen, D. K. Ysebaert, *et al.* Differences in osteopontin up-regulation between proximal and distal tubules after renal ischemia/reperfusion. Kidney Int. Aug 1999;56(2):601-611.

Picard, C., H. von Bernuth, P. Ghandil, *et al.* Clinical features and outcome of patients with IRAK-4 and MyD88 deficiency. Medicine (Baltimore). Nov 2010;89(6):403-425.

Pichler, R. H., N. Franceschini, B. A. Young, *et al.* Pathogenesis of cyclosporine nephropathy: roles of angiotensin II and osteopontin. J Am Soc Nephrol. Oct 1995;6(4):1186-1196.

Pisoni, R., K. M. Wille and A. J. Tolwani. The epidemiology of severe acute kidney injury: from BEST to PICARD, in acute kidney injury: new concepts. Nephron Clin Pract. 2008;109(4):c188-191.

Placido, R., G. Auricchio, S. Falzoni, *et al.* P2X(7) purinergic receptors and extracellular ATP mediate apoptosis of human monocytes/macrophages infected with Mycobacterium tuberculosis reducing the intracellular bacterial viability. Cell Immunol. Nov 2006;244(1):10-18.

Porta, F., J. Takala, C. Weikert, *et al.* Effects of prolonged endotoxemia on liver, skeletal muscle and kidney mitochondrial function. Crit Care. 2006;10(4):R118.

Prowle, J. R., A. Leitch, C. J. Kirwan, *et al.* Positive fluid balance and AKI diagnosis: assessing the extent and duration of 'creatinine dilution'. Intensive Care Med. Jan 2015;41(1):160-161.

Prowle, J. R., Y. L. Liu, E. Licari, *et al.* Oliguria as predictive biomarker of acute kidney injury in critically ill patients. Crit Care. 2011;15(4):R172.

Prowle, J. R., M. P. Molan, E. Hornsey, *et al.* Measurement of renal blood flow by phase-contrast magnetic resonance imaging during septic acute kidney injury: a pilot investigation. Crit Care Med. Jun 2012;40(6):1768-1776.

Qu, Y., L. Franchi, G. Nunez, *et al.* Nonclassical IL-1 beta secretion stimulated by P2X7 receptors is dependent on inflammasome activation and correlated with exosome release in murine macrophages. J Immunol. Aug 1 2007;179(3):1913-1925.

Quoilin, C., A. Mouithys-Mickalad, S. Lecart, *et al.* Evidence of oxidative stress and mitochondrial respiratory chain dysfunction in an in vitro model of sepsis-induced kidney injury. Biochim Biophys Acta. Oct 2014;1837(10):1790-1800.

Ralib, A. M., J. W. Pickering, G. M. Shaw, *et al.* Test characteristics of urinary biomarkers depend on quantitation method in acute kidney injury. J Am Soc Nephrol. Feb 2012;23(2):322-333.

Ranieri, V. M., B. T. Thompson, P. S. Barie, *et al.* Drotrecogin alfa (activated) in adults with septic shock. N Engl J Med. May 31 2012;366(22):2055-2064.

Rassendren, F., G. N. Buell, C. Virginio, *et al.* The permeabilizing ATP receptor, P2X7. Cloning and expression of a human cDNA. J Biol Chem. Feb 28 1997;272(9):5482-5486.

Rector, F., S. Goyal, I. K. Rosenberg, *et al.* Sepsis: a mechanism for vasodilatation in the kidney. Ann Surg. Aug 1973;178(2):222-226.

Rees, A. J. Monocyte and macrophage biology: an overview. Semin Nephrol. May 2010;30(3):216-233.

Remick, D., P. Manohar, G. Bolgos, *et al.* Blockade of tumor necrosis factor reduces lipopolysaccharide lethality, but not the lethality of cecal ligation and puncture. Shock. Aug 1995;4(2):89-95.

Remick, D. G., D. E. Newcomb, G. L. Bolgos, *et al.* Comparison of the mortality and inflammatory response of two models of sepsis: lipopolysaccharide vs. cecal ligation and puncture. Shock. Feb 2000;13(2):110-116.

Ren, G., X. Zhao, L. Zhang, *et al.* Inflammatory cytokine-induced intercellular adhesion molecule-1 and vascular cell adhesion molecule-1 in mesenchymal stem cells are critical for immunosuppression. J Immunol. Mar 1 2010;184(5):2321-2328.

Reynolds, K., B. Novosad, A. Hoffhines, *et al.* Pretreatment with troglitazone decreases lethality during endotoxemia in mice. J Endotoxin Res. 2002;8(4):307-314.

Ricci, Z., D. Cruz and C. Ronco. The RIFLE criteria and mortality in acute kidney injury: A systematic review. Kidney Int. Mar 2008;73(5):538-546.

Ricci, Z., C. Ronco, G. D'Amico, *et al.* Practice patterns in the management of acute renal failure in the critically ill patient: an international survey. Nephrol Dial Transplant. Mar 2006;21(3):690-696.

Rice, T. W., A. P. Wheeler, G. R. Bernard, *et al.* A randomized, double-blind, placebo-controlled trial of TAK-242 for the treatment of severe sepsis. Crit Care Med. Aug 2010;38(8):1685-1694.

Roberts, T. L., A. Idris, J. A. Dunn, *et al.* HIN-200 proteins regulate caspase activation in response to foreign cytoplasmic DNA. Science. Feb 20 2009;323(5917):1057-1060.

Rogers, N. M., D. A. Ferenbach, J. S. Isenberg, *et al.* Dendritic cells and macrophages in the kidney: a spectrum of good and evil. Nat Rev Nephrol. Nov 2014;10(11):625-643.

Ronco, C. and M. Rosner. Acute kidney injury and residual renal function. Crit Care. 2012;16(4):1.

Rosenberg, I. K., S. L. Gupta, C. E. Lucas, *et al.* Renal insufficiency after trauma and sepsis. A prospective functional and ultrastructural analysis. Arch Surg. Aug 1971;103(2):175-183.

Rudiger, A., A. Dyson, K. Felsmann, *et al.* Early functional and transcriptomic changes in the myocardium predict outcome in a long-term rat model of sepsis. Clin Sci (Lond). Mar 2013;124(6):391-401.

Ruperto, N., H. I. Brunner, P. Quartier, *et al.* Two randomized trials of canakinumab in systemic juvenile idiopathic arthritis. N Engl J Med. Dec 20 2012;367(25):2396-2406.

Rusai, K., H. Huang, N. Sayed, *et al.* Administration of interleukin-1 receptor antagonist ameliorates renal ischemia-reperfusion injury. Transpl Int. Jun 2008;21(6):572-580.

Russo, R. A., S. Melo-Gomes, H. J. Lachmann, *et al.* Efficacy and safety of canakinumab therapy in paediatric patients with cryopyrin-associated periodic syndrome: a single-centre, real-world experience. Rheumatology (Oxford). Apr 2014;53(4):665-670.

Sair, M., P. J. Etherington, C. Peter Winlove, *et al.* Tissue oxygenation and perfusion in patients with systemic sepsis. Crit Care Med. Jul 2001;29(7):1343-1349.

Saito, H., E. R. Sherwood, T. K. Varma, *et al.* Effects of aging on mortality, hypothermia, and cytokine induction in mice with endotoxemia or sepsis. Mech Ageing Dev. Dec 2003;124(10-12):1047-1058.

Salomonsson, M., E. Gonzalez, M. Kornfeld, *et al.* The cytosolic chloride concentration in macula densa and cortical thick ascending limb cells. Acta Physiol Scand. Mar 1993;147(3):305-313.

Sasaki, D., A. Yamada, H. Umeno, *et al.* Comparison of the course of biomarker changes and kidney injury in a rat model of drug-induced acute kidney injury. Biomarkers. Nov 2011;16(7):553-566.

Sato, T., Y. Kamiyama, R. T. Jones, *et al.* Ultrastructural study on kidney cell injury following various types of shock in 26 immediate autopsy patients. Adv Shock Res. 1978;1:55-69.

Schmidt, C., K. Hocherl, F. Schweda, *et al.* Regulation of renal sodium transporters during severe inflammation. J Am Soc Nephrol. Apr 2007;18(4):1072-1083.

Schnermann, J., A. E. Persson and B. Agerup. Tubuloglomerular feedback. Nonlinear relation between glomerular hydrostatic pressure and loop of henle perfusion rate. J Clin Invest. Apr 1973;52(4):862-869.

Schnermann, J., H. Weihprecht and J. P. Briggs. Inhibition of tubuloglomerular feedback during adenosine1 receptor blockade. Am J Physiol. Mar 1990;258(3 Pt 2):F553-561.

Schorlemmer, H. U., E. J. Kanzy, K. D. Langner, *et al.* Immunoregulation of SLE-like disease by the IL-1 receptor: disease modifying activity on BDF1 hybrid mice and MRL autoimmune mice. Agents Actions. 1993;39 Spec No:C117-120.

Schrier, R. W. Need to intervene in established acute renal failure. J Am Soc Nephrol. Oct 2004;15(10):2756-2758.

Schrier, R. W. and W. Wang. Acute renal failure and sepsis. N Engl J Med. Jul 8 2004;351(2):159-169.

Schumacker, P. T., N. Chandel and A. G. Agusti. Oxygen conformance of cellular respiration in hepatocytes. Am J Physiol. Oct 1993;265(4 Pt 1):L395-402.

Seely, K. A., J. H. Holthoff, S. T. Burns, *et al.* Hemodynamic changes in the kidney in a pediatric rat model of sepsis-induced acute kidney injury. Am J Physiol Renal Physiol. Jul 2011;301(1):F209-217.

Seija, M., C. Baccino, N. Nin, *et al.* Role of peroxynitrite in sepsis-induced acute kidney injury in an experimental model of sepsis in rats. Shock. Oct 2012;38(4):403-410.

Seok, J., H. S. Warren, A. G. Cuenca, *et al.* Genomic responses in mouse models poorly mimic human inflammatory diseases. Proc Natl Acad Sci U S A. Feb 26 2013;110(9):3507-3512.

Seubert, A., S. Calabro, L. Santini, *et al.* Adjuvanticity of the oil-in-water emulsion MF59 is independent of Nlrp3 inflammasome but requires the adaptor protein MyD88. Proc Natl Acad Sci U S A. Jul 5 2011;108(27):11169-11174.

Shao, X., L. Tian, W. Xu, *et al.* Diagnostic value of urinary kidney injury molecule 1 for acute kidney injury: a meta-analysis. PLoS One. 2014;9(1):e84131.

Sharshar, T., A. Blanchard, M. Paillard, *et al.* Circulating vasopressin levels in septic shock. Crit Care Med. Jun 2003;31(6):1752-1758.

Shiohara, M., S. Taniguchi, J. Masumoto, *et al.* ASC, which is composed of a PYD and a CARD, is up-regulated by inflammation and apoptosis in human neutrophils. Biochem Biophys Res Commun. May 24 2002;293(5):1314-1318.

Siew, E. D., T. A. Ikizler, T. Gebretsadik, *et al.* Elevated urinary IL-18 levels at the time of ICU admission predict adverse clinical outcomes. Clin J Am Soc Nephrol. Aug 2010;5(8):1497-1505.

Skarda, D. E., K. E. Mulier, D. E. Myers, *et al.* Dynamic near-infrared spectroscopy measurements in patients with severe sepsis. Shock. Apr 2007;27(4):348-353.

Sluyter, R., J. G. Dalitz and J. S. Wiley. P2X7 receptor polymorphism impairs extracellular adenosine 5'-triphosphate-induced interleukin-18 release from human monocytes. Genes Immun. Nov 2004;5(7):588-591.

Smith, E. F., 3rd, M. J. Slivjak, J. W. Egan, *et al.* Fluid resuscitation improves survival of endotoxemic or septicemic rats: possible contribution of tumor necrosis factor. Pharmacology. May 1993;46(5):254-267.

Smith, J. A., L. J. Stallons and R. G. Schnellmann. Renal cortical hexokinase and pentose phosphate pathway activation through the EGFR/Akt signaling pathway in endotoxin-induced acute kidney injury. Am J Physiol Renal Physiol. Aug 15 2014;307(4):F435-444.

Sola-Villa, D., M. Camacho, R. Sola, *et al.* IL-1beta induces VEGF, independently of PGE2 induction, mainly through the PI3-K/mTOR pathway in renal mesangial cells. Kidney Int. Dec 2006;70(11):1935-1941.

Soliman, H. M. and J. L. Vincent. Prognostic value of admission serum lactate concentrations in intensive care unit patients. Acta Clin Belg. May-Jun 2010;65(3):176-181.

Spanos, A., S. Jhanji, A. Vivian-Smith, *et al.* Early microvascular changes in sepsis and severe sepsis. Shock. Apr 2010;33(4):387-391.

Staubach, K. H., J. Schroder, F. Stuber, *et al.* Effect of pentoxifylline in severe sepsis: results of a randomized, double-blind, placebo-controlled study. Arch Surg. Jan 1998;133(1):94-100.

Strowig, T., J. Henao-Mejia, E. Elinav, *et al.* Inflammasomes in health and disease. Nature. Jan 19 2012;481(7381):278-286.

Subramanian, R. M., N. Chandel, G. R. Budinger, *et al.* Hypoxic conformance of metabolism in primary rat hepatocytes: a model of hepatic hibernation. Hepatology. Feb 2007;45(2):455-464.

Suffredini, A. F., D. Reda, S. M. Banks, *et al.* Effects of recombinant dimeric TNF receptor on human inflammatory responses following intravenous endotoxin administration. J Immunol. Nov 15 1995;155(10):5038-5045.

Sugiyama, M., K. Kinoshita, K. Kishimoto, *et al.* Deletion of IL-18 receptor ameliorates renal injury in bovine serum albumin-induced glomerulonephritis. Clin Immunol. Jul 2008;128(1):103-108.

Sward, K., F. Valsson, J. Sellgren, *et al.* Differential effects of human atrial natriuretic peptide and furosemide on glomerular filtration rate and renal oxygen consumption in humans. Intensive Care Med. Jan 2005;31(1):79-85.

Takasu, O., J. P. Gaut, E. Watanabe, *et al.* Mechanisms of cardiac and renal dysfunction in patients dying of sepsis. Am J Respir Crit Care Med. Mar 1 2013;187(5):509-517.

Takeda, K., H. Tsutsui, T. Yoshimoto, *et al.* Defective NK cell activity and Th1 response in IL-18-deficient mice. Immunity. Mar 1998;8(3):383-390.

Takeuchi, M., T. Okura, T. Mori, *et al.* Intracellular production of interleukin-18 in human epithelial-like cell lines is enhanced by hyperosmotic stress in vitro. Cell Tissue Res. Sep 1999;297(3):467-473.

Takeuchi, O., K. Hoshino and S. Akira. Cutting edge: TLR2-deficient and MyD88-deficient mice are highly susceptible to Staphylococcus aureus infection. J Immunol. Nov 15 2000;165(10):5392-5396.

Tam, F. W., A. M. Karkar, J. Smith, *et al.* Differential expression of macrophage inflammatory protein-2 and monocyte chemoattractant protein-1 in experimental glomerulonephritis. Kidney Int. Mar 1996;49(3):715-721.

Tam, F. W., J. S. Sanders, A. George, *et al.* Urinary monocyte chemoattractant protein-1 (MCP-1) is a marker of active renal vasculitis. Nephrol Dial Transplant. Nov 2004;19(11):2761-2768.

Tam, F. W., J. Smith, S. J. Cashman, *et al.* Glomerular expression of interleukin-1 receptor antagonist and interleukin-1 beta genes in antibody-mediated glomerulonephritis. Am J Pathol. Jul 1994;145(1):126-136.

Taveira da Silva, A. M., H. C. Kaulbach, F. S. Chuidian, *et al.* Brief report: shock and multiple-organ dysfunction after self-administration of Salmonella endotoxin. N Engl J Med. May 20 1993;328(20):1457-1460.

Taylor, F. B., Jr., A. Chang, C. T. Esmon, *et al.* Protein C prevents the coagulopathic and lethal effects of Escherichia coli infusion in the baboon. J Clin Invest. Mar 1987;79(3):918-925.

Taylor, S. R., M. Gonzalez-Begne, S. Dewhurst, *et al.* Sequential shrinkage and swelling underlie P2X7-stimulated lymphocyte phosphatidylserine exposure and death. J Immunol. Jan 1 2008;180(1):300-308.

Taylor, S. R., C. M. Turner, J. I. Elliott, *et al.* P2X7 deficiency attenuates renal injury in experimental glomerulonephritis. J Am Soc Nephrol. Jun 2009;20(6):1275-1281.

Thijs, L. G. and C. E. Hack. Time course of cytokine levels in sepsis. Intensive Care Med. Nov 1995;21 Suppl 2:S258-263.

Thornberry, N. A., H. G. Bull, J. R. Calaycay, *et al.* A novel heterodimeric cysteine protease is required for interleukin-1 beta processing in monocytes. Nature. Apr 30 1992;356(6372):768-774.

Tian, J., F. Barrantes, Y. Amoateng-Adjepong, *et al.* Rapid reversal of acute kidney injury and hospital outcomes: a retrospective cohort study. Am J Kidney Dis. Jun 2009;53(6):974-981.

Tilahun, A. Y., V. R. Chowdhary, C. S. David, *et al.* Systemic inflammatory response elicited by superantigen destabilizes T regulatory cells, rendering them ineffective during toxic shock syndrome. J Immunol. Sep 15 2014;193(6):2919-2930.

Timoshanko, J. R., A. R. Kitching, Y. Iwakura, *et al.* Contributions of IL-1beta and IL-1alpha to crescentic glomerulonephritis in mice. J Am Soc Nephrol. Apr 2004;15(4):910-918.

Tiwari, M. M., R. W. Brock, J. K. Megyesi, *et al.* Disruption of renal peritubular blood flow in lipopolysaccharide-induced renal failure: role of nitric oxide and caspases. Am J Physiol Renal Physiol. Dec 2005;289(6):F1324-1332.

Togashi, Y., Y. Sakaguchi, M. Miyamoto, *et al.* Urinary cystatin C as a biomarker for acute kidney injury and its immunohistochemical localization in kidney in the CDDP-treated rats. Exp Toxicol Pathol. Nov 2012;64(7-8):797-805.

Tomura, M., S. Maruo, J. Mu, *et al.* Differential capacities of CD4+, CD8+, and CD4-CD8-T cell subsets to express IL-18 receptor and produce IFN-gamma in response to IL-18. J Immunol. Apr 15 1998;160(8):3759-3765.

Tonomura, Y., T. Uehara, E. Yamamoto, *et al.* Decrease in urinary creatinine in acute kidney injury influences diagnostic value of urinary biomarker-to-creatinine ratio in rats. Toxicology. Dec 18 2011;290(2-3):241-248.

Torelli, G., E. Milla, A. Faelli, *et al.* Energy requirement for sodium reabsorption in the in vivo rabbit kidney. Am J Physiol. Sep 1966;211(3):576-580.

Tran, M., D. Tam, A. Bardia, *et al.* PGC-1alpha promotes recovery after acute kidney injury during systemic inflammation in mice. J Clin Invest. Oct 2011;121(10):4003-4014.

Trzeciak, S., J. V. McCoy, R. Phillip Dellinger, *et al.* Early increases in microcirculatory perfusion during protocol-directed resuscitation are associated with reduced multi-organ failure at 24 h in patients with sepsis. Intensive Care Med. Dec 2008;34(12):2210-2217.

Tsuboi, N., Y. Yoshikai, S. Matsuo, *et al.* Roles of toll-like receptors in C-C chemokine production by renal tubular epithelial cells. J Immunol. Aug 15 2002;169(4):2026-2033.

Turkmen, F., G. Isitmangil, I. Berber, *et al.* Comparison of serum creatinine and spot urine interleukin-18 levels following radiocontrast administration. Indian J Nephrol. May 2012;22(3):196-199.

Turnbull, I. R., J. J. Wlzorek, D. Osborne, *et al.* Effects of age on mortality and antibiotic efficacy in cecal ligation and puncture. Shock. Apr 2003;19(4):310-313.

Turner, C. M., B. Ramesh, S. K. Srai, *et al.* Altered ATP-sensitive P2 receptor subtype expression in the Han:SPRD cy/+ rat, a model of autosomal dominant polycystic kidney disease. Cells Tissues Organs. 2004;178(3):168-179.

Turner, C. M., F. W. Tam, P. C. Lai, *et al.* Increased expression of the pro-apoptotic ATP-sensitive P2X7 receptor in experimental and human glomerulonephritis. Nephrol Dial Transplant. Feb 2007;22(2):386-395.

Turner, C. M., O. Vonend, C. Chan, *et al.* The pattern of distribution of selected ATP-sensitive P2 receptor subtypes in normal rat kidney: an immunohistological study. Cells Tissues Organs. 2003;175(2):105-117.

Uchino, S., J. A. Kellum, R. Bellomo, *et al.* Acute renal failure in critically ill patients: a multinational, multicenter study. JAMA. Aug 17 2005;294(7):813-818.

Vallon, V. Tubuloglomerular feedback and the control of glomerular filtration rate. News Physiol Sci. Aug 2003;18:169-174.

Vallon, V. and H. Osswald. Adenosine receptors and the kidney. Handb Exp Pharmacol. 2009;193:443-470.

VanderBrink, B. A., H. Asanuma, K. Hile, *et al.* Interleukin-18 stimulates a positive feedback loop during renal obstruction via interleukin-18 receptor. J Urol. Oct 2011;186(4):1502-1508.

Vanmassenhove, J., R. Vanholder, E. Nagler, *et al.* Urinary and serum biomarkers for the diagnosis of acute kidney injury: an in-depth review of the literature. Nephrol Dial Transplant. Feb 2013;28(2):254-273.

Vilaysane, A., J. Chun, M. E. Seamone, *et al.* The NLRP3 inflammasome promotes renal inflammation and contributes to CKD. J Am Soc Nephrol. Oct 2010;21(10):1732-1744.

Villela, N. R., A. O. dos Santos, M. L. de Miranda, *et al.* Fluid resuscitation therapy in endotoxemic hamsters improves survival and attenuates capillary perfusion deficits and inflammatory responses by a mechanism related to nitric oxide. J Transl Med. 2014;12:232.

von Bernuth, H., C. Picard, Z. Jin, *et al.* Pyogenic bacterial infections in humans with MyD88 deficiency. Science. Aug 1 2008;321(5889):691-696.

Vonend, O., C. M. Turner, C. M. Chan, *et al.* Glomerular expression of the ATP-sensitive P2X receptor in diabetic and hypertensive rat models. Kidney Int. Jul 2004;66(1):157-166.

Waikar, S. S., R. A. Betensky, S. C. Emerson, *et al.* Imperfect gold standards for kidney injury biomarker evaluation. J Am Soc Nephrol. Jan 2012;23(1):13-21.

Waikar, S. S. and J. V. Bonventre. Creatinine kinetics and the definition of acute kidney injury. J Am Soc Nephrol. Mar 2009;20(3):672-679.

Wan, L., C. Langenberg, R. Bellomo, *et al.* Angiotensin II in experimental hyperdynamic sepsis. Crit Care. 2009;13(6):R190.

Wang, J., Q. Long, W. Zhang, *et al.* Protective effects of exogenous interleukin 18-binding protein in a rat model of acute renal ischemia-reperfusion injury. Shock. Mar 2012;37(3):333-340.

Wang, W., S. Faubel, D. Ljubanovic, *et al.* Endotoxemic acute renal failure is attenuated in caspase-1-deficient mice. Am J Physiol Renal Physiol. May 2005;288(5):F997-1004.

Wang, X., G. Z. Feuerstein, J. L. Gu, *et al.* Interleukin-1 beta induces expression of adhesion molecules in human vascular smooth muscle cells and enhances adhesion of leukocytes to smooth muscle cells. Atherosclerosis. May 1995;115(1):89-98.

Ward, J. R., P. W. West, M. P. Ariaans, *et al.* Temporal interleukin-1beta secretion from primary human peripheral blood monocytes by P2X7-independent and P2X7-dependent mechanisms. J Biol Chem. Jul 23 2010;285(30):23147-23158.

Wareham, K., C. Vial, R. C. Wykes, *et al.* Functional evidence for the expression of P2X1, P2X4 and P2X7 receptors in human lung mast cells. Br J Pharmacol. Aug 2009;157(7):1215-1224.

Welter-Stahl, L., C. M. da Silva, J. Schachter, *et al.* Expression of purinergic receptors and modulation of P2X7 function by the inflammatory cytokine IFNgamma in human epithelial cells. Biochim Biophys Acta. May 2009;1788(5):1176-1187.

Wesson, J. A., R. J. Johnson, M. Mazzali, *et al.* Osteopontin is a critical inhibitor of calcium oxalate crystal formation and retention in renal tubules. J Am Soc Nephrol. Jan 2003;14(1):139-147.

Wewers, M. D. and A. Sarkar. P2X(7) receptor and macrophage function. Purinergic Signal. Jun 2009;5(2):189-195.

Whitehouse, T., M. Stotz, V. Taylor, *et al.* Tissue oxygen and hemodynamics in renal medulla, cortex, and corticomedullary junction during hemorrhage-reperfusion. Am J Physiol Renal Physiol. Sep 2006;291(3):F647-653.

Wilcox, C. S. Regulation of renal blood flow by plasma chloride. J Clin Invest. Mar 1983;71(3):726-735.

Williams, K. L., J. D. Lich, J. A. Duncan, *et al.* The CATERPILLER protein monarch-1 is an antagonist of toll-like receptor-, tumor necrosis factor alpha-, and Mycobacterium tuberculosis-induced pro-inflammatory signals. J Biol Chem. Dec 2 2005;280(48):39914-39924.

Wilson, H. L., S. E. Francis, S. K. Dower, *et al.* Secretion of intracellular IL-1 receptor antagonist (type 1) is dependent on P2X7 receptor activation. J Immunol. Jul 15 2004;173(2):1202-1208.

Wolfs, T. G., W. A. Buurman, A. van Schadewijk, *et al.* In vivo expression of Toll-like receptor 2 and 4 by renal epithelial cells: IFN-gamma and TNF-alpha mediated up-regulation during inflammation. J Immunol. Feb 1 2002;168(3):1286-1293.

Wu, H., M. L. Craft, P. Wang, *et al.* IL-18 contributes to renal damage after ischemia-reperfusion. J Am Soc Nephrol. Dec 2008;19(12):2331-2341.

Wu, L., N. Gokden and P. R. Mayeux. Evidence for the role of reactive nitrogen species in polymicrobial sepsis-induced renal peritubular capillary dysfunction and tubular injury. J Am Soc Nephrol. Jun 2007;18(6):1807-1815.

Wu, L. and P. R. Mayeux. Effects of the inducible nitric-oxide synthase inhibitor L-N(6)-(1-iminoethyl)-lysine on microcirculation and reactive nitrogen species generation in the kidney following lipopolysaccharide administration in mice. J Pharmacol Exp Ther. Mar 2007;320(3):1061-1067.

Wulfert, F. M., M. van Meurs, N. F. Kurniati, *et al.* Age-dependent role of microvascular endothelial and polymorphonuclear cells in lipopolysaccharide-induced acute kidney injury. Anesthesiology. Jul 2012;117(1):126-136.

Xie, Y., S. Nishi, S. Iguchi, *et al.* Expression of osteopontin in gentamicin-induced acute tubular necrosis and its recovery process. Kidney Int. Mar 2001;59(3):959-974.

Xie, Y., M. Sakatsume, S. Nishi, *et al.* Expression, roles, receptors, and regulation of osteopontin in the kidney. Kidney Int. Nov 2001;60(5):1645-1657.

Xing, L. and D. G. Remick. Mechanisms of dimethyl sulfoxide augmentation of IL-1 beta production. J Immunol. May 15 2005;174(10):6195-6202.

Xing, L. and D. G. Remick. Mechanisms of oxidant regulation of monocyte chemotactic protein 1 production in human whole blood and isolated mononuclear cells. Shock. Aug 2007;28(2):178-185.

Xing, L. and D. G. Remick. Promoter elements responsible for antioxidant regulation of MCP-1 gene expression. Antioxid Redox Signal. Nov 2007;9(11):1979-1989.

Xu, L. L., M. K. Warren, W. L. Rose, *et al.* Human recombinant monocyte chemotactic protein and other C-C chemokines bind and induce directional migration of dendritic cells in vitro. J Leukoc Biol. Sep 1996;60(3):365-371.

Xu, S. Y., M. Carlson, A. Engstrom*, et al.* Purification and characterization of a human neutrophil lipocalin (HNL) from the secondary granules of human neutrophils. Scand J Clin Lab Invest. Aug 1994;54(5):365-376.

Yamagishi, H., T. Yokoo, T. Imasawa*, et al.* Genetically modified bone marrow-derived vehicle cells site specifically deliver an anti-inflammatory cytokine to inflamed interstitium of obstructive nephropathy. J Immunol. Jan 1 2001;166(1):609-616.

Yang, C. M., S. F. Luo, H. L. Hsieh*, et al.* Interleukin-1beta induces ICAM-1 expression enhancing leukocyte adhesion in human rheumatoid arthritis synovial fibroblasts: involvement of ERK, JNK, AP-1, and NF-kappaB. J Cell Physiol. Aug 2010;224(2):516-526.

Ye, Z., J. D. Lich, C. B. Moore*, et al.* ATP binding by monarch-1/NLRP12 is critical for its inhibitory function. Mol Cell Biol. Mar 2008;28(5):1841-1850.

Yealy, D. M., J. A. Kellum, D. T. Huang*, et al.* A randomized trial of protocol-based care for early septic shock. N Engl J Med. May 1 2014;370(18):1683-1693.

Yu, X. Q., D. J. Nikolic-Paterson, W. Mu*, et al.* A functional role for osteopontin in experimental crescentic glomerulonephritis in the rat. Proc Assoc Am Physicians. Jan-Feb 1998;110(1):50-64.

Zapelini, P. H., G. T. Rezin, M. R. Cardoso*, et al.* Antioxidant treatment reverses mitochondrial dysfunction in a sepsis animal model. Mitochondrion. Jun 2008;8(3):211-218.

Zappacosta, A. R. and B. L. Ashby. Gram-negative sepsis with acute renal failure. Occurrence from acute glomerulonephritis. JAMA. Sep 26 1977;238(13):1389-1390.

Zhang, H., K. L. Hile, H. Asanuma*, et al.* IL-18 mediates proapoptotic signaling in renal tubular cells through a Fas ligand-dependent mechanism. Am J Physiol Renal Physiol. Jul 2011;301(1):F171-178.

Zhang, Z., B. Lu, X. Sheng*, et al.* Cystatin C in prediction of acute kidney injury: a systemic review and meta-analysis. Am J Kidney Dis. Sep 2011;58(3):356-365.

Zhao, J., H. Wang, C. Dai, *et al.* P2X7 blockade attenuates murine lupus nephritis by inhibiting activation of the NLRP3/ASC/caspase 1 pathway. Arthritis Rheum. Dec 2013;65(12):3176-3185.

Zhao, Y., J. Yang, J. Shi, *et al.* The NLRC4 inflammasome receptors for bacterial flagellin and type III secretion apparatus. Nature. Sep 29 2011;477(7366):596-600.

Zhou, F., Z. Peng, R. Murugan, *et al.* Blood purification and mortality in sepsis: a meta-analysis of randomized trials. Crit Care Med. Sep 2013;41(9):2209-2220.

Zhou, W., Q. Guan, C. C. Kwan, *et al.* Loss of clusterin expression worsens renal ischemia-reperfusion injury. Am J Physiol Renal Physiol. Mar 2010;298(3):F568-578.

Zhou, X., B. Ma, Z. Lin, *et al.* Evaluation of the usefulness of novel biomarkers for drug-induced acute kidney injury in beagle dogs. Toxicol Appl Pharmacol. Oct 1 2014;280(1):30-35.

Zolfaghari, P., P. B, D. A, *et al.* The metabolic profile of rodent sepsis: cause for concern? ICM Experimental. 29 October 2013;1(6).

10 Appendix

10.1 AKI definitions

RIFLE Criteria

RIFLE	Creatinine clearance/ GFR Criteria	Urine output criteria
Risk	Serum creatinine x1.5 or GFR decrease >25%	< 0.5ml/kg/h x 6 h
Injury	Serum creatinine x 2 or GFR decrease >50%	< 0.5 ml/kg/h x12 h
Failure	Serum creatinine x3, GFR decrease > 75% or serum creatinine ≥ 352 *µmol/l* with an acute rise >44 *µmol/l*	< 0.3 ml/kg/h x 24 h, or anuria x 12 h
Loss	Persistent acute renal failure = complete loss of kidney function > 4 weeks	
End stage	End-stage kidney disease > 3 months	

AKIN Criteria

AKIN	Creatinine clearance/ GFR Criteria	Urine output criteria
AKIN I	Increase in serum creatinine ≥ 26.4 µmol/l or increase to ≥150-200% (1.5- to 2-fold) from baseline	< 0.5 ml/kg/h for >6 h
AKIN II	Increase in serum creatinine to >200-300% (>2- to 3-fold) from baseline	< 0.5 ml/kg/h for >12 h
AKIN III	Increase in serum creatinine to >300% (>3-fold) from baseline (or serum creatinine ≥354 µmol/l with an acute increase of ≥0.5 mg/dl (44 µmol/l)	< 0.3 ml/kg/h for 24 h or anuria for 12 h

10.2 72hr sepsis and recovery data

(^{a}: Naïve vs. sham; ^{b} sham vs good prognosis sepsis; ^{c} sham vs. poor prognosis sepsis; ^{d} good vs poor prognosis sepsis)

10.2.1 Baseline data

Group	Weight (g)	Temperature (^{o}C)	HR (/min)	SV (mL)	CO (ml/min)
3hr Sham	326 ± 18	37.5 ± 0.2	427 ± 44	0.32 ± 0.02	141 ± 18
3hr Sepsis Good Prognosis	316 ± 9	37.4 ± 0.3	428 ± 40	0.32 ± 0.03	138 ± 18
3hr Sepsis Poor Prognosis	335 ± 29	37.8 ± 0.2	432 ± 32	0.32 ± 0.07	137 ± 16
6hr Sham	314 ± 18	37.4 ± 0.2	384 ± 48	0.34 ± 0.05 ^{b}	136 ± 21 ^{b}
6hr Sepsis Good Prognosis	332 ± 33	37.7 ± 0.5	410 ± 36	0.38 ± 0.04	129 ± 13
6hr Sepsis Poor Prognosis	328 ± 27	37.9 ± 0.5	405 ± 26	0.36 ± 0.07	156 ± 23
12hr Sham	355 ± 37	37.6 ± 0.2	426 ± 26	0.32 ± 0.07	146 ± 31
12hr Sepsis Good Prognosis	324 ± 9	37.4 ± 0.3	416 ± 36	0.35 ± 0.03	146 ± 12
12hr Sepsis Poor Prognosis	326 ± 19	37.3 ± 0.3	418 ± 32	0.32 ± 0.03	135 ± 17
24hr Sham	350 ± 74	37.4 ± 0.5	439 ± 19	0.33 ± 0.04	137 ± 14
24hr Sepsis Good Prognosis	328 ± 25	37.5 ± 0.4	416 ± 35	0.35 ± 0.03	147 ± 18
24hr Sepsis Poor Prognosis	345 ± 66	37.5 ± 0.2	418 ± 34	0.32 ± 0.03 ^{d}	146 ± 12
48hr Sham	342 ± 28	37.4 ± 0.4	394 ± 27	0.35 ± 0.05	135 ± 17
48hr Sepsis Good Prognosis	324 ± 15	37.3 ± 0.2	413 ± 22	0.35 ± 0.06	137 ± 20
72 Sham	337 ± 26	37.6 ± 0.5	400 ± 43	0.39 ± 0.07	143 ± 24
72 Sepsis Good Prognosis	321 ± 9	37.6 ± 0.5	420 ± 33	0.36 ± 0.05	154 ± 21

10.2.2 Preoperative Cardiovascular data

Group	Change in HR (%)	Change in SV (%)	Change in CO (%)
3hr Sham	-1.6 ± 8.4	-7.0 ± 14.6	-9.2 ± 10.6
3hr Sepsis Good Prognosis	4.6 ± 10.6	14.8 ± 19.5	11.4 ± 17.0
3hr Sepsis Poor Prognosis	5.7 ± 8.4	-39 ± 15.5	-36.0 ± 14.2
6hr Sham	-0.4 ± 7.7	-8.0 ± 5.0	-8.6 ± 7.3
6hr Sepsis Good Prognosis	18.8 ± 11.4	-34.2 ± 8.6	-21.9 ± 11.8
6hr Sepsis Poor Prognosis	22.2 ± 9.0	-49.9 ± 12.3	-38.6 ± 16.0
12hr Sham	-0.5 ± 8.8	-4.8 ± 16.4	-5.8 ± 14.9
12hr Sepsis Good Prognosis	9.0 ± 7.5	-35.5 ± 19.8	-29.3 ± 23.9
12hr Sepsis Poor Prognosis	13.7 ± 4.6	-40.0 ± 13.2	-32.0 ± 14.7
24hr Sham	-2.7 ± 6.9	-9.3 ± 11.4	-12.0 ± 10.2
24hr Sepsis Good Prognosis	9.1 ± 13.0	-29.3 ± 14.4	-22.8 ± 18.6
24hr Sepsis Poor Prognosis	14.3 ± 15.3	-32.3 ± 17.4	-25.3 ± 19.9
48hr Sham	-4.1 ± 6.8	-13.5 ± 14.6	-16.8 ± 16.6
48hr Sepsis Good Prognosis	-2.4 ± 9.5	17.3 ± 15.5	-18.9 ± 19.7
72 Sham	-13 ± 8.2	-4.6 ± 14.5	-16.8 ± 16.3
72 Sepsis Good Prognosis	0.6 ± 11.0	-2.7 ± 18.5	-3.6 ± 11.8

Preoperative data

Group	Temperature (°C)	MAP (mmHg)	SVR (dyne.s.cm^5)	DO$_2$ (ml.min^{-1})
Naive	37.5 ± 0.4	116 ± 10	828 ± 103	224 ± 24
3hr Sham	37.5 ± 0.4	139 ± 22	1132 ± 232	209 ± 19
3hr Sepsis Good Prognosis	37.5 ± 0.3	131 ±7	1115 ± 158	221 ± 21
3hr Sepsis Poor Prognosis	38.3 ± 0.9	130 ± 14	1532 ± 156	177 ± 23
6hr Sham	37.4 ± 0.3	117 ± 8	1011 ± 180	191 ± 25
6hr Sepsis Good Prognosis	38.0 ± 0.6	136 ± 13	1174 ± 269	229 ± 51
6hr Sepsis Poor Prognosis	38.5 ± 0.4	137 ± 10	1626 ± 296	174 ± 30
12hr Sham	37.7 ± 0.5	123 ± 8	1022 ± 199	217 ± 32
12hr Sepsis Good Prognosis	38.8 ± 0.5	133 ± 13	1421 ± 365	194 ± 44
12hr Sepsis Poor Prognosis	38.3 ± 0.4	134 ± 11	1496 ± 367	180 ± 35
24hr Sham	37.5 ± 0.4	117 ± 8	941 ± 173	211 ± 42
24hr Sepsis Good Prognosis	38.9 ± 0.5	127 ± 11	1219 ± 272	195 ± 44
24hr Sepsis Poor Prognosis	38.4 ± 0.8	117 ± 20	1307 ± 621	173 ± 44
48hr Sham	38.5 ± 0.8	118 ± 8	1091 ± 230	203 ± 43
48hr Sepsis Good Prognosis	37.9 ± 0.7	112 ± 14	1054 ± 334	183 ± 40
72 Sham	37.8 ± 0.3	127 ± 4	1028 ± 224	222 ± 53
72 Sepsis Good Prognosis	37.5 ± 0.3	117 ± 13	824 ±136	228 ± 45

10.2.3 Arterial Blood Gas

Group	pH	pCO₂ (kPa)	pO₂ (kPa)	SaO₂ (%)	Lactate (mmol/L)	Base Deficit	Hct (%)	Hb (g/dl)
Naive	7.44 ± 0.03	4.8 ± 0.4	11.3 ± 0.8	90 ± 1	1.4 ± 0.4	0.54 ± 1.19	41 ± 2	13.3 ± 0.8
3 h Sham	7.49 ± 0.02	4.6 ± 0.4	12.1 ± 1.1	93 ± 2	0.8 ± 0.1	2.82 ± 1.41	42 ± 2	13.6 ± 0.8
3 h Sepsis Good Prognosis	7.51 ± 0.03	4.1 ± 0.6	11.4 ± 1.3	92 ± 2	1.9 ± 0.5	0.94 ± 1.64	46 ± 4	15.2 ± 1.3
3 h Sepsis Poor Prognosis	7.50 ± 0.02	4.1 ± 0.3	12.0 ± 0.7	93 ± 1	1.7 ± 0.4	0.77 ± 1.07	51 ± 3	16.7 ± 0.9
6h Sham	7.43 ± 0.02	5.2 ± 0.5	11.1 ± 1.1	90 ± 3	1.1 ± 0.2	1.17 ± 1.80	41 ± 3	13.4 ± 1.0
6 h Sepsis Good Prognosis	7.47 ± 0.03	4.5 ± 0.4	10.7 ± 0.8	90 ± 2	1.0 ± 0.1	0.98 ± 1.34	48 ± 4	15.6 ± 1.4
6 h Sepsis Poor Prognosis	7.47 ± 0.04	4.1 ± 0.6	11.2 ± 0.8	92 ± 2	1.4 ± 0.4	-1.31 ± 2.02	51 ± 3	16.5 ± 1.1
12 h Sham	7.45 ± 0.02	5.3 ± 0.4	12.2 ± 1.2	91 ± 2	0.7 + 0.2	3.63 ± 1.33	44 ± 5	14.5 ± 1.6
12 h Sepsis Good Prognosis	7.46 ± 0.03	4.4 ± 0.5	12.4 ± 1.3	92 ± 3	1.2 ± 0.2	-0.82 ± 1.23	49 ± 3	15.9 ± 0.8
12 h Sepsis Poor Prognosis	7.42 ± 0.04	4.8 ± 0.3	11.7 ± 0.9	90 ±3	1.6 ± 0.3	-1.19 ± 2.03	49 ± 3	16.1 ± 0.9
24 h Sham	7.44 ± 0.06	5.0 ± 0.2	11.3 ± 1.4	90 ± 3	0.8 ± 0.6	2.68 ± 1.97	40 ± 4	13.2 ± 0.8
24 h Sepsis Good Prognosis	7.46 ± 0.03	4.4 ± 0.5	11.4 ± 1.8	90 ± 3	2.3 ± 0.5	-0.46 ± 2.11	44 ± 3	14.3 ± 1.0
24 h Sepsis Poor Prognosis	7.54 ± 0.06	4.4 ± 0.8	10.8 ± 2.3	91 ± 4	3.0 ± 1.2	-1.28 ± 3.88	44 ± 4	14.4 ± 1.3
48 h Sham	7.45 ± 0.03	4.8 ± 0.3	12.1 ± 1.4	92 ± 2	1.0 ± 0.2	1.31 ± 2.27	42 ± 8	14.8 ± 1.0
48 h Sepsis Good Prognosis	7.48 ± 0.06	4.6 ± 0.8	13.4 ± 3.2	94 ± 1	2.1 ± 0.9	1.09 ± 3.39	40 ± 6	13.1 ± 2.0
72 h Sham	7.46 ± 0.02	4.7 ± 0.3	11.6 ± 0.5	92 ± 1	1.0 ± 0.1	1.84 ± 1.21	43 ± 1	14.0 ± 0.5
72h Sepsis Good Prognosis	7.46 ± 0.07	4.9 ± 0.7	10.7 ± 4.4	92 ± 4	1.8 ± 0.9	1.40 ± 2.67	40 ± 3	13.2 ± 1.2

10.2.4 Urea and Electrolytes

Group	Na$^+$ (mmol/L)	K$^+$ (mM/L)	Cl$^-$ (mM/L)	HCO$_3^-$ (mM/L)	Urea (mM/L)	Creatinine (μM/L)	Anion Gap (mM/L)	Glucose (mM/L)
Naive	138 ± 4	4.1 ± 0.4	103 ± 3	25.0 ± 0.9	6 ± 1	23 ± 2	13 ± 1	13.8 ± 3.2
3 h Sham	142 ± 1	4.0 ± 0.3	102 ± 1	27.2 ± 1.1	6 ± 1	21 ± 2	17 ± 3	11.4 ± 2.1
3 h Sepsis Good Prognosis	141 ± 3	4.5 ± 0.6	102 ± 2	26.0 ± 1.0	8 ± 2	27 ± 5	18 ± 3	15.0 ± 4.8
3 h Sepsis Poor Prognosis	138 ± 2	4.8 ± 0.2	101 ± 1	25.9 ± 0.8	10 ± 2	31 ± 6	16 ± 1	11.6 ± 1.4
6h Sham	137 ± 2	3.9 ± 0.2	104 ± 3	25.4 ± 1.4	5 ± 1	25 ± 3	12 ± 2	11.2 ± 1.2
6 h Sepsis Good Prognosis	137 ± 4	4.2 ± 0.5	102 ± 5	25.7 ± 1.2	8 ± 4	24 ± 8	13 ± 4	7.9 ± 1.5
6 h Sepsis Poor Prognosis	135 ± 2	4.4 ± 0.7	103 ± 4	24.1 ± 1.5	10 ± 4	30 ± 10	13 ± 5	7.8 ± 2.0
12 h Sham	136 ± 2	3.7 ± 0.5	105 ± 2 [c]	27.5 ± 1.0	5 ± 1	22 ± 5	8 ± 3	11.6 ± 0.8
12 h Sepsis Good Prognosis	140 ± 3	4.1 ± 0.2	105 ± 4	24.3 ± 0.9	5 ± 0	23 ± 3	15 ± 6	7.9 ± 0.5
12 h Sepsis Poor Prognosis	135 ± 2	4.0 ± 0.2	108 ± 3	23.5 ± 1.8	5 ± 1	22 ± 3	7 ± 2	7.1 ± 2.2
24 h Sham	138 ± 2	3.8 ± 0.7	103 ± 3	24.4 ± 1.7	6 ± 1	25 ± 3	12 ± 1	12.5 ± 1.0
24 h Sepsis Good Prognosis	139 ± 3	3.6 ± 0.3	104 ± 4	24.4 ± 1.6	5 ± 1	28 ± 4	14 ± 1	9.1 ± 3.1
24 h Sepsis Poor Prognosis	139 ± 5	3.6 ± 0.4	105 ± 3	23.8 ± 3.0	7 ± 3	33 ± 14	12 ± 4	7.4 ± 2.6
48 h Sham	138 ± 3	3.7 ± 0.3	105 ± 3	25.8 ± 1.9	5 ± 1	26 ± 3	11 ± 3	11.7 ± 2.2
48 h Sepsis Good Prognosis	141 ± 3	4.1 ± 0.6	108 ± 7	25.7 ± 2.9	7 ± 2	29 ± 5	12 ± 4	9.5 ± 1.7
72 h Sham	139 ± 3	4.0 ± 0.5	103 ± 2	26.2 ± 1.1	6 ± 1	27 ± 3	14 ± 2	11.4 ± 1.6
72h Sepsis Good Prognosis	138 ± 3	3.9 ± 0.5	103 ± 3	25.8 ± 2.6	7 ± 1	27 ± 5	13 ± 2	11.6 ± 1.6

10.2.5 Liver Function tests

Group	Albumin (g/L)	ALP (IU/L)	ALT (IU/L)	AST (IU/L)
Naive	34 ± 7	158 ± 21	45 ± 7	101 ± 19
3hr Sham	32 ± 3	123 ± 34	39 ± 11	109 ± 36
3hr Sepsis Good Prognosis	30 ± 3	129 ± 6	36 ± 9	126 ± 26
3hr Sepsis Poor Prognosis	28 ± 2	97 ± 19	37 ± 7	144 ± 22
6hr Sham	28 ± 2	113 ± 32	38 ± 9	125 ± 50
6hr Sepsis Good Prognosis	27 ± 2	129 ± 47	44 ± 12	215 ± 107
6hr Sepsis Poor Prognosis	26 ± 3	138 ± 22	54 ± 20	231 ± 120
12hr Sham	30 ± 2	99 ± 27	38 ± 10	98 ± 16
12hr Sepsis Good Prognosis	31 ± 3	159 ± 52	46 ± 7	146 ± 22
12hr Sepsis Poor Prognosis	24 ± 3	133 ± 16	38 ± 7	134 ± 25
24hr Sham	29 ± 2	116 ± 30	36 ± 8	92 ± 27
24hr Sepsis Good Prognosis	25 ± 3	163 ± 44	32 ± 10	126 ± 45
24hr Sepsis Poor Prognosis	23 ± 3	185 ± 71	34 ± 90	181 ± 107
48hr Sham	31 ± 3	113 ± 27	43 ± 17	105 ± 24
48hr Sepsis Good Prognosis	26 ± 4	250 ± 61	25 ± 6	111 ± 28
72 Sham	29 ± 1	111 ± 20	41 ± 3	93 ± 22
72 Sepsis Good Prognosis	27 ± 4	150 ± 38	28 ± 13	89 ± 21

Serum Cytokines

Group	IL-1β (pg/ml)	IL-6 (pg/ml)	IL-10 (pg/ml)	MCP-1 (ng/ml)	INF-g (pg/ml)	IL-18 (pg/ml)
Naive	1 (1 - 1)	1 (1 - 1)	11 (1 - 36)	54 (45 – 180)	1 (1 - 1)	131 (15 - 237)
3 h Sham	1 (1 - 1)	1 (1 - 1)	185 (1 - 416)	61 (40 – 84)	1 (1 - 1)	192 (107 - 477)
3 h Sepsis Good Prognosis	1134 (1008 - 1296)	2728 (1 - 4521)	930 (634 - 1402)	121 (146 – 880)	1 (1 - 1)	440 (151 - 498)
3 h Sepsis Poor Prognosis	1373 (805 - 1710)	6264 (1 - 10842)	1208 (500 - 1507)	649 (394 – 973)	1 (1 - 1)	310 (210 - 355)
6 h Sham	1 (1 - 1)	1 (1 - 6)	65 (1 - 82)	98 (72 – 118)	16 (15 - 16)	293 (267 - 315)
6 h Sepsis Good Prognosis	1198 (892 - 1604)	16746 (8941 - 24266)	2984 (1956 - 4071)	538 (487 – 635)	47 (35 - 161)	243 (51 - 420)
6 h Sepsis Poor Prognosis	1737 (1293 - 2067)	34971 (13981 - 47523)	5065 (3274 - 6030)	781 (595 – 1018)	23 (21 - 237)	164 (124 - 299)
12 h Sham	1 (1 - 1)	1 (1 - 1)	23 (1 - 47)	100 (67 – 195)	1 (1 - 1)	222 (181 - 263)
12 h Sepsis Good Prognosis	1007 (798 - 1067)	984 (746 - 1552)	2198 (1983 - 2645)	515 (450 – 646)	1 (1 - 1)	132 (103 - 248)
12 h Sepsis Poor Prognosis	1601 (1177 - 1774)	15068 (4330 - 27014)	2655 (1475 - 4113)	728 (511 – 752)	1 (1 - 1)	194 (53 - 375)
24 h Sham	1 (1 - 1)	1 (1 - 1)	325 (106 - 744)	66 (46 – 93)	1 (1 - 1)	96 (36 - 235)
24 hr Sepsis Good Prognosis	481 (207 – 1294)	210 (1 – 1087)	3710 (1889 – 3874)	432 (326 – 576)	1 (1 - 1)	188 (116 – 794)
24 h Sepsis Poor Prognosis	1188 (767 – 2640)	12112 (1 – 44573)	4381 (1702 – 7816)	480 (466 – 826)	1 (1 - 1)	219 (66 – 690)
48 h Sham	1 (1 - 83)	1 (1 - 1)	154 (1 -616)	100 (10 – 107)		185 (164 – 207)
48 h Sepsis Good Prognosis	1361 (163 - 1463)	89 (1 - 255)	2411 (1978 - 4702)	275 (149 – 303)	1 (1 - 1)	339 (223 – 454)
72 h Sham	1 (1 - 1)	1 (1 - 1)	275 (214 - 280)	75 (48 – 106)	1 (1 - 1)	171 (99 – 242)
72 h Sepsis Good Prognosis	148 (67 - 373)	1 (1 - 1)	966 (334 - 1889)	140 (74 – 228)	1 (1 - 1)	209 (200 – 402)

10.2.6 Renal Cytokines

Group	IL-10 (pg/mg protein)	IL-1β (pg/mg protein)	IL-4 (pg/mg protein)	INF-γ (pg/mg protein)	MCP-1 (pg/mg protein)
Naive	286 (224 - 446)	104 (100 - 124)	866 (642 -1144)	10808 (6175 - 11858)	253 (195 - 3008)
3 h Sham	414 (363 - 585)	33 (18 - 74)	503 (480 - 563)	6250 (5867 - 7706)	508 (417 - 523)
3 h Sepsis Good Prognosis	389 (388 -568)	108 (75 - 117)	487 (289 - 576	4536 (4223 - 6425)	621 (481 - 692)
3 h Sepsis Poor Prognosis	326 (230 - 444)	86 (65 - 143)	303 (225 - 424)	7271 (3838 - 8446)	681 (523 - 871)
6 h Sham	316 (212 - 344)	88 (76 - 144)	967 (696 - 1480)	10982 (7303 - 12379)	322 (180 - 538)
6 h Sepsis Good Prognosis	241 (240 - 320)	213 (147 - 233)	647 (488 - 734)	12977 (11109 - 12873)	504 (167 - 704)
6 h Sepsis Poor Prognosis	256 (222 - 318)	177 (110 - 277)	936 (636 - 1560)	9007 (6133 - 13567)	687 (493 - 859)
12 h Sham	392 (281 - 445)	114 (91 - 144)	769 (717 - 856)	9384 (7862 - 11515)	426 (302 - 580)
12 h Sepsis Good Prognosis	313 (209 - 327)	190 (168 - 226)	781 (447 - 893)	3799 (3602 - 4607)	569 (525 - 647)
12 h Sepsis Poor Prognosis	343 (228 - 437)	201 (152 - 270)	964 (886 - 1242)	8753 (8508 - 9610)	414 (263 - 717)
24 h Sham	326 (228 - 665)	171 (165 - 178)	1080 (930 - 1088)	9279 (9275 - 11886)	520 (110 - 705)
24 hr Sepsis Good Prognosis	355 (208 – 628)	157 (140 – 309)	1114 (842 – 1485)	9090 (4608 – 10945)	729 (573 – 1273)
24 h Sepsis Poor Prognosis	276 (270 – 359)	218 (167 – 280)	833 (595 – 1017)	3767 (2920 – 5227)	542 (218 – 948)
48 h Sham	204 (180 - 515)	126 (71 - 403)	907 (568 - 1093)	7434 (5469 - 9170)	402 (69 - 555)
48 h Sepsis Good Prognosis	436 (378 - 459)	216 (147 - 278)	1125 (917 - 1275)	7962 (3429 - 13908)	592 (422 - 702)
72 h Sham	456 (439 - 518)	140 (114 - 152)	844 (744 - 913)	11953 (10542 - 16858)	432 (226 - 504)
72 h Sepsis Good Prognosis	268 (166 - 477)	68 (66 - 100)	749 (703 - 973)	9394 (7521 - 11757)	437 (280 - 454)

10.2.7 Serum Biomarkers

Group	Serum NGAL (pg/ml)	Serum Cyst C (ng/ml)
Naive	38 (26 - 56)	2163 (1830 - 2389)
3 h Sham	442 (354 - 668)	2725 (2177 - 2946)
3 h Sepsis Good Prognosis	1807 (1449 - 2183)	2770 (2439 - 3201)
3 h Sepsis Poor Prognosis	3405 (1417 - 4640)	2883 (2839 - 3000)
6 h Sham	849 (691 - 905)	1948 (1617 - 2328)
6 h Sepsis Good Prognosis	9044 (6430 - 10959)	1876 (1816 - 2395)
6 h Sepsis Poor Prognosis	7860 (5808 - 7997)	2462 (2270 - 2588)
12 h Sham	121 (106 - 236)	1977 (1940 – 2055)
12 h Sepsis Good Prognosis	6622 (6184 - 7723)	2364 (2328 - 2365)
12 h Sepsis Poor Prognosis	13936 (8533 - 14449)	2217 (1895 - 2958)
24 h Sham	408 (269 - 692)	2091 (1773 - 2361)
24 h Sepsis Good Prognosis	13272 (13187 - 16766)	2525 (2226 – 2882)
24 h Sepsis Poor Prognosis	13450 (10278 - 17792)	2836 (2776 – 3158)
48 h Sham	843 (396 - 1887)	1749 (1713 - 2444)
48 h Sepsis Good Prognosis	5257 (50 - 14531)	2342 (1987 - 2492)
72 h Sham	1408 (433 - 6009)	2845 (1895 - 3108)
72 h Sepsis Good Prognosis	8830 (2920 - 14445)	2503 (2338 - 3089)

10.2.8 Urine biomarkers- 1

Group	Urine NGAL (ng/ml)	Urine CystC (pg/ml)	Urine IL18 (pg/ml)	Urine MCP-1 (pg/ml)
Naive	279 (218 – 421)	234 (164 - 256)	7288 (5641 - 8771)	6300 (4925 - 6827)
3 h Sham	1133 (895 - 1549)	283 (227 - 286)	7261 (5800 - 8268)	7121 (5912 - 7496)
3 h Sepsis Good Prognosis	2379 (1807 - 3456)	137 (69 - 279)	3174 (241 - 4164)	4413 (2764 - 4506)
3 h Sepsis Poor Prognosis	6024 (3709 - 6266)	323 (223 - 378)	3206 (2896 - 5344)	4098 (3074 - 7308)
6 h Sham	2315 (886 - 3026)	220 (123 - 271)	2259 (1651 - 6796)	2592 (1594 - 7377)
6 h Sepsis Good Prognosis	6360 (6023 - 7643)	273 (228 - 350)	1256 (665 - 2064)	1403 (646 - 2314)
6 h Sepsis Poor Prognosis	7267 (7016 - 7645)	238 (80 - 382)	5930 (1896 - 7847)	2326 (2225 - 6709)
12 h Sham	454 (376 - 2057)	53 (23 - 176)	2038 (1270 - 6266)	1472 (937 - 3435)
12 h Sepsis Good Prognosis	8396 (8152 - 9364)	245 (200 - 245)	5880 (3233 - 7261)	6790 (6258 - 8202)
12 h Sepsis Poor Prognosis	9358 (8343 - 9740)	245 (213 - 287)	2654 (1421 - 3807)	4245 (2986 - 4432)
24 h Sham	2611 (1197 - 2978)	71 (48 - 102)	990 (323 - 3286)	1619 (657 - 3644)
24 h Sepsis Good Prognosis	32625 (28307 - 40179)	436 (217 - 577)	3656 (769 - 4832)	5247 (1391 - 6041)
24 h Sepsis Poor Prognosis	30435 (29885 - 123555)	343 (242 - 740)	1100 (725 - 2576)	2280 (1740 - 4119)
48 h Sham	3878 (3192 - 4426)	90 (77 - 106)	1764 (924 - 5012)	1978 (984 - 4712)
48 h Sepsis Good Prognosis	30733 (11969 - 42586)	365 (254 - 608)	7014 (3782 - 11900)	6363 (3620 - 8275)
72 h Sham	2133 (1201 - 2396)	155 (93 - 170)	2914 (2647 - 4185)	3432 (3005 - 4416)
72 h Sepsis Good Prognosis	4082 (3811 - 11478)	209 (207 - 374)	1587 (1446 - 4935)	2213 (1794 - 4225)

10.2.9 Urine biomarkers- 2

Group	Urine Calbindin (ng/ml)	Urine Clusterin (ng/ml)	Urine KIM-1 (ng/ml)	Urine Osteopontin (ng/ml)
Naive	51 (0 -66)	21 (19 - 36)	250 (200 - 320)	2210 (910 - 2510)
3 h Sham	97 (57 - 99)	95 (76 - 151)	260 (210 - 370)	390 (210 - 720)
3 h Sepsis Good Prognosis	159 (91 - 235)	174 (110 - 202)	320 (180 -990)	460 (190 - 930)
3 h Sepsis Poor Prognosis	112 (50 - 134)	182 (180 - 283)	640 (400 - 670)	500 (320 - 560)
6 h Sham	67 (45 - 89)	133 (49 - 198)	120 (90 - 520)	920 (480 - 1620)
6 h Sepsis Good Prognosis	79 (72 - 158)	138 (42 - 328)	2510 (290 - 3960)	610 (280 - 720)
6 h Sepsis Poor Prognosis	186 (165 - 217)	344 (50 - 880)	1480 (770 - 5500)	810 (620 - 920)
12 h Sham	29 (0 -50)	21 (5 - 24)	0 (0 - 30)	420 (150 - 580)
12 h Sepsis Good Prognosis	74 (72 - 83)	20 (17 - 46)	610 (430 -740)	430 (390 - 630)
12 h Sepsis Poor Prognosis	80 (62 - 89)	145 (80 - 251)	2490 (1560 -3080)	770 (720 - 960)
24 h Sham	64 (29 - 124)	18 (15 - 48)	120 (70 - 190)	850 (480 -860)
24 h Sepsis Good Prognosis	59 (45 - 82)	153 (89 - 208)	450 (160 - 570)	470 (70 - 1000)
24 h Sepsis Poor Prognosis	51 (36 - 191)	183 (48 - 339)	212 (110 - 520)	100 (60 - 290)
48 h Sham	82 (57 - 130)	55 (34 - 168)	240 (110 - 370)	630 (220 - 1010)
48 h Sepsis Good Prognosis	63 (58 - 167)	175 (88 - 381)	770 (420 - 960)	820 (190 - 1370)
72 h Sham	73 (51 - 95)	29 (20 -45)	400 (290 - 420)	230 (210 - 560)
72 h Sepsis Good Prognosis	67 (52 - 82)	119 (78 - 128)	500 (320 - 650)	460 (140 - 890)

10.2.10 Urine Electrolytes

Group	Urine Na$^+$ (mmol/l)	Urine Cr (mmol/l)	Fe Na$^+$
Naive	44 (30 - 109)	4.8 (3.1 - 11.2)	2.35 (0.85 - 2.92)
3 h Sham	81 (45 - 84)	2.2 (2.0 - 2.7)	0.43 (0.30 - 0.46)
3 h Sepsis Good Prognosis	32 (18 - 48)	1.9 (1.4 - 5.9)	0.21 (0.09 - 0.46)
3 h Sepsis Poor Prognosis	23 (21 - 30)	6.0 (5.3 - 10.4)	0.07 (0.06 - 0.08)
6 h Sham	40 (36 - 45)	1.6 (1.5 - 1.8)	0.44 (0.39 - 0.49)
6 h Sepsis Good Prognosis	36 (14 - 89)	1.7 (0.9 - 2.5)	0.60 (0.25 - 0.84)
6 h Sepsis Poor Prognosis	30 (29 - 63)	2.6 (2.3 - 11.8)	0.18 (0.11 - 0.22)
12 h Sham	60 (54 - 66)	1.2 (1.0 - 1.3)	0.67 (0.65 - 0.85)
12 h Sepsis Good Prognosis	45 (37 - 57)	1.3 (1.2 - 1.4)	0.54 (0.51 - 0.65)
12 h Sepsis Poor Prognosis	38 (33 - 66)	1.6 (1.3 - 2.5)	0.39 (0.22 - 0.82)
24 h Sham	38 (33 – 66)	1.6 (1.3 - 2.5)	0.39 (0.22 - 0.82)
24 h Sepsis Good Prognosis	59 (39 - 116)	2.2 (1.6 - 2.4)	0.76 (0.33 - 1.27)
24 h Sepsis Poor Prognosis	23 (14 - 45)	3.7 (2.0 - 7.5)	0.21 (0.13 - 0.25)
48 h Sham	63 (45 - 82)	2.7 (2.1 - 3.7)	0.47 (-.39 - 0.54)
48 h Sepsis Good Prognosis	74 (18 - 107)	4.7 (1.6 - 5.9)	0.23 (0.09 - -0.47)
72 h Sham	90 (71 - 126)	3.2 (2.7 - 3.5)	0.53 (0.46 - 0.58)
72 h Sepsis Good Prognosis	75 (57 - 108)	3.3 (2.6 - 4.4)	0.40 (0.29 - 0.44)

10.2.11 Renal Macrophages

Group	Serum- Renal MCP-1	Renal Glomerular macrophages	Renal interstitial macrophages
Naive	NA	0 (0 - 0.4)	3.0 (2.4 - 4.3)
3 h Sham	0.0086 (0.0044 - 0.0131)	0.0 (0.0 - 0.0)	0.0 (0.0 - 0.0)
3 h Sepsis Good Prognosis	0.0033 (0.0008 - 0.0039)	0.0 (0.0 - 0.0)	0.0 (0.0 - 0.0)
3 h Sepsis Poor Prognosis	0.0011 (0.0008 - 0.0023)	0.0 (0.0 - 0.0)	0.0 (0.0 - 0.0)
6 h Sham	0.0031 (0.0015 - 0.0070)	0.8 (0.4 - 5.4)	6.6 (2.6 - 12.5)
6 h Sepsis Good Prognosis	0.0011 (0.0007 - 0.0014)	2.1 (0.0 - 3.7)	24.5 (0.0 - 35.0)
6 h Sepsis Poor Prognosis	0.0007 (0.0007 - 0.0009)	1.5 (0.4 - 4.0)	15.0 (1.0 - 50.0)
12 h Sham	0.0046 (0.0031 -0.0052)	0.2 (0.0 -0.3)	1.3 (0.0 - 6.0)
12 h Sepsis Good Prognosis	0.0012 (0.0011 - 0.0013)	0.0 (0.0 - 0.7)	0.0 (0.0 - 10.5)
12 h Sepsis Poor Prognosis	0.0009 (0.0005 - 0.0015)	3.7 (2.4 - 5.7)	27.5 (16.0 - 46.0)
24 h Sham	0.0119 (0.0071 - 0.0149)	0.4 (0.2 - 0.6)	4.4 (2.8 - 12.0)
24 h Sepsis Good Prognosis	0.0019 (00013 - 0.0022)	1.6 (0.0 - 2.6)	19.0 (13.0 - 40.0)
24 h Sepsis Poor Prognosis	0.0011 (0.0009 - 0.0015)	1.3 (1.1 - 1.7)	41.0 (21.2 - 45.0)
48 h Sham	0.0040 (0.0035 - 0.0044)	0.3 (0.1 - 3.2)	5.9 (4.0 - 21.1)
48 h Sepsis Good Prognosis	0.0025 (0.0021 - 0.0030)	6.0 (0.0 -11.0)	47.0 (0.0 -202.0)
72 h Sham	0.0067 (0.0021 - 0.0089)	0.8 (0.4 - 0.9)	10.6 (7.6 - 13.1)
72 h Sepsis Good Prognosis	0.0041 (0.0015 - 0.0082)	6.0 (2.4 - 9.9)	43.5 (24.5 - 83.0)

10.2.12 Effect of fluid resuscitation

* p<0.05 compared to resuscitated septic animal

	Fluid resuscitated	No fluid resuscitation
Change in cardiac output (%)	-26 (-38 - -7)	-35 (-56 - -29)
Change in stroke volume (%)	-38 (-49 - -25)	-49 (-62 - -37)
Change in heart rate (%)	19 (10 – 41)	25 (16 – 27)
Global O$_2$ delivery (ml.min^{-1})	183 (153 – 194)	185 (124 – 195)
Mean arterial pressure (mmHg)	138 (127 – 145)	136 (123 – 143)
Temperature (^{o}C)	38.4 (38.1 – 38.8)	39.3 (38.6 – 39.6)

	Fluid resuscitated	No fluid resuscitation
Lactate (mmol.l^{-1})	1.2 (1.0 – 1.5)	1.6 (1.5 – 1.7) *
Base Excess (mmol.l^{-1})	0.6 (0.0 – 2.1)	-2.3 (-3.0 - -0.6)
Urea (mmol.l^{-1})	6.4 (5.3 – 7.0)	8.1 (6.8 – 9.8) *
Creatinine (μmol^{-1})	23.0 (21.0 -27.5)	32.0 (26.0 – 34.0) *
Haematocrit (%)	48 (42 – 51)	50 (45 – 55)
O$_2$ Saturation (%)	90 (89 – 91)	90 (89 – 91)

10.3 Renal Haemodynamics

- p<0.05 for sham vs. sepsis (at corresponding time points);
- [§] p<0.05 for Naïve vs. sepsis. ( ) indicated approaching significance (p 0.05-.0.06)

10.3.1 Baseline Variables

	6hr		24hr	
	Sham n = 6	Septic n = 6	Sham n = 7	Septic n = 8
Weight (g)	330 ± 25	332 ± 25	351 ± 32	332 ± 26
Stroke volume (mL)	0.36 ± 0.03	0.35 ± 0.04	0.34 ± 0.03	0.35 ± 0.03
Heart rate (min^{-1})	425 ± 23	410 ± 30	428 ± 27	424 ± 31
Cardiac output (ml/min)	152 ± 11	142 ± 18	146 ±14	149 ± 8

10.3.2 Systemic variables

	Naive	Sham 6 h	Sepsis 6 h	Sham 24 h	Sepsis 24 h
Weight (g)	348 (326 - 359)	325 (305 - 358)	332 (320 - 345)	365 (323 -370)	323 (313 - 330)
Temperature (^{o}C)	37.5 (37.1 - 37.8)	37.2 (36.8 - 37.4) *	38.4 (38.1 - 38.6) §	37.4 (36.9 - 37.8) *	38.3 (38.0 - 38.4) §
Mean Arterial Pressure (mmHg)	113 (108 - 123)	118 (110 - 120)	120 (115 - 128)	120 (110 - 130)	115 (110 - 130)
Syst vasc resist (dyne.s.cm^5)	860 (173 - 914)	884 (747 - 1026)	994 (929 - 1092) §	903 (876 - 1088)	979 (966 - 1137)
Change in heart rate (%)	-	4 (3 - 6) $^{(*)}$	16 (10 – 19) §	-7 (-8 - -5) *	6 (-3 - 9)
Change in cardiac output (%)	-	-12 (-15 - -12)	-23 (-39 - 1) $^{(§)}$	-13 (-22 - -5)	-24 (-43 - 10) §
Change in stroke volume (%)	-	-16 (-17 - 0)	-34 (-56 - -12) §	-2 (-10 - 2) *	-29 (-39 - -15) §
SaO$_2$ (%)	90 (89 - 91)	89 (87 - 90)	92 (91 - 94)	92 (88 - 93)	88 (86 - 91)
Global DO$_2$ (ml.min^{-1})	227 (209 - 239)	217 (216 - 224)	216 (203 - 227)	220 (210 - 239)	217 (205 - 224)
Glucose (mmol.l^{-1})	13 (11 - 16)	12 (11 - 12)	12 (10 - 12)	14 (11 - 15) *	10 (9 -11) §
Lactate (mmol.l^{-1})	1.3 (1.0 - 1.6)	1.5 (1.2 - 1.8)	1.5 (1.2 - 1.6)	1.3 (1.3 - 1.7) *	1.7 (1.6 - 2.5)
Anion Gap (mmol.l^{-1})	13 (12 - 14)	14 (13 - 16)	15 (12 - 16)	12 (12 - 14)	12 (11 - 13)

Syst vasc resist = systemic vascular resistance

10.3.3 Renal haemodynamic variables

	Naive	Sham 6 h	Sepsis 6 h	Sham 24 h	Sepsis 24 h
RBF (ml.min^{-1})	16.3 (15.1 - 19.5)	20.7 (18.0 - 22.0)	16.4 (15.8 - 20.0)	20.2 (18.0 - 23.0) *	16.6 (16.2 - 18.6)
Renal DO$_2$ (ml.min^{-1})	27 (24 - 33)	34 (28 - 38)	30 (28 - 36)	37 (33 -39) *	28 (27 - 34)
Renal/Global DO$_2$ (%)	12 (10 - 14)	16 (12 - 17)	14 (12 - 18)	16 (14 - 19)	16 (12 - 16)
Renal VO$_2$ (ml.min^{-1})	11 (10 - 14)	9 (8 - 13)	8 (7 - 11) [§]	15 (11 - 19)	12 (11 - 13)
ERO$_2$ (%)	45 (36 - 53)	30 (24 - 40)	29 (23 - 31) [§]	44 (34 - 47)	43 (34 - 44)
Renal vein lactate (mmol.l^{-1})	1.3 (1.1 - 1.5)	1.8 (1.4 - 2.2)	1.7 (1.2 - 2.2)	2.3 (1.8 - 3.1) *	3.9 (2.2 - 4.6) [§]
Lactate Consumption (umol.min^{-1})	-0.15 (-0.20 - 0.05)	-0.20 (-0.008 - 0.003)	-0.20 (-0.004 - 0.00)	-0.05 (-0.14 - -0.04)	-0.13 (-0.17 - -0.07)
Renal vein Glucose (mmol.l^{-1})	19 (15 - 20)	18 (16 - 19)	16 (13 - 18)	21 (15 - 24) *	13 (4 - 16)
Glucose Consumption (mmol.l^{-1})	-0.04 (-0.05 - -0.03)	-0.06 (-0.08 - -0.03)	-0.04 (-0.06 - -0.02)	-0.08 (-0.1 - -0.04) *	-0.02 (-0.04 - 0.04) [§]
Renal Cortex pO$_2$ (mmHg)	12.8 (12.3 - 14.5)	12.5 (11.5 - 13.0)	11.9 (10.5 - 13.8)	13.0 (11.0 - 18.0) *	10.8 (7.5 - 11.5) [§]

10.4 Antagonist data

a: p < 0,05 for DMSO vs DMSO/P2X7 for 6 or 24hr. b: DMSO vs untreated. C: DMSO/P2X7 vs. untreated. D: Pre-treatment vs. untreated

10.4.1 Baseline data

Group	Weight (g)	Temperature (^{o}C)
6 h sepsis untreated	340 (308 – 373)	37.4 (37.1 – 38.0)
6 h high dose DMSO	311 (295 - 370)	37.6 (37.5 - 37.8)
6 h high dose P2X$_7$	360 (350 – 380)	37.6 (37.5 - 38.2)
24 h sepsis untreated	338 (330 – 340)	37.4 (37.2 – 37.8)
24 h low dose DMSO	330 (327 - 3340)	37.9 (37.5 - 38.3)
24 h high dose DMSO	333 (315 - 350)	37.4 (37.3 - 38.0)
24 h low dose DMSO/P2X$_7$	336 (317 - 340)	37.5 (37.5 - 37.9)
24 h high dose DMSO/P2X$_7$	346 (317 - 360)	37.6 (37.2 - 37.8)
24 h P2X$_7$ pretreatment	380 (360 - 388)	37.7 (37.3 - 38.0)

10.4.2 Baseline CVS

Group	HR (/min)	SV (mL)	CO (ml/min)
6 h sepsis untreated	408 (385 – 435)	0.36 (0.33 – 0.40)	153 (136 – 161)
6 h high dose DMSO	421 (408 - 436)	0.33 (0.28 - 0.38)	134 (130 - 156)
6 h high dose P2X$_7$	394 (373 - 431)	0.31 (0.28 - 0.39)	133 (113 - 147)
24 h sepsis untreated	404 (384 – 429)	0.31 (0.30 – 0.33)	132 (120 – 137)
24 h low dose DMSO	384 (370 - 409)	0.34 (0.31 - 0.34)	125 (115 -146)
24 h high dose DMSO	401 (390 - 453)	0.34 (0.33 - 0.42)	151 (143 - 162)
24 h low dose DMSO/P2X$_7$	412 (410 - 432)	0.35 (0.31 - 0.36)	146 (199 - 155)
24 h high dose DMSO/P2X$_7$	425 (408 - 437)	0.33 (0.31 - 0.36)	140 (130 - 153)
24 h P2X$_7$ pretreatment	429 (412 - 453)	0.34 (0.30 - 0.36)	149 (132 - 151)

10.4.3 Preoperative CVS data

Group	Change in HR (%)	Change in SV (%)	Change in CO (%)
6 h sepsis untreated	16 (14 – 29)	-49 (-56 - -37)	-41 (-47 - -27)
6 h high dose DMSO	15 (10 - 18)	-32 (-42 - -28)	-27 (-31 - 19)
6 h high dose P2X$_7$	16 (14 - 18) [c]	-38 (-50 - -35)	-29 (-42 - 23)
24 h sepsis untreated	19 (2 – 22)	-31 (-37 - -24)	-23 (-34 - -12)
24 h low dose DMSO	13 (9 - 14)	-29 (-36 - -25)	-23 (-27 - -15)
24 h high dose DMSO	5 (-2 - 16)	-22 (-39 - 15)	-22 (-36 - -13)
24 h low dose DMSO/P2X$_7$	6 (4 - 11)	-17 (-21 - -6)	-10 (-21 - 5)
24 h high dose DMSO/P2X$_7$	-1 (-6 - 7) [c]	-25 (-30 - 16) [c]	-23 (-27 - -16)
24 h P2X$_7$ pretreatment	7 (0 - 9) [d]	-29 (-30 - 0)	-22 (-26 - -1)

10.4.4 Preoperative data

Group	Temperature (^{o}C)	MAP (mmHg)	SVR (dyne.s.cm^5)	DO$_2$ (ml.min^{-1})
6 h sepsis untreated	39.7 (39.1 – 39.7)	138 (128 – 153)	1681 (1240 – 1774)	174 (146 – 214)
6 h high dose DMSO	38.4 (38.3 - 39.0)	135 (130 - 137)	1312 (1048 - 1704)	199 (176 - 233)
6 h high dose P2X$_7$	38.7 (38.6 - 38.7)	136 (135 - 145)	1358 (1311 - 1572)	217 (199 -231)
24 h sepsis untreated	38.2 (37.6 -38.6)	125 (110 – 125)	1078 (1009 – 1217)	184 (170 – 190)
24 h low dose DMSO	38.2 (37.9 - 38.7)	127 (120 - 128)	1111 (883 - 1193)	190 (160 - 198)
24 h high dose DMSO	38.3 (37.8 - 38.5)	127 (112 - 134)	1126 (871 - 1244)	198 (183 - 224)
24 h low dose DMSO/P2X$_7$	38.5 (38.1 - 38.5)	132 (126 - 137)	1033 (969 - 1156)	226 (217 - 241)
24 h high dose DMSO/P2X$_7$	38.2 (37.6 - 38.7)	123 (117 - 130)	1105 (817 - 1265)	185 (174 - 234)
24 h P2X$_7$ pretreatment	38.1 (37.1 - 38.5)	130 (125 - 140) [a]	1120 (1089 -1128)	219 (203 - 240) [a]

10.4.5 Arterial Blood Gas

Group	pH	pCO$_2$ (kPa)	pO$_2$ (kPa)	SaO$_2$ (%)	Lactate (mmol/L)	Base Deficit	Hct (%)	Hb (g/dl)
6 h sepsis untreated	7.47 (7.44–7.52)	4.1 (3.9–4.6)	11.3 (10.5–11.7)	91 (90–93)	1.2 (0.9 – 1.2)	-0.5 (-0.7–0.9)	51 (47 – 53)	16.7 (15.2-17.4)
6 h high dose DMSO	7.44 (7.43-7.50)	4.5 (4.0-4.8)	12.0 (11.1-12.8)[b]	93 (92-94)[b]	1.0 (0.9-1.0)[b]	-0.2 (-1.6- -0.1)	50 (48 -51)	16.5 (15.7-16.7)
6 h high dose P2X$_7$	7.45 (7.40-7.46)	4.4 (4.0-4.7)	11.9 (11.6-12.3)[c]	94 (92-95)[c]	1.2 (1.1-1.3)[a]	-1.6 (-2.6- -0.3)	55 (53-55)[a,c]	18.0 (17.3-18.1)[a,c]
24 h sepsis untreated	7.44 (7.44–7.49)	4.1 (4.1–4.7)	12.1 (11.3–12.6)	92 (89–93)	2.2 (2 – 2.4)	-0.3 (-2.2- -0.5)	45 (45 – 46)	14.7 (13.6–14.9)
24 h low dose DMSO	7.48 (7.47-7.48)	4.5 (4.0- .7)	12.1 (11.4-12.7)	93 (91-93)	2.1 (1.2-2.8)	1.2 (-0.8 - 2.5)	44 (43 - 45)	14.5 (14.1-14.8)
24 h high dose DMSO	7.48 (7.46-7.48)	4.4 (4.3-4.8)	12.0 (11.7-12.2)	93 (91-94)[b]	2.2 (2.1-2.2)	1.5 (0.0- 2.0)[b]	43 (42 - 45)	14.1 (13.7-14.7)
24 h low dose DMSO/P2X$_7$	7.50 (7.46-7.56)	4.2 (4.1-4.9)	12.6 (12.3-13.1)	93 (92-95)	2.4 (1.16-2.6)	-0.1 (-0.1- 1)	46 (43 - 49)	14.9 (14.1-15.9)
24 h high dose DMSO/P2X$_7$	7.45 (7.42-7.46)	4.42 (4.2-4.9)	12.1 (10.3-12.9)	93 (90-94)	1.4 (0.9-1.8)[a,c]	0.2 (-2.0- 1.7)	45 (41 - 45)	14.6 (13.5-14.9)
24 h P2X$_7$ pretreat	7.48 (7.46-7,48)	4.8 (4.6-4.9)	11.8 (9.9-13.1)	93 (88-94)[d]	1.7 (1.4-2.3)[(d)]	1.9 (0.3- 2.1)[d]	46 (43 - 47)	15.2 (15.0-15.3)

10.4.6 Urea and Electrolytes

Group	Na$^+$ (mmol/L)	K$^+$ (mmol/L)	Cl$^-$ (mmol/L)	HCO$_3^-$ (mmol/L)	Urea (mmol/L)	Creatinine (μmol/L)	Anion Gap (mmol/L)	Glucose (mmol/L)
6 h sepsis untreated	138 (134 – 140)	4.6 (4.2 – 4.8)	100 (94 – 102)	24.7 (23.7 – 26.2)	7.8 (6.1–17.9)	25 (17 – 36)	19 (18 – 20)	7.0 (6.2 – 7.6)
6 h high dose DMSO	136 (136 - 139)	4.3 (4.2 - 4.6)	100 (99 - 107)	24.6 (24.1 - 24.7)	7.4 (7.1 -8.2)	19 (15 - 23)[b]	17 (4 - 18)	6.5 (6.0 - 7.1)[b]
6 h high dose P2X$_7$	137 (136 - 141)	4.3 (4.3 - 4.3)	109 (99 - 113)	24.1 (22.3 - 24.8)	9.7 (7.0 - 12.9)	26 (24 - 31)[a]	9 (6 - 18)	7.7 (7.3 - 8.1)[a]
24 h sepsis untreated	143 (136 – 144)	3.7 (3.6 – 3.8)	106 (104–108)	24.8 (23.2 – 25.5)	5.3 (5.1 – 5.6)	25 (22 – 27)	15 (13 – 17)	8.5 (7.9 – 9.2)
24 h low dose DMSO	140 (137 - 142)	3.7 (3.6 - 4.0)	106 (103 - 106)	25.9 (24.3 - 26.6)	4.5 (4.1 - 5.8)	28 (26 - 32)	12 (12 - 13)	9.4 (8.7 - 9.7)
24 h high dose DMSO	143 (141 - 144)[b]	3.7 (3.6 - 4.1)	105 (104 - 107)	26.2 (24.9-26.6)[b]	4.7 (4.4 5.4)[b]	23 (20 - 26)[b]	16 (13 - 17)	8.6 (8.1 - 9.6)
24 h low dose DMSO/P2X$_7$	140 (135 - 142)	3.9 (3.8 - 3.9)	107 (104 - 108)	25.4 (25.1 - 25.5)	4.4 (3.9 - 4.5)	26 (25 - 27)	11 (9 - 12)	9.4 (8.7 - 10.4)
24 h high dose DMSO/P2X$_7$	142 (139 - 143)[c]	3.6 (3.3 - 3.9)	107 (105 - 109)[c]	25.2 (23.3 -26.1)	4.4 (4.1 - 4.9)[c]	23 (18 - 26)[c]	13 (11 - 14)[a]	8.7 (8.0 - 10.5)[c]
24 h P2X$_7$ pretreat	143 (142-143)[d]	3.5 (3.4 - 4.0)	106 (105 - 106)	26.4 (24.4-26.6)[d]	4.3 (3.6-4.6)[d]	22 (19 - 22)[d]	14 (14 - 16)	8.9 (8.5 - 9.2)

10.4.7 Liver Function tests

Group	Albumin (g/l)	ALP (IU/L)	ALT (IU/L)	AST (IU/L)
6 h sepsis untreated	28 (27 – 30)	127 (100 – 152)	50 (45 – 544)	206 (167 – 248)
6 h high dose DMSO	25 (23 - 27)	131 (109 - 143)	45 (42 - 55)	180 (162 - 207)
6 h high dose P2X$_7$	26 (25 - 28)	132 (112 - 145)	48 (47 - 55)	199 (180 -259)
24 h sepsis untreated	23 (21 – 24)	138 (114 – 173)	31 (29 – 44)	143 (123 – 212)
24 h low dose DMSO	29 (25 - 32)	144 (116 - 185)	36 (33 - 47)	140 (122 - 145)
24 h high dose DMSO	24 (22 - 25)	179 (142 - 205)	31 (27 - 33)	140 (113 - 154)
24 h low dose DMSO/P2X$_7$	26 (26 - 27)	158 (138 - 168)	28 (27 - 37)	127 (116 - 146)
24 h high dose DMSO/P2X$_7$	27 (25 - 28) [a, c]	142 (128 - 191)	33 (31 - 35)	118 (95 - 129) [c]
24 h P2X$_7$ pretreatment	25 (23 - 28)	131 (121 - 163)	29 (27 - 31)	114 (114 - 125)

10.4.8 Serum Cytokines

Group	IL-1β (pg/ml)	IL-6 (pg/ml)	IL-10 (pg/ml)	MCP-1 (ng/ml)	IL-18 (pg/ml)
6 h sepsis untreated	1737 (1473 – 1944)	13980 (8697–31736)	4017 (2164 – 6340)	538 (481 – 1018)	299 (164–386)
6 h high dose DMSO	1924 (1853 - 2218)	25036 (20255-25947)	2576 (2378 - 3616)	668 (572 - 763)	-
6 h high dose P2X$_7$	1989 (1214 - 2382)	20643 (18217-29203)	3152 (2297 - 4870)	568 (392 - 698)	-
24 h sepsis untreated	1462 (907 – 2245)	1 (1 – 2477)	2997 (1717 – 3792)	470 (403 – 502)	188 (66 – 317)
24 h low dose DMSO	584 (487 - 1395)	1 (1 - 1)	4071 (1975 - 5309)	336 (164 - 406)	-
24 h high dose DMSO	1808 (973 - 2657)	450 (43 - 1148)	2034 (393 - 4681)	704 (519 - 734)	210 (164 - 745)
24 h low dose DMSO/P2X$_7$	609 (556 - 957)	1 (1 - 1)	2202 (2013 - 3035)	429 (370 - 479)	-
24 h high dose DMSO/P2X$_7$	768 (178 - 1456)	1 (1 - 3274)	2387 (2122 - 4587)	514 (164 - 769)	93 (93 - 201) [c]
24 h P2X$_7$ pretreatment	661 (281 - 1395) [d]	972 (1 - 1993)	3384 (2378 - 6340)	384 (318 - 500)	-

10.4.9 Renal Cytokines

Group	IL-10 (pg/mg protein)	IL-1β (pg/mg protein)	INF-γ (pg/mg protein)	IL-4 (pg/mg protein)	MCP-1 (pg/mg protein)	Serum/Renal MCP-1 gradient
6 h sepsis untreated	248 (186 – 318)	128 (101 – 162)	6707 (6133 – 6818)	625 (488 – 936)	590 (318 – 704)	0.0007 (0.0007–0.0009)
6 h high dose DMSO	126 (112 - 147)	126 (112 - 147)	8652 (7917 - 8834)	1028 (824 - 1805)	624 (512 - 688)	0.0009 (0.0009 - 0.001)
6 h high dose P2X$_7$	70 (60 - 100)[c]	70 (60-100)[c]	7110 (5615 - 9104)	1801 (675 - 2342)	390 (264-457)[a,c]	0.00065 (0.0005-0.001)
24 h sepsis untreated	276 (270 – 322)	170 (144–279)	3767 (3205 – 4821)	946 (639 – 1200)	641 (425 – 1080)	0.0013 (0.0007–0.0015)
24 h low dose DMSO	212 (130 - 265)	162 (136-220)	7779 (7165 - 9927)	537 (480 - 1132)	702 (422 - 817)	0.00185 (0.0015-0.003)
24 h high dose DMSO	219 (211 - 252)	210 (128-256)	4126 (3243 - 6713)	751 (593 - 871)	902 (627 - 1155)	0.0013 (0.0011-0.0021)
24 h low dose DMSO/P2X$_7$	308 (258 - 348)	165 (111-224)	8986 (6408 - 9307)	779 (664 - 792)	610 (175 - 647)	0.00145 (0.0002-0.0017)
24 h high dose DMSO/P2X$_7$	224 (169 - 331)	280 (195-380)	7584 (4387 - 9544)	593 (480 -1218)	741 (394 - 830)	0.0015 (0.0012-0.0024)
24 h P2X$_7$ pretreatment	188 (184 - 256)	222 (212 - 238)	8607 (7982-12227)[d]	1048 (895 - 1225)	836 (560 - 968)	0.00225 (0.0018-0.0041)

10.4.10 Urine biomarkers

Group	Urine NGAL (μg/ml)	Urine KIM-1 (ng/ml)	Urine IL-18 (ng/ml)	Urine MCP-1 (ng/ml)	Osteopontin (ng/ml)	Clusterin (ng/ml)	Calbindin (ng/ml)
6 h sepsis untreated	27 (24 – 38)	2.4 (1.2 – 4.4)	3643 (1266 – 5674)	3284 (1343 – 5619)	0.78 (0.28 – 1.02)	43 (33 – 232)	180 (157–244)
6 h high dose DMSO	20 (17 - 33)	1.82 (1.03 - 2.14)	2021 (1605 - 2421)	3152 (2350 -3538)	0.88 (0.36 - 1.81)	253 (245 - 319)	119 (119 - 141)
6 h high dose $P2X_7$	23 (23 - 27)	2.80 (1.97 - 6.1)	2844 (2462 - 3534)	4360 (3888-4926) [a,c]	1.02 (0.73 - 1.44)	205 (152 - 536)	264 (118 - 452)
24 h sepsis untreated	39 (24 – 46)	0.44 (0.11 – 0.45)	769 (725 – 2576)	1740 (1391 – 4119)	0.09 (0.08 – 0.29)	175 (130 – 338)	46 (36 – 52)
24 h low dose DMSO	29 (21 - 32)	-	-	-	-	-	-
24 h high dose DMSO	30 (25 - 44)	0.36 (0.15 - 0.64)	2085 (1497 - 3899)	2710 (1336 - 5009)	0.37 (0.33 - 0.58)	307 (227 - 667)	89 (75 - 112)
24 h low dose DMSO/$P2X_7$	29 (24 - 30)	-	-	-	-	-	-
24 h high-dose DMSO/$P2X_7$	23 (15 - 40)	0.31 (0.21 - 0.61)	3505 (2880-5979) [c]	3044 (2608 - 5701)	1.02 (0.37-1.53) [c]	290 (89 - 699)	100 (68 - 120)
24 h $P2X_7$ pretreatment	39 (35 - 52)	0.27 (0.16 - 0.31)	4104 (1245 - 5781)	3965 (1595 - 5201)	0.66 (0.66 -0.96)	240 (205 - 264)	142 (63 - 144)